


Theoretical investigation of second
electric-field-induced
second-harmonic-generation
(ESHG) virial coefficients



Roshna Mariam Jacob



*Submitted in partial fulfilment of the
requirements for the degree of
Doctor of Philosophy in Physics in the
School of Chemistry and Physics,
University of KwaZulu-Natal.*

School of Chemistry and Physics
University of KwaZulu-Natal
Private Bag X01, Pietermaritzburg
Scottsville 3209, South Africa

Supervisor: Dr V W Couling

2025

Abstract

The molecular theory of the second electric-field-induced second-harmonic generation (ESHG) virial coefficient B_γ describing the effects of interacting pairs of molecules on the molecular hyperpolarizability is reviewed, and then extended to include contributions arising from the permanent electric quadrupole moments and the dipole-dipole-quadrupole hyperpolarizabilities of the molecules. The classical long-range dipole-induced-dipole model is used to describe the interactions between pairs of molecules. The molecular (hyper)polarizability tensor components required in the calculations have been obtained by *ab initio* computation using DALTON.

This investigation has been limited to non-dipolar species, where the permanent electric quadrupole moment is the leading multipole moment. The expressions obtained for contributions to B_γ are evaluated numerically for the H₂, N₂, CO₂ and C₂H₄ molecules.

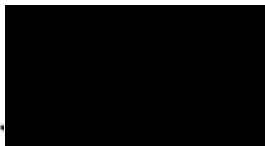
For CO₂ and C₂H₄, the quadrupole-induced and dipole-dipole-quadrupole hyperpolarizability contributions become significant, and the calculated B_γ virial coefficients indicate that the pair-interaction contributions arising for CO₂ and for C₂H₄ are large enough to be comfortably measurable by Shelton's ESHG apparatus and electrode arrays.

Declaration


I, Roshna Mariam Jacob, declare that

1. The research reported in this thesis, except where otherwise indicated, is my original research.
2. This thesis has not been submitted for any degree or examination at any other university.
3. This thesis does not contain other persons' data, pictures, graphs or other information, unless specifically acknowledged as being sourced from other persons.
4. This thesis does not contain any other persons' writing, unless specifically acknowledged as being sourced from other researchers. Where other written sources have been quoted, then:
 - (a) their words have been rewritten but the general information attributed to them has been referenced;
 - (b) where their exact words have been used, their writing has been placed inside quotation marks, and referenced.

5. This thesis does not contain text, graphics or tables copied and pasted from the internet, unless specifically acknowledged, and the source being detailed in the thesis and in the References sections.

Signed 

I hereby certify that this statement is correct.

Signed 

V W Couling
Supervisor

Acknowledgments

Undertaking this PhD has been a truly life-changing experience for me and it would not have been possible to do without the support and guidance that I received from many people. Many people have contributed to this thesis in various ways; including but not limited to literature search, acquisition and access to resources, providing insights and personal support. I thank all of them.

First and foremost, I would like to thank God Almighty for giving me the strength, knowledge, ability and opportunity to undertake this research study and to persevere and complete it satisfactorily. Without his blessings, this achievement would not have been possible.

Foremost, I would to express my deep sense of gratitude and profound respect to my supervisor Dr Vincent W Couling for the continuous support of my PhD work and research with great patience, encouragement, motivation, enthusiasm and immense knowledge. Without his guidance and constant feedback this PhD would not have been achievable. He has inspired me to become an independent researcher and helped me realize the power of critical reasoning. Also, I gratefully acknowledge the financial support he provided me to complete the work. I could not have imagined having a better advisor and mentor for my PhD study.

Many thanks also to Dr N Dlamini for his constant help to overcome the burdens

in the computational part of my work.

Thanks to members of my research group Mr Prathap, Mr Mzumagezi, Mr Preshen, Mr Verlan and Mr Mzwadile. In addition to, special thanks to UKZN Physics staffs, particularly Mr Ravin and Mr Mzungezi for the unwavering support, and who kept the postgraduate lab lively whenever the going got tough. Besides, a very special thank you to Dr Francis for his invaluable advice and feedback on my research and for always being so supportive of my work. I am also very grateful to everyone in my UKZN Physics department who all helped me in numerous ways during various stages of my PhD.

I acknowledge financial support from the following bodies;

- (i) The National Research Foundation (NRF), South Africa through Grants No. 106020, 92786, and 93562.
- (ii) The University of KwaZulu-Natal - PhD fee remission.

I cannot forget friends who went through hard times together, cheered me on, and celebrated each accomplishment: Dr Fikisiwe Gebashe, Mr Mzungezi Cypriyan

I would like to express my gratitude to my parents-in-law Mr Sunny Mathew and Mrs Susan Sunny for their unfailing emotional support.

I feel a deep sense of gratitude for my grand parents Late Mr CJ Thomas, Mrs Marykutty Thomas, Mr PM Koruth and Mrs Elizabeth Varghese who formed part of my vision and taught me good things that really matter in life.

A special thanks to my brother Roshith Jacob, sister in law Mable Ann, and my nephew Adam Rosh for for helping in whatever way they could during this challeng-

ing period. Also been generous with their love and encouragement despite the long distance between us.

I owe my deepest gratitude towards my better half Samson for his eternal support and understanding of my goals and aspirations. His infallible love and support has always been my strength. His patience and sacrifice will remain my inspiration throughout my life. Without his help, I would not have been able to complete much of what I have done and become who I am.

I deeply thank my parents, Jacob Thomas and Anila Jacob for their unconditional trust, timely encouragement, endless patience and constant prayers. It was their love that raised me up again when I got weary. Their infallible love and support has always been my strength. Their patience and sacrifice will remain my inspiration throughout my life. I am also very much grateful to all my family members for their constant inspiration and encouragement.

Last but not the least, this thesis is dedicated to my precious child Pearl Marybeth Samson who brought so much joy into my life and reminds me of what truly matters.

As always it is impossible to mention everybody who had an impact to this work however there are those whose spiritual support is even more important.

Contents

1	Review and Introduction	1
1.1	Review	1
1.1.1	Nonlinear optics (NLO)	1
1.1.2	Electric-field-induced second-harmonic generation (either ESHG or EFISH)	4
1.2	Interaction-induced hyperpolarizabilities	8
1.3	The aim of this project	11
2	Molecular Electric Properties	14
2.1	Introduction	14
2.2	The multipole expansion	15
2.3	The microscopic field-induced multipole moments	20
2.4	The macroscopic induced dipole density	40
2.5	The transition from microscopic to macroscopic polarization	45
2.6	Concluding remarks	48
3	The Theory of ESHG for an Ideal Gas	49
3.1	Electromagnetic theory in dielectric media	49
3.2	The dielectric constant of an ideal gas	51
3.3	The index of refraction of an ideal gas	62
3.4	ESHG in an ideal gas	68
3.4.1	Static and dynamic fields with parallel polarization	69

3.4.2	Dynamic field polarized perpendicular to static field	77
4	The Theory of ESHG for a Real Gas	82
4.1	Interacting non-dipolar molecules	82
4.2	The molecular-property tensors	119
4.2.1	Molecules of D_{2h} symmetry	119
4.2.2	Molecules of $D_{\infty h}$ symmetry	125
5	Results	131
5.1	Hydrogen	131
5.2	Nitrogen	144
5.3	Carbon Dioxide	157
5.4	Ethene	168
5.5	Concluding Remarks	178
A		181
A.1	Fortran Program to calculate the $\gamma_1\alpha_1$ contribution to B_γ	181
	Bibliography	197

List of Tables

2.1	Typical linear and nonlinear optical processes.	25
5.1	The intermolecular potential parameters and quadrupole moment of H ₂ used in the calculation of B_γ	132
5.2	H ₂ mean polarizabilities, polarizability anisotropies, and deduced polarizability tensor components for zero frequency and relevant optical frequencies.† All values are in SI units. ^a	133
5.3	Components of the ESHG second hyperpolarizability $\gamma_{ijkl}(-2\omega; \omega, \omega, 0)$ for H ₂ calculated in this work using a CCSD wavefunction and a t-aug-cc-pVQZ basis set. All values are in atomic units. ^a	134
5.4	Components of the ESHG second hyperpolarizability $\gamma_{ijkl}(-2\omega; \omega, \omega, 0)$ for H ₂ calculated by Bishop <i>et al.</i> using accurate James-Coolidge type wavefunctions and an extended basis set.† All values are in atomic units. ^a	135
5.5	Components of the SHG dipole-dipole-quadrupole hyperpolarizabilities $B_{ijkl}(-2\omega; \omega, \omega)$ and $D_{ijkl}(-2\omega; \omega, \omega)$ for H ₂ calculated <i>ab initio</i> in this work using a CCSD wavefunction and a t-aug-cc-pVQZ basis set. All values are in atomic units. ^a	136
5.6	The relative magnitudes of the contributions to B_γ for H ₂ at $T = 200$ K	138
5.7	The relative magnitudes of the contributions to B_γ for H ₂ at $T = 298$ K	139
5.8	The relative magnitudes of the contributions to B_γ for H ₂ at $T = 400$ K	140

5.9	The relative magnitudes of the contributions to B_γ for H_2 at $T = 500$ K	141
5.10	A summary of the calculated B_γ values for H_2	142
5.11	The intermolecular potential parameters and quadrupole moment of N_2 used in the calculation of B_γ .	144
5.12	N_2 mean polarizabilities, polarizability anisotropies, and deduced polarizability tensor components for zero frequency and relevant optical frequencies. [†] All values are in SI units. ^a	145
5.13	Components of the ESHG second hyperpolarizability $\gamma_{ijkl}(-2\omega; \omega, \omega, 0)$ for N_2 calculated in this work using a CCSD wavefunction and a t-aug-cc-pVTZ basis set. All values are in atomic units. ^a	147
5.14	Components of the SHG dipole-dipole-quadrupole hyperpolarizabilities $B_{ijkl}(-2\omega; \omega, \omega)$ and $D_{ijkl}(-2\omega; \omega, \omega)$ for N_2 calculated <i>ab initio</i> in this work using a CCSD wavefunction and a t-aug-cc-pVTZ basis set. All values are in atomic units. ^a	148
5.15	The relative magnitudes of the contributions to B_γ for N_2 at $T = 200$ K	150
5.16	The relative magnitudes of the contributions to B_γ for N_2 at $T = 298$ K	151
5.17	The relative magnitudes of the contributions to B_γ for N_2 at $T = 400$ K	152
5.18	The relative magnitudes of the contributions to B_γ for N_2 at $T = 500$ K	153
5.19	A summary of the calculated B_γ values for N_2	154
5.20	The intermolecular potential parameters and quadrupole moment of CO_2 used in the calculation of B_γ .	157
5.21	CO_2 mean polarizabilities, polarizability anisotropies, and deduced polarizability tensor components for zero frequency and relevant optical frequencies. [†] All values are in SI units. ^a	158
5.22	Components of the ESHG second hyperpolarizability $\gamma_{ijkl}(-2\omega; \omega, \omega, 0)$ for CO_2 calculated in this work using a CCSD wavefunction and a t-aug-cc-pVTZ basis set. All values are in atomic units. ^a	160

5.23	Components of the SHG dipole-dipole-quadrupole hyperpolarizabilities $B_{ijkl}(-2\omega; \omega, \omega)$ and $D_{ijkl}(-2\omega; \omega, \omega)$ for CO ₂ calculated <i>ab initio</i> in this work using a CCSD wavefunction and a t-aug-cc-pVTZ basis set. All values are in atomic units. ^a	161
5.24	The relative magnitudes of the contributions to B_γ for CO ₂ at $T = 200$ K	163
5.25	The relative magnitudes of the contributions to B_γ for CO ₂ at $T = 298$ K	164
5.26	The relative magnitudes of the contributions to B_γ for CO ₂ at $T = 400$ K	165
5.27	The relative magnitudes of the contributions to B_γ for CO ₂ at $T = 500$ K	166
5.28	A summary of the calculated B_γ values for CO ₂	167
5.29	The intermolecular potential parameters and quadrupole moment of C ₂ H ₄ used in the calculation of B_γ	168
5.30	C ₂ H ₄ mean polarizabilities, polarizability anisotropies, and polarizability tensor components for zero frequency and relevant optical frequencies. The data are calculated in this work using a CCSD wavefunction and a t-aug-cc-pVTZ basis set. All values are in SI units. ^a	169
5.31	Experimentally deduced mean polarizabilities, polarizability anisotropies, and polarizability tensor components for C ₂ H ₄ for zero frequency and relevant optical frequencies. All values are in SI units.	169
5.32	Components of the ESHG second hyperpolarizability $\gamma_{ijkl}(-2\omega; \omega, \omega, 0)$ for C ₂ H ₄ calculated using a CCSD wavefunction and a t-aug-cc-pVTZ basis set. All values are in atomic units. ^a	171

5.33	Components of the SHG dipole-dipole-quadrupole hyperpolarizabilities $B_{ijkl}(-2\omega; \omega, \omega)$ and $D_{ijkl}(-2\omega; \omega, \omega)$ for C_2H_4 calculated <i>ab initio</i> in this work using a CCSD wavefunction and a t-aug-cc-pVTZ basis set. All values are in au. ^a	172
5.34	The relative magnitudes of the contributions to B_γ for C_2H_4 at $T = 200$ K	174
5.35	The relative magnitudes of the contributions to B_γ for C_2H_4 at $T = 298$ K	175
5.36	The relative magnitudes of the contributions to B_γ for C_2H_4 at $T = 400$ K	176
5.37	The relative magnitudes of the contributions to B_γ for C_2H_4 at $T = 500$ K	177
5.38	A summary of the calculated B_γ values for C_2H_4	178

List of Abbreviations

CC3	iterative approximate coupled cluster singles, doubles, and triples
CCSD	coupled cluster method with single and double replacements
CO ₂	carbon dioxide
C ₂ H ₄	ethene
DID	dipole-induced-dipole
DOSD	dipole oscillator strength distribution
EFISH	electric-field-induced second-harmonic generation
ESHG	electric-field-induced second-harmonic generation
H ₂	hydrogen
N ₂	nitrogen
NLO	nonlinear optics
QID	quadrupole-induced-dipole
SCF	self-consistent field
SHG	second-harmonic generation
t-aug-cc-pVQZ	triply-augmented correlation-consistent polarized valence quadruple zeta
t-aug-cc-pVTZ	triply-augmented correlation-consistent polarized valence triple zeta

Chapter 1

Review and Introduction

1.1 Review

1.1.1 Nonlinear optics (NLO)

In 1931, Maria Goeppert-Mayer presented in her PhD thesis the quantum-mechanical theory predicting two-photon absorption (or two-photon excitation) [1]. This was the first nonlinear optical effect to be predicted, her pioneering theory accounting for the simultaneous absorption by a single atom of two photons, exciting the atom from an initial electronic state (typically the ground state) to one of higher energy (usually an excited electronic state). The two photons can be of the same frequency, or, for so-called *non-degenerate* two-photon absorption, of different frequencies. The probability of two-photon absorption is found to depend quadratically on the light intensity, making it a NLO process. It was almost three decades later, and only after the invention of the laser in 1960 (which provided a source for the required high-intensity radiation), that experimental observation of two-photon absorption was at last realised. At Bell Labs, Kaiser and Garrett irradiated Eu^{2+} doped CaF_2 crystals with the red monochromatic light ($\lambda = 694.3 \text{ nm}$) from a pulsed ruby laser, and generated blue fluorescent light at around 425.0 nm through the process of two-photon-excited fluorescence [2].

Around a month prior to Kaiser and Garrett publishing their work on two-photon absorption, Franken, Hill, Peters and Weinreich reported their discovery of the NLO process of second-harmonic generation (SHG): on passing the beam from a ruby laser through a quartz crystal, they observed the production of ultraviolet photons ($\lambda = 347.1$ nm) at double the frequency of the incident photons [3].

The quantum-mechanical processes for two-photon absorption and for SHG are different, and have been comprehensively explained in various modern texts (see, for recent examples, references [4–6]). The essential mechanisms of the two processes are now briefly reviewed:

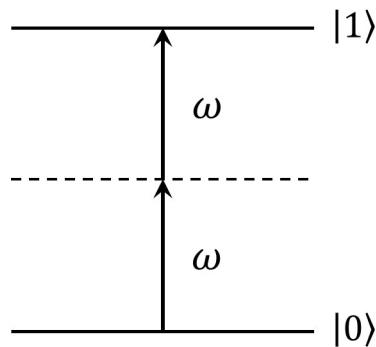


Figure 1.1: Energy-level diagram representing the two-photon absorption process.

In two-photon absorption, which is represented in Figure 1.1, an atom or molecule in the sample simultaneously absorbs two photons from the irradiating laser beam, and usually makes a transition from its ground electronic state (labelled by the ket $|0\rangle$) to its first excited electronic state $|1\rangle$.

Figure 1.2 on the other hand represents the process of optical second-harmonic generation. Here, two incident photons of frequency ω from the optical field are almost simultaneously incident on the molecule, and in a single quantum-mechanical pro-

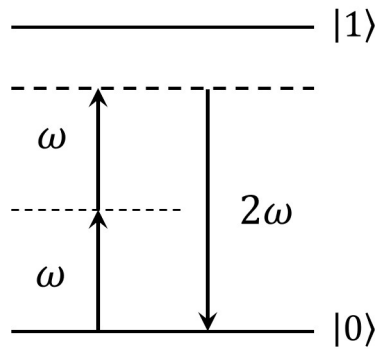


Figure 1.2: Energy-level diagram for the SHG process indicating the two incident photons, each of frequency ω , and the emitted photon of frequency 2ω .

cess are annihilated, almost instantaneously creating a scattered photon of the sum frequency 2ω . The solid lines represent real electronic energy eigenstates of the free atom or molecule, whereas the dashed lines represent virtual levels, these being the combined energy of the ground electronic state and of one, or both, of the simultaneously incident photons.

The discovery of SHG is generally taken as the birth of the field of nonlinear optics. It was Nicolaas Bloembergen who rapidly developed the theoretical basis for many nonlinear optical processes, as described in his 1965 monograph *Nonlinear Optics* [7], which was based on the lectures which he delivered at Harvard University in 1963 for a course on quantum electronics. Bloembergen was jointly awarded the Nobel Prize in Physics in 1981, being singled out in the presentation speech for having, together with his collaborators, “founded a new field of science we now call non-linear optics . . . where two or more beams of laser light are mixed in order to produce laser light of a different wavelength” [8].

The SHG experiment of Franken *et al.* precipitated a sudden explosion of discovery of nonlinear optical phenomena, as evidenced by the early review article of Franken and Ward [9]. Amongst these was the discovery of electric-field-induced second-harmonic generation, the effect which is the subject of the present investiga-

tion.

1.1.2 Electric-field-induced second-harmonic generation (either ESHG or EFISH)

In 1962, Terhune, Maker and Savage were the first to observe electric-field-induced second-harmonic generation, when they propagated light from a ruby laser through a calcite crystal in the presence of a dc electric field, producing SHG photons [10, 11]. For normal SHG (*i.e.* that arising from electric dipole transitions) to occur, the medium cannot be isotropic, meaning that it *must* lack a centre of inversion. Calcite crystal is a naturally isotropic medium, but the application of a dc electric field induces polarization in the medium, thereby destroying the inversion symmetry and so permitting optical SHG arising from electric dipole transitions [9]. Terhune *et al.* even observed the faint production of SHG photons in calcite in the absence of an applied dc electric field [10, 11], these arising from electric quadrupole and magnetic dipole transitions [12–15].

In 1968, Mayer reported on ESHG experiments for various gases and liquids [16]. Shortly thereafter, Kielich developed a molecular-tensor theory to account for ESHG, by invoking classical statistical mechanics to relate the macroscopic susceptibility to the microscopic hyperpolarizabilities [17–21]. The third-order nonlinear susceptibility $\chi^{(3)}(2\omega)$ is the measurable observable in an ESHG experiment, and the theory of Kielich yields, for a gas-phase ESHG measurement where the light-wave field is plane polarized in the same direction as the applied dc electric field,

$$\chi^{(3)}(2\omega) = \frac{1}{6} f_L(0) f_L^2(\omega) f_L(2\omega) \frac{\mathcal{N}}{\varepsilon_0} \Gamma. \quad (1.1)$$

Here, $f_L(\omega)$ is the Lorentz local-field factor at frequency ω , $f_L(0)$ is the local-field factor for the static applied field, \mathcal{N} is the molecular number density, and Γ is the

orientationally averaged microscopic second hyperpolarizability

$$\Gamma = \left[\gamma_{\parallel}^{\text{ESHG}} + \frac{\mu_0}{3kT} \beta_{\parallel}^{\text{SHG}} \right], \quad (1.2)$$

with $\gamma_{\parallel}^{\text{ESHG}}$ being the scalar component of the second molecular hyperpolarizability, μ_0 the permanent molecular electric dipole moment (if there is one), k the Boltzmann constant, T the absolute temperature of the gas, and $\beta_{\parallel}^{\text{SHG}}$ the vector component of the first hyperpolarizability in the direction of the permanent dipole moment. Equations (1.1) and (1.2) will be formally derived in Section 3.4.1 of Chapter 3, where a full account of the tensor notation will also be provided.

The two terms in the expression for Γ in equation (1.2) arise from different mechanisms. The source of the temperature-independent second-hyperpolarizability contribution is the distortion of the electronic structure of the individual molecules in the sample by the applied static electric field. The temperature-dependent first hyperpolarizability term, on the other hand, is due to the orientational effect of the electric field on the permanent molecular dipole moments, which tend to become partially aligned. Both atoms and non-dipolar molecules are centrosymmetric, with μ_0 and $\beta_{\parallel}^{\text{SHG}}$ being zero. For them, the orientation term makes no contribution to Γ and an ESHG measurement at room temperature will suffice to yield knowledge of $\gamma_{\parallel}^{\text{ESHG}}$. Conversely, dipolar molecules are non-centrosymmetric, and so for them, both $\gamma_{\parallel}^{\text{ESHG}}$ and $\beta_{\parallel}^{\text{SHG}}$ will contribute to Γ . This means that for dipolar molecules, temperature-dependent measurements of the ESHG are necessary if values of $\gamma_{\parallel}^{\text{ESHG}}$ and $\beta_{\parallel}^{\text{SHG}}$ are to be extracted.

The typical experimental procedure for measuring ESHG in gaseous media entails passing a laser beam with oscillating electric field $\mathcal{E}_{\alpha} \cos(\omega t)$ through the sample while in the presence of a static applied electric field E_{α} , which permits the gen-

eration of a weak, collinear beam of frequency-doubled photons. Mayer *et al.* undertook the first ESHG measurements of gases [16], investigating a number of small molecules.

From 1971 through to 1985, Ward's research group undertook a systematic series of ESHG experiments for gaseous media, making use of a single pair of cylindrical electrodes and a pulsed ruby laser ($\lambda = 694.3$ nm) [22–29]. The density of each gas was gradually varied to obtain a maximum signal, corresponding to the coherence length of the gas matching the length of the electrostatic region. As a consequence of the dispersion of the refractive index, the fundamental wave generating the SHG and the second-harmonic wave travel at different velocities through the medium. By increasing the path-length of the medium under the influence of the applied electric field (to increase the intensity of the SHG signal), the second-harmonic waves generated at either end of the sample will get further out of phase with each other, and ultimately they will interfere destructively rather than constructively. Increasing the sample length any further than this will reduce the amplitude of the resultant second-harmonic wave. Since a method to achieve phase matching had not yet been established, the cylindrical electrodes served to optimize the length of the electrostatic region to avoid this problem, and consequently a high-power pulsed laser was essential if a detectable SHG signal was to be achieved. For gases of atoms or non-dipolar molecules, room temperature measurements sufficed, while for dipolar species, the apparatus was modified to allow for measurements over the temperature range 295 to 600 K.

In 1982, Buckingham and Shelton described a gas-phase ESHG experimental arrangement to realise periodic phase matching [30], allowing for an increase in the number of second-harmonic photons of around four orders of magnitude. A continuous wave laser beam with a power of around 1 W could now be used to excite

the gas sample under study, and they used an argon-ion laser, allowing for measurements at all six of the laser wavelengths, namely 514.5, 501.7, 496.5, 488.0, 476.5 and 457.9 nm. Combined with the ruby laser measurements at $\lambda = 694.3$ nm of Ward's group, this would at last allow the frequency dependence of the second hyperpolarizability of isolated atoms and non-dipolar molecules to be measured in the visible region of the electromagnetic spectrum. By employing a periodic array of cylindrical electrodes, the density of the gas sample could be continuously varied until the coherence length of the gas matched the spatial period of the electrodes, hence greatly enhancing the SHG signal. Since 1982, Shelton's research group has employed this periodic-phase-matching technique to yield the most accurate measurements of the dispersion of the hyperpolarizability of atoms and small, mostly non-dipolar, molecules to date [30–53].

In 1990, Shelton measured Γ for 16 atoms and molecules using room-temperature gas-phase ESHG at the two near-infrared wavelengths 1064 and 1319 nm [45]. This served to extend the spectral range of the measured dispersion curves to the widest possible range. In 1993, Shelton and Donley enclosed their ESHG cell in an oven, permitting measurements over a range of gas temperatures from room temperature up to 200 °C. They measured the temperature-dependence of Γ for the polar molecule acetonitrile (mixed in a buffer gas of N_2) using an argon-ion laser to provide an excitation beam of wavelength 514.5 nm [47], extracting values of $\gamma_{\parallel}^{\text{ESHG}}$ and $\beta_{\parallel}^{\text{SHG}}$ for acetonitrile. In 1998, Kaatz, Donley and Shelton measured $\gamma_{\parallel}^{\text{ESHG}}$ and $\beta_{\parallel}^{\text{SHG}}$ for eight molecules at $\lambda = 1064$ nm by measuring gas-phase ESHG, and by measuring the temperature dependence of the ESHG for the strongly polar molecules [50]. In 2015, Couling and Shelton reported temperature-dependent gas-phase ESHG measurements of the dipolar molecule $(\text{CH}_3)_2\text{O}$ using five different excitation wavelengths over the range $488 \text{ nm} < \lambda < 1064 \text{ nm}$ [51]. This allowed, for the first time, for the extraction of benchmark-quality dispersion curves for $\gamma_{\parallel}^{\text{ESHG}}$ and for $\beta_{\parallel}^{\text{SHG}}$

for an isolated dipolar molecule from gas-phase ESHG measurements.

1.2 Interaction-induced hyperpolarizabilities

The field of electro-optics bridges the two essential modern technologies of electronics and photonics. Information technology requires the creation, manipulation, transportation and detection of information, and this occurs by means of electrons, photons, phonons or plasmons [54]. In essence, electro-optics allows for information to be converted between the electronic and photonic domains. Nonlinear-optical (NLO) materials allow for optical harmonic generation and signal processing. Much experimental and theoretical effort has been expended in studying the NLO properties of molecules to find new materials which possess the desired NLO requirements [55]. The current state-of-the-art in NLO materials is discussed in the recent review article of Zheludev and Kivshar, wherein they examine metamaterials as a means of realising tunable, switchable, nonlinear and sensing functionalities [56]. Metamaterials are artificial electromagnetic media which have been structured on the subwavelength scale. They argue that future metadevices will see photonic devices rivalling conventional electronic devices for telecommunications systems as well as for consumer products like mobile phones.

NLO materials are generally in the condensed phase, so that theoretical and computational attempts to predict their NLO properties are hampered by the presence of many subtle physical effects which are not present in the case of an isolated molecule [57, 58]. Theoretical and experimental understanding of the NLO properties of isolated molecules is an important precursor in the development of an understanding of NLO properties in the condensed phase. Accurate experimental measurements

of the hyperpolarizabilities of isolated molecules in the gas phase provide useful benchmarks for the computationalists who are perpetually refining their *ab initio* quantum computational techniques. Two recent review articles provide an excellent overview of the theory of molecular nonlinear optics [59, 60].

In the condensed phase, interatomic and intermolecular interactions can have a significant effect on the NLO properties of materials. The complexity in unravelling the particular contributions of the many effects at play has provided the impetus to understand the simplest of intermolecular interaction effects, namely that of interatomic and intermolecular pair interactions in the gas phase on the atomic or molecular hyperpolarizabilities. To this end, Donley and Shelton have developed experimental and analytical techniques at the 0.1% level to obtain accurate measurements of the effects of intermolecular pair interactions on dc ESHG molecular hyperpolarizabilities $\gamma^{\text{ESHG}}(-2\omega; \omega, \omega, 0)$ for the atoms and non-dipolar molecules He, Ar, H₂ and N₂ [48]. Their measured pair-interaction contributions were then compared with calculated values obtained from a classical dipole-induced-dipole (DID) model. Their model was found to underestimate the magnitude of the density dependence of the hyperpolarizability by a factor of *ca.* 2, and it had the opposite sign. Buckingham, Concannon and Hands subsequently made use of a classical DID model to investigate the effect of dipolar interaction on the independent components of the hyperpolarizability of a pair of spherical atoms for five different NLO effects, including ESHG [61, 62]. They found Donley and Shelton's expression for the DID contribution to the pair hyperpolarizability to differ from the original expression derived by Hunt [63], leading to the correction of Donley and Shelton's expression by the numerical factor 19/60 [49]. The DID model was thus underestimating the magnitude of the observed density dependence of the hyperpolarizabilities by a factor of about 6, and was still having the opposite sign. The conclusion reached by Donley and Shelton was that the DID model, which assumes classical multipole interactions

even at very short range, does not account for the short-range “electron overlap” contribution. *Ab initio* quantum-mechanical calculations which take into account the electron overlap would be required to establish whether this is the reason, or part of the reason, for the discrepancy found between experiment and theory. Donley and Shelton suggested other avenues of future investigation to make refinements to the classical multipole interaction theory to increase its accuracy. This included using more accurate intermolecular potential functions, using correct values for the independent tensor components of the molecular hyperpolarizabilities (they had assumed the molecules to possess spherical symmetry), inclusion of the effects of the permanent electric quadrupole moments of the H₂ and N₂ molecules as well as the effects arising from higher-order response tensors, and inclusion of fluctuations in the moments which give a quantum correction to DID, especially for less massive molecules.

Buckingham and Concannon investigated the question of electron overlap at short range, undertaking *ab initio* SCF calculations of the polarizability and second hyperpolarizability for interacting pairs of atoms at various internuclear separations [61]. The DID model is based on the long-range theory of intermolecular interactions, the molecules being assumed to retain their individual identities even at short-range internuclear separations. For these short range interactions, the electron clouds, and hence the wavefunctions, of the two molecules begin to overlap [64]. Their *ab initio* quantum mechanical calculations show that for interacting helium atoms, for long-range interatomic separations of 0.35 nm or more, the calculated classical and quantum mechanical interaction-induced effects on the second hyperpolarizability agree very well. However, for short-range separations of less than 0.35 nm, the classical model (which neglects the electron overlap effects) predicts larger interaction-induced effects than the the SCF calculations (which do account for electron overlap) [61].

There have been a few more-recent studies of collision-induced hyperpolarizabilities between pairs of atoms, [65–72]. While the *ab initio* computations have become increasingly accurate, they have simultaneously become increasingly demanding of computational resources, which explains why calculations have not been easily extended to molecules [73]. Koch *et al.* have utilized the frequency-dependent interaction-induced second hyperpolarizabilities calculated *ab initio* for helium and argon [67] to evaluate the ESHG second virial coefficients for these atoms using a semi-classical approach [69]. The computed interaction-induced second hyperpolarizabilities are seen to be quite sensitive to the choice of basis set, and so calculations using more extended and diffuse basis sets were performed to try and improve agreement with experiment. The ESHG second virial coefficients obtained for Ar show a dramatic dependence on choice of basis set, and are positive while the virial coefficients for He are negative. Donley and Shelton measured the density dependence of hyperpolarizability ratios, and when their experimental determinations for argon and hydrogen, and for hydrogen and helium, are combined the result has the opposite sign to the calculated value of Koch *et al.*

1.3 The aim of this project

Recent studies of interaction-induced contributions to the Kerr electro-optic effect raise interesting questions for the ESHG effect. A brief review is required to give context.

In 1955, Buckingham and Pople developed a molecular-tensor theory to account for the Kerr-effect in ideal gases of atoms or axially-symmetric molecules [74]. Buckingham went on to provide a statistical-mechanical theory of the Kerr constant which

accounted for the density-dependence of the Kerr effect in real gases of atoms or axially-symmetric molecules [75]. In 1983, Buckingham, Galwas and Fan-Chen included the collision-induced polarizability into this theory, and found that it made the largest contribution to B_K [76]. Their calculated B_K coefficients were in reasonable agreement with the measured data for the fluoromethanes over the experimental temperature range, though the experimental values do have a large uncertainty (around 50%).

Couling and Graham extended Buckingham's theory to dipolar molecules, including higher-order molecular-interaction terms to ensure convergence [77]. Calculations for CH_3F , CH_2F_2 , CHF_3 , SO_2 , $(\text{CH}_3)_2\text{O}$, CH_3COCH_3 and H_2S over a range of temperature are mostly within the uncertainty limits of the available experimental data [77–79]. Quadrupole and field gradient contributions were assumed to be negligible for molecules with large permanent dipole moments, but should probably be included for non-dipolar molecules. Quadrupole–induced-dipole (QID) molecular-interaction contributions were investigated by Couling and Naidoo in 2017, calculating B_K for CO_2 , C_2H_4 and C_2H_6 . Agreement with the measured data was generally favourable [80]. Of especial relevance to the present ESHG investigation is the fact that molecules with a larger quadrupole moment and polarizability anisotropy had substantial contributions from the QID interaction, these sometimes even exceeding the pure polarizability term contributions.

Couling and Mhlongo extended the molecular-tensor theory of the Kerr effect to include contributions to B_K from the optical-frequency second hyperpolarizability $\gamma^K(-\omega; \omega, 0, 0)$ [81]. These were found to be non-negligible.

If QID contributions can be substantial for the linear interaction-induced polarizability, the question arises as to whether, especially for non-dipolar molecules with

significant quadrupole moments, the QID effects for the interaction-induced hyperpolarizability will be similarly significant. Might this account for the discrepancy between the measured ESHG virial coefficients and those calculated using the DID model?

In an attempt to answer this question, this project extends the molecular-tensor theory of ESHG to include, in the classical DID long-range model, the contributions to B_γ arising from the permanent molecular quadrupole moments and from the second-harmonic dipole-dipole-quadrupole hyperpolarizabilities. The non-dipolar molecules H_2 , N_2 , CO_2 and C_2H_4 are investigated, the latter two having relatively large permanent quadrupole moments. Since the DALTON molecular electronic-structure program allows the molecular-property tensor components to be accurately calculated, the full molecular symmetry can be taken into account.

It should be noted that, for an isolated molecule, Kielich has already considered second-harmonic generation (SHG) arising from higher-order tensors, both for electric dipole scattering, where the electric field gradient of the incident light wave distorts the electronic structure of the molecule thereby inducing additional dipole moment, and for electric quadrupole scattering where the electric field of the light wave induces an electric quadrupole moment [82]. Kielich described both processes by means of the dipole-dipole-quadrupole hyperpolarizability $B_{ijkl}(-2\omega; \omega, \omega)$, tabulating the non-zero and independent tensor components for all point groups. He assumed the quadrupole-dipole-dipole tensor $D_{ijkl}(-2\omega; \omega, \omega) = B_{klij}(-2\omega; \omega, \omega)$ [82], but our analysis will reveal this to be an approximation at optical frequencies, the relationship holding true only in the static limit where, as described by Buckingham in his classic review on permanent and induced molecular moments and long-range intermolecular forces, $D_{ijkl}(0; 0, 0) = B_{klij}(0; 0, 0)$ [83].

Chapter 2

Molecular Electric Properties

2.1 Introduction

The permanent multipole moments of a molecule (e.g. its electric dipole and quadrupole moments) are fundamental properties which describe the molecular charge distribution, while the molecular (hyper)polarizabilities describe the distortion of the molecular charge distribution by applied fields or the fields arising from the permanent or induced moments of neighbouring molecules [83–86]. These permanent multipole moments and polarizabilities provide key insight into molecular structure and intermolecular forces, and are crucial to the development of the molecular-tensor theory of electro-optic effects such as the dielectric, refractivity and Kerr effects. Hence they are now reviewed in sufficient detail to permit the subsequent development of the ESHG theory, which is presented in Chapters 3 (ideal gas) and 4 (real gas).

2.2 The multipole expansion

The simplest possible intermolecular interaction is that between two molecules. A full description of this pair interaction is in fact a many-body problem since the effects of all the individual charges upon each other needs to be accounted for. This full description is essentially intractable, and simplifications are required. For example, electrostatic theory can be employed provided the internal motion of the electrons within a molecule, and the motion of the molecule as a whole, are disregarded. On the condition that the separation of the two molecules is sufficiently large (*i.e.* greater than the molecular dimensions), the electrostatic potential of a molecule can then be expanded about an arbitrary origin which is chosen to be close to the charges. This gives rise to a series of moments of charge which are measurable, and which can then be invoked to characterize the molecule.

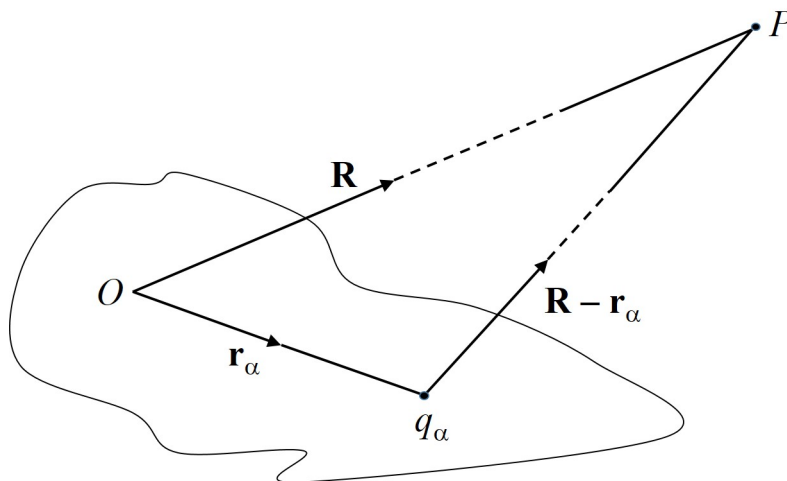


Figure 2.1: The coordinates and notation used in the generation of the multipole expansion of a discrete charge distribution.

Consider N discrete charges q_α ($\alpha = 1, 2, \dots, N$) which are distributed within a vacuum. Let the charges have displacement vectors \mathbf{r}_α from an arbitrary origin O which is chosen to be either within, or close to, the distribution as indicated in

Figure 2.1. The electrostatic potential ϕ which arises at any arbitrary point P with displacement vector \mathbf{R} from O is given by

$$\phi(\mathbf{R}) = \frac{1}{4\pi\epsilon_0} \sum_{\alpha=1}^N \frac{q_\alpha}{|\mathbf{R} - \mathbf{r}_\alpha|} . \quad (2.1)$$

Provided that the distance to P is much greater than the dimensions of the charge distribution (*i.e.* $R > r_\alpha$), then the binomial theorem can be used to expand the denominator of this summation, yielding

$$\phi(\mathbf{R}) = \frac{1}{4\pi\epsilon_0} \left[\frac{1}{R} \sum_{\alpha} q_\alpha + \frac{R_\alpha}{R^3} \sum_{\alpha} q_\alpha r_{\alpha i} + \frac{3R_i R_j - R^2 \delta_{ij}}{2R^5} \sum_{\alpha} q_\alpha r_{\alpha i} r_{\alpha j} + \cdots \right] . \quad (2.2)$$

Here, the Roman subscripts i, j, \dots , denote tensor components, which can be equal to the Cartesian components 1, 2 or 3 of molecule-fixed axes $O(1, 2, 3)$. The Einstein summation convention is invoked, whereby a repeated Roman subscript denotes a summation over all three Cartesian components. δ_{ij} is the Kronecker delta tensor, with $\delta_{ij} = 1$ if $i = j$, $\delta_{ij} = 0$ if $i \neq j$. The electric moments of the distribution are:

the total charge

$$q = \sum_{\alpha} q_\alpha , \quad (2.3)$$

the electric dipole moment

$$\mu_i = \sum_{\alpha} q_\alpha r_{\alpha i} , \quad (2.4)$$

and the primitive (or traced) electric quadrupole moment

$$Q_{ij} = \sum_{\alpha} q_\alpha r_{\alpha i} r_{\alpha j} . \quad (2.5)$$

The higher-order moments (i.e. octopole, hexadecapole, \dots) will not be considered in this work, since they make successively smaller contributions to the electrostatic potential, and we will be considering non-dipolar molecules which possess a permanent electric quadrupole moment as the leading moment. The electric quadrupole moment defined in equation (2.5) is the primitive (or traced) quadrupole moment. An alternative definition known as the traceless quadrupole moment is useful since it describes the departure from spherical symmetry of the charge distribution: [84]

$$\Theta_{ij} = \frac{1}{2} (3Q_{ij} - Q_{kk}\delta_{ij}) = \frac{1}{2} \sum_{\alpha} q_{\alpha} (3r_{\alpha i}r_{\alpha j} - r_{\alpha}^2\delta_{ij}) . \quad (2.6)$$

Here $\Theta_{ii} = 0$, hence the name “traceless”.

The electrostatic potential of the charge distribution can be written in terms of these moments of charge, becoming

$$\phi(\mathbf{R}) = \frac{1}{R} q + \frac{R_i}{R^3} \mu_i + \frac{3R_iR_j - R^2\delta_{ij}}{3R^5} \Theta_{ij} + \dots . \quad (2.7)$$

In this expression, the terms for successively higher multipole moments make contributions which grow successively smaller by a factor of the order $\frac{1}{R}$. A consequence of this is that the leading non-zero moment will provide a reasonable description of the electrostatic potential ϕ at point P as long as the distance R is sufficiently large. Since the contribution to the expanded property arising from each of the multipole moments depends only on the displacement \mathbf{R} of point P from O , the multipole moments are considered to be located at the origin O .

If an electrostatic field \mathbf{E} is applied to the charge distribution, the distribution will

experience a net force \mathbf{F} given by

$$F_i = \sum_{\alpha} q_{\alpha} E_{\alpha i} = q(E_i)_0 + \mu_j (\nabla_j E_i)_0 + \frac{1}{3} \Theta_{jk} (\nabla_k \nabla_j E_i)_0 + \dots \quad (2.8)$$

Here, the field and its derivatives are determined at the origin O about which the Taylor expansion of the field has been taken. From equation (2.8), it can be shown that a dipolar charge distribution will experience a torque in a region of uniform field, or that a quadrupolar charge distribution will experience a torque in a region of uniform field gradient. Equation (2.8) can be used to determine the potential energy U of the charge distribution in the presence of an applied electrostatic field \mathbf{E} [86, 87]

$$U = - \int_{r_1(\mathbf{E}=0)}^{r_2(\mathbf{E}=\mathbf{E})} F_i dr_i = q\phi - \int_0^{\mathbf{E}} \mu_i dE_i - \frac{1}{3} \int_0^{\mathbf{E}} \Theta_{ij} d(\nabla_j E_i) - \dots \quad (2.9)$$

For a rigid charge distribution, only the permanent multipole moments will contribute to equation (2.9), giving

$$U = q\phi - \mu_i^{(0)} E_i - \frac{1}{3} \Theta_{ij}^{(0)} \nabla_j E_i - \dots \quad (2.10)$$

Here, the permanent multipole moments are identified by a superscript (0) .

For an axially symmetric charge distribution, each multipole moment is determined by a single scalar quantity, namely q , μ , Θ , \dots ; for example, the quadrupole moment Θ_{ij} has principal components $\Theta_{33} = \Theta$, $\Theta_{11} = \Theta_{22} = -\frac{1}{2}\Theta$.

The effect of a change of origin on a quadrupole moment can be established by moving O by \mathbf{r}' to O' . The quadrupole moment Θ' relative to the new origin O' is

$$\Theta'_{ij} = \frac{1}{2} \sum_{\alpha} q_{\alpha} (3r'_{\alpha i} r'_{\alpha j} - (r'_{\alpha})^2 \delta_{ij}) \quad (2.11)$$

which becomes

$$\Theta'_{ij} = \Theta_{ij} - \frac{3}{2}\mu_i r'_j - \frac{3}{2}\mu_j r'_i + \mu_k r'_k \delta_{ij} + \frac{1}{2}q \{3r'_i r'_j - (r')^2 \delta_{ij}\} . \quad (2.12)$$

The quadrupole moment is seen to be independent of the choice of origin provided both q and μ_i are zero. More generally, it is possible to show that only the leading non-zero electric multipole moment is independent of the choice of origin. For a dipolar molecule, the quadrupole moment *will* depend on the location of the origin. In this work, we will only consider non-dipolar molecules.

2.3 The microscopic field-induced multipole moments

The permanent multipole moments describing the static molecular charge distribution in the preceding section are identified by a superscript ⁽⁰⁾, so that a molecule's permanent electric dipole and quadrupole moments are denoted by $\mu_i^{(0)}$ and $\Theta_{ij}^{(0)}$ respectively. When the molecule is in weak interaction with fixed external charges, such that the applied static electric field and field gradient at the origin (at which the point multipoles are located) are E_i and E_{ij} respectively, the charges in the molecular distribution will be displaced from their field-free positions to new equilibrium positions. The corresponding total dipole and quadrupole moments of the molecule can be described by Taylor-series expansions in the field and field gradient, giving [83]

$$\begin{aligned} \mu_i = \mu_i^{(0)} + \alpha_{ij}E_j + \frac{1}{2!}\beta_{ijk}E_jE_k + \frac{1}{3!}\gamma_{ijkl}E_jE_kE_l \\ + \frac{1}{3}A_{ijk}E_{jk} + \frac{1}{3}B_{ijkl}E_jE_{kl} + \dots, \end{aligned} \quad (2.13)$$

and

$$\Theta_{ij} = \Theta_{ij}^{(0)} + \mathcal{A}_{ijk}E_k + \frac{1}{2!}D_{ijkl}E_kE_l + C_{ijkl}E_{kl} + \dots. \quad (2.14)$$

The induced electric-dipole moment is thus

$$\begin{aligned} \mu_i - \mu_i^{(0)} = \alpha_{ij}E_j + \frac{1}{2}\beta_{ijk}E_jE_k + \frac{1}{6}\gamma_{ijkl}E_jE_kE_l \\ + \frac{1}{3}A_{ijk}E_{jk} + \frac{1}{3}B_{ijkl}E_jE_{kl} + \dots, \end{aligned} \quad (2.15)$$

while the induced electric quadrupole moment is

$$\Theta_{ij} - \Theta_{ij}^{(0)} = \mathcal{A}_{ijk}E_k + \frac{1}{2}D_{ijkl}E_kE_l + C_{ijkl}E_{kl} + \dots \quad (2.16)$$

In these expressions, terms which depend linearly on field strengths are termed polarizabilities, while those which have a nonlinear dependence on field strengths are called hyperpolarizabilities, a term coined by Coulson, Maccoll and Sutton [88]. α_{ij} is known as the static (dipole) polarizability, while β_{ijk} and γ_{ijkl} are the first and second (dipole) hyperpolarizabilities. A_{ijk} , \mathcal{A}_{ijk} and C_{ijkl} are field-gradient polarizabilities, while B_{ijkl} and D_{ijkl} are field-gradient hyperpolarizabilities. All of these (hyper)polarizabilities are independent of the applied fields so that they are properties of the unperturbed charge distribution.

Equations (2.13) and (2.14) are obtained on purely phenomenological grounds. These equations can be derived using quantum-mechanical time-independent perturbation theory, which yields explicit expressions for the (hyper)polarizability tensors [89, 90]. The quantum-mechanical expressions for the (hyper)polarizabilities reveal any relationships which might exist between the tensors, as well as any intrinsic symmetry which might exist between the tensor subscripts of a particular tensor. For example, in equations (2.13) and (2.14), the tensors A_{ijk} and \mathcal{A}_{ijk} are related by $\mathcal{A}_{ijk} = A_{kij}$, while the tensors B_{ijkl} and D_{ijkl} are related by $D_{ijkl} = B_{klij}$. Hence Eq (2.14) can be written

$$\Theta_{ij} = \Theta_{ij}^{(0)} + A_{kij}E_k + \frac{1}{2!}B_{klij}E_kE_l + C_{ijkl}E_{kl} + \dots \quad (2.17)$$

α_{ij} , β_{ijk} and γ_{ijkl} are symmetric in all suffixes, while A_{ijk} is symmetric in jk , B_{ijkl} is symmetric in ij and kl , and C_{ijkl} is symmetric in ij and kl and in the pairs $(ij), (kl)$.

Consider a perturbing electric field which is comprised of a static component and

one or more dynamic components given by [91]

$$E_i(t) = \frac{1}{2} \sum_{\omega \geq 0} \left[E_i^\omega e^{-i\omega t} + E_i^{-\omega} e^{i\omega t} \right] \quad (2.18)$$

where, since the applied field is real, $[E_i^\omega]^* = E_i^{-\omega}$. This can be written in the more succinct form

$$E_i(t) = \frac{1}{2} \sum_{\omega} E_i^\omega e^{-i\omega t} \quad (2.19)$$

where the summation now includes both positive and negative frequencies. Similarly, a perturbing electric field gradient comprised of a static component and one or more dynamic components will be

$$E_{ij}(t) = \frac{1}{2} \sum_{\omega \geq 0} \left[E_{ij}^\omega e^{-i\omega t} + E_{ij}^{-\omega} e^{i\omega t} \right] \quad (2.20)$$

where $[E_{ij}^\omega]^* = E_{ij}^{-\omega}$. This, in turn, can be written more succinctly as

$$E_{ij}(t) = \frac{1}{2} \sum_{\omega} E_{ij}^\omega e^{-i\omega t} , \quad (2.21)$$

this summation now including both positive and negative frequencies. The corresponding total dipole and quadrupole moments of the molecule can be described by

Taylor-series expansions in the dynamic field and field gradient, giving

$$\begin{aligned}
 \mu_i(t) = & \mu_i^{(0)} + \sum_{\omega_1} \alpha_{ij}(-(\omega_\sigma = \omega_1); \omega_1) \frac{1}{2} E_j^{\omega_1} e^{-i\omega_\sigma t} \\
 & + \frac{1}{2} \sum_{\omega_1, \omega_2} \beta_{ijk}(-(\omega_\sigma = \omega_1 + \omega_2); \omega_1, \omega_2) \frac{1}{2} E_j^{\omega_1} \frac{1}{2} E_k^{\omega_2} e^{-i\omega_\sigma t} \\
 & + \frac{1}{6} \sum_{\omega_1, \omega_2, \omega_3} \gamma_{ijkl}(-(\omega_\sigma = \omega_1 + \omega_2 + \omega_3); \omega_1, \omega_2, \omega_3) \frac{1}{2} E_j^{\omega_1} \frac{1}{2} E_k^{\omega_2} \frac{1}{2} E_l^{\omega_3} e^{-i\omega_\sigma t} \\
 & + \frac{1}{3} \sum_{\omega_1} A_{ijk}(-(\omega_\sigma = \omega_1); \omega_1) \frac{1}{2} E_{jk}^{\omega_\sigma} e^{-i\omega_\sigma t} \\
 & + \frac{1}{6} \sum_{\omega_1, \omega_2} B_{ijkl}(-(\omega_\sigma = \omega_1 + \omega_2); \omega_1, \omega_2) \frac{1}{2} E_j^{\omega_1} \frac{1}{2} E_{kl}^{\omega_2} e^{-i\omega_\sigma t} \\
 & + \frac{1}{6} \sum_{\omega_1, \omega_2} \mathcal{B}_{ijkl}(-(\omega_\sigma = \omega_1 + \omega_2); \omega_1, \omega_2) \frac{1}{2} E_{jk}^{\omega_1} \frac{1}{2} E_l^{\omega_2} e^{-i\omega_\sigma t} + \dots
 \end{aligned} \tag{2.22}$$

and

$$\begin{aligned}
 \Theta_{ij}(t) = & \Theta_{ij}^{(0)} + \sum_{\omega_1} \mathcal{A}_{ijk}(-(\omega_\sigma = \omega_1); \omega_1) \frac{1}{2} E_k^{\omega_1} e^{-i\omega_\sigma t} \\
 & + \frac{1}{2} \sum_{\omega_1, \omega_2} D_{ijkl}(-(\omega_\sigma = \omega_1 + \omega_2); \omega_1, \omega_2) \frac{1}{2} E_k^{\omega_1} \frac{1}{2} E_l^{\omega_2} e^{-i\omega_\sigma t} \\
 & + \sum_{\omega_1} C_{ijkl}(-(\omega_\sigma = \omega_1); \omega_1) \frac{1}{2} E_{kl}^{\omega_1} e^{-i\omega_\sigma t} + \dots
 \end{aligned} \tag{2.23}$$

The summations over frequency $\sum_{\omega_1, \dots, \omega_n}$ ensure summation over all distinct sets of $\omega_1, \dots, \omega_n$, since the spectrum of monochromatic waves in the incident light beam in equations (2.18) to (2.21) could, in principle, contain several distinct sets of frequencies $\omega_1, \dots, \omega_n$ which satisfy $\omega_\sigma = \omega_1 + \omega_2 + \dots + \omega_n$. In practice, experimentalists usually ensure that there is only one set of frequencies $\omega_1, \dots, \omega_n$, and so from now on the summations $\sum_{\omega_1, \dots, \omega_n}$ will be omitted, although

they remain implied. Since a factor of $\frac{1}{2}$ was included in the definition of the applied dynamic electric field and field gradient in equations (2.18) to (2.21), a factor of $\frac{1}{2}$ appears with each occurrence of $E_i^{\omega_q}$ and $E_{ij}^{\omega_q}$ occurring in equations (2.22) and (2.23) (provided that the frequency $\omega_q \neq 0$). This is not a universal convention (though it is probably the most frequently utilized), with some researchers choosing an alternative convention where the factor of $\frac{1}{2}$ is omitted [92]. Keeping track of the various numerical factors is tedious, and can become the source of errors, which is why it was suggested to combine these into a single numerical factor $K(-\omega_\sigma; \omega_1, \dots, \omega_n)$ [93, 94], which for terms depending on powers of the electric field is formally defined as [91]

$$K(-\omega_\sigma; \omega_1, \dots, \omega_n) = 2^{l+m-n} p \quad (2.24)$$

where p is the number of distinct permutations of $\omega_1, \dots, \omega_n$, while n is the order of nonlinearity (e.g. $\beta_{i,j,k}(-\omega_\sigma; \omega_1, \omega_2)$ in equation (2.22) is quadratic in the field, so that it is of second-order nonlinearity). m is the number of frequencies in the set $\omega_1, \dots, \omega_n$ which are zero (i.e. for static dc fields), and $l = 1$ if $\omega_\sigma \neq 0$, otherwise $l = 0$. Table (2.1) provides values of K for several typical nonlinear optical processes. Equation (2.22) becomes

$$\begin{aligned} \mu_i(t) = & \mu_i^{(0)} + \alpha_{ij}(-\omega_\sigma; \omega_1) E_j^{\omega_1} e^{-i\omega_\sigma t} \\ & + \frac{1}{2} K(-\omega_\sigma; \omega_1, \omega_2) \beta_{ijk}(-\omega_\sigma; \omega_1, \omega_2) E_j^{\omega_1} E_k^{\omega_2} e^{-i\omega_\sigma t} \\ & + \frac{1}{6} K(-\omega_\sigma; \omega_1, \omega_2, \omega_3) \gamma_{ijkl}(-\omega_\sigma; \omega_1, \omega_2, \omega_3) E_j^{\omega_1} E_k^{\omega_2} E_l^{\omega_3} e^{-i\omega_\sigma t} + \dots \end{aligned} \quad (2.25)$$

Table 2.1: Typical linear and nonlinear optical processes.

Process	Property	K
First-order linear optical processes		
Static polarizability	$\alpha(0; 0)$	1
Linear absorption/emission and refractive index	$\alpha(-\omega; \omega)$	1
Second-order nonlinear optical (NLO) processes		
Static first hyperpolarizability	$\beta(0; 0, 0)$	1
Optical rectification (OR)	$\beta(0; \omega, -\omega)$	$\frac{1}{2}$
dc-Pockels effect (dc-P) ^a	$\beta(-\omega; \omega, 0)$	2
Second harmonic generation (SHG)	$\beta(-2\omega; \omega, \omega)$	$\frac{1}{2}$
Three-wave mixing ^b	$\beta(-(\omega_3 = \omega_1 \pm \omega_2); \omega_1, \pm\omega_2)$	1
Third-order NLO processes		
Static second hyperpolarizability	$\gamma(0; 0, 0, 0)$	1
dc-Optical rectification (dc-OR) ^c	$\gamma(0; \omega, -\omega, 0)$	$\frac{3}{2}$
dc-Kerr effect (dc-K) ^d	$\gamma(-\omega; \omega, 0, 0)$	3
ac-Kerr effect (ac-K) ^e	$\gamma(-\omega_1; \omega_1, \omega_2, -\omega_2)$	$\frac{3}{2}$
Intensity-dependent refractive index (IDRI) ^f	$\gamma(-\omega; \omega, -\omega, \omega)$	$\frac{3}{4}$
dc-Second harmonic generation (dc-SHG) ^g	$\gamma(-2\omega; \omega, \omega, 0)$	$\frac{3}{2}$
Third harmonic generation (THG)	$\gamma(-3\omega; \omega, \omega, \omega)$	$\frac{1}{4}$
Four-wave mixing (FWM) ^h	$\gamma(-(\omega_4 = \omega_1 + \omega_2 + \omega_3); \omega_1, \omega_2, \omega_3)$	$\frac{3}{2}$

^aor Electro-optical Pockels effect (EOPE)

^bor Sum and difference frequency generation (SFG, DFG)

^cor Electric-field-induced optical rectification (EFIOR)

^dor Electro-optical Kerr effect (EOKE)

^eor Optical Kerr effect (OKE)

^for Degenerate four-wave mixing(DFWM)

^gor Electric-field-induced second harmonic generation (EFISH or ESHG)

^hthis is but one example of FWM, where three photons of different frequency are annihilated, and a fourth photon is created having a frequency that is the sum of the three input photon frequencies (an example of SFG). In general, FWM can occur when interactions between two or three optical frequencies produce two or one new frequencies.

It is important to note that experimentally measured (hyper)polarizabilities contain both electronic and vibrational contributions [95]. In this project, the electronic contributions to the hyperpolarizabilities are calculated *ab initio*, since these are generally the dominant contributions to optical-frequency hyperpolarizabilities. Both zero-point vibrational averages and pure vibrational contributions can, however, sometimes be sizeable, especially for static properties. Wherever vibrational contributions have been determined in the literature, these are included in the discussion of the results presented for each molecule in Chapter 5.

Although equations (2.22) and (2.23) have been obtained phenomenologically, they can also be formally derived using quantum-mechanical perturbation theory, which provides explicit sum-over-states expressions for the electronic contribution to the static and optical-frequency polarizability tensors [83, 86]. These expressions allow for any intrinsic symmetry of the tensor subscripts to be ascertained, and for any relationships between the various tensors to be deduced. In this vein, Orr and Ward utilized perturbation theory to obtain general quantum-mechanical sum-over-states expressions for the optical-frequency molecular hyperpolarizabilities [94], which yields for the second hyperpolarizability $\gamma_{ijkl}(-\omega_\sigma; \omega_1, \omega_2, \omega_3)$ (where ω_1 , ω_2 and ω_3 are the frequencies of the distinct monochromatic waves in the incident beam of light, and $\omega_\sigma = \omega_1 + \omega_2 + \omega_3$ is the sum of these frequencies) the expression [89, 94]

$$\begin{aligned} \gamma_{ijkl}(-\omega_\sigma; \omega_1, \omega_2, \omega_3) = & \frac{1}{\hbar^3} \sum_P \left[\sum_{m,n,p(\neq g)} \frac{\langle g|\mu_i|m\rangle \langle m|\bar{\mu}_l|n\rangle \langle n|\bar{\mu}_k|p\rangle \langle p|\mu_j|g\rangle}{(\omega_{mg} - \omega_\sigma)(\omega_{ng} - \omega_1 - \omega_2)(\omega_{pg} - \omega_1)} \right. \\ & \left. - \sum_{m,n(\neq g)} \frac{\langle g|\mu_i|m\rangle \langle m|\mu_l|g\rangle \langle g|\mu_k|n\rangle \langle n|\mu_j|g\rangle}{(\omega_{mg} - \omega_\sigma)(\omega_{ng} - \omega_1)(\omega_{ng} + \omega_2)} \right]. \end{aligned} \quad (2.26)$$

Here, $|g\rangle$ and $|m\rangle$ are ground-state and excited-state electronic wavefunctions respectively and $\hbar\omega_{mg}$ is the energy difference between them, while \sum_P is the sum

over all permutations of the frequency/operator pairs $(-\omega_\sigma/\mu_i)$, (ω_1/μ_j) , (ω_2/μ_k) , (ω_3/μ_l) . $\mu_i = \sum_\alpha q_\alpha r_{\alpha i}$ is the electric dipole moment operator with q_α the α^{th} element of charge at point \mathbf{r}_α in the discrete molecular charge distribution measured relative to an origin O which is fixed at a point within the molecule (generally at the centre-of-mass). For a multipole operator Ω , the barred notation $\langle m|\bar{\Omega}|n\rangle$ is shorthand for $\langle m|\Omega|n\rangle - \langle g|\Omega|g\rangle\delta_{mn}$ [94], where δ_{mn} is the Kronecker delta ($\delta_{mn} = 1$ if $m = n$, $\delta_{mn} = 0$ if $m \neq n$).

Bishop has followed the formalism of Orr and Ward to obtain the general perturbation-theory expression for the optical-frequency dipole-dipole-quadrupole hyperpolarizability $B_{ijkl}(-\omega_\sigma; \omega_1, \omega_2)$ [95, 96]:

$$B_{ijkl}(-\omega_\sigma; \omega_1, \omega_2) = \frac{1}{\hbar^2} \sum_P \sum_{m(\neq g)} \sum_{n(\neq g)} \frac{\langle g|\mu_i|m\rangle \langle m|\bar{\mu}_j|n\rangle \langle n|\Theta_{kl}|g\rangle}{(\omega_{mg} - \omega_\sigma)(\omega_{ng} - \omega_2)}, \quad (2.27)$$

where $\Theta_{ij} = \Theta_{ji} = \frac{1}{2} \sum_\alpha q_\alpha (3r_{\alpha i}r_{\alpha j} - r_\alpha^2 \delta_{ij})$ is the traceless quadrupole-moment operator, $\omega_\sigma = \omega_1 + \omega_2$, and where \sum_P is the sum over the permutations of the pairs $(-\omega_\sigma/\mu_i)$, (ω_1/μ_j) , (ω_2/Θ_{kl}) . Using this same formalism, the expression for the dipole-quadrupole-dipole hyperpolarizability is obtained:

$$\mathcal{B}_{ijkl}(-\omega_\sigma; \omega_1, \omega_2) = \frac{1}{\hbar^2} \sum_P \sum_{m(\neq g)} \sum_{n(\neq g)} \frac{\langle g|\mu_i|m\rangle \langle m|\bar{\Theta}_{jk}|n\rangle \langle n|\mu_l|g\rangle}{(\omega_{mg} - \omega_\sigma)(\omega_{ng} - \omega_2)} \quad (2.28)$$

where \sum_P is the sum over the permutations of the pairs $(-\omega_\sigma/\mu_i)$, (ω_1/Θ_{jk}) , (ω_2/μ_l) , and for the quadrupole-dipole-dipole hyperpolarizability the expression

$$D_{ijkl}(-\omega_\sigma; \omega_1, \omega_2) = \frac{1}{\hbar^2} \sum_P \sum_{m(\neq g)} \sum_{n(\neq g)} \frac{\langle g|\Theta_{ij}|m\rangle \langle m|\bar{\mu}_k|n\rangle \langle n|\mu_l|g\rangle}{(\omega_{mg} - \omega_\sigma)(\omega_{ng} - \omega_2)} \quad (2.29)$$

where \sum_P is the sum over the permutations of the pairs $(-\omega_\sigma/\Theta_{ij})$, (ω_1/μ_k) , (ω_2/μ_l) . The response-function formalism provides a more compact notation for

equations (2.26) to (2.29), giving [97–99]

$$\gamma_{ijkl}(-\omega_\sigma; \omega_1, \omega_2, \omega_3) = -\langle\langle \mu_i; \mu_j, \mu_k, \mu_l \rangle\rangle_{\omega_1, \omega_2, \omega_3}, \quad (2.30)$$

$$B_{ijkl}(-\omega_\sigma; \omega_1, \omega_2) = \langle\langle \mu_i; \mu_j, \Theta_{kl} \rangle\rangle_{\omega_1, \omega_2}, \quad (2.31)$$

$$\mathcal{B}_{ijkl}(-\omega_\sigma; \omega_1, \omega_2) = \langle\langle \mu_i; \Theta_{jk}, \mu_l \rangle\rangle_{\omega_1, \omega_2}, \quad (2.32)$$

and

$$D_{ijkl}(-\omega_\sigma; \omega_1, \omega_2) = \langle\langle \Theta_{ij}; \mu_k, \mu_l \rangle\rangle_{\omega_1, \omega_2}. \quad (2.33)$$

A common experimental configuration is the application of a static field with amplitude $E_i^{\omega=0} = E_i^0$ together with a single, monochromatic laser beam having a field with frequency ω and amplitude E_i^ω . Equation (2.19) yields

$$E_i(t) = E_i^0 + E_i^\omega \cos(\omega t). \quad (2.34)$$

The notation can be compressed by writing the static field as $E_i^0 \equiv E_i$ and the dynamic field amplitude as $E_i^\omega \equiv \mathcal{E}_i$, so that

$$E_i(t) = E_i + \mathcal{E}_i \cos(\omega t). \quad (2.35)$$

If there is also a static applied electric field gradient of amplitude $E_{ij}^{\omega=0} = E_{ij}^0$, combined with the field gradient of the light wave, which has amplitude E_{ij}^ω , then

equation (2.20) becomes

$$E_{ij}(t) = E_{ij}^0 + E_{ij}^\omega \cos(\omega t). \quad (2.36)$$

This notation is similarly compressed by writing the static field gradient as $E_{ij}^0 \equiv E_{ij}$ and the dynamic field-gradient amplitude as $E_{ij}^\omega \equiv \mathcal{E}_{ij}$ so that

$$E_{ij}(t) = E_{ij} + \mathcal{E}_{ij} \cos(\omega t). \quad (2.37)$$

Substituting equations (2.35) and (2.37) into equation (2.22), the electric dipole moment of a molecule becomes

$$\begin{aligned} \mu_i(t) = & \mu_i^{(0)} + \alpha_{ij}(-\omega_\sigma; \omega_1) \left(E_j + \mathcal{E}_j \cos(\omega t) \right) \\ & + \frac{1}{2} \beta_{ijk}(-\omega_\sigma; \omega_1, \omega_2) \left(E_j + \mathcal{E}_j \cos(\omega t) \right) \left(E_k + \mathcal{E}_k \cos(\omega t) \right) \\ & + \frac{1}{6} \gamma_{ijkl}(-\omega_\sigma; \omega_1, \omega_2, \omega_3) \left(E_j + \mathcal{E}_j \cos(\omega t) \right) \left(E_k + \mathcal{E}_k \cos(\omega t) \right) \left(E_l + \mathcal{E}_l \cos(\omega t) \right) \\ & + \frac{1}{3} A_{ijk}(-\omega_\sigma; \omega_1) \left(E_{jk} + \mathcal{E}_{jk} \cos(\omega t) \right) \\ & + \frac{1}{6} B_{ijkl}(-\omega_\sigma; \omega_1, \omega_2) \left(E_j + \mathcal{E}_j \cos(\omega t) \right) \left(E_{kl} + \mathcal{E}_{kl} \cos(\omega t) \right) \\ & + \frac{1}{6} \mathcal{B}_{ijkl}(-\omega_\sigma; \omega_1, \omega_2) \left(E_{jk} + \mathcal{E}_{jk} \cos(\omega t) \right) \left(E_l + \mathcal{E}_l \cos(\omega t) \right) + \dots \end{aligned} \quad (2.38)$$

Here the frequency arguments of the (hyper)polarizabilities have not yet been made explicit in terms of the frequency ω of the laser beam light, since terms in $\cos^2(\omega t)$ will be seen to have both a dc component and a component oscillating at frequency 2ω , while terms in $\cos^3(\omega t)$ will have components oscillating at the frequencies ω

and 3ω . Equation (2.38) yields

$$\begin{aligned}
\mu_i(t) = & \mu_i^{(0)} + \alpha_{ij}(-\omega_\sigma; \omega_1) E_j + \alpha_{ij}(-\omega_\sigma; \omega_1) \mathcal{E}_j \cos(\omega t) \\
& + \frac{1}{2} \beta_{ijk}(-\omega_\sigma; \omega_1, \omega_2) E_j E_k \\
& + \frac{1}{2} \left[\beta_{ijk}(-\omega_\sigma; \omega_1, \omega_2) E_j \mathcal{E}_k + \beta_{ijk}(-\omega_\sigma; \omega_1, \omega_2) \mathcal{E}_j E_k \right] \cos(\omega t) \\
& + \frac{1}{2} \beta_{ijk}(-\omega_\sigma; \omega_1, \omega_2) \mathcal{E}_j \mathcal{E}_k \cos^2(\omega t) \\
& + \frac{1}{6} \gamma_{ijkl}(-\omega_\sigma; \omega_1, \omega_2, \omega_3) E_j E_k E_l \\
& + \frac{1}{6} \left[\gamma_{ijkl}(-\omega_\sigma; \omega_1, \omega_2, \omega_3) E_j E_k \mathcal{E}_l + \gamma_{ijkl}(-\omega_\sigma; \omega_1, \omega_2, \omega_3) E_j \mathcal{E}_k E_l \right. \\
& \quad \left. + \gamma_{ijkl}(-\omega_\sigma; \omega_1, \omega_2, \omega_3) \mathcal{E}_j E_k E_l \right] \cos(\omega t) \\
& + \frac{1}{6} \left[\gamma_{ijkl}(-\omega_\sigma; \omega_1, \omega_2, \omega_3) E_j \mathcal{E}_k \mathcal{E}_l + \gamma_{ijkl}(-\omega_\sigma; \omega_1, \omega_2, \omega_3) \mathcal{E}_j E_k \mathcal{E}_l \right. \\
& \quad \left. + \gamma_{ijkl}(-\omega_\sigma; \omega_1, \omega_2, \omega_3) \mathcal{E}_j \mathcal{E}_k E_l \right] \cos^2(\omega t) \\
& + \frac{1}{6} \gamma_{ijkl}(-\omega_\sigma; \omega_1, \omega_2, \omega_3) \mathcal{E}_j \mathcal{E}_k \mathcal{E}_l \cos^3(\omega t) \\
& + \frac{1}{3} A_{ijk}(-\omega_\sigma; \omega_1) E_{jk} + \frac{1}{3} A_{ijk}(-\omega_\sigma; \omega_1) \mathcal{E}_{jk} \cos(\omega t) \\
& + \frac{1}{6} B_{ijkl}(-\omega_\sigma; \omega_1, \omega_2) E_j E_{kl} \\
& + \frac{1}{6} B_{ijkl}(-\omega_\sigma; \omega_1, \omega_2) E_j \mathcal{E}_{kl} \cos(\omega t) + \frac{1}{6} B_{ijkl}(-\omega_\sigma; \omega_1, \omega_2) \mathcal{E}_j E_{kl} \cos(\omega t) \\
& + \frac{1}{6} B_{ijkl}(-\omega_\sigma; \omega_1, \omega_2) \mathcal{E}_j \mathcal{E}_{kl} \cos^2(\omega t) \\
& + \frac{1}{6} \mathcal{B}_{ijkl}(-\omega_\sigma; \omega_1, \omega_2) E_{jk} E_l \\
& + \frac{1}{6} \mathcal{B}_{ijkl}(-\omega_\sigma; \omega_1, \omega_2) E_{jk} \mathcal{E}_l \cos(\omega t) + \frac{1}{6} \mathcal{B}_{ijkl}(-\omega_\sigma; \omega_1, \omega_2) \mathcal{E}_{jk} E_l \cos(\omega t) \\
& + \frac{1}{6} \mathcal{B}_{ijkl}(-\omega_\sigma; \omega_1, \omega_2) \mathcal{E}_{jk} \mathcal{E}_l \cos^2(\omega t) + \dots
\end{aligned} \tag{2.39}$$

The trigonometric identity

$$\cos \phi \cos \theta = \frac{1}{2} [\cos(\phi + \theta) + \cos(\phi - \theta)] \quad (2.40)$$

gives

$$\cos^2(\omega t) = \frac{1}{2} + \frac{1}{2} \cos(2\omega t) \quad (2.41)$$

and

$$\cos^3(\omega t) = \frac{3}{4} \cos(\omega t) + \frac{1}{4} \cos(3\omega t) , \quad (2.42)$$

so that equation (2.39) simplifies to

$$\begin{aligned}
\mu_i(t) = & \mu_i^{(0)} + \alpha_{ij}(-\omega_\sigma; \omega_1) E_j + \alpha_{ij}(-\omega_\sigma; \omega_1) \mathcal{E}_j \cos(\omega t) \\
& + \frac{1}{2} \beta_{ijk}(-\omega_\sigma; \omega_1, \omega_2) E_j E_k \\
& + \frac{1}{2} \left[\beta_{ijk}(-\omega_\sigma; \omega_1, \omega_2) E_j \mathcal{E}_k + \beta_{ijk}(-\omega_\sigma; \omega_1, \omega_2) \mathcal{E}_j E_k \right] \cos(\omega t) \\
& + \frac{1}{2} \beta_{ijk}(-\omega_\sigma; \omega_1, \omega_2) \mathcal{E}_j \mathcal{E}_k \left(\frac{1}{2} + \frac{1}{2} \cos(2\omega t) \right) \\
& + \frac{1}{6} \gamma_{ijkl}(-\omega_\sigma; \omega_1, \omega_2, \omega_3) E_j E_k E_l \\
& + \frac{1}{6} \left[\gamma_{ijkl}(-\omega_\sigma; \omega_1, \omega_2, \omega_3) E_j E_k \mathcal{E}_l + \gamma_{ijkl}(-\omega_\sigma; \omega_1, \omega_2, \omega_3) E_j \mathcal{E}_k E_l \right. \\
& \quad \left. + \gamma_{ijkl}(-\omega_\sigma; \omega_1, \omega_2, \omega_3) \mathcal{E}_j E_k E_l \right] \cos(\omega t) \\
& + \frac{1}{6} \left[\gamma_{ijkl}(-\omega_\sigma; \omega_1, \omega_2, \omega_3) E_j \mathcal{E}_k \mathcal{E}_l + \gamma_{ijkl}(-\omega_\sigma; \omega_1, \omega_2, \omega_3) \mathcal{E}_j E_k \mathcal{E}_l \right. \\
& \quad \left. + \gamma_{ijkl}(-\omega_\sigma; \omega_1, \omega_2, \omega_3) \mathcal{E}_j \mathcal{E}_k E_l \right] \left(\frac{1}{2} + \frac{1}{2} \cos(2\omega t) \right) \\
& + \frac{1}{6} \gamma_{ijkl}(-\omega_\sigma; \omega_1, \omega_2, \omega_3) \mathcal{E}_j \mathcal{E}_k \mathcal{E}_l \left(\frac{3}{4} \cos(\omega t) + \frac{1}{4} \cos(3\omega t) \right) \\
& + \frac{1}{3} A_{ijk}(-\omega_\sigma; \omega_1) E_{jk} + \frac{1}{3} A_{ijk}(-\omega_\sigma; \omega_1) \mathcal{E}_{jk} \cos(\omega t) \\
& + \frac{1}{6} B_{ijkl}(-\omega_\sigma; \omega_1, \omega_2) E_j E_{kl} \\
& + \frac{1}{6} B_{ijkl}(-\omega_\sigma; \omega_1, \omega_2) E_j \mathcal{E}_{kl} \cos(\omega t) + \frac{1}{6} B_{ijkl}(-\omega_\sigma; \omega_1, \omega_2) \mathcal{E}_j E_{kl} \cos(\omega t) \\
& + \frac{1}{6} B_{ijkl}(-\omega_\sigma; \omega_1, \omega_2) \mathcal{E}_j \mathcal{E}_{kl} \left(\frac{1}{2} + \frac{1}{2} \cos(2\omega t) \right) \\
& + \frac{1}{6} \mathcal{B}_{ijkl}(-\omega_\sigma; \omega_1, \omega_2) E_{jk} E_l \\
& + \frac{1}{6} \mathcal{B}_{ijkl}(-\omega_\sigma; \omega_1, \omega_2) E_{jk} \mathcal{E}_l \cos(\omega t) + \frac{1}{6} \mathcal{B}_{ijkl}(-\omega_\sigma; \omega_1, \omega_2) \mathcal{E}_{jk} E_l \cos(\omega t) \\
& + \frac{1}{6} \mathcal{B}_{ijkl}(-\omega_\sigma; \omega_1, \omega_2) \mathcal{E}_{jk} \mathcal{E}_l \left(\frac{1}{2} + \frac{1}{2} \cos(2\omega t) \right) + \dots
\end{aligned}
\tag{2.43}$$

The frequency arguments of the (hyper)polarizabilities can now be made explicit:

$$\begin{aligned}
 \mu_i(t) = & \mu_i^{(0)} + \alpha_{ij}(0; 0)E_j + \alpha_{ij}(-\omega; \omega)\mathcal{E}_j \cos(\omega t) + \frac{1}{2}\beta_{ijk}(0; 0, 0)E_j E_k \\
 & + \frac{1}{2} \left[\beta_{ijk}(-\omega; 0, \omega)E_j \mathcal{E}_k + \beta_{ijk}(-\omega; \omega, 0)\mathcal{E}_j E_k \right] \cos(\omega t) \\
 & + \frac{1}{4}\beta_{ijk}(0; \omega, -\omega)\mathcal{E}_j \mathcal{E}_k + \frac{1}{4}\beta_{ijk}(-2\omega; \omega, \omega)\mathcal{E}_j \mathcal{E}_k \cos(2\omega t) \\
 & + \frac{1}{6}\gamma_{ijkl}(0; 0, 0, 0)E_j E_k E_l \\
 & + \frac{1}{6} \left[\gamma_{ijkl}(-\omega; 0, 0, \omega)E_j E_k \mathcal{E}_l + \gamma_{ijkl}(-\omega; 0, \omega, 0)E_j \mathcal{E}_k E_l \right. \\
 & \quad \left. + \gamma_{ijkl}(-\omega; \omega, 0, 0)\mathcal{E}_j E_k E_l \right] \cos(\omega t) \\
 & + \frac{1}{12} \left[\gamma_{ijkl}(0; 0, \omega, -\omega)E_j \mathcal{E}_k \mathcal{E}_l + \gamma_{ijkl}(0; \omega, 0, -\omega)\mathcal{E}_j E_k \mathcal{E}_l \right. \\
 & \quad \left. + \gamma_{ijkl}(0; \omega, -\omega, 0)\mathcal{E}_j \mathcal{E}_k E_l \right] \\
 & + \frac{1}{12} \left[\gamma_{ijkl}(-2\omega; 0, \omega, \omega)E_j \mathcal{E}_k \mathcal{E}_l + \gamma_{ijkl}(-2\omega; \omega, 0, \omega)\mathcal{E}_j E_k \mathcal{E}_l \right. \\
 & \quad \left. + \gamma_{ijkl}(-2\omega; \omega, \omega, 0)\mathcal{E}_j \mathcal{E}_k E_l \right] \cos(2\omega t) \\
 & + \frac{1}{8}\gamma_{ijkl}(-\omega; \omega, -\omega, \omega)\mathcal{E}_j \mathcal{E}_k \mathcal{E}_l \cos(\omega t) + \frac{1}{24}\gamma_{ijkl}(-3\omega; \omega, \omega, \omega)\mathcal{E}_j \mathcal{E}_k \mathcal{E}_l \cos(3\omega t) \\
 & + \frac{1}{3}A_{ijk}(0; 0)E_{jk} + \frac{1}{3}A_{ijk}(-\omega; \omega)\mathcal{E}_{jk} \cos(\omega t) \\
 & + \frac{1}{6}B_{ijkl}(0; 0, 0)E_j E_{kl} \\
 & + \frac{1}{6}B_{ijkl}(-\omega; 0, \omega)E_j \mathcal{E}_{kl} \cos(\omega t) + \frac{1}{6}B_{ijkl}(-\omega; \omega, 0)\mathcal{E}_j E_{kl} \cos(\omega t) \\
 & + \frac{1}{12}B_{ijkl}(0; \omega, -\omega)\mathcal{E}_j \mathcal{E}_{kl} + \frac{1}{12}B_{ijkl}(-2\omega; \omega, \omega)\mathcal{E}_j \mathcal{E}_{kl} \cos(2\omega t) \\
 & + \frac{1}{6}\mathcal{B}_{ijkl}(0; 0, 0)E_{jk} E_l \\
 & + \frac{1}{6}\mathcal{B}_{ijkl}(-\omega; 0, \omega)E_{jk} \mathcal{E}_l \cos(\omega t) + \frac{1}{6}\mathcal{B}_{ijkl}(-\omega; \omega, 0)\mathcal{E}_{jk} E_l \cos(\omega t) \\
 & + \frac{1}{12}\mathcal{B}_{ijkl}(0; \omega, -\omega)\mathcal{E}_{jk} \mathcal{E}_l + \frac{1}{12}\mathcal{B}_{ijkl}(-2\omega; \omega, \omega)\mathcal{E}_{jk} \mathcal{E}_l \cos(2\omega t) + \dots
 \end{aligned}
 \tag{2.44}$$

The quantum-mechanical expressions for the hyperpolarizabilities given in equations (2.26) to (2.29) allow for any relationships between them to be deduced. The static B - and \mathcal{B} -tensors are related by

$$\mathcal{B}_{ijkl}(0; 0, 0) = B_{iljk}(0; 0, 0) \quad (2.45)$$

so that

$$\mathcal{B}_{ijkl}(0; 0, 0)E_{jk}E_l = B_{iljk}(0; 0, 0)E_{jk}E_l . \quad (2.46)$$

$B_{iljk}(0; 0, 0)E_{jk}E_l$ can be rewritten as $B_{ijkl}(0; 0, 0)E_jE_{kl}$ by relabelling the dummy subscripts. The dynamic first-harmonic dipole-dipole-quadrupole hyperpolarizability tensors $\mathcal{B}_{ijkl}(-\omega; 0, \omega)$ and $B_{iljk}(-\omega; \omega, 0)$ are related by

$$\mathcal{B}_{ijkl}(-\omega; 0, \omega) = B_{iljk}(-\omega; \omega, 0) \quad (2.47)$$

so that

$$\mathcal{B}_{ijkl}(-\omega; 0, \omega)E_{jk}\mathcal{E}_l \cos(\omega t) = B_{iljk}(-\omega; \omega, 0)E_{jk}\mathcal{E}_l \cos(\omega t) , \quad (2.48)$$

where $B_{iljk}(-\omega; \omega, 0)E_{jk}\mathcal{E}_l$ can be written $B_{ijkl}(-\omega; \omega, 0)\mathcal{E}_jE_{kl}$. Similarly, the tensors $B_{ijkl}(-\omega; 0, \omega)$ and $\mathcal{B}_{iklj}(-\omega; \omega, 0)$ are related through

$$B_{ijkl}(-\omega; 0, \omega) = \mathcal{B}_{iklj}(-\omega; \omega, 0) \quad (2.49)$$

so that

$$B_{ijkl}(-\omega; 0, \omega)E_j\mathcal{E}_{kl} \cos(\omega t) = \mathcal{B}_{iklj}(-\omega; \omega, 0)E_j\mathcal{E}_{kl} \cos(\omega t) , \quad (2.50)$$

where $\mathcal{B}_{iklj}(-\omega; \omega, 0)E_j\mathcal{E}_{kl}$ is the same as $\mathcal{B}_{ijkl}(-\omega; \omega, 0)\mathcal{E}_{jk}E_l$. The frequency-

doubled dipole-dipole-quadrupole hyperpolarizabilities, which are of especial relevance to this project, have the relationship

$$\mathcal{B}_{ijkl}(-2\omega; \omega, \omega) = B_{iljk}(-2\omega; \omega, \omega) \quad (2.51)$$

so that

$$\mathcal{B}_{ijkl}(-2\omega; \omega, \omega) \mathcal{E}_j \mathcal{E}_k \mathcal{E}_l = B_{iljk}(-2\omega; \omega, \omega) \mathcal{E}_j \mathcal{E}_k \mathcal{E}_l. \quad (2.52)$$

Relabelling of the dummy subscripts allows $B_{iljk}(-2\omega; \omega, \omega) \mathcal{E}_j \mathcal{E}_k \mathcal{E}_l$ to be rewritten as $B_{ijkl}(-2\omega; \omega, \omega) \mathcal{E}_j \mathcal{E}_k \mathcal{E}_l$.

The molecular dipole moment in equation (2.44) becomes

$$\begin{aligned} \mu_i(t) = & \left[\mu_i^{(0)} + \alpha_{ij}(0; 0) E_j + \frac{1}{2} \beta_{ijk}(0; 0, 0) E_j E_k + \frac{1}{4} \beta_{ijk}(0; \omega, -\omega) \mathcal{E}_j \mathcal{E}_k \right. \\ & + \frac{1}{6} \gamma_{ijkl}(0; 0, 0, 0) E_j E_k E_l + \frac{1}{4} \gamma_{ijkl}(0; \omega, -\omega, 0) \mathcal{E}_j \mathcal{E}_k E_l \\ & \left. + \frac{1}{3} A_{ijk}(0; 0) E_{jk} + \frac{1}{3} B_{ijkl}(0; 0, 0) E_j E_{kl} + \frac{1}{6} B_{ijkl}(0; \omega, -\omega) \mathcal{E}_j \mathcal{E}_{kl} \right] \\ & + \left[\alpha_{ij}(-\omega; \omega) \mathcal{E}_j + \beta_{ijk}(-\omega; \omega, 0) \mathcal{E}_j E_k + \frac{1}{2} \gamma_{ijkl}(-\omega; \omega, 0, 0) \mathcal{E}_j E_k E_l \right. \\ & + \frac{1}{8} \gamma_{ijkl}(-\omega; \omega, -\omega, \omega) \mathcal{E}_j \mathcal{E}_k \mathcal{E}_l + \frac{1}{3} A_{ijk}(-\omega; \omega) \mathcal{E}_{jk} \\ & \left. + \frac{1}{3} B_{ijkl}(-\omega; \omega, 0) \mathcal{E}_j E_{kl} + \frac{1}{3} \mathcal{B}_{ijkl}(-\omega; \omega, 0) \mathcal{E}_j \mathcal{E}_k E_l \right] \cos(\omega t) \\ & + \left[\frac{1}{4} \beta_{ijk}(-2\omega; \omega, \omega) \mathcal{E}_j \mathcal{E}_k + \frac{1}{4} \gamma_{ijkl}(-2\omega; \omega, \omega, 0) \mathcal{E}_j \mathcal{E}_k E_l \right. \\ & \left. + \frac{1}{6} B_{ijkl}(-2\omega; \omega, \omega) \mathcal{E}_j \mathcal{E}_{kl} \right] \cos(2\omega t) \\ & + \left[\frac{1}{24} \gamma_{ijkl}(-3\omega; \omega, \omega, \omega) \mathcal{E}_j \mathcal{E}_k \mathcal{E}_l \right] \cos(3\omega t) + \dots \end{aligned} \quad (2.53)$$

Hence the polarization can be written as

$$\mu_i(t) = \mu_i^0 + \mu_i^\omega \cos(\omega t) + \mu_i^{2\omega} \cos(2\omega t) + \mu_i^{3\omega} \cos(3\omega t) + \dots \quad (2.54)$$

where the Fourier amplitudes are

$$\begin{aligned} \mu_i^0 &= \mu_i^{(0)} + \alpha_{ij}(0; 0)E_j + \frac{1}{2}\beta_{ijk}(0; 0, 0)E_jE_k + \frac{1}{4}\beta_{ijk}(0; \omega, -\omega)\mathcal{E}_j\mathcal{E}_k \\ &+ \frac{1}{6}\gamma_{ijkl}(0; 0, 0, 0)E_jE_kE_l + \frac{1}{4}\gamma_{ijkl}(0; -\omega, \omega, 0)\mathcal{E}_j\mathcal{E}_kE_l \\ &+ \frac{1}{3}A_{ijk}(0; 0)E_{jk} + \frac{1}{3}B_{ijkl}(0; 0, 0)E_jE_{kl} + \frac{1}{6}B_{ijkl}(0; -\omega, \omega)\mathcal{E}_j\mathcal{E}_{kl}, \end{aligned} \quad (2.55)$$

$$\begin{aligned} \mu_i^\omega &= \alpha_{ij}(-\omega; \omega)\mathcal{E}_j + \beta_{ijk}(-\omega; \omega, 0)\mathcal{E}_jE_k + \frac{1}{2}\gamma_{ijkl}(-\omega; \omega, 0, 0)\mathcal{E}_jE_kE_l \\ &+ \frac{1}{8}\gamma_{ijkl}(-\omega; \omega, -\omega, \omega)\mathcal{E}_j\mathcal{E}_k\mathcal{E}_l + \frac{1}{3}A_{ijk}(-\omega; \omega)\mathcal{E}_{jk} \\ &+ \frac{1}{3}B_{ijkl}(-\omega; \omega, 0)\mathcal{E}_jE_{kl} + \frac{1}{3}B_{ijkl}(-\omega; \omega, 0)\mathcal{E}_{jk}E_l, \end{aligned} \quad (2.56)$$

$$\begin{aligned} \mu_i^{2\omega} &= \frac{1}{4}\beta_{ijk}(-2\omega; \omega, \omega)\mathcal{E}_j\mathcal{E}_k + \frac{1}{4}\gamma_{ijkl}(-2\omega; \omega, \omega, 0)\mathcal{E}_j\mathcal{E}_kE_l \\ &+ \frac{1}{6}B_{ijkl}(-2\omega; \omega, \omega)\mathcal{E}_j\mathcal{E}_{kl}, \end{aligned} \quad (2.57)$$

and

$$\mu_i^{3\omega} = \frac{1}{24}\gamma_{ijkl}(-3\omega; \omega, \omega, \omega)\mathcal{E}_j\mathcal{E}_k\mathcal{E}_l. \quad (2.58)$$

A similar treatment of the molecular electric quadrupole moment of equation (2.23)

yields, after substitution of equations (2.35) and (2.37),

$$\begin{aligned}
\Theta_{ij}(t) &= \Theta_{ij}^{(0)} + \mathcal{A}_{ijk}(-\omega_\sigma; \omega_1) \left(E_k + \mathcal{E}_k \cos(\omega t) \right) \\
&\quad + \frac{1}{2} D_{ijkl}(-\omega_\sigma; \omega_1, \omega_2) \left(E_k + \mathcal{E}_k \cos(\omega t) \right) \left(E_l + \mathcal{E}_l \cos(\omega t) \right) \\
&\quad + C_{ijkl}(-\omega_\sigma; \omega_1) \left(E_{kl} + \mathcal{E}_{kl} \cos(\omega t) \right) + \dots .
\end{aligned} \tag{2.59}$$

This expands to

$$\begin{aligned}
\Theta_{ij}(t) &= \Theta_{ij}^{(0)} + \mathcal{A}_{ijk}(-\omega_\sigma; \omega_1) E_k + \mathcal{A}_{ijk}(-\omega_\sigma; \omega_1) \mathcal{E}_k \cos(\omega t) \\
&\quad + \frac{1}{2} D_{ijkl}(-\omega_\sigma; \omega_1, \omega_2) E_k E_l \\
&\quad + \frac{1}{2} D_{ijkl}(-\omega_\sigma; \omega_1, \omega_2) E_k \mathcal{E}_l \cos(\omega t) \\
&\quad + \frac{1}{2} D_{ijkl}(-\omega_\sigma; \omega_1, \omega_2) \mathcal{E}_k E_l \cos(\omega t) \\
&\quad + \frac{1}{2} D_{ijkl}(-\omega_\sigma; \omega_1, \omega_2) \mathcal{E}_k \mathcal{E}_l \cos^2(\omega t) \\
&\quad + C_{ijkl}(-\omega_\sigma; \omega_1) E_{kl} + C_{ijkl}(-\omega_\sigma; \omega_1) \mathcal{E}_{kl} \cos(\omega t) + \dots .
\end{aligned} \tag{2.60}$$

Substitution of the trigonometric identity in equation (2.41) yields

$$\begin{aligned}
\Theta_{ij}(t) &= \Theta_{ij}^{(0)} + \mathcal{A}_{ijk}(-\omega_\sigma; \omega_1) E_k + \mathcal{A}_{ijk}(-\omega_\sigma; \omega_1) \mathcal{E}_k \cos(\omega t) \\
&+ \frac{1}{2} D_{ijkl}(-\omega_\sigma; \omega_1, \omega_2) E_k E_l \\
&+ \frac{1}{2} D_{ijkl}(-\omega_\sigma; \omega_1, \omega_2) E_k \mathcal{E}_l \cos(\omega t) \\
&+ \frac{1}{2} D_{ijkl}(-\omega_\sigma; \omega_1, \omega_2) \mathcal{E}_k E_l \cos(\omega t) \\
&+ \frac{1}{2} D_{ijkl}(-\omega_\sigma; \omega_1, \omega_2) \mathcal{E}_k \mathcal{E}_l \left(\frac{1}{2} + \frac{1}{2} \cos(2\omega t) \right) \\
&+ C_{ijkl}(-\omega_\sigma; \omega_1) E_{kl} + C_{ijkl}(-\omega_\sigma; \omega_1) \mathcal{E}_{kl} \cos(\omega t) + \dots
\end{aligned} \tag{2.61}$$

The frequency arguments of the (hyper)polarizabilities can now be made explicit:

$$\begin{aligned}
\Theta_{ij}(t) &= \Theta_{ij}^{(0)} + \mathcal{A}_{ijk}(0; 0) E_k + \mathcal{A}_{ijk}(-\omega; \omega) \mathcal{E}_k \cos(\omega t) \\
&+ \frac{1}{2} D_{ijkl}(0; 0, 0) E_k E_l \\
&+ \frac{1}{2} D_{ijkl}(-\omega; 0, \omega) E_k \mathcal{E}_l \cos(\omega t) \\
&+ \frac{1}{2} D_{ijkl}(-\omega; \omega, 0) \mathcal{E}_k E_l \cos(\omega t) \\
&+ \frac{1}{4} D_{ijkl}(0; -\omega, \omega) \mathcal{E}_k \mathcal{E}_l \\
&+ \frac{1}{4} D_{ijkl}(-2\omega; \omega, \omega) \mathcal{E}_k \mathcal{E}_l \cos(2\omega t) \\
&+ C_{ijkl}(0; 0) E_{kl} + C_{ijkl}(-\omega; \omega) \mathcal{E}_{kl} \cos(\omega t) + \dots
\end{aligned} \tag{2.62}$$

This yields

$$\begin{aligned}
\Theta_{ij}(t) = & \left[\Theta_{ij}^{(0)} + \mathcal{A}_{ijk}(0;0)E_k + \frac{1}{2}D_{ijkl}(0;0,0)E_kE_l + \frac{1}{4}D_{ijkl}(0;-\omega,\omega)\mathcal{E}_k\mathcal{E}_l \right. \\
& \left. + C_{ijkl}(0;0)E_{kl} \right] \\
& + \left[\mathcal{A}_{ijk}(-\omega;\omega)\mathcal{E}_k + D_{ijkl}(-\omega;\omega,0)\mathcal{E}_kE_l + C_{ijkl}(-\omega;\omega)\mathcal{E}_{kl} \right] \cos(\omega t) \\
& + \left[\frac{1}{4}D_{ijkl}(-2\omega;\omega,\omega)\mathcal{E}_k\mathcal{E}_l \right] \cos(2\omega t) + \dots .
\end{aligned} \tag{2.63}$$

The quantum-mechanical expressions for the hyperpolarizabilities in equations (2.27) to (2.29) yield for the static B - and D -tensors the relationship

$$D_{ijkl}(0;0,0) = B_{klij}(0;0,0) ,$$

while the first-harmonic hyperpolarizabilities have the relationship

$$D_{ijkl}(-\omega;\omega,0) = B_{klij}(-\omega;0,\omega) .$$

The total quadrupole moment becomes

$$\begin{aligned}
\Theta_{ij}(t) = & \left[\Theta_{ij}^{(0)} + \mathcal{A}_{ijk}(0;0)E_k + \frac{1}{2}B_{klij}(0;0,0)E_kE_l + \frac{1}{4}D_{ijkl}(0;-\omega,\omega)\mathcal{E}_k\mathcal{E}_l \right. \\
& \left. + C_{ijkl}(0;0)E_{kl} \right] \\
& + \left[\mathcal{A}_{ijk}(-\omega;\omega)\mathcal{E}_k + B_{klij}(-\omega;0,\omega)\mathcal{E}_kE_l + C_{ijkl}(-\omega;\omega)\mathcal{E}_{kl} \right] \cos(\omega t) \\
& + \left[\frac{1}{4}D_{ijkl}(-2\omega;\omega,\omega)\mathcal{E}_k\mathcal{E}_l \right] \cos(2\omega t) + \dots .
\end{aligned} \tag{2.64}$$

Hence the quadrupole moment can be written as

$$\Theta_{ij}(t) = \Theta_{ij}^0 + \Theta_{ij}^\omega \cos(\omega t) + \Theta_{ij}^{2\omega} \cos(2\omega t) + \dots \quad (2.65)$$

where the Fourier amplitudes are

$$\begin{aligned} \Theta_{ij}^0 = & \Theta_{ij}^{(0)} + \mathcal{A}_{ijk}(0; 0)E_k + \frac{1}{2}B_{kl ij}(0; 0, 0)E_k E_l + \frac{1}{4}D_{ijkl}(0; -\omega, \omega)\mathcal{E}_k \mathcal{E}_l \\ & + C_{ijkl}(0; 0)E_{kl}, \end{aligned} \quad (2.66)$$

$$\Theta_{ij}^\omega = \mathcal{A}_{ijk}(-\omega; \omega)\mathcal{E}_k + B_{kl ij}(-\omega; 0, \omega)\mathcal{E}_k E_l + C_{ijkl}(-\omega; \omega)\mathcal{E}_{kl}, \quad (2.67)$$

and

$$\Theta_{ij}^{2\omega} = \frac{1}{4}D_{ijkl}(-2\omega; \omega, \omega)\mathcal{E}_k \mathcal{E}_l. \quad (2.68)$$

2.4 The macroscopic induced dipole density

The macroscopic polarization (or macroscopic electric dipole moment per unit volume) of a medium under the influence of an applied electric field can be described as a power series in the field:

$$P_\alpha(t) = P_\alpha^{(0)}(t) + P_\alpha^{(1)}(t) + P_\alpha^{(2)}(t) + P_\alpha^{(3)}(t) + \dots, \quad (2.69)$$

where $P_\alpha^{(0)}(t)$ is independent of the field, while $P_\alpha^{(1)}(t)$ is linear in the field, $P_\alpha^{(2)}(t)$ is quadratic in the field, *etc.* $P_\alpha^{(0)}(t)$ is the permanent polarization which is present in some crystals. For an isotropic medium, $P_\alpha^{(0)}(t) = 0$. Here, the polarization $P_\alpha(t)$ is referred to space-fixed axes since it is generally measured in the laboratory frame.

As in equation (2.19), the dynamic component of the macroscopic applied electric field $E_\alpha(t)$ can be written as

$$E_\alpha(t) = \frac{1}{2} \sum_{\omega} E_\alpha^\omega e^{-i\omega t}, \quad (2.70)$$

where the summation is over both positive and negative frequencies. The expansion terms of equation (2.69) can be written as

$$P_\alpha^{(n)}(t) = \varepsilon_0 \sum_{\omega_1, \dots, \omega_n} \chi_{\alpha\beta\dots\varepsilon}^{(n)}(-\omega_\sigma; \omega_1, \dots, \omega_n) \frac{1}{2} E_\beta^{\omega_1} \dots \frac{1}{2} E_\varepsilon^{\omega_n} e^{-i\omega_\sigma t}, \quad (2.71)$$

where ω_σ denotes the sum of optical frequencies, *i.e.* $\omega_\sigma = \sum_{i=1}^n \omega_i$. The macroscopic polarization becomes

$$\begin{aligned} P_\alpha(t) = & \varepsilon_0 \sum_{\omega_1} \chi_{\alpha\beta}^{(1)}(-\omega_\sigma; \omega_1) \frac{1}{2} E_\beta^{\omega_1} e^{-i\omega_\sigma t} + \varepsilon_0 \sum_{\omega_1, \omega_2} \chi_{\alpha\beta\gamma}^{(2)}(-\omega_\sigma; \omega_1, \omega_2) \frac{1}{2} E_\beta^{\omega_1} \frac{1}{2} E_\gamma^{\omega_2} e^{-i\omega_\sigma t} \\ & + \varepsilon_0 \sum_{\omega_1, \omega_2, \omega_3} \chi_{\alpha\beta\gamma\delta}^{(3)}(-\omega_\sigma; \omega_1, \omega_2, \omega_3) \frac{1}{2} E_\beta^{\omega_1} \frac{1}{2} E_\gamma^{\omega_2} \frac{1}{2} E_\delta^{\omega_3} e^{-i\omega_\sigma t} + \dots \end{aligned} \quad (2.72)$$

For NLO processes such as SHG, THG and ESHG in non-resonant spectral regions, a monochromatic laser beam (with single frequency ω) induces the NLO process. In the case of ESHG, the light beam travels through the medium while it is subjected to an applied uniform static electric field. The general case of application of a static field with amplitude $E_\alpha(\omega = 0) = E_\omega^0$ together with a laser beam having a field with single frequency ω and amplitude $E_\alpha(\omega) = E_\alpha^\omega$ will be considered. The net applied field can be written as

$$E_\alpha(t) = E_\alpha^0 + E_\alpha^\omega \cos(\omega t). \quad (2.73)$$

The notation can be simplified as done previously in the case of the microscopic multipole expansion, by writing the static field as $E_\omega^0 \equiv E_\alpha$ and the dynamic field amplitude as $E_\alpha^\omega \equiv \mathcal{E}_\alpha$, so that

$$E_\alpha(t) = E_\alpha + \mathcal{E}_\alpha \cos(\omega t). \quad (2.74)$$

The expansion terms $P_\alpha^{(n)}(t)$ of equation (2.69) can each be written as a Fourier series having the general form

$$P_\alpha^{(n)}(t) = P_\alpha^{(n)}(0) + P_\alpha^{(n)}(\omega) \cos(\omega t) + P_\alpha^{(n)}(2\omega) \cos(2\omega t) + \dots \quad (2.75)$$

For an isotropic medium such as a gas, $P_\alpha^{(0)}(t) = 0$, while the first-order polarization will be

$$\begin{aligned} P_\alpha^{(1)}(t) &= \varepsilon_0 \chi_{\alpha\beta}^{(1)}(-\omega_\sigma; \omega_1) E_\beta(t) \\ &= \varepsilon_0 \chi_{\alpha\beta}^{(1)}(0; 0) E_\beta + \varepsilon_0 \chi_{\alpha\beta}^{(1)}(-\omega; \omega) \mathcal{E}_\beta \cos(\omega t). \end{aligned} \quad (2.76)$$

The second-order polarization is

$$\begin{aligned} P_\alpha^{(2)}(t) &= \varepsilon_0 \chi_{\alpha\beta\gamma}^{(2)}(-\omega_\sigma; \omega_1, \omega_2) E_\beta(t) E_\gamma(t) \\ &= \varepsilon_0 \chi_{\alpha\beta\gamma}^{(2)}(-\omega_\sigma; \omega_1, \omega_2) \left(E_\beta + \mathcal{E}_\beta \cos(\omega t) \right) \left(E_\gamma + \mathcal{E}_\gamma \cos(\omega t) \right) \\ &= \varepsilon_0 \left[\chi_{\alpha\beta\gamma}^{(2)}(0; 0, 0) E_\beta E_\gamma + 2\chi_{\alpha\beta\gamma}^{(2)}(-\omega; \omega, 0) \mathcal{E}_\beta E_\gamma \cos(\omega t) \right. \\ &\quad \left. + \chi_{\alpha\beta\gamma}^{(2)}(-\omega_\sigma; \omega_1, \omega_2) \mathcal{E}_\beta \mathcal{E}_\gamma \cos^2(\omega t) \right]. \end{aligned} \quad (2.77)$$

The trigonometric identity given in equation (2.41), namely

$$\cos^2(\omega t) = \frac{1}{2} + \frac{1}{2} \cos(2\omega t), \quad (2.78)$$

allows equation (2.77) to be recast as

$$\begin{aligned}
P_\alpha^{(2)}(t) = \varepsilon_0 & \left[\chi_{\alpha\beta\gamma}^{(2)}(0; 0, 0) E_\beta E_\gamma + \frac{1}{2} \chi_{\alpha\beta\gamma}^{(2)}(0; \omega, -\omega) \mathcal{E}_\beta \mathcal{E}_\gamma \right. \\
& \left. + 2\chi_{\alpha\beta\gamma}^{(2)}(-\omega; \omega, 0) \mathcal{E}_\beta E_\gamma \cos(\omega t) + \frac{1}{2} \chi_{\alpha\beta\gamma}^{(2)}(-2\omega; \omega, \omega) \mathcal{E}_\beta \mathcal{E}_\gamma \cos(2\omega t) \right].
\end{aligned} \tag{2.79}$$

Finally, the third-order polarization is

$$\begin{aligned}
P_\alpha^{(3)}(t) &= \varepsilon_0 \chi_{\alpha\beta\gamma\delta}^{(3)}(-\omega_\sigma; \omega_1, \omega_2, \omega_3) E_\beta(t) E_\gamma(t) E_\delta(t) \\
&= \varepsilon_0 \chi_{\alpha\beta\gamma\delta}^{(3)}(-\omega_\sigma; \omega_1, \omega_2, \omega_3) \left(E_\beta + \mathcal{E}_\beta \cos(\omega t) \right) \left(E_\gamma + \mathcal{E}_\gamma \cos(\omega t) \right) \left(E_\delta + \mathcal{E}_\delta \cos(\omega t) \right) \\
&= \varepsilon_0 \left[\chi_{\alpha\beta\gamma\delta}^{(3)}(-\omega_\sigma; \omega_1, \omega_2, \omega_3) E_\beta E_\gamma E_\delta + \left(\chi_{\alpha\beta\gamma\delta}^{(3)}(-\omega_\sigma; \omega_1, \omega_2, \omega_3) E_\beta E_\gamma \mathcal{E}_\delta \right. \right. \\
&\quad \left. \left. + \chi_{\alpha\beta\gamma\delta}^{(3)}(-\omega_\sigma; \omega_1, \omega_2, \omega_3) E_\beta \mathcal{E}_\gamma E_\delta + \chi_{\alpha\beta\gamma\delta}^{(3)}(-\omega_\sigma; \omega_1, \omega_2, \omega_3) \mathcal{E}_\beta E_\gamma E_\delta \right) \cos(\omega t) \right. \\
&\quad \left. + \left(\chi_{\alpha\beta\gamma\delta}^{(3)}(-\omega_\sigma; \omega_1, \omega_2, \omega_3) E_\beta \mathcal{E}_\gamma \mathcal{E}_\delta + \chi_{\alpha\beta\gamma\delta}^{(3)}(-\omega_\sigma; \omega_1, \omega_2, \omega_3) \mathcal{E}_\beta E_\gamma \mathcal{E}_\delta \right. \right. \\
&\quad \left. \left. + \left(\chi_{\alpha\beta\gamma\delta}^{(3)}(-\omega_\sigma; \omega_1, \omega_2, \omega_3) \mathcal{E}_\beta \mathcal{E}_\gamma E_\delta \right) \cos^2(\omega t) \right. \right. \\
&\quad \left. \left. + \chi_{\alpha\beta\gamma\delta}^{(3)}(-\omega_\sigma; \omega_1, \omega_2, \omega_3) \mathcal{E}_\beta \mathcal{E}_\gamma \mathcal{E}_\delta \cos^3(\omega t) \right] .
\end{aligned} \tag{2.80}$$

The trigonometric identity given in equation (2.42), namely

$$\cos^3(\omega t) = \frac{3}{4} \cos(\omega t) + \frac{1}{4} \cos(3\omega t) , \tag{2.81}$$

is now also required. Substituted together with equation (2.78) into equation (2.80), $P_\alpha^{(3)}(t)$ becomes

$$\begin{aligned}
P_\alpha^{(3)}(t) = \varepsilon_0 & \left[\chi_{\alpha\beta\gamma\delta}^{(3)}(0; 0, 0, 0) E_\beta E_\gamma E_\delta + \frac{3}{2} \chi_{\alpha\beta\gamma\delta}^{(3)}(0; -\omega, \omega, 0) \mathcal{E}_\beta \mathcal{E}_\gamma E_\delta \right. \\
& + 3 \chi_{\alpha\beta\gamma\delta}^{(3)}(-\omega; \omega, 0, 0) \mathcal{E}_\beta E_\gamma E_\delta \cos(\omega t) \\
& + \frac{3}{4} \chi_{\alpha\beta\gamma\delta}^{(3)}(-\omega; \omega, -\omega, \omega) \mathcal{E}_\beta \mathcal{E}_\gamma \mathcal{E}_\delta \cos(\omega t) \\
& + \frac{3}{2} \chi_{\alpha\beta\gamma\delta}^{(3)}(-2\omega; \omega, \omega, 0) \mathcal{E}_\beta \mathcal{E}_\gamma E_\delta \cos(2\omega t) \\
& \left. + \frac{1}{4} \chi_{\alpha\beta\gamma\delta}^{(3)}(-3\omega; \omega, \omega, \omega) \mathcal{E}_\beta \mathcal{E}_\gamma \mathcal{E}_\delta \cos(3\omega t) \right].
\end{aligned} \tag{2.82}$$

The polarizability Fourier amplitude responsible for SHG is

$$P_\alpha^{(2)}(2\omega) = \frac{1}{2} \varepsilon_0 \chi_{\alpha\beta\gamma}^{(2)}(-2\omega; \omega, \omega) \mathcal{E}_\beta \mathcal{E}_\gamma \tag{2.83}$$

while that responsible for THG is

$$P_\alpha^{(3)}(3\omega) = \frac{1}{4} \varepsilon_0 \chi_{\alpha\beta\gamma\delta}^{(3)}(-3\omega; \omega, \omega, \omega) \mathcal{E}_\beta \mathcal{E}_\gamma \mathcal{E}_\delta. \tag{2.84}$$

The polarizability amplitude which gives rise to ESHG is

$$P_\alpha^{(3)}(2\omega) = \frac{3}{2} \varepsilon_0 \chi_{\alpha\beta\gamma\delta}^{(3)}(-2\omega; \omega, \omega, 0) \mathcal{E}_\beta \mathcal{E}_\gamma E_\delta. \tag{2.85}$$

2.5 The transition from microscopic to macroscopic polarization

The link between the induced microscopic molecular dipole moment and the induced macroscopic polarization of a fluid is provided by [100, 101]

$$P_\alpha = \mathcal{N} \bar{\mu}_\alpha = \frac{N_A}{V_m} \bar{\mu}_\alpha \quad (2.86)$$

where $\bar{\mu}_\alpha$ is the orientational average of the electric dipole moment of a molecule and \mathcal{N} is the number density of molecules, N_A being Avogadro's number, and V_m the molar volume.

In equation (2.86), the macroscopic polarization P_α is for a medium under the influence of a macroscopic applied electric field. It needs to be recognized that the macroscopic Maxwell field E_α inside matter is a macroscopic spatial average, since the microscopic charge distribution (comprised of electrons and nuclei) and resulting fields are rapidly varying in an intractably complicated manner, necessitating simplification. The spatial averaging is a mathematical procedure which smooths out the microscopic spatial variations observed on length scales of the order of molecular dimensions, yielding slowly varying macroscopic sources and fields [101, 102]. The macroscopic electric field has contributions both from sources external to the material system (e.g. charges on a parallel-plate capacitor), and from the charges of all the molecules comprising the system (e.g. a dielectric fluid inserted to fill the space between the plates of the capacitor).

The microscopic polarization μ_α in equation (2.86) is for a single molecule under the influence of the microscopic *local* electric field acting on the molecule. This local field E_α^{loc} is the field arising from all external sources and from all of the molecules

within the sample *with the exception* of the single molecule under consideration, and is different to the applied field E_α . To obtain the macroscopic susceptibilities from the microscopic (hyper)polarizabilities thus requires knowledge of the relationship between the local and macroscopic fields. For rarefied gases, where the refractive index approaches unity, the distinction between the local field and the macroscopic field becomes negligible. In dense isotropic media such as non-dipolar fluids or cubic crystals, Lorentz [103] was able to show that

$$E_\alpha^{\text{loc}} = E_\alpha + \frac{1}{3\epsilon_0} P_\alpha. \quad (2.87)$$

Kirkwood [104] considered a dielectric sphere of macroscopic dimension which is small enough to be treated as a mathematical point, but which contains a sufficient number of molecules such that molecular fluctuations average out to a constant value. Assuming that the dominant contribution to the local field arises from the linear polarizability of the surrounding molecules, he was able express equation (2.87) as

$$E_\alpha^{\text{loc}} = \frac{\epsilon_r(\omega) + 2}{3} E_\alpha, \quad (2.88)$$

where $\epsilon_r(\omega)$ is the frequency-dependent dielectric constant for a dynamic applied field $E_\alpha \equiv E_\alpha^\omega$. For a static applied field $E_\alpha \equiv E_\alpha^0$, equation (2.88) becomes

$$E_\alpha^{\text{loc}} = \frac{\epsilon_r + 2}{3} E_\alpha, \quad (2.89)$$

where ϵ_r is the static dielectric constant. Here, E_α^{loc} is called the Lorentz local field, while the Lorentz local field factor relating the local and applied fields is

$$f_L(\omega) = \frac{\epsilon_r(\omega) + 2}{3} \quad (2.90)$$

for dynamic fields, and

$$f_L(0) = \frac{\varepsilon_r + 2}{3} \quad (2.91)$$

for static fields. Fortunately, the mathematical simplicity afforded by the spherical shape of the dielectric material does not lead to a loss of generality, since the dielectric constant ε_r of a material is independent of the shape of the sample under consideration.

For a fluid comprised of dipolar molecules, the external field will not only induce dipoles, but will also tend to orient the permanent molecular dipole moments. Onsager refined the Lorentz model to account for the orientational reactive forces which are exerted between dipolar molecules [105], obtaining the Onsager local field factor

$$f_O(0) = \frac{\varepsilon_r(\varepsilon_r(\infty) + 2)}{\varepsilon_r(\infty) + 2\varepsilon_r}, \quad (2.92)$$

where $\varepsilon_r(\infty)$ is the dielectric constant obtained through extrapolation of $\varepsilon_r(\omega)$ to high frequencies. If the applied field arises from a visible beam of light, the electric field oscillates at optical frequency, and molecular inertial effects prevent any alignment of dipoles with the alternating field, so that the Lorentz local field factor in equation (2.90) still suffices, even for a dense fluid comprised of dipolar molecules.

Armstrong *et. al* have shown that the local field factors obtained above for linear polarizabilities are readily extended to nonlinear (hyper)polarizabilities [12]. Boyd provides a full derivation [6] based on the procedure of Bloembergen [106], showing that equation (2.86) is valid for the Maxwell nonlinear polarization provided that in the average of the electric dipole moment of a molecule, not only are each of the incident local fields multiplied by their local field correction factor, but a local field factor must also be included for the field generated by the nonlinear interaction (*i.e.*

for the induced dipole which oscillates at the frequency ω_σ).

2.6 Concluding remarks

First, a word of caution. In the scientific literature, the use of different conventions in the definition of hyperpolarizabilities has resulted in significant confusion in the comparison between hyperpolarizabilities either measured or calculated by different research groups. The relationship between nonlinear susceptibilities and hyperpolarizabilities defined using the various different conventions has been examined by Willetts, Rice, Burland and Shelton [107], and re-examined by Reis [92]. One of the reasons we have been particular in deriving from first principles the multipole expansion, the total molecular dipole moment, and the macroscopic susceptibilities in this chapter is to provide a coherent foundation for the theory in subsequent chapters, and a definitive means of comparing the conventions used here with the others encountered in the literature.

In conclusion, the multipole expansion has successfully related many macroscopic electromagnetic phenomena in matter to the microscopic structure of individual molecules in gases (or of unit cells in crystals) [83, 86]. By means of it, the description of two interacting molecules can be simplified provided the separation of the molecules is sufficiently large, allowing the individual molecules to be characterized by a series of moments of charge. Equipped with the multipole expansion and the expression for the total molecular electric dipole moment in the presence of both a uniform static applied electric field and a dynamic light-wave electric field, it will be possible to relate the induced dc ESHG to these microscopic (hyper)polarizabilities and multipole moments.

Chapter 3

The Theory of ESHG for an Ideal Gas

3.1 Electromagnetic theory in dielectric media

All electromagnetic phenomena which depend on the macroscopic electric field $\mathbf{E}(\mathbf{r}, t)$ and magnetic field $\mathbf{B}(\mathbf{r}, t)$ are described by Maxwell's macroscopic equations

$$\nabla \cdot \mathbf{D} = \rho_f, \quad (3.1)$$

$$\nabla \times \mathbf{E} = -\frac{\partial \mathbf{B}}{\partial t}, \quad (3.2)$$

$$\nabla \cdot \mathbf{B} = 0, \quad (3.3)$$

and

$$\nabla \times \mathbf{H} = \mathbf{J}_f + \frac{\partial \mathbf{D}}{\partial t}. \quad (3.4)$$

Here, ρ_f and \mathbf{J}_f are the macroscopic “free” charge and current densities respectively, and the auxiliary macroscopic response fields, to the order of electric and magnetic dipole respectively, are defined as

$$\mathbf{D}(\mathbf{r}, t) = \varepsilon_0 \mathbf{E}(\mathbf{r}, t) + \mathbf{P}(\mathbf{r}, t) \quad (3.5)$$

and

$$\mathbf{H}(\mathbf{r}, t) = \mu_0^{-1} \mathbf{B}(\mathbf{r}, t) - \mathbf{M}(\mathbf{r}, t). \quad (3.6)$$

\mathbf{D} and \mathbf{H} can be termed response fields because the electric dipole moment density \mathbf{P} and the magnetic dipole moment density \mathbf{M} include induced contributions arising from the response of matter to externally applied electric and magnetic fields respectively.

In this work, we will be considering dielectric media, which means that there are no free charges (*i.e.* $\rho_f = 0$) and no significant currents (*i.e.* $\mathbf{J}_f = 0$). It is sufficient in this project to work to electric dipole order, which means that the dipole magnetization term \mathbf{M} should *not* be included in equation (3.6). As has been articulated in detail by Raab and de Lange [86], the reason for this is that in an application involving an electromagnetic response, the multipole contributions to \mathbf{D} and \mathbf{H} should be of comparable magnitude. \mathbf{M} is of magnetic dipole order, and is of the same multipole order as the electric quadrupole contribution to \mathbf{D} [86].

In the following two sections, we review the linear electro-optical effects of the dielectric constant (for an ideal gas in the presence of a static applied electric field) and the refractive index (for an ideal gas traversed by an applied monochromatic light-wave field), which are both determined by the linear polarizability α . This prepares the groundwork for tackling the molecular-tensor theory for dc ESHG, which

is the analogous effect for the nonlinear hyperpolarizability γ . It also serves to establish the technique of orientational averaging, thus permitting the formulation of a relationship between the macroscopic dipole polarization P_α and the microscopic dipole μ_α of an individual molecule for the various electro-optical effects.

3.2 The dielectric constant of an ideal gas

Consider a sample of an ideal gas containing a number density \mathcal{N} of identical molecules ($\mathcal{N} = N_A/V_m$ where N_A is Avogadro's number and V_m is the molar volume). This fluid is a homogeneous medium, and in the absence of any external applied fields is isotropic on a macroscopic scale. Such a nonconducting material is termed a dielectric. If the gas sample is placed in a uniform external static electric field \mathbf{E} , the applied field will induce a polarization of the medium through two possible mechanisms, namely from partial orientation of permanent molecular electric dipole moments (if these exist), and through distortion of the electronic structure of the molecules. The polarization of the medium results in a partial cancellation of the electric field inside the dielectric, the resultant field remaining finite. Even for a gas of non-dipolar molecules, the external field will induce electric dipoles and higher multipoles in the molecules. The electric dipole approximation neglects the contributions arising from these higher-order multipoles.

In the following analysis, it will be sufficient to work to electric-dipole order, so that the auxiliary field \mathbf{D} within the medium (which is often called the electric displacement) is related to the macroscopic Maxwellian field \mathbf{E} by

$$D_\alpha = \varepsilon_0 E_\alpha + P_\alpha \quad (3.7)$$

where \mathbf{D} and \mathbf{E} have been written in tensor notation as D_α and E_α respectively, ε_0 is the permittivity of free space, and where P_α is the macroscopic dipole moment per

unit volume, or dipole moment density, sometimes also called the dipole polarization. (Throughout this thesis, Greek tensor subscripts pertain to the laboratory frame, while Roman tensor subscripts pertain to molecule-fixed axes.) Since

$$D_\alpha = \varepsilon_r \varepsilon_0 E_\alpha \quad (3.8)$$

where ε_r is the static dielectric constant, equation (3.7) becomes

$$\begin{aligned} P_\alpha &= D_\alpha - \varepsilon_0 E_\alpha \\ &= \varepsilon_0 (\varepsilon_r - 1) E_\alpha. \end{aligned} \quad (3.9)$$

Recall from equation (2.76) that the first-order (*i.e.* linear) macroscopic static polarization is

$$P_\alpha^{(1)} = \varepsilon_0 \chi_{\alpha\beta}^{(1)}(0; 0) E_\beta. \quad (3.10)$$

This equation is general, in that it accounts for the response of an anisotropic medium (as is the case for various crystalline media) to an applied field. Since we are dealing specifically with gaseous media, which are isotropic, the induced dipole will be parallel to the applied field, so that equation (3.10) reduces to

$$P_\alpha = \varepsilon_0 \chi_e E_\alpha. \quad (3.11)$$

Here the dimensionless scalar macroscopic quantity χ_e is termed the electric susceptibility of the medium under consideration. Comparison of equations (3.9) and (3.11) yields

$$\chi_e = (\varepsilon_r - 1). \quad (3.12)$$

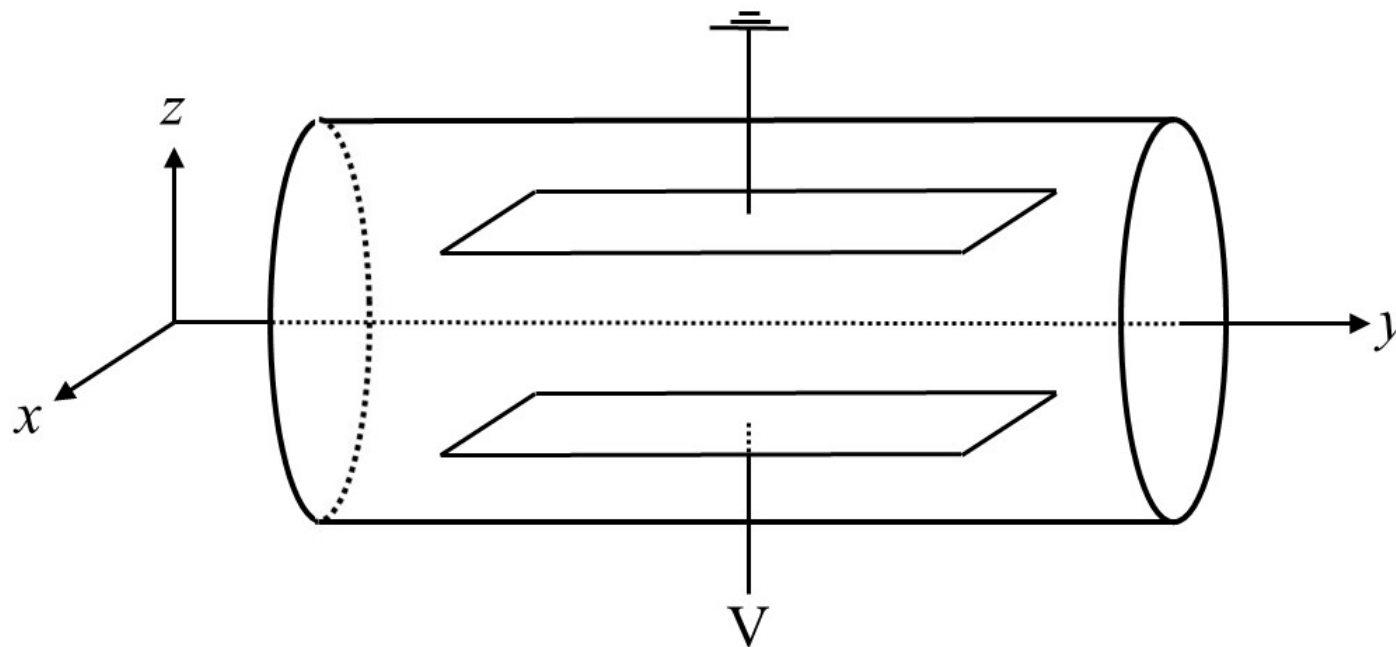


Figure 3.1: Schematic of a dielectric cell containing a parallel-plate capacitor the capacitance of which can be measured with a vacuum between the plates, or with the plates filled with a dielectric fluid. The laboratory reference frame $O(x,y,z)$ is oriented such that the z -axis is parallel to the direction of the uniform static electric field between the plates.

Experimentally, the dielectric constant of a dielectric can be measured using a parallel-plate capacitor with fixed potential, as shown in Figure 3.1. If the capacitor has a vacuum capacitance of C_0 , and if the dielectric is then allowed to fill the space between the plates while the potential difference V between the plates is held constant, the capacitance becomes $C = \epsilon_r C_0$. Note that the electric field between the plates remains fixed at $E = V/d$ (where d is the plate separation) whether the dielectric is present or absent. As dielectric is admitted, charge will flow to the plates so that the polarization charge of the adjacent dielectric surfaces will be exactly cancelled, as described on pp. 172-173 of Reference [102]. Various research groups have used refined experimental techniques to obtain accurate measurements of the dielectric constants of gases, such as reported in References [108, 109].

In equation (3.9) the macroscopic polarization can be related to the orientational average of the electric dipole moment of a molecule *via* equation (2.86) so that

$$P_\alpha = \epsilon_0(\epsilon_r - 1)E_\alpha = \mathcal{N} \bar{\mu}_\alpha = \frac{N_A}{V_m} \bar{\mu}_\alpha \quad (3.13)$$

where $\bar{\mu}_\alpha$ is the orientational average of the electric dipole moment of a molecule and \mathcal{N} is the number of molecules per unit volume. The space-fixed laboratory frame $O(x, y, z)$ is oriented such that the z -axis is in the direction of the applied uniform field, giving $\mathbf{E} = (0, 0, E_z)$. The induced polarization density in equation (3.13) simplifies to $P_z = \mathcal{N} \bar{\mu}_z$ since the random molecular orientation in directions perpendicular to the applied field means that the perpendicular polarization contributions $P_x = \mathcal{N} \bar{\mu}_x$ and $P_y = \mathcal{N} \bar{\mu}_y$ will average to zero:

$$P_z = \epsilon_0(\epsilon_r - 1)E_z = \frac{N_A}{V_m} \bar{\mu}_z. \quad (3.14)$$

It is reasonable to assume (for all but the lightest of molecules) that the rotational energy levels are sufficiently close for the orientation σ to be treated as continuous,

so that a classical rather than quantum mechanical treatment will suffice. This permits a Boltzmann-type weighting factor to be used in determining the orientational average $\bar{\mu}_z$ [74, 110]. The biased orientational average of a molecular quantity X in configuration σ in the presence of the biasing influence of the applied field \mathbf{E} is

$$\bar{X} = \overline{X(\sigma, \mathbf{E})} = \frac{\int X(\sigma, \mathbf{E}) e^{-U(\sigma, \mathbf{E})/kT} d\sigma}{\int e^{-U(\sigma, \mathbf{E})/kT} d\sigma}. \quad (3.15)$$

Here, $U(\sigma, \mathbf{E})$ is the energy of the molecule, given by

$$U(\sigma, \mathbf{E}) = - \int_0^{\mathbf{E}} \mu_i dE_i. \quad (3.16)$$

As discussed in Section 2.5, a microscopic quantity X is for a single molecule under the influence of the *local* field acting on the molecule. Rather than correcting for each instance of the field using equation (2.89), it is more convenient to proceed using the applied (Maxwell) field, bearing in mind that once the final expression for \bar{X} has been obtained, adjustments for the local field factor must then be made as appropriate. The biased average \bar{X} is converted into isotropic averages through a Taylor series expansion of \bar{X} in powers of E_α ,

$$\bar{X} = \overline{X(\sigma, \mathbf{E})} = A + B E_\alpha + C E_\alpha^2 + \dots, \quad (3.17)$$

where

$$A = \left(\overline{X(\sigma, \mathbf{E})} \right)_{E_\alpha=0}, \quad B = \left(\frac{\partial \overline{X(\sigma, \mathbf{E})}}{\partial E_\alpha} \right)_{E_\alpha=0} \quad \text{and} \quad C = \frac{1}{2} \left(\frac{\partial^2 \overline{X(\sigma, \mathbf{E})}}{\partial E_\alpha^2} \right)_{E_\alpha=0}. \quad (3.18)$$

The isotropic average of a property $X(\sigma, \mathbf{E})$ with $\mathbf{E} = 0$ is denoted as $\langle X \rangle$, and is

$$\langle X \rangle = \frac{\int X(\sigma, 0) e^{-U(\sigma, 0)/kT} d\sigma}{\int e^{-U(\sigma, 0)/kT} d\sigma}. \quad (3.19)$$

The coefficients in equation (3.18) are now evaluated from equation (3.15), where the partial derivatives will be evaluated using the product rule. Firstly,

$$A = \langle X \rangle. \quad (3.20)$$

The Leibnitz integral rule, in the special case where the limits of integration are constants (given by a and b below), states that [111]

$$\frac{d}{dx} \left(\int_a^b f(x, t) dt \right) = \int_a^b \frac{\partial}{\partial x} f(x, t) dt. \quad (3.21)$$

Hence,

$$\begin{aligned} \left(\frac{\partial \overline{X(\sigma, \mathbf{E})}}{\partial E_\alpha} \right) &= \frac{\int \frac{\partial X(\sigma, \mathbf{E})}{\partial E_\alpha} e^{-U(\sigma, \mathbf{E})/kT} d\sigma}{\int e^{-U(\sigma, \mathbf{E})/kT} d\sigma} - \frac{1}{kT} \frac{\int X(\sigma, \mathbf{E}) \frac{\partial U(\sigma, \mathbf{E})}{\partial E_\alpha} e^{-U(\sigma, \mathbf{E})/kT} d\sigma}{\int e^{-U(\sigma, \mathbf{E})/kT} d\sigma} \\ &+ \frac{1}{kT} \frac{\left(\int X(\sigma, \mathbf{E}) e^{-U(\sigma, \mathbf{E})/kT} d\sigma \right) \left(\int \frac{\partial U(\sigma, \mathbf{E})}{\partial E_\alpha} e^{-U(\sigma, \mathbf{E})/kT} d\sigma \right)}{\left(\int e^{-U(\sigma, \mathbf{E})/kT} d\sigma \right)^2}, \end{aligned} \quad (3.22)$$

where $\left(\frac{\partial \overline{X(\sigma, \mathbf{E})}}{\partial E_\alpha} \right)$ is the partial derivative of the Boltzmann average $\overline{X(\sigma, \mathbf{E})}$ with respect to the applied field E_α , so that

$$B = \left(\frac{\partial \overline{X(\sigma, \mathbf{E})}}{\partial E_\alpha} \right)_{E_\alpha=0} = \left\langle \frac{\partial X}{\partial E_\alpha} \right\rangle - \frac{1}{kT} \left\langle X \frac{\partial U}{\partial E_\alpha} \right\rangle + \frac{1}{kT} \langle X \rangle \left\langle \frac{\partial U}{\partial E_\alpha} \right\rangle. \quad (3.23)$$

The expression for C is obtained in an analogous procedure to that for B above. The double partial derivative of $\overline{X(\sigma, \mathbf{E})}$ which appears in equation (3.18) is evaluated

by taking $\partial/\partial E_\alpha$ of $\left(\overline{\partial X(\sigma, \mathbf{E})/\partial E_\alpha}\right)$ in equation (3.22), which yields

$$\begin{aligned}
C = & \frac{1}{2} \left\langle \frac{\partial^2 X}{\partial E_\alpha^2} \right\rangle - \frac{1}{2kT} \left\{ 2 \left\langle \frac{\partial X}{\partial E_\alpha} \frac{\partial U}{\partial E_\alpha} \right\rangle - 2 \left\langle \frac{\partial X}{\partial E_\alpha} \right\rangle \left\langle \frac{\partial U}{\partial E_\alpha} \right\rangle \right. \\
& \left. + \left\langle X \frac{\partial^2 U}{\partial E_\alpha^2} \right\rangle - \langle X \rangle \left\langle \frac{\partial^2 U}{\partial E_\alpha^2} \right\rangle \right\} \\
& + \frac{1}{2k^2T^2} \left\{ \left\langle X \left(\frac{\partial U}{\partial E_\alpha} \right)^2 \right\rangle - \langle X \rangle \left\langle \left(\frac{\partial U}{\partial E_\alpha} \right)^2 \right\rangle \right. \\
& \left. - 2 \left\langle X \frac{\partial U}{\partial E_\alpha} \right\rangle \left\langle \frac{\partial U}{\partial E_\alpha} \right\rangle + 2 \langle X \rangle \left\langle \frac{\partial U}{\partial E_\alpha} \right\rangle \left\langle \frac{\partial U}{\partial E_\alpha} \right\rangle \right\}.
\end{aligned} \tag{3.24}$$

From equation (2.55), for a molecule in a uniform static external electric field \mathbf{E} the total dipole moment is given by

$$\mu_i = \mu_i^{(0)} + \alpha_{ij}(0; 0) E_j + \frac{1}{2} \beta_{ijk}(0; 0, 0) E_j E_k + \frac{1}{6} \gamma_{ijkl}(0; 0, 0, 0) E_j E_k E_l + \dots \tag{3.25}$$

Equation (3.25) in equation (3.16) yields

$$\begin{aligned}
U(\sigma, \mathbf{E}) = & U^{(0)} - \mu_i^{(0)} E_i - \frac{1}{2} \alpha_{ij}(0; 0) E_i E_j - \frac{1}{6} \beta_{ijk}(0; 0, 0) E_i E_j E_k \\
& - \frac{1}{24} \gamma_{ijkl}(0; 0, 0, 0) E_i E_j E_k E_l - \dots \tag{3.26}
\end{aligned}$$

The transformation of the electric field from the laboratory frame (*i.e.* space-fixed axes) into molecule-fixed axes is obtained using the direction cosine as follows:

$$E_i = a_\alpha^i E_\alpha \tag{3.27}$$

Since the electric field E_α has as its only non-zero component E_z , E_i becomes

$E_z a_z^i = E_z a_i^z$, so that equations (3.25) and (3.26) become

$$\mu_i = \mu_i^{(0)} + \alpha_{ij}(0;0)E_z a_j^z + \frac{1}{2}\beta_{ijk}(0;0,0)E_z^2 a_j^z a_k^z + \frac{1}{6}\gamma_{ijkl}(0;0,0,0)E_z^3 a_j^z a_k^z a_l^z + \dots \quad (3.28)$$

and

$$U(\sigma, \mathbf{E}) = U^{(0)} - \mu_i^{(0)} E_z a_i^z - \frac{1}{2}\alpha_{ij}(0;0)E_z^2 a_i^z a_j^z - \frac{1}{6}\beta_{ijk}(0;0,0)E_z^3 a_i^z a_j^z a_k^z - \frac{1}{24}\gamma_{ijkl}(0;0,0,0)E_z^4 a_i^z a_j^z a_k^z a_l^z - \dots \quad (3.29)$$

Equation (3.17) provides

$$\bar{\mu}_z = \overline{\mu_z(\sigma, \mathbf{E})} = A + B E_z + C E_z^2 + \dots, \quad (3.30)$$

where

$$A = \left(\overline{\mu_z(\sigma, \mathbf{E})} \right)_{E_z=0}, \quad B = \left(\frac{\partial \overline{\mu_z(\sigma, \mathbf{E})}}{\partial E_z} \right)_{E_z=0} \quad \text{and} \quad C = \frac{1}{2} \left(\frac{\partial^2 \overline{\mu_z(\sigma, \mathbf{E})}}{\partial E_z^2} \right)_{E_z=0}. \quad (3.31)$$

Obtaining expressions for A , B and C requires evaluation of the isotropic averages of the direction cosines or products of directions cosines, the procedures for which are well-established [74, 85, 112]. Many of the isotropic averages evaluate to zero, for example

$$\langle a_i^x \rangle = \langle a_i^y \rangle = \langle a_i^z \rangle = 0. \quad (3.32)$$

The non-vanishing isotropic averages used in this work are now summarized:

$$\langle a_i^x a_j^x \rangle = \langle a_i^y a_j^y \rangle = \langle a_i^z a_j^z \rangle = \frac{1}{3} \delta_{ij}, \quad (3.33)$$

$$\langle a_i^x a_j^y a_k^z \rangle = \frac{1}{6} \varepsilon_{ijk} \quad (3.34)$$

where ε_{ijk} is the Levi-Civita tensor, which is +1 or -1 if i, j, k is respectively an even or odd permutation of 1, 2, 3, or is zero if any two of the subscripts i, j, k are the same,

$$\langle a_i^x a_j^x a_k^x a_l^x \rangle = \langle a_i^y a_j^y a_k^y a_l^y \rangle = \langle a_i^z a_j^z a_k^z a_l^z \rangle = \frac{1}{15} (\delta_{ij} \delta_{kl} + \delta_{ik} \delta_{jl} + \delta_{il} \delta_{jk}) \quad (3.35)$$

and

$$\langle a_i^x a_j^x a_k^y a_l^y \rangle = \langle a_i^y a_j^y a_k^z a_l^z \rangle = \langle a_i^z a_j^z a_k^x a_l^x \rangle = \frac{1}{30} (4\delta_{ij} \delta_{kl} - \delta_{ik} \delta_{jl} - \delta_{il} \delta_{jk}) . \quad (3.36)$$

Equation (3.28) gives

$$\begin{aligned} \mu_z(\sigma, \mathbf{E}) = \mu_i a_i^z &= \mu_i^{(0)} a_i^z + \alpha_{ij}(0; 0) E_z a_i^z a_j^z + \frac{1}{2} \beta_{ijk}(0; 0, 0) E_z^2 a_i^z a_j^z a_k^z \\ &+ \frac{1}{6} \gamma_{ijkl}(0; 0, 0, 0) E_z^3 a_i^z a_j^z a_k^z a_l^z + \dots , \end{aligned} \quad (3.37)$$

so that equation (3.31) yields

$$A = \left(\overline{\mu_z(\sigma, \mathbf{E})} \right)_{E_z=0} = \langle \mu_z \rangle . \quad (3.38)$$

By setting $E_z = 0$ in equation (3.37) this becomes

$$A = \mu_i^{(0)} \langle a_i^z \rangle = 0 . \quad (3.39)$$

In a similar fashion, use of equation (3.23) yields

$$B = \left(\frac{\partial \overline{\mu_z}}{\partial E_z} \right)_{E_z=0} = \left\langle \frac{\partial \mu_z}{\partial E_z} \right\rangle - \frac{1}{kT} \left\langle \mu_z \frac{\partial U}{\partial E_z} \right\rangle + \frac{1}{kT} \langle \mu_z \rangle \left\langle \frac{\partial U}{\partial E_z} \right\rangle . \quad (3.40)$$

Since $A = \langle \mu_z \rangle = 0$, the expression for B reduces to

$$B = \left\langle \frac{\partial \mu_z}{\partial E_z} \right\rangle - \frac{1}{kT} \left\langle \mu_z \frac{\partial U}{\partial E_z} \right\rangle. \quad (3.41)$$

Equation (3.37) provides

$$\left(\frac{\partial \mu_z}{\partial E_z} \right)_{E_z=0} = \alpha_{ij}(0; 0) a_i^z a_j^z, \quad (3.42)$$

so that

$$\left\langle \frac{\partial \mu_z}{\partial E_z} \right\rangle = \alpha_{ij}(0; 0) \langle a_i^z a_j^z \rangle = \frac{1}{3} \alpha_{ij}(0; 0) \delta_{ij} = \frac{1}{3} \alpha_{ii}(0; 0) = \alpha(0; 0) \quad (3.43)$$

where

$$\alpha(0; 0) = \frac{1}{3} \alpha_{ii}(0; 0) = \frac{1}{3} (\alpha_{11}(0; 0) + \alpha_{22}(0; 0) + \alpha_{33}(0; 0)) \quad (3.44)$$

is the mean static polarizability.

Similarly, equation (3.29) provides

$$\left(\frac{\partial U}{\partial E_z} \right)_{E_z=0} = -\mu_j^{(0)} a_j^z \quad (3.45)$$

so that

$$\left(\mu_z \frac{\partial U}{\partial E_z} \right)_{E_z=0} = -\mu_i^{(0)} \mu_j^{(0)} a_i^z a_j^z \quad (3.46)$$

and

$$\left\langle \mu_z \frac{\partial U}{\partial E_z} \right\rangle = -\mu_i^{(0)} \mu_j^{(0)} \langle a_i^z a_j^z \rangle = -\frac{1}{3} \mu_i^{(0)} \mu_j^{(0)} \delta_{ij} = -\frac{1}{3} (\mu_i^{(0)})^2. \quad (3.47)$$

A similar analysis yields $C = 0$. The leading non-vanishing term in the expansion

of $\bar{\mu}_z$ is thus in E_z , and gathering the terms in equation (3.41) yields

$$B = \left(\alpha(0;0) + \frac{(\mu_i^{(0)})^2}{3kT} \right) \quad (3.48)$$

such that equation (3.30) becomes

$$\bar{\mu}_z = \left(\alpha(0;0) + \frac{(\mu_i^{(0)})^2}{3kT} \right) E_z . \quad (3.49)$$

Bearing in mind the earlier caveat that this expression for the orientational average $\bar{\mu}_z$ is for a single molecule under the influence of the *local* electric field acting on the molecule, it must now be written explicitly as

$$\bar{\mu}_z = \left(\alpha(0;0) + \frac{(\mu_i^{(0)})^2}{3kT} \right) E_z^{\text{loc}} . \quad (3.50)$$

The classic Langevin-Debye result [113–116] is obtained if the Lorentz local field factor $f_L(0)$ for a static applied electric field, given by equation (2.92), is used to relate the local and applied fields *via* $E_\alpha^{\text{loc}} = f_L(0) E_\alpha$ for *both* the distortion and orientation components of equation (3.50), which then becomes

$$\bar{\mu}_z = \left(\alpha(0;0) + \frac{(\mu_i^{(0)})^2}{3kT} \right) \left(\frac{\varepsilon_r + 2}{3} \right) E_z . \quad (3.51)$$

Substituting equation (3.51) into equation (3.14) for the dipole polarization yields

$$P_z = \varepsilon_0(\varepsilon_r - 1)E_z = \frac{N_A}{V_m} \left(\frac{\varepsilon_r + 2}{3} \right) \left(\alpha(0;0) + \frac{(\mu_i^{(0)})^2}{3kT} \right) E_z , \quad (3.52)$$

which when rearranged for the total (or molar) polarization ${}_T P$ provides the Langevin-

Debye equation

$${}_T P = \frac{\varepsilon_r - 1}{\varepsilon_r + 2} V_m = \frac{N_A}{3\varepsilon_0} \left(\alpha(0; 0) + \frac{(\mu_i^{(0)})^2}{3kT} \right). \quad (3.53)$$

In the case of a gaseous dielectric comprised of non-dipolar molecules, where there is no permanent electric dipole moment, the Langevin-Debye equation reduces to the Clausius-Mossotti equation [117, 118]

$${}_T P = \frac{\varepsilon_r - 1}{\varepsilon_r + 2} V_m = \frac{N_A \alpha(0; 0)}{3\varepsilon_0}. \quad (3.54)$$

Osager refined the Langevin-Debye equation, showing that one cannot use the Lorentz local field factor to relate the Maxwell field to the local field of the term in equation (3.50) which describes the partial orientation of permanent dipole moments, since it does not account for the orientational reactive forces which are exerted between dipolar molecules [105]. Rather, the Onsager local field factor given in equation (2.92) should be used. This subtlety is probed in detail by Böttcher [100], and is not further examined here since this project only considers gases comprised of non-dipolar molecules.

3.3 The index of refraction of an ideal gas

The theory of the refractive index n of an ideal gas is closely analagous to that for the dielectric constant ε_r of an ideal gas presented in the previous section. The equation linking the two theories is

$$n^2 = \varepsilon_r \mu_r, \quad (3.55)$$

where departures of the relative permeability μ_r from $\mu_r = 1$ is assumed to be negligible for dilute gases comprised of non-magnetic molecules. In the theory of

the dielectric constant of an ideal gas, the gas sample was placed in a uniform static electric field \mathbf{E} . For the theory of the refractive index of an ideal gas, this static electric field is replaced by the dynamic electric field of a light beam, which is typically a monochromatic laser beam with electric field $\mathcal{E}_\alpha \cos(\omega t)$, as illustrated in Figure 3.2. Equation (3.9) for the macroscopic dipole moment density, P_α , becomes

$$P_\alpha(t) = \varepsilon_0 \left(\varepsilon_r(\omega) - 1 \right) \mathcal{E}_\alpha \cos(\omega t) \quad (3.56)$$

where $\varepsilon_r(\omega)$ is the frequency-dependent dielectric constant of the gas, and $\mathcal{E}_\alpha \cos(\omega t)$ is the oscillating macroscopic Maxwellian electric field of the light wave (of frequency ω). The polarizability Fourier amplitude is

$$P_\alpha(\omega) = \varepsilon_0 \left(\varepsilon_r(\omega) - 1 \right) \mathcal{E}_\alpha \quad (3.57)$$

which can be compared to that obtained from equation (2.76), which accounts in general for an anisotropic medium:

$$P_\alpha^{(1)}(\omega) = \varepsilon_0 \chi_{\alpha\beta}^{(1)}(-\omega; \omega) \mathcal{E}_\beta. \quad (3.58)$$

For a gaseous medium, which is isotropic, this reduces to

$$P_\alpha(\omega) = \varepsilon_0 \chi_e(\omega) \mathcal{E}_\alpha \quad (3.59)$$

where the scalar quantity $\chi_e(\omega)$ is the dynamic electric susceptibility of the medium under investigation. Equations (3.57), (3.55) and (3.59) yield

$$\chi_e(\omega) = \left(\varepsilon_r(\omega) - 1 \right) = \left(n^2(\omega) - 1 \right). \quad (3.60)$$

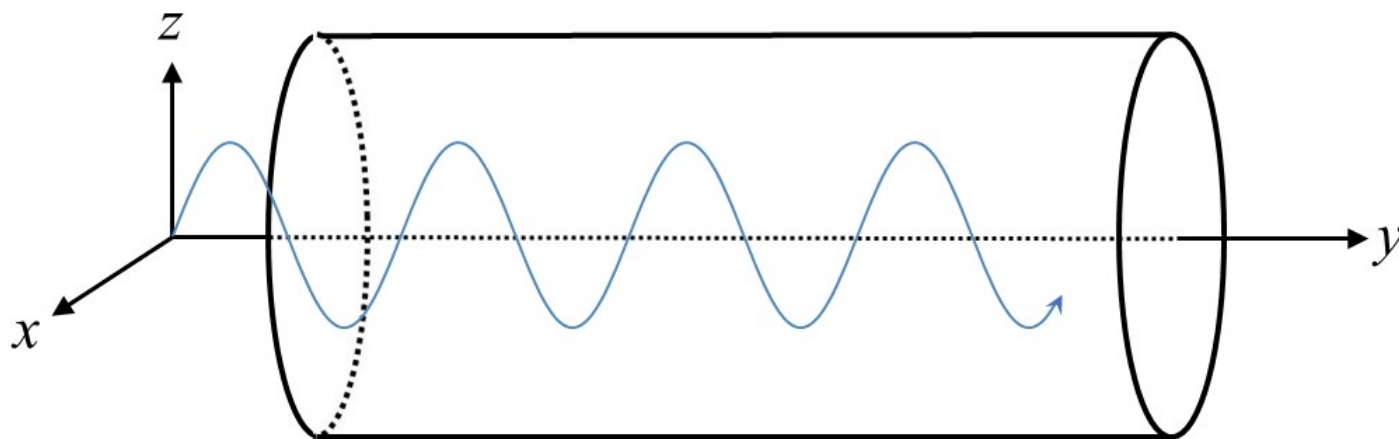


Figure 3.2: Schematic of a refractivity cell which would be placed in one arm of an interferometer. The laboratory reference frame $O(x,y,z)$ is oriented such that the z -axis is parallel to the direction of the oscillating electric field of the light wave.

The refractive index of a dielectric is typically measured interferometrically, using a monochromatic laser beam of known frequency. For example, using a Michelson interferometer, an evacuated cell with optical windows can be placed in the light path along one arm of the interferometer, and can then be slowly filled with the desired gas to a known final pressure. As the gas fills the cell, there will be fringe shifts (which arise because the wavelength of the light inside the gas changes), and these fringe shifts can be used to determine the refractive index. More sophisticated interferometric techniques for measuring the refractive indices of gases have been reported in the literature, for example [119–121].

Equations (3.57) and (2.86) combine to give

$$P_\alpha(\omega) = \varepsilon_0(\varepsilon_r(\omega) - 1)\mathcal{E}_\alpha = \mathcal{N}\bar{\mu}_\alpha = \frac{N_A}{V_m}\bar{\mu}_\alpha. \quad (3.61)$$

If the incident beam is plane polarized (a condition which is not necessary, but which helps to simplify the theoretical analysis), and the laboratory frame $O(x, y, z)$ is oriented such that y is in the direction of propagation of the light beam, the electric field of which oscillates in the yz plane such that $\mathcal{E}_\alpha = (0, 0, \mathcal{E}_z)$, then the induced polarization density simplifies to $P_z = \mathcal{N}\bar{\mu}_z$, and equation (3.61) becomes

$$P_z(\omega) = \varepsilon_0(\varepsilon_r(\omega) - 1)\mathcal{E}_z = \frac{N_A}{V_m}\bar{\mu}_z. \quad (3.62)$$

From equation (2.9), for a molecule in the presence of the light-wave electric field the total dipole moment is given by

$$\mu_i = \mu_i^{(0)} + \alpha_{ij}(-\omega; \omega)\mathcal{E}_j + \frac{1}{8}\gamma_{ijkl}(-\omega; \omega, -\omega, \omega)\mathcal{E}_j\mathcal{E}_k\mathcal{E}_l + \dots \quad (3.63)$$

The biased orientational average $\bar{\mu}_z$ in equation (3.61) is evaluated using a procedure analogous to that for the dielectric constant in Section (3.2). In the present case,

with the applied field oscillating at optical frequency, molecular inertial effects prevent any alignment of dipoles with the alternating field, so that the energy $U(\sigma, \mathcal{E}_z)$ of the molecule is simply the free energy of the molecule,

$$U(\sigma, \mathcal{E}_z) = U(\sigma) = U^{(0)} . \quad (3.64)$$

Here, the biased average $\bar{\mu}_z$ is converted into isotropic averages through a Taylor series expansion of $\bar{\mu}_z$ in powers of \mathcal{E}_z , namely

$$\bar{\mu}_z = \overline{\mu_z(\sigma, \mathcal{E})} = A + B \mathcal{E}_z + C \mathcal{E}_z^2 + \dots , \quad (3.65)$$

where

$$A = \left(\overline{\mu_z(\sigma, \mathcal{E})} \right)_{\mathcal{E}_z=0} , \quad B = \left(\frac{\partial \overline{\mu_z(\sigma, \mathcal{E})}}{\partial \mathcal{E}_z} \right)_{\mathcal{E}_z=0} \quad \text{and} \quad C = \frac{1}{2} \left(\frac{\partial^2 \overline{\mu_z(\sigma, \mathcal{E})}}{\partial \mathcal{E}_z^2} \right)_{\mathcal{E}_z=0} . \quad (3.66)$$

The leading non-vanishing term in the expansion is

$$B = \left\langle \frac{\partial \mu_z}{\partial \mathcal{E}_z} \right\rangle - \frac{1}{kT} \left\langle \mu_z \frac{\partial U}{\partial \mathcal{E}_z} \right\rangle , \quad (3.67)$$

and since from equation (3.64)

$$\frac{\partial U}{\partial \mathcal{E}_z} = 0 , \quad (3.68)$$

the temperature-dependent term in equation (3.67) drops to zero, this being a direct consequence of the light-wave field having no orienting effect on the molecules in the gas sample. B reduces to the contribution arising from distortion by the light-wave

field of the electronic structure of the molecules:

$$B = \left\langle \frac{\partial \mu_z}{\partial \mathcal{E}_z} \right\rangle. \quad (3.69)$$

Equation (3.63) gives

$$\mu_i = \mu_i^{(0)} + \alpha_{ij}(-\omega; \omega) \mathcal{E}_z a_j^z + \frac{1}{8} \gamma_{ijkl}(-\omega; \omega, -\omega, \omega) \mathcal{E}_z^3 a_j^z a_k^z a_l^z + \dots, \quad (3.70)$$

so that

$$\mu_z(\sigma, \mathcal{E}) = \mu_i a_i^z = \mu_i^{(0)} a_i^z + \alpha_{ij}(-\omega; \omega) \mathcal{E}_z a_i^z a_j^z + \frac{1}{8} \gamma_{ijkl}(-\omega; \omega, -\omega, \omega) \mathcal{E}_z^3 a_i^z a_j^z a_k^z a_l^z + \dots. \quad (3.71)$$

Hence,

$$\left(\frac{\partial \mu_z}{\partial \mathcal{E}_z} \right)_{\mathcal{E}_z=0} = \alpha_{ij}(-\omega; \omega) a_i^z a_j^z, \quad (3.72)$$

so that

$$B = \left\langle \frac{\partial \mu_z}{\partial \mathcal{E}_z} \right\rangle = \alpha_{ij}(-\omega; \omega) \langle a_i^z a_j^z \rangle = \frac{1}{3} \alpha_{ij}(-\omega; \omega) \delta_{ij} = \frac{1}{3} \alpha_{ii}(-\omega; \omega) = \alpha(-\omega; \omega) \quad (3.73)$$

where

$$\alpha(-\omega; \omega) = \frac{1}{3} \alpha_{ii}(-\omega; \omega) = \frac{1}{3} \left(\alpha_{11}(-\omega; \omega) + \alpha_{22}(-\omega; \omega) + \alpha_{33}(-\omega; \omega) \right) \quad (3.74)$$

is the mean dynamic polarizability. Equation (3.65) becomes

$$\bar{\mu}_z = \alpha(-\omega; \omega) \mathcal{E}_z, \quad (3.75)$$

where \mathcal{E}_z is the *local* field acting on the molecule, so that this expression for $\bar{\mu}_z$

should be written explicitly as

$$\bar{\mu}_z = \alpha(-\omega; \omega) \mathcal{E}_z^{\text{loc}}. \quad (3.76)$$

Invoking the Lorentz local field factor $f_L(\omega)$ for dynamic fields, given in equation (2.90), and substituting into equation (3.62) yields

$$P_z(\omega) = \varepsilon_0 (\varepsilon_r(\omega) - 1) \mathcal{E}_z = \frac{N_A}{V_m} \alpha(-\omega; \omega) \left(\frac{\varepsilon_r(\omega) + 2}{3} \right) \mathcal{E}_z. \quad (3.77)$$

This equation, together with equation (3.55), yields the Lorentz-Lorenz relation for the molar refraction R_m of an ideal gas [122, 123]

$$R_m = \frac{n^2 - 1}{n^2 + 2} V_m = \frac{N_A}{3\varepsilon_0} \alpha(-\omega; \omega). \quad (3.78)$$

3.4 ESHG in an ideal gas

In dc ESHG the medium is perturbed by a combination of both a static and a dynamic electric field by passing a polarized laser beam with oscillating electric field $\mathcal{E}_\alpha \cos(\omega t)$ through the gas in the presence of a static applied electric field E_α , as shown in Figure 3.3. The space-fixed laboratory frame $O(x, y, z)$ is oriented such that the z -axis is in the direction of the applied uniform field, giving $\mathbf{E} = (0, 0, E_z)$. The most common experimental arrangement has the light-wave field also polarized in the z -direction, and propagating in the y -direction, and this will be treated in the next section. The other significant experimental arrangement, which has the optical field polarized perpendicular to the static field (*i.e.* in the x -direction), will be treated in Section 3.4.2.

3.4.1 Static and dynamic fields with parallel polarization

The third-order polarization Fourier amplitude which gives rise to ESHG has been provided in equation (2.85), namely

$$P_\alpha^{(3)}(2\omega) = \frac{3}{2}\varepsilon_0\chi_{\alpha\beta\gamma\delta}^{(3)}(-2\omega; \omega, \omega, 0)\mathcal{E}_\beta\mathcal{E}_\gamma E_\delta. \quad (3.79)$$

This macroscopic polarization is related to the orientational average of a single molecule's electric dipole moment *via* equation (2.86), so that

$$P_\alpha^{(3)}(2\omega) = \frac{3}{2}\varepsilon_0\chi_{\alpha\beta\gamma\delta}^{(3)}(-2\omega; \omega, \omega, 0)\mathcal{E}_\beta\mathcal{E}_\gamma E_\delta = \mathcal{N}\overline{\mu_\alpha^{2\omega}} = \frac{N_A}{V_m}\overline{\mu_\alpha^{2\omega}}. \quad (3.80)$$

As was found for the linear electromagnetic effects of dielectric constant and refractive index (explored in sections 3.2 and 3.3, respectively), the induced polarization density in equation (3.80) simplifies to $P_z = \mathcal{N}\overline{\mu_z^{2\omega}}$ since the random molecular orientation in directions perpendicular to the applied fields means that the perpendicular polarization contributions $P_x = \mathcal{N}\overline{\mu_x^{2\omega}}$ and $P_y = \mathcal{N}\overline{\mu_y^{2\omega}}$ will average to zero:

$$P_z^{(3)}(2\omega) = \frac{3}{2}\varepsilon_0\chi_{z\beta\gamma\delta}^{(3)}(-2\omega; \omega, \omega, 0)\mathcal{E}_\beta\mathcal{E}_\gamma E_\delta = \frac{N_A}{V_m}\overline{\mu_z^{2\omega}}. \quad (3.81)$$

Here the experimental arrangement has the light-wave field polarized in the same direction as the applied static field, both in the z -direction of the laboratory frame, so that this becomes

$$P_z^{(3)}(2\omega) = \frac{3}{2}\varepsilon_0\chi_{zzzz}^{(3)}(-2\omega; \omega, \omega, 0)\mathcal{E}_z^2 E_z = \frac{N_A}{V_m}\overline{\mu_z^{2\omega}}. \quad (3.82)$$

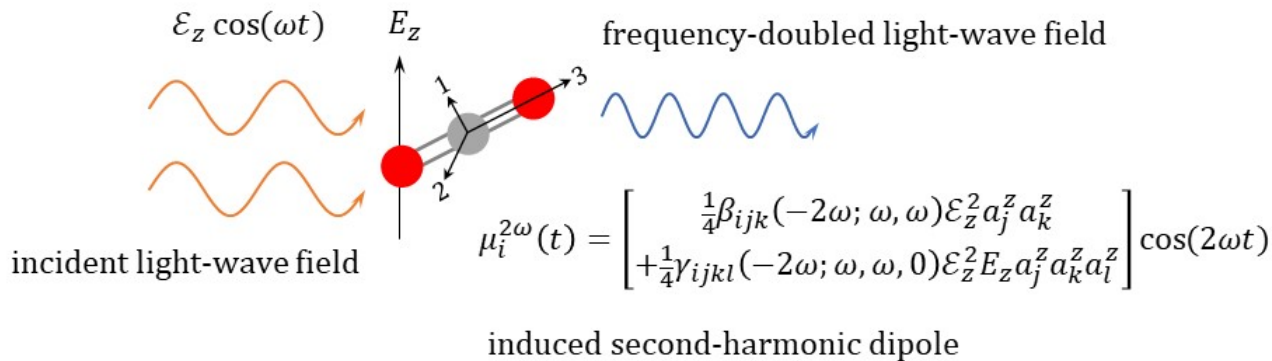


Figure 3.3: Schematic of the ESHG experiment for the particular case of static and dynamic fields having parallel polarization. The laboratory reference frame $O(x, y, z)$ is oriented such that the z -axis is parallel to the direction of both the uniform static electric field and the oscillating light-wave field. A carbon dioxide molecule is shown with molecule-fixed axes $O(1, 2, 3)$. The induced second-harmonic dipole moment yields the frequency-doubled light wave.

The task that remains is to evaluate $\overline{\mu_z^{2\omega}}$. For an isolated molecule within a sample of ideal gas in the presence of combined static and dynamic electric fields with parallel polarization, the total dipole moment oscillating at frequency 2ω is given by equation (2.57), namely

$$\mu_i^{2\omega} = \frac{1}{4}\beta_{ijk}(-2\omega; \omega, \omega)\mathcal{E}_j\mathcal{E}_k + \frac{1}{4}\gamma_{ijkl}(-2\omega; \omega, \omega, 0)\mathcal{E}_j\mathcal{E}_k E_l + \dots \quad (3.83)$$

Using the direction cosines $a_i^\alpha = a_\alpha^i$ between the α space-fixed axes and the i molecule-fixed axes, and with both fields polarized in the z -direction, the relationships between the applied fields expressed in molecule-fixed axes and space-fixed axes becomes

$$E_i = E_\alpha a_\alpha^i = E_z a_z^i \quad (3.84)$$

and

$$\mathcal{E}_i = \mathcal{E}_\alpha a_\alpha^i = \mathcal{E}_z a_z^i . \quad (3.85)$$

Then

$$\mu_i^{2\omega} = \frac{1}{4}\beta_{ijk}(-2\omega; \omega, \omega)\mathcal{E}_z^2 a_j^z a_k^z + \frac{1}{4}\gamma_{ijkl}(-2\omega; \omega, \omega, 0)\mathcal{E}_z^2 E_z a_j^z a_k^z a_l^z + \dots \quad (3.86)$$

with

$$\mu_z^{2\omega} = \mu_i^{2\omega} a_i^z . \quad (3.87)$$

The energy of the molecule is also required when evaluating the orientational average of $\mu_z^{2\omega}$, and is obtained from the total molecular electric dipole moment μ_i in the presence of the light-wave field and the applied field, bearing in mind that the terms in the optical field \mathcal{E}_α must in fact be omitted, since \mathcal{E}_α has no orienting effect on

a molecule. μ_i is given by equation (2.55) with terms in \mathcal{E}_i set to zero, yielding the same result as for equation (3.25) in the analysis of the dielectric constant, namely

$$\mu_i = \mu_i^{(0)} + \alpha_{ij}(0;0)E_j + \frac{1}{2}\beta_{ijk}(0;0,0)E_jE_k + \frac{1}{6}\gamma_{ijkl}(0;0,0,0)E_jE_kE_l + \dots . \quad (3.88)$$

From equation (3.16), for a neutral molecule in a uniform applied electric field,

$$U(\sigma, \mathbf{E}) = - \int_0^{\mathbf{E}} \mu_i dE_i . \quad (3.89)$$

Substituting equation (3.88) into this gives an expression for the energy of the molecule that is identical to the one in equation (3.26),

$$\begin{aligned} U(\sigma, \mathbf{E}) = U^{(0)} - \mu_i^{(0)}E_i - \frac{1}{2}\alpha_{ij}(0;0)E_iE_j - \frac{1}{6}\beta_{ijk}(0;0,0)E_iE_jE_k \\ - \frac{1}{24}\gamma_{ijkl}(0;0,0,0)E_iE_jE_kE_l - \dots . \end{aligned} \quad (3.90)$$

Setting $E_i = E_z a_z^i$ in equation (3.90) establishes the expression for the energy that will be required in deriving $\overline{\mu_z^{2\omega}}$:

$$\begin{aligned} U(\sigma, \mathbf{E}) = U^{(0)} - \mu_i^{(0)}E_z a_z^i - \frac{1}{2}\alpha_{ij}(0;0)E_z^2 a_z^i a_z^j - \frac{1}{6}\beta_{ijk}(0;0,0)E_z^3 a_z^i a_z^j a_z^k \\ - \frac{1}{24}\gamma_{ijkl}(0;0,0,0)E_z^4 a_z^i a_z^j a_z^k a_z^l - \dots . \end{aligned} \quad (3.91)$$

In a procedure analagous to the treatment of the linear electro-optic effects in Sections 3.2 and 3.3, the biased average $\overline{\mu_z^{2\omega}}$ is converted into isotropic averages through a Taylor series expansion of $\overline{\mu_z^{2\omega}}$ in powers of the applied field E_z .

$$\overline{\mu_z^{2\omega}} = \overline{\mu_z^{2\omega}(\sigma, \mathbf{E})} = A + B E_z + C E_z^2 + \dots , \quad (3.92)$$

where

$$A = \left(\overline{\mu_z^{2\omega}(\sigma, \mathbf{E})} \right)_{E_z=0}, \quad (3.93)$$

$$B = \left(\frac{\partial \overline{\mu_z^{2\omega}(\sigma, \mathbf{E})}}{\partial E_z} \right)_{E_z=0} \quad (3.94)$$

and

$$C = \frac{1}{2} \left(\frac{\partial^2 \overline{\mu_z^{2\omega}(\sigma, \mathbf{E})}}{\partial E_z^2} \right)_{E_z=0}. \quad (3.95)$$

From equations (3.86) and (3.87),

$$\begin{aligned} \mu_z^{2\omega}(\sigma, \mathbf{E}) &= \mu_i^{2\omega} a_i^z = \frac{1}{4} \beta_{ijk}(-2\omega; \omega, \omega) \mathcal{E}_z^2 a_i^z a_j^z a_k^z \\ &+ \frac{1}{4} \gamma_{ijkl}(-2\omega; \omega, \omega, 0) \mathcal{E}_z^2 E_z a_i^z a_j^z a_k^z a_l^z + \dots \end{aligned} \quad (3.96)$$

It follows that

$$A = \left(\overline{\mu_z^{2\omega}(\sigma, \mathbf{E})} \right)_{E_z=0} = \frac{1}{4} \beta_{ijk}(-2\omega; \omega, \omega) \mathcal{E}_z^2 \langle a_i^z a_j^z a_k^z \rangle = 0 \quad (3.97)$$

since, according to equation (3.34), $\langle a_i^z a_j^z a_k^z \rangle = 0$.

The leading term is B , which has been evaluated in equation (3.40), giving

$$B = \left(\frac{\partial \overline{\mu_z^{2\omega}}}{\partial E_z} \right)_{E_z=0} = \left\langle \frac{\partial \mu_z^{2\omega}}{\partial E_z} \right\rangle - \frac{1}{kT} \left\langle \mu_z^{2\omega} \frac{\partial U}{\partial E_z} \right\rangle + \frac{1}{kT} \langle \mu_z^{2\omega} \rangle \left\langle \frac{\partial U}{\partial E_z} \right\rangle. \quad (3.98)$$

Since $A = \langle \mu_z^{2\omega} \rangle = 0$, the expression for B reduces to

$$B = \left\langle \frac{\partial \mu_z^{2\omega}}{\partial E_z} \right\rangle - \frac{1}{kT} \left\langle \mu_z^{2\omega} \frac{\partial U}{\partial E_z} \right\rangle. \quad (3.99)$$

Equation (3.96) provides

$$\left(\frac{\partial \mu_z^{2\omega}}{\partial E_z} \right)_{E_z=0} = \frac{1}{4} \gamma_{ijkl}(-2\omega; \omega, \omega, 0) \mathcal{E}_z^2 a_i^z a_j^z a_k^z a_l^z, \quad (3.100)$$

and so

$$\begin{aligned} \left\langle \frac{\partial \mu_z^{2\omega}}{\partial E_z} \right\rangle &= \frac{1}{4} \gamma_{ijkl}(-2\omega; \omega, \omega, 0) \mathcal{E}_z^2 \left\langle a_i^z a_j^z a_k^z a_l^z \right\rangle \\ &= \frac{1}{4} \gamma_{ijkl}(-2\omega; \omega, \omega, 0) \mathcal{E}_z^2 \cdot \frac{1}{15} \left(\delta_{ij} \delta_{kl} + \delta_{ik} \delta_{jl} + \delta_{il} \delta_{jk} \right) \\ &= \frac{1}{60} \left[\gamma_{iijj}(-2\omega; \omega, \omega, 0) + \gamma_{ijij}(-2\omega; \omega, \omega, 0) + \gamma_{ijji}(-2\omega; \omega, \omega, 0) \right] \mathcal{E}_z^2. \end{aligned} \quad (3.101)$$

Since $\gamma_{ijkl}(-2\omega; \omega, \omega, 0)$ is symmetric in the suffices jk , equation (3.101) reduces to

$$\left\langle \frac{\partial \mu_z^{2\omega}}{\partial E_z} \right\rangle = \frac{1}{60} \left[2\gamma_{iijj}(-2\omega; \omega, \omega, 0) + \gamma_{ijji}(-2\omega; \omega, \omega, 0) \right] \mathcal{E}_z^2. \quad (3.102)$$

From equation (3.96),

$$\left(\mu_z^{2\omega} \right)_{E_z=0} = \frac{1}{4} \beta_{ijk}(-2\omega; \omega, \omega) \mathcal{E}_z^2 a_i^z a_j^z a_k^z, \quad (3.103)$$

while from equation (3.91)

$$\left(\frac{\partial U}{\partial E_z} \right)_{E_z=0} = -\mu_l^{(0)} a_l^z, \quad (3.104)$$

so that

$$\left(\mu_z^{2\omega} \frac{\partial U}{\partial E_z} \right)_{E_z=0} = -\frac{1}{4} \beta_{ijk}(-2\omega; \omega, \omega) \mu_l^{(0)} \mathcal{E}_z^2 a_i^z a_j^z a_k^z a_l^z. \quad (3.105)$$

Hence

$$\begin{aligned} \left\langle \mu_z^{2\omega} \frac{\partial U}{\partial E_z} \right\rangle &= -\frac{1}{4} \beta_{ijk}(-2\omega; \omega, \omega) \mu_l^{(0)} \mathcal{E}_z^2 \left\langle a_i^z a_j^z a_k^z a_l^z \right\rangle \\ &= -\frac{1}{4} \beta_{ijk}(-2\omega; \omega, \omega) \mu_l^{(0)} \mathcal{E}_z^2 \cdot \frac{1}{15} \left(\delta_{ij} \delta_{kl} + \delta_{ik} \delta_{jl} + \delta_{il} \delta_{jk} \right) \\ &= -\frac{1}{60} \left[\beta_{iij}(-2\omega; \omega, \omega) \mu_j^{(0)} + \beta_{iji}(-2\omega; \omega, \omega) \mu_j^{(0)} + \beta_{jii}(-2\omega; \omega, \omega) \mu_j^{(0)} \right] \mathcal{E}_z^2. \end{aligned} \quad (3.106)$$

$\beta_{ijk}(-2\omega; \omega, \omega)$ is symmetric in the suffices jk so that equation (3.106) reduces to

$$\left\langle \mu_z^{2\omega} \frac{\partial U}{\partial E_z} \right\rangle = -\frac{1}{60} \left[2\beta_{iij}(-2\omega; \omega, \omega) \mu_j^{(0)} + \beta_{jii}(-2\omega; \omega, \omega) \mu_j^{(0)} \right] \mathcal{E}_z^2. \quad (3.107)$$

From equation (3.92),

$$\overline{\mu_z^{2\omega}} = B E_z = \left[\left\langle \frac{\partial \mu_z^{2\omega}}{\partial E_z} \right\rangle - \frac{1}{kT} \left\langle \mu_z^{2\omega} \frac{\partial U}{\partial E_z} \right\rangle \right] E_z, \quad (3.108)$$

hence

$$\overline{\mu_z^{2\omega}} = \frac{1}{4} \left[\gamma_{\parallel}^{\text{ESHG}} + \frac{\mu_3}{3kT} \beta_{\parallel}^{\text{ESHG}} \right] \mathcal{E}_z^2 E_z. \quad (3.109)$$

Here the experimentally measurable hyperpolarizabilities $\gamma_{\parallel}^{\text{ESHG}}$ and $\beta_{\parallel}^{\text{SHG}}$ have a parallel subscript to indicate that both applied fields (static and dynamic) have parallel polarization, and from equations (3.102) and (3.107) respectively, they are

given by

$$\gamma_{\parallel}^{\text{ESHG}} = \frac{1}{15} \left(2\gamma_{iijj}(-2\omega; \omega, \omega, 0) + \gamma_{ijji}(-2\omega; \omega, \omega, 0) \right) \quad (3.110)$$

and

$$\beta_{\parallel}^{\text{SHG}} = \frac{1}{5} \left(2\beta_{iiz}(-2\omega; \omega, \omega) + \beta_{3ii}(-2\omega; \omega, \omega) \right). \quad (3.111)$$

In equation (3.109), it must be remembered that each of the incident fields are local fields, and these are now written explicitly as such:

$$\overline{\mu_z^{2\omega}} = \frac{1}{4} \left[\gamma_{\parallel}^{\text{ESHG}} + \frac{\mu_3}{3kT} \beta_{\parallel}^{\text{SHG}} \right] (\mathcal{E}_z^{\text{loc}})^2 E_z^{\text{loc}}. \quad (3.112)$$

The local fields are related to the applied fields *via* equation (2.92) for the Lorentz local field factor $f_L(0)$ for the static applied field and *via* equation (2.90) for the Lorentz local field factor $f_L(\omega)$ for the applied light-wave field. In addition, a local field correction factor $f_L(2\omega)$ must also be included for the field generated by the nonlinear action, arising from the induced dipole oscillating at frequency 2ω . Hence, equation (3.112) becomes

$$\overline{\mu_z^{2\omega}} = f_L(0) f_L^2(\omega) f_L(2\omega) \frac{1}{4} \left[\gamma_{\parallel}^{\text{ESHG}} + \frac{\mu_3}{3kT} \beta_{\parallel}^{\text{SHG}} \right] \mathcal{E}_z^2 E_z \quad (3.113)$$

where

$$\begin{aligned} f_L(0) f_L^2(\omega) f_L(2\omega) &= \left(\frac{\varepsilon_r + 2}{3} \right) \left(\frac{\varepsilon_r(\omega) + 2}{3} \right)^2 \left(\frac{\varepsilon_r(2\omega) + 2}{3} \right) \\ &= \left(\frac{\varepsilon_r + 2}{3} \right) \left(\frac{n_\omega^2 + 2}{3} \right)^2 \left(\frac{n_{2\omega}^2 + 2}{3} \right). \end{aligned} \quad (3.114)$$

Here, n_ω is the refractive index of the gas at frequency ω . While equation (3.113) will hold for a gas of non-dipolar molecules at lower pressures, for a gas at higher

pressures or comprised of strongly dipolar molecules, the Lorentz local field factor $f_L(0)$ for the static applied field would need to be replaced by the Onsager local field factor $f_O(0)$ given in equation (2.92).

The third-order polarization given in equation (3.82) is

$$P_z^{(3)}(2\omega) = \frac{3}{2}\varepsilon_0\chi_{zzzz}^{(3)}(-2\omega; \omega, \omega, 0)\mathcal{E}_z^2 E_z = \frac{N_A}{V_m}\overline{\mu_z^{2\omega}}, \quad (3.115)$$

and substituting in for $\overline{\mu_z^{2\omega}}$ given by equation (3.113), it follows that

$$\frac{3}{2}\varepsilon_0\chi_{zzzz}^{(3)}(-2\omega; \omega, \omega, 0)\mathcal{E}_z^2 E_z = \frac{N_A}{V_m}f_L(0)f_L^2(\omega)f_L(2\omega)\frac{1}{4}\left[\gamma_{\parallel}^{\text{ESHG}} + \frac{\mu_3}{3kT}\beta_{\parallel}^{\text{SHG}}\right]\mathcal{E}_z^2 E_z. \quad (3.116)$$

Hence, the third-order susceptibility is found to be

$$\chi_{zzzz}^{(3)}(-2\omega; \omega, \omega, 0) = \frac{1}{6}f_L(0)f_L^2(\omega)f_L(2\omega)\frac{N_A}{\varepsilon_0 V_m}\left[\gamma_{\parallel}^{\text{ESHG}} + \frac{\mu_3}{3kT}\beta_{\parallel}^{\text{SHG}}\right]. \quad (3.117)$$

This equation was first obtained by Kielich [17–21], and has been used in the extraction of molecular hyperpolarizabilities from gas-phase measurements of the third-order nonlinear optical susceptibilities of a range of atoms and small molecules [22–53].

Attention is now focused on the case in which the optical field is polarized perpendicular to the static field.

3.4.2 Dynamic field polarized perpendicular to static field

dc ESHG experiments have also been undertaken with the light-wave field polarized perpendicular to the static applied field [22, 23, 25–28]. If the laboratory frame $O(x, y, z)$ is oriented such that the relatively strong static applied field is in the

z -direction while the (relatively weak) oscillating optical field is polarized in the x -direction, then $E_i = E_z a_z^i$ and $\mathcal{E}_i = \mathcal{E}_x a_x^i$. Here, the surviving third-order polarization Fourier amplitude is

$$\begin{aligned} P_z^{(3)}(2\omega) &= \frac{3}{2} \varepsilon_0 \chi_{z\beta\gamma\delta}^{(3)}(-2\omega; \omega, \omega, 0) \mathcal{E}_\beta \mathcal{E}_\gamma E_\delta = \frac{N_A}{V_m} \overline{\mu_z^{2\omega}} \\ &= \frac{3}{2} \varepsilon_0 \chi_{zxzx}^{(3)}(-2\omega; \omega, \omega, 0) \mathcal{E}_x^2 E_z = \frac{N_A}{V_m} \overline{\mu_z^{2\omega}}. \end{aligned} \quad (3.118)$$

For a molecule in the gas, the total dipole moment oscillating at frequency 2ω as given by equation (3.83) becomes

$$\mu_i^{2\omega} = \frac{1}{4} \beta_{ijk}(-2\omega; \omega, \omega) \mathcal{E}_x^2 a_j^x a_k^x + \frac{1}{4} \gamma_{ijkl}(-2\omega; \omega, \omega, 0) \mathcal{E}_x^2 E_z a_j^x a_k^x a_l^z + \dots \quad (3.119)$$

Hence,

$$\begin{aligned} \mu_z^{2\omega}(\sigma, \mathbf{E}) &= \mu_i^{2\omega} a_i^z = \frac{1}{4} \beta_{ijk}(-2\omega; \omega, \omega) \mathcal{E}_x^2 a_i^z a_j^x a_k^x \\ &\quad + \frac{1}{4} \gamma_{ijkl}(-2\omega; \omega, \omega, 0) \mathcal{E}_x^2 E_z a_i^z a_j^x a_k^x a_l^z + \dots \end{aligned} \quad (3.120)$$

The energy of the molecule remains as given in equation (3.91), namely

$$\begin{aligned} U(\sigma, \mathbf{E}) &= U^{(0)} - \mu_i^{(0)} E_z a_i^z - \frac{1}{2} \alpha_{ij}(0; 0) E_z^2 a_i^z a_j^z - \frac{1}{6} \beta_{ijk}(0; 0, 0) E_z^3 a_i^z a_j^z a_k^z \\ &\quad - \frac{1}{24} \gamma_{ijkl}(0; 0, 0, 0) E_z^4 a_i^z a_j^z a_k^z a_l^z - \dots \end{aligned} \quad (3.121)$$

Again, the biased average $\overline{\mu_z^{2\omega}}$ is converted into isotropic averages through a Taylor series expansion of $\overline{\mu_z^{2\omega}}$ in powers of the applied field E_z :

$$\overline{\mu_z^{2\omega}} = \overline{\mu_z^{2\omega}(\sigma, \mathbf{E})} = A + B E_z + C E_z^2 + \dots, \quad (3.122)$$

where the leading surviving term remains

$$B = \left\langle \frac{\partial \mu_z^{2\omega}}{\partial E_z} \right\rangle - \frac{1}{kT} \left\langle \mu_z^{2\omega} \frac{\partial U}{\partial E_z} \right\rangle. \quad (3.123)$$

Equation (3.120) provides

$$\left(\frac{\partial \mu_z^{2\omega}}{\partial E_z} \right)_{E_z=0} = \frac{1}{4} \gamma_{ijkl}(-2\omega; \omega, \omega, 0) \mathcal{E}_x^2 a_i^z a_j^x a_k^x a_l^z, \quad (3.124)$$

so that

$$\begin{aligned} \left\langle \frac{\partial \mu_z^{2\omega}}{\partial E_z} \right\rangle &= \frac{1}{4} \gamma_{ijkl}(-2\omega; \omega, \omega, 0) \mathcal{E}_x^2 \left\langle a_j^x a_k^x a_i^z a_l^z \right\rangle \\ &= \frac{1}{4} \gamma_{ijkl}(-2\omega; \omega, \omega, 0) \mathcal{E}_x^2 \cdot \frac{1}{30} \left(4\delta_{jk}\delta_{il} - \delta_{ji}\delta_{kl} - \delta_{jl}\delta_{ki} \right) \\ &= \frac{1}{120} \left[4\gamma_{ijji}(-2\omega; \omega, \omega, 0) - \gamma_{iijj}(-2\omega; \omega, \omega, 0) - \gamma_{ijij}(-2\omega; \omega, \omega, 0) \right] \mathcal{E}_x^2 \\ &= \frac{1}{120} \left[4\gamma_{ijji}(-2\omega; \omega, \omega, 0) - 2\gamma_{iijj}(-2\omega; \omega, \omega, 0) \right] \mathcal{E}_x^2 \\ &= \frac{1}{60} \left[2\gamma_{ijji}(-2\omega; \omega, \omega, 0) - \gamma_{iijj}(-2\omega; \omega, \omega, 0) \right] \mathcal{E}_x^2. \end{aligned} \quad (3.125)$$

From equation (3.120),

$$\left(\mu_z^{2\omega} \right)_{E_z=0} = \frac{1}{4} \beta_{ijk}(-2\omega; \omega, \omega) \mathcal{E}_x^2 a_i^z a_j^x a_k^x, \quad (3.126)$$

while from equation (3.121)

$$\left(\frac{\partial U}{\partial E_z} \right)_{E_z=0} = -\mu_l^{(0)} a_l^z, \quad (3.127)$$

so that

$$\left(\mu_z^{2\omega} \frac{\partial U}{\partial E_z} \right)_{E_z=0} = -\frac{1}{4} \beta_{ijk}(-2\omega; \omega, \omega) \mu_l^{(0)} \mathcal{E}_x^2 a_i^z a_j^x a_k^x a_l^z. \quad (3.128)$$

Hence

$$\begin{aligned} \left\langle \mu_z^{2\omega} \frac{\partial U}{\partial E_z} \right\rangle &= -\frac{1}{4} \beta_{ijk}(-2\omega; \omega, \omega) \mu_l^{(0)} \mathcal{E}_x^2 \left\langle a_i^z a_j^x a_k^x a_l^z \right\rangle \\ &= -\frac{1}{4} \beta_{ijk}(-2\omega; \omega, \omega) \mu_l^{(0)} \mathcal{E}_x^2 \cdot \frac{1}{30} \left(4\delta_{jk}\delta_{il} - \delta_{ji}\delta_{kl} - \delta_{jl}\delta_{ki} \right) \\ &= -\frac{1}{120} \left[4\beta_{jii}(-2\omega; \omega, \omega) \mu_j^{(0)} - \beta_{iij}(-2\omega; \omega, \omega) \mu_j^{(0)} - \beta_{iji}(-2\omega; \omega, \omega) \mu_j^{(0)} \right] \mathcal{E}_x^2 \\ &= -\frac{1}{60} \left[2\beta_{jii}(-2\omega; \omega, \omega) \mu_j^{(0)} - \beta_{iij}(-2\omega; \omega, \omega) \mu_j^{(0)} \right] \mathcal{E}_x^2. \end{aligned} \quad (3.129)$$

From equation (3.122),

$$\overline{\mu_z^{2\omega}} = B E_z = \left[\left\langle \frac{\partial \mu_z^{2\omega}}{\partial E_z} \right\rangle - \frac{1}{kT} \left\langle \mu_z^{2\omega} \frac{\partial U}{\partial E_z} \right\rangle \right] E_z, \quad (3.130)$$

hence

$$\overline{\mu_z^{2\omega}} = \frac{1}{4} \left[\gamma_{\perp}^{\text{ESHG}} + \frac{\mu_3}{3kT} \beta_{\perp}^{\text{SHG}} \right] \mathcal{E}_x^2 E_z. \quad (3.131)$$

Here the experimentally measurable hyperpolarizabilities $\gamma_{\perp}^{\text{ESHG}}$ and $\beta_{\perp}^{\text{SHG}}$ have a perpendicular subscript to indicate that the optical applied field is perpendicular to the static field, and from equations (3.125) and (3.129) respectively, they are given by

$$\gamma_{\perp}^{\text{ESHG}} = \frac{1}{15} \left(2\gamma_{ijji}(-2\omega; \omega, \omega, 0) - \gamma_{iijj}(-2\omega; \omega, \omega, 0) \right) \quad (3.132)$$

and

$$\beta_{\perp}^{\text{ESHG}} = \frac{1}{5} \left(2\beta_{3ii}(-2\omega; \omega, \omega) - \beta_{ii3}(-2\omega; \omega, \omega) \right). \quad (3.133)$$

The applied fields in equation (3.131) are local fields, which are written explicitly as

$$\overline{\mu_z^{2\omega}} = \frac{1}{4} \left[\gamma_{\perp}^{\text{ESHG}} + \frac{\mu_3}{3kT} \beta_{\perp}^{\text{SHG}} \right] (\mathcal{E}_x^{\text{loc}})^2 E_z^{\text{loc}}. \quad (3.134)$$

Equation (3.134) becomes

$$\overline{\mu_z^{2\omega}} = f_{\text{L}}(0) f_{\text{L}}^2(\omega) f_{\text{L}}(2\omega) \frac{1}{4} \left[\gamma_{\perp}^{\text{ESHG}} + \frac{\mu_3}{3kT} \beta_{\perp}^{\text{SHG}} \right] \mathcal{E}_x^2 E_z \quad (3.135)$$

where \mathcal{E}_x and E_z are the applied macroscopic fields, and where the Lorentz local field factors are

$$f_{\text{L}}(0) f_{\text{L}}^2(\omega) f_{\text{L}}(2\omega) = \left(\frac{\varepsilon_r + 2}{3} \right) \left(\frac{n_{\omega}^2 + 2}{3} \right)^2 \left(\frac{n_{2\omega}^2 + 2}{3} \right). \quad (3.136)$$

Substituting equation (3.135) into equation (3.118) and rearranging for the third-order susceptibility yields

$$\chi_{zzxz}^{(3)}(-2\omega; \omega, \omega, 0) = \frac{1}{6} f_{\text{L}}(0) f_{\text{L}}^2(\omega) f_{\text{L}}(2\omega) \frac{N_{\text{A}}}{\varepsilon_0 V_{\text{m}}} \left[\gamma_{\perp}^{\text{ESHG}} + \frac{\mu_3}{3kT} \beta_{\perp}^{\text{SHG}} \right]. \quad (3.137)$$

Single-temperature gas-phase measurements of the third-order macroscopic susceptibility $\chi_{zzxz}^{(3)}(-2\omega; \omega, \omega, 0)$ for atoms or non-dipolar molecules (for which μ_3 and $\beta_{\perp}^{\text{SHG}}$ are both zero) allow for the extraction of $\gamma_{\perp}^{\text{ESHG}}$. For dipolar molecules, temperature-dependent measurements of $\chi_{zzxz}^{(3)}(-2\omega; \omega, \omega, 0)$ are required if both first and second molecular hyperpolarizabilities are to be deduced.

In the next chapter, a theory to account for the effects of intermolecular pair interactions on ESHG in a real gas will be developed.

Chapter 4

The Theory of ESHG for a Real Gas

4.1 Interacting non-dipolar molecules

In the previous chapter, the molecular-tensor theory to account for ESHG in an ideal gas was reviewed. In this chapter, the theory is extended to account for ESHG in a real gas. For these higher gas densities, the approach adopted by Buckingham and Pople for the treatment of intermolecular interaction effects *via* a virial expansion is followed [124]. This approach is now briefly reviewed:

A range of electromagnetic properties of gases are found to be proportional to the number density of the constituent molecules. For ideal gases, this proportionality will be exact since there are no interactions between the molecules, each molecule existing as an independent system. For real gases, where intermolecular interactions occur, the electromagnetic properties display a non-linear dependence on the number density of the molecules.

In 1956, Buckingham and Pople accounted for these intermolecular interaction ef-

fects through the use of a virial-type expansion [124]. If Q is a measurable molecular-optic property of a real gas, Q can be expressed as a virial expansion in inverse powers of the molar volume V_m :

$$Q = A_Q + \frac{B_Q}{V_m} + \frac{C_Q}{V_m^2} + \dots . \quad (4.1)$$

Here, the first virial coefficient A_Q is the ideal gas contribution to Q , B_Q is the second virial coefficient accounting for the contribution to Q from interacting pairs of molecules, while the third virial coefficient C_Q gives the contribution arising from interacting triplets. The virial coefficients are functions only of the temperature, or in the case of molecular-optical phenomena, of temperature and the wavelength of the light [124].

For a mole of ideal-gas molecules, the N_A mean contributions \bar{q} of the individual isolated molecules sum to the molar quantity Q , so that

$$Q = A_Q = N_A \bar{q} . \quad (4.2)$$

At higher gas densities, a representative molecule 1 in the sample will, on occasion, be interacting with a neighbouring molecule 2. If the relative intermolecular configuration is described by τ , then their contribution to Q at any given instant will be $q_{12}(\tau)$. Treating molecule 1 as half of an interacting pair, its contribution to Q at a given instant is $\frac{1}{2}q_{12}(\tau)$. Neglecting triplet and higher-order interactions, Q becomes

$$Q = N_A \left\{ \bar{q} + \int_{\tau} \left[\frac{1}{2}q_{12}(\tau) - \bar{q} \right] P(\tau) d\tau \right\} , \quad (4.3)$$

where $P(\tau) d\tau$ is the probability that molecule 1 has a neighbour in the range $(\tau, \tau + d\tau)$. The relationship between the intermolecular potential energy $U_{12}(\tau)$ and the

probability function is given by

$$P(\tau) = \frac{N_A}{\Omega V_m} e^{-U_{12}(\tau)/kT} , \quad (4.4)$$

where $\Omega = V_m^{-1} \int_{\tau} d\tau$. From equation (4.1),

$$B_Q = \lim_{V_m \rightarrow \infty} (Q - A_Q) V_m , \quad (4.5)$$

which combined with equations (4.2) to (4.4) gives

$$B_Q = \frac{N_A^2}{\Omega} \int_{\tau} \left[\frac{1}{2} q_{12}(\tau) - \bar{q} \right] e^{-U_{12}(\tau)/kT} d\tau . \quad (4.6)$$

This general expression for B_Q can be applied to whichever molecular-optical property Q is under consideration. In this project, it is applied to the second ESHG virial coefficient B_γ for interacting pairs of non-dipolar molecules.

Recall from equations (3.108), (3.112) and (3.113) that for an ideal gas in the presence of a static applied electric field and an oscillating light-wave electric field which are parallel (in the z space-fixed direction),

$$\begin{aligned} \overline{\mu_z^{2\omega}} &= \overline{\mu_z(2\omega)} = B E_z^{\text{loc}} = \left(\frac{\partial \overline{\mu_z^{2\omega}}}{\partial E_z^{\text{loc}}} \right)_{E_z^{\text{loc}}=0} E_z^{\text{loc}} \\ &= \left[\left\langle \frac{\partial \mu_z^{2\omega}}{\partial E_z^{\text{loc}}} \right\rangle - \frac{1}{kT} \left\langle \mu_z^{2\omega} \frac{\partial U}{\partial E_z^{\text{loc}}} \right\rangle \right] E_z^{\text{loc}} \\ &= f_L(0) f_L^2(\omega) f_L(2\omega) \frac{1}{4} \left[\gamma_{\parallel}^{\text{ESHG}} + \frac{\mu_3}{3kT} \beta_{\parallel}^{\text{SHG}} \right] \mathcal{E}_z^2 E_z \end{aligned} \quad (4.7)$$

where $\overline{\mu_z^{2\omega}}$ is the average over all configurations σ of the quantity $\mu_i^{2\omega} a_i^z$ of a representative isolated molecule in the presence of the biasing influence of the applied field.

The macroscopic measurable quantity in an ESHG experiment is the third-order susceptibility $\chi_{zzzz}^{(3)}(-2\omega; \omega, \omega, 0)$, which for an ideal gas is related to $\overline{\mu_z^{2\omega}}$ in equations (3.82) to (3.117). From equation (3.117) one can define a molar ESHG constant ${}_m\Gamma$ as

$${}_m\Gamma = \frac{6\varepsilon_0\chi_{zzzz}^{(3)}(-2\omega; \omega, \omega, 0)}{f_L(0)f_L^2(\omega)f_L(2\omega)}V_m. \quad (4.8)$$

For higher gas pressures, the density dependence of the molar ESHG constant, ${}_m\Gamma(V_m)$, could then be expressed by a virial expansion analogous to equation (4.1), where the ideal-gas ${}_m\Gamma$ would be the first virial coefficient.

However, in Donley and Shelton's publication on the measurement of hyperpolarizabilities for interacting molecular pairs, they utilise a virial expansion of the measured density-dependent *molecular* hyperpolarizability $\Gamma(V_m)$ for non-dipolar molecules

$$\Gamma(V_m) = \frac{{}_m\Gamma(V_m)}{N_A} = A_\gamma + \frac{B_\gamma}{V_m} + \dots \quad (4.9)$$

where A_γ is the ideal-gas density-independent molecular hyperpolarizability $\gamma_{\parallel}^{\text{ESHG}}$, and where B_γ is the second ESHG virial coefficient. This is analogous to equation (4.1) where only the left-hand side has been divided by N_A , so that the expansion is no longer for macroscopic molar virial coefficients, but rather for microscopic molecular virial coefficients, yielding

$$\frac{Q}{N_A} = A_Q + \frac{B_Q}{V_m} + \frac{C_Q}{V_m^2} + \dots \quad (4.10)$$

Equations (4.2), (4.3) and (4.6) respectively become

$$\frac{Q}{N_A} = A_Q = \bar{q} , \quad (4.11)$$

$$\frac{Q}{N_A} = \bar{q} + \int_{\tau} \left[\frac{1}{2} q_{12}(\tau) - \bar{q} \right] P(\tau) d\tau , \quad (4.12)$$

and

$$B_Q = \frac{N_A}{\Omega} \int_{\tau} \left[\frac{1}{2} q_{12}(\tau) - \bar{q} \right] e^{-U_{12}(\tau)/kT} d\tau . \quad (4.13)$$

For an ESHG measurement at higher gas densities, the contribution of a representative molecule 1 to the macroscopic susceptibility is not always given by equation (4.7), there now being times when molecule 1 has to be treated as half of an interacting pair. When molecule 1 is in the presence of a neighbouring molecule 2, their relative configuration being specified by τ , then the instantaneous contribution of molecule 1 to the macroscopic susceptibility is $\frac{1}{2}\mu_z^{(12)}(2\omega)$ where

$$\mu_z^{(12)}(2\omega) = \mu_z^{(12)}(2\omega, \tau, \mathbf{E}) = \mu_i^{(12)}(2\omega) a_i^z . \quad (4.14)$$

$\mu_i^{(12)}(2\omega)$ is the induced second-harmonic dipole of the interacting pair, and a full expression for this must now be derived. Obtaining the biased orientational average $\overline{\mu_z^{(12)}(2\omega, \tau, \mathbf{E})}$ requires that the molecular pair is allowed to rotate as a rigid whole (in the fixed configuration τ) in the presence of the biasing influence of the applied uniform electric field E_a . This biased average is then converted into isotropic averages by means of a Taylor expansion in powers of E_z , in a procedure analagous to that performed in the case of an isolated molecule in equations (3.92) through to (3.114). (It is implicitly understood that these molecular properties experience local fields, and to circumvent laborious notation, the appropriate local field factor

corrections will only be applied to the end results.) The leading term emerges as

$$\overline{\mu_z^{(12)}(2\omega, \tau, \mathbf{E})}_{E_z=0} = \left(\frac{\overline{\partial \mu_z^{(12)}(2\omega, \tau, \mathbf{E})}}{\partial E_z} \right)_{E_z=0} E_z \quad (4.15)$$

where

$$\left(\frac{\overline{\partial \mu_z^{(12)}(2\omega, \tau, \mathbf{E})}}{\partial E_z} \right)_{E_z=0} = \left\langle \frac{\partial \mu_z^{(12)}(2\omega)}{\partial E_z} \right\rangle - \frac{1}{kT} \left\langle \mu_z^{(12)}(2\omega) \frac{\partial U^{(12)}}{\partial E_z} \right\rangle. \quad (4.16)$$

$U^{(12)} = U^{(12)}(\tau, 0)$ is the potential energy of the interacting pair of molecules when the applied field is removed. The quantities inside the angular brackets are initially referred to the molecule-fixed axes $O(1, 2, 3)$ of molecule 1. For a given interaction configuration τ , the tensor product in $O(1, 2, 3)$ will be fixed. Allowing the pair to rotate as a rigid whole in the laboratory frame $O(x, y, z)$, the average projection of the pair properties, referred to $O(1, 2, 3)$, will be averaged into $O(x, y, z)$ over all orientations. Averaging over the pair-interaction parameters τ can subsequently be undertaken.

We follow Donley and Shelton in writing the density dependence of the molecular ESHG constant $\Gamma(V_m)$ as the virial expansion contained in equation (4.9), namely

$$\Gamma(V_m) = \frac{m\Gamma(V_m)}{N_A} = A_\gamma + \frac{B_\gamma}{V_m} + \dots \quad (4.17)$$

Only gases of non-dipolar molecules will be considered in this work, and for an ideal gas of non-dipolar molecules, equation (3.112) yields

$$\overline{\mu_z^{2\omega}} = \frac{1}{4} \Gamma \mathcal{E}_z^2 E_z \quad (4.18)$$

where $\Gamma = \gamma_{\parallel}^{\text{ESHG}}$, and where the fields are all local fields. Hence the first ESHG

virial coefficient is

$$A_\gamma = \Gamma = \gamma_{\parallel}^{\text{ESHG}} = \frac{4}{\mathcal{E}_z^2 E_z} \cdot \overline{\mu_z^{2\omega}} = \frac{4}{\mathcal{E}_z^2} \left(\frac{\partial \overline{\mu_z^{2\omega}}}{\partial E_z} \right)_{E_z=0}. \quad (4.19)$$

From equation (4.13) B_γ is seen to be

$$\begin{aligned} B_\gamma &= \frac{N_A}{\Omega} \cdot \frac{4}{\mathcal{E}_z^2 E_z} \int_{\tau} \left[\frac{1}{2} \mu_z^{(12)}(2\omega, \tau, \mathbf{E}) - \overline{\mu_z(2\omega)} \right] e^{-U_{12}(\tau)/kT} d\tau \\ &= \frac{4N_A}{\Omega \mathcal{E}_z^2} \int_{\tau} \left[\frac{1}{2} \left(\frac{\partial \mu_z^{(12)}(2\omega, \tau, \mathbf{E})}{\partial E_z} \right)_{E_z=0} - \left(\frac{\partial \overline{\mu_z(2\omega)}}{\partial E_z} \right)_{E_z=0} \right] e^{-U_{12}(\tau)/kT} d\tau. \end{aligned} \quad (4.20)$$

The relative configuration τ of the two interacting molecules can be represented by the following seven parameters \dots the intermolecular separation R , the Euler angles α_1, β_1 and γ_1 defining the direction cosines a_i^α between the laboratory frame $O(x, y, z)$ (referred to by $\alpha, \beta, \gamma \dots$) and the molecule-fixed axes $O(1, 2, 3)$ of molecule 1 (referred to by $i, j, k \dots$), and the Euler angles α_2, β_2 and γ_2 defining the direction cosines a_i^α between the laboratory frame and the molecule-fixed axes $O(1', 2', 3')$ of molecule 2 (referred to by $i', j', k' \dots$). These parameters are fully described elsewhere [77, 125], together with evaluation of the normalization constant as $\Omega = (8\pi^2)^2$. The direction cosine tensors are found to be

$$\begin{aligned} a_i^\alpha &= \begin{bmatrix} \cos\gamma_1 & \sin\gamma_1 & 0 \\ -\sin\gamma_1 & \cos\gamma_1 & 0 \\ 0 & 0 & 1 \end{bmatrix} \begin{bmatrix} \cos\beta_1 & 0 & -\sin\beta_1 \\ 0 & 1 & 0 \\ \sin\beta_1 & 0 & \cos\beta_1 \end{bmatrix} \begin{bmatrix} \cos\alpha_1 & \sin\alpha_1 & 0 \\ -\sin\alpha_1 & \cos\alpha_1 & 0 \\ 0 & 0 & 1 \end{bmatrix} \\ &= \begin{bmatrix} \cos\alpha_1 \cos\beta_1 \cos\gamma_1 - \sin\alpha_1 \sin\gamma_1 & \sin\alpha_1 \cos\beta_1 \cos\gamma_1 + \cos\alpha_1 \sin\gamma_1 & -\sin\beta_1 \cos\gamma_1 \\ -\cos\alpha_1 \cos\beta_1 \sin\gamma_1 - \sin\alpha_1 \cos\gamma_1 & -\sin\alpha_1 \cos\beta_1 \sin\gamma_1 + \cos\alpha_1 \cos\gamma_1 & \sin\beta_1 \sin\gamma_1 \\ \cos\alpha_1 \sin\beta_1 & \sin\alpha_1 \sin\beta_1 & \cos\beta_1 \end{bmatrix}, \end{aligned} \quad (4.21)$$

$$a_{ij}^{\alpha} = \begin{bmatrix} \cos\alpha_2\cos\beta_2\cos\gamma_2 - \sin\alpha_2\sin\gamma_2 & \sin\alpha_2\cos\beta_2\cos\gamma_2 + \cos\alpha_2\sin\gamma_2 & -\sin\beta_2\cos\gamma_2 \\ -\cos\alpha_2\cos\beta_2\sin\gamma_2 - \sin\alpha_2\cos\gamma_2 & -\sin\alpha_2\cos\beta_2\sin\gamma_2 + \cos\alpha_2\cos\gamma_2 & \sin\beta_2\sin\gamma_2 \\ \cos\alpha_2\sin\beta_2 & \sin\alpha_2\sin\beta_2 & \cos\beta_2 \end{bmatrix}. \quad (4.22)$$

Equation (4.20) becomes

$$B_{\gamma} = \frac{N_A}{4\pi^3 \mathcal{E}_z^2} \int_{R=0}^{\infty} \int_{\alpha_1=0}^{2\pi} \int_{\beta_1=0}^{\pi} \int_{\gamma_1=0}^{2\pi} \int_{\alpha_2=0}^{2\pi} \int_{\beta_2=0}^{\pi} \int_{\gamma_2=0}^{2\pi} \\ \times \left[\frac{1}{2} \left(\frac{\overline{\partial\mu_z^{(12)}(2\omega, \tau, \mathbf{E})}}{\partial E_z} \right)_{E_z=0} - \left(\frac{\overline{\partial\mu_z(2\omega)}}{\partial E_z} \right)_{E_z=0} \right] e^{-U_{12}(\tau)/kT} \quad (4.23) \\ \times R^2 \sin\beta_1 \sin\beta_2 dR d\alpha_1 d\beta_1 d\gamma_1 d\alpha_2 d\beta_2 d\gamma_2 .$$

Integration over the pair interaction coordinates in equation (4.23) requires knowledge of both the intermolecular potential $U_{12}(\tau)$, and the expression

$$\frac{1}{2} \left(\frac{\overline{\partial\mu_z^{(12)}(2\omega, F)}}{\partial E_z} \right)_{E_z=0} \quad (4.24)$$

which contains the induced second-harmonic dipole $\mu_i^{(12)}(2\omega)$ of the interacting pair.

At this juncture, certain assumptions are made which need to be qualified. The interacting molecules are assumed to always retain their separate identities so that the classical long-range DID model can be invoked. In the long-range limit this will hold true, but at short ranges (*i.e.* of the order of molecular dimensions or smaller) the charge distributions of the molecules can start overlapping, so that classical multipole theory cannot adequately describe the interactions. A definitive description of the effects of the overlap of the molecular wavefunctions requires high-level *ab initio* quantum-mechanical calculations utilizing large basis sets with diffuse

basis functions, and taking into account electron correlation effects. Such calculations are computationally demanding even for interacting atoms and quasi-spherical molecules, and remain almost intractable for interacting molecules of low symmetry. By treating small molecules as if they retain their separate identities even in the region of overlap, the molecular interactions for Rayleigh light-scattering [125–128] and the Kerr effect [76–79] have been successfully modelled, with agreement between measured and calculated second virial coefficients of within 10% or better being realised. This perhaps provides some justification for the simplifying assumption. If this also holds true for the interaction-induced hyperpolarizabilities of molecules, then equation (4.14) can be written as

$$\mu_z^{(12)}(2\omega) = \mu_z^{(12)}(2\omega, \tau, \mathbf{E}) = \mu_i^{(12)}(2\omega) a_i^z = \left(\mu_i^{(1)}(2\omega) + \mu_i^{(2)}(2\omega) \right) a_i^z . \quad (4.25)$$

The potential energy of the interacting pair of molecules in the presence of the static applied field is [76]

$$U^{(12)}(\tau, \mathbf{E}) = U^{(12)}(\tau, 0) - \int_0^{\mathbf{E}} \mu_i^{(12)}(\tau, \mathbf{E}) dE_i , \quad (4.26)$$

where $\mu_i^{(12)}$ is the total dipole moment of the pair in the presence of \mathbf{E} which, using the above arguments, can be written as

$$\mu_i^{(12)}(0) = \mu_i^{(1)}(0) + \mu_i^{(2)}(0). \quad (4.27)$$

Here $\mu_i^{(p)}(0)$ is the total dipole of molecule p in the presence of E_i and molecule q, the terms in the light-wave field \mathcal{E}_i being omitted since \mathcal{E}_i does not orient a molecule. Hence, for interacting pairs of non-dipolar molecules the total static dipole and quadrupole moments induced in molecule p are provided by equations (2.55) and

(2.66) respectively, giving

$$\begin{aligned} \mu_i^{(p)}(0) &= \alpha_{ij}^{(p)}(0; 0) \left(E_j + F_j^{(p)} \right) + \frac{1}{6} \gamma_{ijkl}^{(p)}(0; 0, 0, 0) \left(E_j + F_j^{(p)} \right) \left(E_k + F_k^{(p)} \right) \left(E_l + F_l^{(p)} \right) \\ &\quad + \frac{1}{3} B_{ijkl}^{(p)}(0; 0, 0) \left(E_j + F_j^{(p)} \right) F_{kl}^{(p)} + \dots, \end{aligned} \quad (4.28)$$

and

$$\Theta_{ij}^{(p)}(0) = \Theta_{0ij}^{(p)} + C_{ijkl}^{(p)}(0; 0) F_{kl}^{(p)} + \frac{1}{2} D_{ijkl}^{(p)}(0; 0, 0) \left(E_k + F_k^{(p)} \right) \left(E_l + F_l^{(p)} \right) + \dots. \quad (4.29)$$

In these equations, $\Theta_{0ij}^{(p)}$ is the permanent molecular electric quadrupole moment of molecule p, and $F_j^{(p)}$ and $F_{jk}^{(p)}$ are the static field and field gradient arising at molecule p due to both the induced dipole and the permanent and induced quadrupole moments of molecule q.

Buckingham's T -tensors [83] are now invoked to aid with the analysis. $F_j^{(p)}$ is given by

$$F_j^{(p)} = T_{jk}^{(p)} \mu_k^{(q)}(0) - \frac{1}{3} T_{jkl}^{(p)} \Theta_{kl}^{(q)}(0), \quad (4.30)$$

while $F_{jk}^{(p)}$ is given by

$$F_{jk}^{(p)} = T_{jkl}^{(p)} \mu_l^{(q)}(0) - \frac{1}{3} T_{jklm}^{(p)} \Theta_{lm}^{(q)}(0), \quad (4.31)$$

where

$$T_{jk}^{(1)} = \frac{1}{4\pi\epsilon_0} \nabla_j \nabla_k R^{-1} = \frac{1}{4\pi\epsilon_0} (3R_j R_k - R^2 \delta_{jk}) R^{-5} \quad (4.32)$$

and

$$\begin{aligned}
 T_{jkl}^{(1)} &= -\frac{1}{4\pi\epsilon_0} \nabla_j \nabla_k \nabla_l R^{-1} \\
 &= \frac{3}{4\pi\epsilon_0} \left[5R_j R_k R_l - R^2 (R_j \delta_{kl} + R_k \delta_{jl} + R_l \delta_{jk}) \right] R^{-7}
 \end{aligned} \tag{4.33}$$

are the second and third rank T -tensors respectively. In these equations, \mathbf{R} is the vector from the origin of molecule 1 to the origin of molecule 2. Buckingham has also shown that

$$\mathbf{T}^{(1)} = (-1)^n \mathbf{T}^{(2)} \tag{4.34}$$

where n is the order of the T -tensor, so that the superscript may be omitted from T -tensors of even rank.

The higher-order (hyper)polarizabilities in equations (4.28) and (4.29) will henceforth be assumed to contribute negligibly to the second average in equation (4.16) since they will result in tensor products of higher-order polarizabilities. Consequently, $\Theta_{ij}^{(p)}(0)$ will be described solely by the leading contribution arising from the permanent quadrupole moment of the molecule. $\mu_i^{(p)}(0)$ and $\Theta_{ij}^{(p)}(0)$ become

$$\mu_i^{(p)}(0) = \alpha_{ij}^{(p)}(0;0) \left(E_j + F_j^{(p)} \right) + \dots, \tag{4.35}$$

$$\Theta_{ij}^{(p)}(0) = \Theta_{0ij}^{(p)} + \dots. \tag{4.36}$$

For molecule q the respective equations are

$$\mu_j^{(q)}(0) = \alpha_{jk}^{(p)}(0;0) \left(E_k + F_k^{(q)} \right) + \dots \tag{4.37}$$

and

$$\Theta_{jk}^{(q)}(0) = \Theta_{0jk}^{(q)} + \dots \quad (4.38)$$

with

$$F_k^{(q)} = T_{kl}\mu_l^{(p)}(0) - \frac{1}{3}T_{klm}^{(q)}\Theta_{lm}^{(p)}(0). \quad (4.39)$$

Successive substitutions of $F_j^{(p)}$ and $F_k^{(q)}$ into equation (4.35) give the interaction-induced contributions to the total static dipole $\mu_i^{(p)}(0)$ of molecule p as

$$\begin{aligned} \mu_i^{(p)}(0) = & -\frac{1}{3} \left(\alpha_{ij}^{(p)}(0;0)T_{jkv}^{(p)}\Theta_{0kv}^{(q)} + \alpha_{ij}^{(p)}(0;0)T_{jk}\alpha_{kl}^{(q)}(0;0)T_{lmv}^{(q)}\Theta_{0mv}^{(p)} \right. \\ & + \alpha_{ij}^{(p)}(0;0)T_{jk}\alpha_{kl}^{(q)}(0;0)T_{lm}\alpha_{mn}^{(p)}(0;0)T_{npv}^{(p)}\Theta_{0pv}^{(q)} \\ & \left. + \alpha_{ij}^{(p)}(0;0)T_{jk}\alpha_{kl}^{(q)}(0;0)T_{lm}\alpha_{mn}^{(p)}(0;0)T_{np}\alpha_{pq}^{(q)}(0;0)T_{qrv}^{(q)}\Theta_{0rv}^{(p)} + \dots \right) \\ & + \left(\alpha_{iv}^{(p)}(0;0) + \alpha_{ij}^{(p)}(0;0)T_{jk}\alpha_{kv}^{(q)}(0;0) + \alpha_{ij}^{(p)}(0;0)T_{jk}\alpha_{kl}^{(q)}(0;0)T_{lm}\alpha_{mv}^{(p)}(0;0) \right. \\ & + \alpha_{ij}^{(p)}(0;0)T_{jk}\alpha_{kl}^{(q)}(0;0)T_{lm}\alpha_{mn}^{(p)}(0;0)T_{np}\alpha_{pv}^{(q)}(0;0) \\ & \left. + \alpha_{ij}^{(p)}(0;0)T_{jk}\alpha_{kl}^{(q)}(0;0)T_{lm}\alpha_{mn}^{(p)}(0;0)T_{np}\alpha_{pq}^{(q)}(0;0)T_{qr}\alpha_{rv}^{(p)}(0;0) + \dots \right) E_v \\ & + O(E^2) + \dots \end{aligned} \quad (4.40)$$

Hence, using equations (4.40) and (4.27), equation (4.26) becomes

$$U^{(12)}(\tau, \mathbf{E}) = U^{(12)}(\tau, 0) + U^{(1)}(\tau, \mathbf{E}) + U^{(2)}(\tau, \mathbf{E}) \quad (4.41)$$

where

$$\begin{aligned}
U^{(p)}(\tau, \mathbf{E}) = & \frac{1}{3} \left(\alpha_{ij}^{(p)}(0; 0) T_{jkv}^{(p)} \Theta_{0kv}^{(q)} + \alpha_{ij}^{(p)}(0; 0) T_{jk} \alpha_{kl}^{(q)}(0; 0) T_{lmv}^{(q)} \Theta_{0mv}^{(p)} \right. \\
& + \alpha_{ij}^{(p)}(0; 0) T_{jk} \alpha_{kl}^{(q)}(0; 0) T_{lm} \alpha_{mn}^{(p)}(0; 0) T_{npv}^{(p)} \Theta_{0pv}^{(q)} \\
& + \alpha_{ij}^{(p)}(0; 0) T_{jk} \alpha_{kl}^{(q)}(0; 0) T_{lm} \alpha_{mn}^{(p)}(0; 0) T_{np} \alpha_{pq}^{(q)}(0; 0) T_{qrv}^{(q)} \Theta_{0rv}^{(p)} \\
& \left. + \dots \right) E_z a_i^z \\
& - \frac{1}{2} \left(\alpha_{iv}^{(p)}(0; 0) + \alpha_{ij}^{(p)}(0; 0) T_{jk} \alpha_{kv}^{(q)}(0; 0) \right. \\
& + \alpha_{ij}^{(p)}(0; 0) T_{jk} \alpha_{kl}^{(q)}(0; 0) T_{lm} \alpha_{mv}^{(p)}(0; 0) \\
& + \alpha_{ij}^{(p)}(0; 0) T_{jk} \alpha_{kl}^{(q)}(0; 0) T_{lm} \alpha_{mn}^{(p)}(0; 0) T_{np} \alpha_{pv}^{(q)}(0; 0) \\
& + \alpha_{ij}^{(p)}(0; 0) T_{jk} \alpha_{kl}^{(q)}(0; 0) T_{lm} \alpha_{mn}^{(p)}(0; 0) T_{np} \alpha_{pq}^{(q)}(0; 0) T_{qr} \alpha_{rv}^{(p)}(0; 0) \\
& \left. + \dots \right) E_z^2 a_i^z a_v^z \\
& - O(E^3) - \dots .
\end{aligned} \tag{4.42}$$

Equation (4.34) allows the third-rank T -tensors in equation (4.42) to be written as $T_{jkl}^{(1)} = -T_{jkl}^{(2)} = T_{jkl}$, so that the respective energies $U^{(1)}(\tau, \mathbf{E})$ and $U^{(2)}(\tau, \mathbf{E})$ of

molecules 1 and 2 can be written explicitly as

$$\begin{aligned}
U^{(1)}(\tau, \mathbf{E}) = & \frac{1}{3} \left(\alpha_{ab}^{(1)}(0; 0) T_{bgh} \Theta_{0gh}^{(2)} - \alpha_{ab}^{(1)}(0; 0) T_{bc} \alpha_{cd}^{(2)}(0; 0) T_{dgh} \Theta_{0gh}^{(1)} \right. \\
& + \alpha_{ab}^{(1)}(0; 0) T_{bc} \alpha_{cd}^{(2)}(0; 0) T_{de} \alpha_{ef}^{(1)}(0; 0) T_{fgh} \Theta_{0gh}^{(2)} \\
& - \alpha_{ab}^{(1)}(0; 0) T_{bc} \alpha_{cd}^{(2)}(0; 0) T_{de} \alpha_{ef}^{(1)}(0; 0) T_{fs} \alpha_{st}^{(2)}(0; 0) T_{tgh} \Theta_{0gh}^{(1)} \\
& \left. + \dots \right) E_z a_a^z \\
& - \frac{1}{2} \left(\alpha_{ah}^{(1)}(0; 0) + \alpha_{ab}^{(1)}(0; 0) T_{bc} \alpha_{ch}^{(2)}(0; 0) \right. \\
& + \alpha_{ab}^{(1)}(0; 0) T_{bc} \alpha_{cd}^{(2)}(0; 0) T_{de} \alpha_{eh}^{(1)}(0; 0) \\
& + \alpha_{ab}^{(1)}(0; 0) T_{bc} \alpha_{cd}^{(2)}(0; 0) T_{de} \alpha_{ef}^{(1)}(0; 0) T_{fg} \alpha_{gh}^{(2)}(0; 0) \\
& + \alpha_{ab}^{(1)}(0; 0) T_{bc} \alpha_{cd}^{(2)}(0; 0) T_{de} \alpha_{ef}^{(1)}(0; 0) T_{fg} \alpha_{gs}^{(2)}(0; 0) T_{st} \alpha_{th}^{(1)}(0; 0) \\
& \left. + \dots \right) E_z^2 a_a^z a_h^z \\
& - O(E^3) - \dots,
\end{aligned} \tag{4.43}$$

and

$$\begin{aligned}
U^{(2)}(\tau, \mathbf{E}) = & \frac{1}{3} \left(-\alpha_{ab}^{(2)}(0; 0) T_{bgh} \Theta_{0gh}^{(1)} + \alpha_{ab}^{(2)}(0; 0) T_{bc} \alpha_{cd}^{(1)}(0; 0) T_{dgh} \Theta_{0gh}^{(2)} \right. \\
& - \alpha_{ab}^{(2)}(0; 0) T_{bc} \alpha_{cd}^{(1)}(0; 0) T_{de} \alpha_{ef}^{(2)}(0; 0) T_{fgh} \Theta_{0gh}^{(1)} \\
& + \alpha_{ab}^{(2)}(0; 0) T_{bc} \alpha_{cd}^{(1)}(0; 0) T_{de} \alpha_{ef}^{(2)}(0; 0) T_{fs} \alpha_{st}^{(1)}(0; 0) T_{tgh} \Theta_{0gh}^{(2)} \\
& \left. + \dots \right) E_z a_a^z \\
& - \frac{1}{2} \left(\alpha_{ah}^{(2)}(0; 0) + \alpha_{ab}^{(2)}(0; 0) T_{bc} \alpha_{ch}^{(1)}(0; 0) \right. \\
& + \alpha_{ab}^{(2)}(0; 0) T_{bc} \alpha_{cd}^{(1)}(0; 0) T_{de} \alpha_{eh}^{(2)}(0; 0) \\
& + \alpha_{ab}^{(2)}(0; 0) T_{bc} \alpha_{cd}^{(1)}(0; 0) T_{de} \alpha_{ef}^{(2)}(0; 0) T_{fg} \alpha_{gh}^{(1)}(0; 0) \\
& + \alpha_{ab}^{(2)}(0; 0) T_{bc} \alpha_{cd}^{(1)}(0; 0) T_{de} \alpha_{ef}^{(2)}(0; 0) T_{fg} \alpha_{gs}^{(1)}(0; 0) T_{st} \alpha_{th}^{(2)}(0; 0) \\
& \left. + \dots \right) E_z^2 a_a^z a_h^z \\
& - O(E^3) - \dots
\end{aligned} \tag{4.44}$$

Attention is now focussed upon the second-harmonic oscillating dipole moment of molecule p, $\mu_i^{(p)}(2\omega)$, which is induced partly by the oscillating light-wave field \mathcal{E}_j and partly by the field $\mathcal{F}_j^{(p)}$ arising at molecule p due to the oscillating moments on molecule q, as illustrated schematically in Figure 4.1, so that

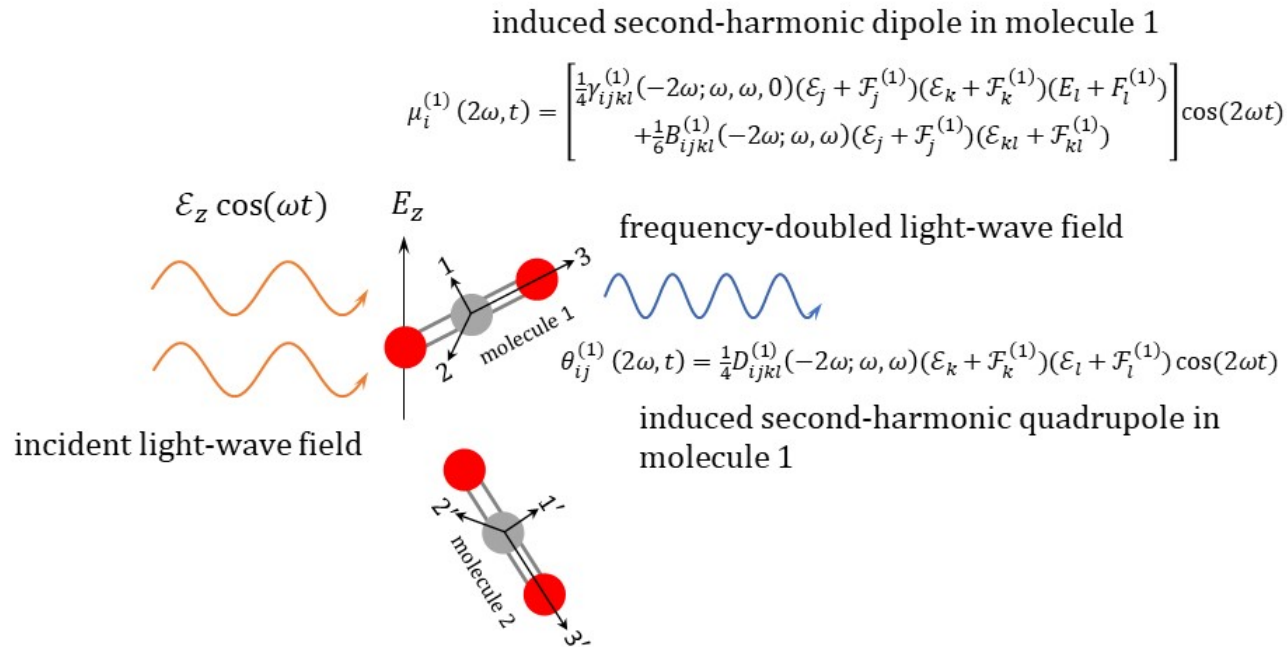


Figure 4.1: Schematic of the ESHG experiment for a dense gas with static and dynamic fields having parallel polarization. The laboratory reference frame $O(x, y, z)$ is oriented such that the z -axis is parallel to the direction of both the uniform static electric field and the oscillating light-wave field. A pair of interacting carbon dioxide molecules is shown with molecule-fixed axes $O(1, 2, 3)$ for molecule 1 and $O(1', 2', 3')$ for molecule 2. The induced second-harmonic dipole and quadrupole moments yield the frequency-doubled light wave.

$$\begin{aligned}
\mu_i^{(p)}(2\omega) &= \alpha_{ij}^{(p)}(-2\omega; 2\omega) \mathcal{F}_j^{(p)}(2\omega) \\
&+ \frac{1}{4} \gamma_{ijkl}^{(p)}(-2\omega; \omega, \omega, 0) \left(\mathcal{E}_j + \mathcal{F}_j^{(p)}(\omega) \right) \left(\mathcal{E}_k + \mathcal{F}_k^{(p)}(\omega) \right) \left(E_l + F_l^{(p)} \right) \\
&+ \frac{1}{6} B_{ijkl}^{(p)}(-2\omega; \omega, \omega) \left(\mathcal{E}_j + \mathcal{F}_j^{(p)}(\omega) \right) \left(\mathcal{E}_{kl} + \mathcal{F}_{kl}^{(p)}(\omega) \right) .
\end{aligned} \tag{4.45}$$

$\gamma_{ijkl}(-2\omega; \omega, \omega, 0)$ is symmetric in jk , and assuming the field gradient \mathcal{E}_{kl} of the light wave to be negligibly small, this expression reduces to

$$\begin{aligned}
\mu_i^{(p)}(2\omega) &= \alpha_{ij}^{(p)}(-2\omega; 2\omega) \mathcal{F}_j^{(p)}(2\omega) \\
&+ \frac{1}{4} \gamma_{ijkl}^{(p)}(-2\omega; \omega, \omega, 0) \left(\mathcal{E}_j \mathcal{E}_k + 2\mathcal{E}_j \mathcal{F}_k^{(p)}(\omega) + \mathcal{F}_j^{(p)}(\omega) \mathcal{F}_k^{(p)}(\omega) \right) \left(E_l + F_l^{(p)} \right) \\
&+ \frac{1}{6} B_{ijkl}^{(p)}(-2\omega; \omega, \omega) \left(\mathcal{E}_j + \mathcal{F}_j^{(p)}(\omega) \right) \mathcal{F}_{kl}^{(p)}(\omega) .
\end{aligned} \tag{4.46}$$

The second-harmonic oscillating quadrupole of molecule p is

$$\Theta_{ij}^{(p)}(2\omega) = \frac{1}{4} D_{ijkl}^{(p)}(-2\omega; \omega, \omega) \left(\mathcal{E}_k + \mathcal{F}_k^{(p)}(\omega) \right) \left(\mathcal{E}_l + \mathcal{F}_l^{(p)}(\omega) \right) , \tag{4.47}$$

which, since $D_{ijkl}(-2\omega; \omega, \omega)$ is symmetric in kl , reduces to

$$\Theta_{ij}^{(p)}(2\omega) = \frac{1}{4} D_{ijkl}^{(p)}(-2\omega; \omega, \omega) \left(\mathcal{E}_k \mathcal{E}_l + 2\mathcal{E}_k \mathcal{F}_l^{(p)}(\omega) + \mathcal{F}_k^{(p)}(\omega) \mathcal{F}_l^{(p)}(\omega) \right) . \tag{4.48}$$

With the aid of the second- and third-rank T -tensors [83], $\mathcal{F}_j^{(p)}(2\omega)$, $\mathcal{F}_j^{(p)}(\omega)$ and

$\mathcal{F}_{jk}^{(p)}(\omega)$ have the form

$$\mathcal{F}_j^{(p)}(2\omega) = T_{jk}^{(p)} \mu_k^{(q)}(2\omega) - \frac{1}{3} T_{jkl}^{(p)} \Theta_{kl}^{(q)}(2\omega), \quad (4.49)$$

$$\mathcal{F}_j^{(p)}(\omega) = T_{jk}^{(p)} \mu_k^{(q)}(\omega) - \frac{1}{3} T_{jkl}^{(p)} \Theta_{kl}^{(q)}(\omega), \quad (4.50)$$

and

$$\mathcal{F}_{jk}^{(p)}(\omega) = T_{jkl}^{(p)} \mu_l^{(q)}(\omega). \quad (4.51)$$

Here the induced dipole on molecule q oscillating at 2ω is

$$\begin{aligned} \mu_k^{(q)}(2\omega) &= \alpha_{kl}^{(q)}(-2\omega; 2\omega) \mathcal{F}_l^{(q)}(2\omega) \\ &+ \frac{1}{4} \gamma_{klmn}^{(q)}(-2\omega; \omega, \omega, 0) \left(\mathcal{E}_l \mathcal{E}_m + 2\mathcal{E}_l \mathcal{F}_m^{(q)}(\omega) + \mathcal{F}_l^{(q)}(\omega) \mathcal{F}_m^{(q)}(\omega) \right) (E_n + F_n^{(q)}) \\ &+ \frac{1}{6} B_{klmn}^{(q)}(-2\omega; \omega, \omega) \left(\mathcal{E}_l + \mathcal{F}_l^{(q)}(\omega) \right) \mathcal{F}_{mn}^{(q)}(\omega), \end{aligned} \quad (4.52)$$

the induced quadrupole on molecule q oscillating at 2ω is

$$\Theta_{kl}^{(q)}(2\omega) = \frac{1}{4} D_{klmn}^{(q)}(-2\omega; \omega, \omega) \left(\mathcal{E}_m \mathcal{E}_n + 2\mathcal{E}_m \mathcal{F}_n^{(q)}(\omega) + \mathcal{F}_m^{(q)}(\omega) \mathcal{F}_n^{(q)}(\omega) \right), \quad (4.53)$$

the induced dipole on molecule q oscillating at ω is

$$\begin{aligned}
\mu_j^{(q)}(\omega) &= \alpha_{jk}^{(q)}(-\omega; \omega) \left(\mathcal{E}_k + \mathcal{F}_k^{(q)}(\omega) \right) \\
&+ \frac{1}{2} \gamma_{jkab}^{(q)}(-\omega; \omega, 0, 0) \left(\mathcal{E}_k + \mathcal{F}_k^{(q)}(\omega) \right) \left(E_a + F_a^{(q)} \right) \left(E_b + F_b^{(q)} \right) \\
&+ \frac{1}{3} B_{jkab}^{(q)}(-\omega; \omega, 0) \left(\mathcal{E}_k + \mathcal{F}_k^{(q)}(\omega) \right) F_{ab}^{(q)} \\
&+ \frac{1}{3} \mathcal{B}_{jkla}^{(q)}(-\omega; \omega, 0) \left(\mathcal{E}_{kl} + \mathcal{F}_{kl}^{(q)}(\omega) \right) \left(E_a + F_a^{(q)} \right),
\end{aligned} \tag{4.54}$$

and the induced quadrupole on molecule q oscillating at ω is

$$\Theta_{jk}^{(q)}(\omega) = D_{jklm}^{(q)}(-\omega; \omega, 0) \left(\mathcal{E}_l + \mathcal{F}_l^{(q)} \right) \left(E_m + F_m^{(q)} \right) + C_{jklm}^{(q)}(-\omega; \omega) \left(\mathcal{E}_{lm} + \mathcal{F}_{lm}^{(q)} \right). \tag{4.55}$$

The field gradient of the light wave appearing in equations (4.54) and (4.55), namely \mathcal{E}_{kl} and \mathcal{E}_{lm} respectively, will also be assumed to be negligibly small. In turn,

$$\mathcal{F}_n^{(q)} = T_{np}^{(q)} \mu_p^{(p)}. \tag{4.56}$$

If equations (4.55) and (4.56) are substituted into equation (4.49), followed by successive substitutions of $\mathcal{F}_j^{(p)}$ and $\mathcal{F}_n^{(q)}$, a series of terms contributing to the net field $\mathcal{F}_j^{(p)}$ in equation (4.49) is obtained, which, when substituted into equation (4.45), yields the required expression for the total oscillating dipole moment induced on molecule p by the light-wave field in the presence of the neighbouring molecule q . This expression is now provided in full, with terms up to the order required in the ensuing calculations. To conserve space, since the frequency arguments for γ_{ijkl} are always $(-2\omega; \omega, \omega, 0)$, these are omitted (except for the first occurrence). Similarly, the frequency arguments for both B_{ijkl} and D_{ijkl} are consistently $(-2\omega; \omega, \omega)$, so that these too are omitted (save for the introductory terms).

$$\begin{aligned}
\mu_i^{(p)}(2\omega) = & \frac{1}{4} \left(\gamma_{iwvh}^{(p)}(-2\omega; \omega, \omega, 0) + 2\gamma_{ivjh}^{(p)} T_{jk} \alpha_{kw}^{(q)}(-\omega; \omega) + \alpha_{ij}^{(p)}(-2\omega; 2\omega) T_{jk} \gamma_{kvwh}^{(q)} + \gamma_{ivwa}^{(p)} T_{ab} \alpha_{bh}^{(q)}(0; 0) + 2\gamma_{ivjh}^{(p)} T_{jk} \alpha_{kl}^{(q)}(-\omega; \omega) T_{lm} \alpha_{mw}^{(p)}(-\omega; \omega) \right. \\
& + \gamma_{ijph}^{(p)} T_{jk} \alpha_{kv}^{(q)}(-\omega; \omega) T_{pq} \alpha_{qw}^{(q)}(-\omega; \omega) + 2\alpha_{ij}^{(p)}(-2\omega; 2\omega) T_{jk} \gamma_{kvlh}^{(q)} T_{lm} \alpha_{mw}^{(p)}(-\omega; \omega) + \alpha_{ij}^{(p)}(-2\omega; 2\omega) T_{jk} \alpha_{kl}^{(q)}(-2\omega; 2\omega) T_{lm} \gamma_{mvwh}^{(p)} \\
& + \alpha_{ij}^{(p)}(-2\omega; 2\omega) T_{jk} \gamma_{kvwa}^{(q)} T_{ab} \alpha_{bh}^{(p)}(0; 0) + 2\gamma_{ivja}^{(p)} T_{jk} \alpha_{kw}^{(q)}(-\omega; \omega) T_{ab} \alpha_{bh}^{(q)}(0; 0) + \gamma_{ivwa}^{(p)} T_{ab} \alpha_{bc}^{(q)}(0; 0) T_{cd} \alpha_{dh}^{(p)}(0; 0) \\
& + 2\gamma_{ivjh}^{(p)} T_{jk} \alpha_{kl}^{(q)}(-\omega; \omega) T_{lm} \alpha_{mn}^{(p)}(-\omega; \omega) T_{np} \alpha_{pw}^{(q)}(-\omega; \omega) + 2\gamma_{ijph}^{(p)} T_{jk} \alpha_{kv}^{(q)}(-\omega; \omega) T_{pq} \alpha_{qr}^{(q)}(-\omega; \omega) T_{rs} \alpha_{sw}^{(p)}(-\omega; \omega) \\
& + 2\alpha_{ij}^{(p)}(-2\omega; 2\omega) T_{jk} \gamma_{kvlh}^{(q)} T_{lm} \alpha_{mn}^{(p)}(-\omega; \omega) T_{np} \alpha_{pw}^{(q)}(-\omega; \omega) + \alpha_{ij}^{(p)}(-2\omega; 2\omega) T_{jk} \gamma_{klph}^{(q)} T_{lm} \alpha_{mv}^{(p)}(-\omega; \omega) T_{pq} \alpha_{qw}^{(p)}(-\omega; \omega) \\
& + 2\alpha_{ij}^{(p)}(-2\omega; 2\omega) T_{jk} \alpha_{kl}^{(q)}(-2\omega; 2\omega) T_{lm} \gamma_{mvnh}^{(p)} T_{np} \alpha_{pw}^{(q)}(-\omega; \omega) + \alpha_{ij}^{(p)}(-2\omega; 2\omega) T_{jk} \alpha_{kl}^{(q)}(-2\omega; 2\omega) T_{lm} \alpha_{mn}^{(p)}(-2\omega; 2\omega) T_{np} \gamma_{pvwh}^{(q)} \\
& + \alpha_{ij}^{(p)}(-2\omega; 2\omega) T_{jk} \alpha_{kl}^{(q)}(-2\omega; 2\omega) T_{lm} \gamma_{mvwn}^{(p)} T_{np} \alpha_{ph}^{(q)}(0; 0) + 2\alpha_{ij}^{(p)}(-2\omega; 2\omega) T_{jk} \gamma_{kvma}^{(q)} T_{mn} \alpha_{nw}^{(p)}(-\omega; \omega) T_{ab} \alpha_{bh}^{(p)}(0; 0) \\
& + \alpha_{ij}^{(p)}(-2\omega; 2\omega) T_{jk} \gamma_{kvwa}^{(q)} T_{ab} \alpha_{bc}^{(p)}(0; 0) T_{cd} \alpha_{dh}^{(q)}(0; 0) + \gamma_{ijpa}^{(p)} T_{jk} \alpha_{kv}^{(q)}(-\omega; \omega) T_{pq} \alpha_{qw}^{(q)}(-\omega; \omega) T_{ab} \alpha_{bh}^{(q)}(0; 0) \\
& + 2\gamma_{ivja}^{(p)} T_{jk} \alpha_{kl}^{(q)}(-\omega; \omega) T_{lm} \alpha_{mw}^{(p)}(-\omega; \omega) T_{ab} \alpha_{bh}^{(q)}(0; 0) + 2\gamma_{ivja}^{(p)} T_{jk} \alpha_{kw}^{(q)}(-\omega; \omega) T_{ab} \alpha_{bc}^{(q)}(0; 0) T_{cd} \alpha_{dh}^{(p)}(0; 0) \\
& + \gamma_{ivwa}^{(p)} T_{ab} \alpha_{bc}^{(q)}(0; 0) T_{cd} \alpha_{de}^{(p)}(0; 0) T_{ef} \alpha_{fh}^{(q)}(0; 0) + 2\gamma_{ivjh}^{(p)} T_{jk} \alpha_{kl}^{(q)}(-\omega; \omega) T_{lm} \alpha_{mn}^{(p)}(-\omega; \omega) T_{np} \alpha_{pq}^{(q)}(-\omega; \omega) T_{qr} \alpha_{rw}^{(p)}(-\omega; \omega) \\
& + 2\gamma_{ijph}^{(p)} T_{jk} \alpha_{kv}^{(q)}(-\omega; \omega) T_{pq} \alpha_{qr}^{(q)}(-\omega; \omega) T_{rs} \alpha_{st}^{(p)}(-\omega; \omega) T_{tu} \alpha_{uw}^{(q)}(-\omega; \omega) + \gamma_{ijph}^{(p)} T_{jk} \alpha_{kl}^{(q)}(-\omega; \omega) T_{lm} \alpha_{mv}^{(p)}(-\omega; \omega) T_{pq} \alpha_{qr}^{(q)}(-\omega; \omega) T_{rs} \alpha_{sw}^{(p)}(-\omega; \omega) \\
& + 2\gamma_{ivja}^{(p)} T_{jk} \alpha_{kl}^{(q)}(-\omega; \omega) T_{lm} \alpha_{mn}^{(p)}(-\omega; \omega) T_{np} \alpha_{pw}^{(q)}(-\omega; \omega) T_{ab} \alpha_{bh}^{(q)}(0; 0) + 2\gamma_{ijpa}^{(p)} T_{jk} \alpha_{kv}^{(q)}(-\omega; \omega) T_{pq} \alpha_{qr}^{(q)}(-\omega; \omega) T_{rs} \alpha_{sw}^{(p)}(-\omega; \omega) T_{ab} \alpha_{bh}^{(q)}(0; 0) \\
& + 2\gamma_{ivja}^{(p)} T_{jk} \alpha_{kl}^{(q)}(-\omega; \omega) T_{lm} \alpha_{mw}^{(p)}(-\omega; \omega) T_{ab} \alpha_{bc}^{(q)}(0; 0) T_{cd} \alpha_{dh}^{(p)}(0; 0) + \gamma_{ijpa}^{(p)} T_{jk} \alpha_{kv}^{(q)}(-\omega; \omega) T_{pq} \alpha_{qw}^{(q)}(-\omega; \omega) T_{ab} \alpha_{bc}^{(q)}(0; 0) T_{cd} \alpha_{dh}^{(p)}(0; 0) \\
& + 2\gamma_{ivja}^{(p)} T_{jk} \alpha_{kw}^{(q)}(-\omega; \omega) T_{ab} \alpha_{bc}^{(q)}(0; 0) T_{cd} \alpha_{de}^{(p)}(0; 0) T_{ef} \alpha_{fh}^{(q)}(0; 0) + \gamma_{ivwa}^{(p)} T_{ab} \alpha_{bc}^{(q)}(0; 0) T_{cd} \alpha_{de}^{(p)}(0; 0) T_{ef} \alpha_{fg}^{(q)}(0; 0) T_{gj} \alpha_{jh}^{(p)}(0; 0) \\
& + 2\alpha_{ij}^{(p)}(-2\omega; 2\omega) T_{jk} \gamma_{kvlh}^{(q)} T_{lm} \alpha_{mn}^{(p)}(-\omega; \omega) T_{np} \alpha_{pw}^{(q)}(-\omega; \omega) T_{qr} \alpha_{rw}^{(p)}(-\omega; \omega) + \alpha_{ij}^{(p)}(-2\omega; 2\omega) T_{jk} \gamma_{klph}^{(q)} T_{lm} \alpha_{mv}^{(p)}(-\omega; \omega) T_{pq} \alpha_{qr}^{(p)}(-\omega; \omega) T_{rs} \alpha_{sw}^{(q)}(-\omega; \omega)
\end{aligned}$$

(continued over the page ...)

$$\begin{aligned}
& + 2\alpha_{ij}^{(p)}(-2\omega; 2\omega)T_{jk}\alpha_{kl}^{(q)}(-2\omega; 2\omega)T_{lm}\gamma_{m\nu nh}^{(p)}T_{np}\alpha_{pq}^{(q)}(-\omega; \omega)T_{qr}\alpha_{rw}^{(p)}(-\omega; \omega) + \alpha_{ij}^{(p)}(-2\omega; 2\omega)T_{jk}\alpha_{kl}^{(q)}(-2\omega; 2\omega)T_{lm}\gamma_{mnqh}^{(p)}T_{np}\alpha_{pv}^{(q)}(-\omega; \omega)T_{qr}\alpha_{rw}^{(q)}(-\omega; \omega) \\
& + 2\alpha_{ij}^{(p)}(-2\omega; 2\omega)T_{jk}\alpha_{kl}^{(q)}(-2\omega; 2\omega)T_{lm}\alpha_{mn}^{(p)}(-2\omega; 2\omega)T_{np}\gamma_{pvqh}^{(q)}T_{qr}\alpha_{rw}^{(p)}(-\omega; \omega) + \alpha_{ij}^{(p)}(-2\omega; 2\omega)T_{jk}\alpha_{kl}^{(q)}(-2\omega; 2\omega)T_{lm}\alpha_{mn}^{(p)}(-2\omega; 2\omega)T_{np}\alpha_{pq}^{(q)}(-2\omega; 2\omega)T_{qr}\gamma_{rvwh}^{(p)} \\
& + 2\alpha_{ij}^{(p)}(-2\omega; 2\omega)T_{jk}\gamma_{klva}^{(q)}T_{lm}\alpha_{mn}^{(p)}(-\omega; \omega)T_{np}\alpha_{pw}^{(q)}(-2\omega; 2\omega)T_{ab}\alpha_{bh}^{(p)}(0; 0) + \alpha_{ij}^{(p)}(-2\omega; 2\omega)T_{jk}\gamma_{klpa}^{(q)}T_{lm}\alpha_{mv}^{(p)}(-\omega; \omega)T_{pq}\alpha_{qw}^{(p)}(-2\omega; 2\omega)T_{ab}\alpha_{bh}^{(p)}(0; 0) \\
& + 2\alpha_{ij}^{(p)}(-2\omega; 2\omega)T_{jk}\alpha_{kl}^{(q)}(-2\omega; 2\omega)T_{lm}\gamma_{m\nu na}^{(p)}T_{np}\alpha_{pw}^{(q)}(-\omega; \omega)T_{ab}\alpha_{bh}^{(q)}(0; 0) + \alpha_{ij}^{(p)}(-2\omega; 2\omega)T_{jk}\alpha_{kl}^{(q)}(-2\omega; 2\omega)T_{lm}\alpha_{mn}^{(p)}(-2\omega; 2\omega)T_{np}\gamma_{pvwa}^{(q)}T_{ab}\alpha_{bh}^{(p)}(0; 0) \\
& + 2\alpha_{ij}^{(p)}(-2\omega; 2\omega)T_{jk}\gamma_{klva}^{(q)}T_{lm}\alpha_{mw}^{(p)}(-\omega; \omega)T_{ab}\alpha_{bc}^{(p)}(0; 0)T_{cd}\alpha_{dh}^{(q)}(0; 0) + \alpha_{ij}^{(p)}(-2\omega; 2\omega)T_{jk}\alpha_{kl}^{(q)}(-2\omega; 2\omega)T_{lm}\gamma_{mvwa}^{(p)}T_{ab}\alpha_{bc}^{(q)}(0; 0)T_{cd}\alpha_{dh}^{(p)}(0; 0) \\
& + \alpha_{ij}^{(p)}(-2\omega; 2\omega)T_{jk}\gamma_{kvwa}^{(q)}T_{ab}\alpha_{bc}^{(p)}(0; 0)T_{cd}\alpha_{de}^{(q)}(0; 0)T_{ef}\alpha_{fh}^{(p)}(0; 0) + \dots \Big) \mathcal{E}_v \mathcal{E}_w E_h \\
& - \frac{1}{12} \left(\gamma_{ivwj}^{(p)}(-2\omega; \omega, \omega, 0)T_{jqr}^{(p)}\Theta_{0qr}^{(q)} + 2\gamma_{ivjl}^{(p)}T_{jk}\alpha_{kw}^{(q)}(-\omega; \omega)T_{lqr}^{(p)}\Theta_{0qr}^{(q)} + \alpha_{ij}^{(p)}(-2\omega; 2\omega)T_{jk}\gamma_{kvwl}^{(q)}T_{lqr}^{(q)}\Theta_{0qr}^{(p)} + \gamma_{ivwj}^{(p)}T_{jk}\alpha_{kl}^{(q)}(0; 0)T_{lqr}^{(q)}\Theta_{0qr}^{(p)} \right. \\
& \quad + 2\gamma_{ivjp}^{(p)}T_{jk}\alpha_{kl}^{(q)}(-\omega; \omega)T_{lm}\alpha_{mw}^{(p)}(-\omega; \omega)T_{pqr}^{(p)}\Theta_{0qr}^{(q)} + \gamma_{ijlp}^{(p)}T_{jk}\alpha_{kv}^{(q)}(-\omega; \omega)T_{lm}\alpha_{mw}^{(q)}(-\omega; \omega)T_{pqr}^{(p)}\Theta_{0qr}^{(q)} + 2\alpha_{ij}^{(p)}(-2\omega; 2\omega)T_{jk}\gamma_{kvlp}^{(q)}T_{lm}\alpha_{mw}^{(p)}(-\omega; \omega)T_{pqr}^{(q)}\Theta_{0qr}^{(p)} \\
& \quad + \alpha_{ij}^{(p)}(-2\omega; 2\omega)T_{jk}\alpha_{kl}^{(q)}(-2\omega; 2\omega)T_{lm}\gamma_{mvwp}^{(p)}T_{pqr}^{(p)}\Theta_{0qr}^{(q)} + \alpha_{ij}^{(p)}(-2\omega; 2\omega)T_{jk}\gamma_{kvwl}^{(q)}T_{lm}\alpha_{mp}^{(p)}(0; 0)T_{pqr}^{(p)}\Theta_{0qr}^{(q)} + 2\gamma_{ivjl}^{(p)}T_{jk}\alpha_{kw}^{(q)}(-\omega; \omega)T_{lm}\alpha_{mp}^{(q)}(0; 0)T_{pqr}^{(q)}\Theta_{0qr}^{(p)} \\
& \quad \left. + \gamma_{ivwj}^{(p)}T_{jk}\alpha_{kl}^{(q)}(0; 0)T_{lm}\alpha_{mp}^{(p)}(0; 0)T_{pqr}^{(p)}\Theta_{0qr}^{(q)} + \dots \right) \mathcal{E}_v \mathcal{E}_w \\
& + \frac{1}{6} \left(B_{ivjk}^{(p)}(-2\omega; \omega, \omega)T_{jkl}^{(p)}\alpha_{lw}^{(q)}(-\omega; \omega) + \alpha_{ij}^{(p)}(-2\omega; 2\omega)T_{jk}B_{kvlm}^{(q)}T_{lmn}^{(q)}\alpha_{nw}^{(p)}(-\omega; \omega) + B_{ivjk}^{(p)}T_{jkl}^{(p)}\alpha_{lm}^{(q)}(-\omega; \omega)T_{mn}\alpha_{nw}^{(p)}(-\omega; \omega) \right. \\
& \quad \left. + B_{ijlm}^{(p)}T_{jk}\alpha_{kv}^{(q)}(-\omega; \omega)T_{lmn}^{(p)}\alpha_{nw}^{(q)}(-\omega; \omega) + \dots \right) \mathcal{E}_v \mathcal{E}_w \\
& - \frac{1}{12} \left(\alpha_{ij}^{(p)}(-2\omega; 2\omega)T_{jkl}^{(p)}D_{klvw}^{(q)}(-2\omega; \omega, \omega) + \alpha_{ij}^{(p)}(-2\omega; 2\omega)T_{jk}\alpha_{kl}^{(q)}(-2\omega; 2\omega)T_{lmn}^{(q)}D_{mnvw}^{(p)} + 2\alpha_{ij}^{(p)}(-2\omega; 2\omega)T_{jkl}^{(p)}D_{klvm}^{(q)}T_{mn}\alpha_{nw}^{(p)}(-\omega; \omega) + \dots \right) \mathcal{E}_v \mathcal{E}_w
\end{aligned}$$

(4.57)

In the laboratory frame, $\mu_z^{(1)}(2\omega) = \mu_i^{(1)}(2\omega)a_i^z$, which together with the simplification $T_{jkl}^{(1)} = -T_{jkl}^{(2)} = T_{jkl}$ gives

$$\begin{aligned}
\mu_z^{(1)}(2\omega) = & \frac{1}{4} \left(\gamma_{ivwh}^{(1)}(-2\omega; \omega, \omega, 0) + 2\gamma_{ivjh}^{(1)} T_{jk} \alpha_{kw}^{(2)}(-\omega; \omega) + \alpha_{ij}^{(1)}(-2\omega; 2\omega) T_{jk} \gamma_{kvwh}^{(2)} + \gamma_{ivwa}^{(1)} T_{ab} \alpha_{bh}^{(2)}(0; 0) + 2\gamma_{ivjh}^{(1)} T_{jk} \alpha_{kl}^{(2)}(-\omega; \omega) T_{lm} \alpha_{mw}^{(1)}(-\omega; \omega) \right. \\
& + \gamma_{ijph}^{(1)} T_{jk} \alpha_{kv}^{(2)}(-\omega; \omega) T_{pq} \alpha_{qw}^{(2)}(-\omega; \omega) + 2\alpha_{ij}^{(1)}(-2\omega; 2\omega) T_{jk} \gamma_{kvlh}^{(2)} T_{lm} \alpha_{mw}^{(1)}(-\omega; \omega) + \alpha_{ij}^{(1)}(-2\omega; 2\omega) T_{jk} \alpha_{kl}^{(2)}(-2\omega; 2\omega) T_{lm} \gamma_{mvwh}^{(1)} \\
& + \alpha_{ij}^{(1)}(-2\omega; 2\omega) T_{jk} \gamma_{kvwa}^{(2)} T_{ab} \alpha_{bh}^{(1)}(0; 0) + 2\gamma_{ivja}^{(1)} T_{jk} \alpha_{kw}^{(2)}(-\omega; \omega) T_{ab} \alpha_{bh}^{(2)}(0; 0) + \gamma_{ivwa}^{(1)} T_{ab} \alpha_{bc}^{(2)}(0; 0) T_{cd} \alpha_{dh}^{(1)}(0; 0) \\
& + 2\gamma_{ivjh}^{(1)} T_{jk} \alpha_{kl}^{(2)}(-\omega; \omega) T_{lm} \alpha_{mn}^{(1)}(-\omega; \omega) T_{np} \alpha_{pw}^{(2)}(-\omega; \omega) + 2\gamma_{ijph}^{(1)} T_{jk} \alpha_{kv}^{(2)}(-\omega; \omega) T_{pq} \alpha_{qr}^{(2)}(-\omega; \omega) T_{rs} \alpha_{sw}^{(1)}(-\omega; \omega) \\
& + 2\alpha_{ij}^{(1)}(-2\omega; 2\omega) T_{jk} \gamma_{kvlh}^{(2)} T_{lm} \alpha_{mn}^{(1)}(-\omega; \omega) T_{np} \alpha_{pw}^{(2)}(-\omega; \omega) + \alpha_{ij}^{(1)}(-2\omega; 2\omega) T_{jk} \gamma_{klph}^{(2)} T_{lm} \alpha_{mv}^{(1)}(-\omega; \omega) T_{pq} \alpha_{qw}^{(1)}(-\omega; \omega) \\
& + 2\alpha_{ij}^{(1)}(-2\omega; 2\omega) T_{jk} \alpha_{kl}^{(2)}(-2\omega; 2\omega) T_{lm} \gamma_{mvnh}^{(1)} T_{np} \alpha_{pw}^{(2)}(-\omega; \omega) + \alpha_{ij}^{(1)}(-2\omega; 2\omega) T_{jk} \alpha_{kl}^{(2)}(-2\omega; 2\omega) T_{lm} \alpha_{mn}^{(1)}(-2\omega; 2\omega) T_{np} \gamma_{pvwh}^{(2)} \\
& + \alpha_{ij}^{(1)}(-2\omega; 2\omega) T_{jk} \alpha_{kl}^{(2)}(-2\omega; 2\omega) T_{lm} \gamma_{mvwn}^{(1)} T_{np} \alpha_{ph}^{(2)}(0; 0) + 2\alpha_{ij}^{(1)}(-2\omega; 2\omega) T_{jk} \gamma_{kvma}^{(2)} T_{mn} \alpha_{nw}^{(1)}(-\omega; \omega) T_{ab} \alpha_{bh}^{(1)}(0; 0) \\
& + \alpha_{ij}^{(1)}(-2\omega; 2\omega) T_{jk} \gamma_{kvwa}^{(2)} T_{ab} \alpha_{bc}^{(1)}(0; 0) T_{cd} \alpha_{dh}^{(2)}(0; 0) + \gamma_{ijpa}^{(1)} T_{jk} \alpha_{kv}^{(2)}(-\omega; \omega) T_{pq} \alpha_{qw}^{(2)}(-\omega; \omega) T_{ab} \alpha_{bh}^{(2)}(0; 0) \\
& + 2\gamma_{ivja}^{(1)} T_{jk} \alpha_{kl}^{(2)}(-\omega; \omega) T_{lm} \alpha_{mw}^{(1)}(-\omega; \omega) T_{ab} \alpha_{bh}^{(2)}(0; 0) + 2\gamma_{ivja}^{(1)} T_{jk} \alpha_{kw}^{(2)}(-\omega; \omega) T_{ab} \alpha_{bc}^{(2)}(0; 0) T_{cd} \alpha_{dh}^{(1)}(0; 0) \\
& + \gamma_{ivwa}^{(1)} T_{ab} \alpha_{bc}^{(2)}(0; 0) T_{cd} \alpha_{de}^{(1)}(0; 0) T_{ef} \alpha_{fh}^{(2)}(0; 0) + 2\gamma_{ivjh}^{(1)} T_{jk} \alpha_{kl}^{(2)}(-\omega; \omega) T_{lm} \alpha_{mn}^{(1)}(-\omega; \omega) T_{np} \alpha_{pq}^{(2)}(-\omega; \omega) T_{qr} \alpha_{rw}^{(1)}(-\omega; \omega) \\
& + 2\gamma_{ijph}^{(1)} T_{jk} \alpha_{kv}^{(2)}(-\omega; \omega) T_{pq} \alpha_{qr}^{(2)}(-\omega; \omega) T_{rs} \alpha_{st}^{(1)}(-\omega; \omega) T_{tu} \alpha_{uv}^{(2)}(-\omega; \omega) + \gamma_{ijph}^{(1)} T_{jk} \alpha_{kl}^{(2)}(-\omega; \omega) T_{lm} \alpha_{mv}^{(1)}(-\omega; \omega) T_{pq} \alpha_{qr}^{(2)}(-\omega; \omega) T_{rs} \alpha_{sw}^{(1)}(-\omega; \omega) \\
& + 2\gamma_{ivja}^{(1)} T_{jk} \alpha_{kl}^{(2)}(-\omega; \omega) T_{lm} \alpha_{mn}^{(1)}(-\omega; \omega) T_{np} \alpha_{pw}^{(2)}(-\omega; \omega) T_{ab} \alpha_{bh}^{(2)}(0; 0) + 2\gamma_{ijpa}^{(1)} T_{jk} \alpha_{kv}^{(2)}(-\omega; \omega) T_{pq} \alpha_{qr}^{(2)}(-\omega; \omega) T_{rs} \alpha_{sw}^{(1)}(-\omega; \omega) T_{ab} \alpha_{bh}^{(2)}(0; 0) \\
& + 2\gamma_{ivja}^{(1)} T_{jk} \alpha_{kl}^{(2)}(-\omega; \omega) T_{lm} \alpha_{mw}^{(1)}(-\omega; \omega) T_{ab} \alpha_{bc}^{(2)}(0; 0) T_{cd} \alpha_{dh}^{(1)}(0; 0) + \gamma_{ijpa}^{(1)} T_{jk} \alpha_{kv}^{(2)}(-\omega; \omega) T_{pq} \alpha_{qw}^{(2)}(-\omega; \omega) T_{ab} \alpha_{bc}^{(2)}(0; 0) T_{cd} \alpha_{dh}^{(1)}(0; 0) \\
& + 2\gamma_{ivja}^{(1)} T_{jk} \alpha_{kw}^{(2)}(-\omega; \omega) T_{ab} \alpha_{bc}^{(2)}(0; 0) T_{cd} \alpha_{de}^{(1)}(0; 0) T_{ef} \alpha_{fh}^{(2)}(0; 0) + \gamma_{ivwa}^{(1)} T_{ab} \alpha_{bc}^{(2)}(0; 0) T_{cd} \alpha_{de}^{(1)}(0; 0) T_{ef} \alpha_{fg}^{(2)}(0; 0) T_{gj} \alpha_{jh}^{(1)}(0; 0)
\end{aligned}$$

(continued over the page ...)

$$\begin{aligned}
& + 2\alpha_{ij}^{(1)}(-2\omega; 2\omega)T_{jk}\gamma_{kvlh}^{(2)}T_{lm}\alpha_{mn}^{(1)}(-\omega; \omega)T_{np}\alpha_{pq}^{(2)}(-\omega; \omega)T_{qr}\alpha_{rw}^{(1)}(-\omega; \omega) + \alpha_{ij}^{(1)}(-2\omega; 2\omega)T_{jk}\gamma_{klph}^{(2)}T_{lm}\alpha_{mv}^{(1)}(-\omega; \omega)T_{pq}\alpha_{qr}^{(1)}(-\omega; \omega)T_{rs}\alpha_{sw}^{(2)}(-\omega; \omega) \\
& + 2\alpha_{ij}^{(1)}(-2\omega; 2\omega)T_{jk}\alpha_{kl}^{(2)}(-2\omega; 2\omega)T_{lm}\gamma_{mvnh}^{(1)}T_{np}\alpha_{pq}^{(2)}(-\omega; \omega)T_{qr}\alpha_{rw}^{(1)}(-\omega; \omega) + \alpha_{ij}^{(1)}(-2\omega; 2\omega)T_{jk}\alpha_{kl}^{(2)}(-2\omega; 2\omega)T_{lm}\gamma_{mnqh}^{(1)}T_{np}\alpha_{pv}^{(2)}(-\omega; \omega)T_{qr}\alpha_{rw}^{(2)}(-\omega; \omega) \\
& + 2\alpha_{ij}^{(1)}(-2\omega; 2\omega)T_{jk}\alpha_{kl}^{(2)}(-2\omega; 2\omega)T_{lm}\alpha_{mn}^{(1)}(-2\omega; 2\omega)T_{np}\gamma_{pvqh}^{(2)}T_{qr}\alpha_{rw}^{(1)}(-\omega; \omega) + \alpha_{ij}^{(1)}(-2\omega; 2\omega)T_{jk}\alpha_{kl}^{(2)}(-2\omega; 2\omega)T_{lm}\alpha_{mn}^{(1)}(-2\omega; 2\omega)T_{np}\alpha_{pq}^{(2)}(-2\omega; 2\omega)T_{qr}\gamma_{rvwh}^{(1)} \\
& + 2\alpha_{ij}^{(1)}(-2\omega; 2\omega)T_{jk}\gamma_{kvla}^{(2)}T_{lm}\alpha_{mn}^{(1)}(-\omega; \omega)T_{np}\alpha_{pw}^{(2)}(-2\omega; 2\omega)T_{ab}\alpha_{bh}^{(1)}(0; 0) + \alpha_{ij}^{(1)}(-2\omega; 2\omega)T_{jk}\gamma_{klpa}^{(2)}T_{lm}\alpha_{mv}^{(1)}(-\omega; \omega)T_{pq}\alpha_{qw}^{(1)}(-2\omega; 2\omega)T_{ab}\alpha_{bh}^{(1)}(0; 0) \\
& + 2\alpha_{ij}^{(1)}(-2\omega; 2\omega)T_{jk}\alpha_{kl}^{(2)}(-2\omega; 2\omega)T_{lm}\gamma_{mvna}^{(1)}T_{np}\alpha_{pw}^{(2)}(-\omega; \omega)T_{ab}\alpha_{bh}^{(2)}(0; 0) + \alpha_{ij}^{(1)}(-2\omega; 2\omega)T_{jk}\alpha_{kl}^{(2)}(-2\omega; 2\omega)T_{lm}\alpha_{mn}^{(1)}(-2\omega; 2\omega)T_{np}\gamma_{pvwa}^{(2)}T_{ab}\alpha_{bh}^{(1)}(0; 0) \\
& + 2\alpha_{ij}^{(1)}(-2\omega; 2\omega)T_{jk}\gamma_{kvla}^{(2)}T_{lm}\alpha_{mw}^{(1)}(-\omega; \omega)T_{ab}\alpha_{bc}^{(1)}(0; 0)T_{cd}\alpha_{dh}^{(2)}(0; 0) + \alpha_{ij}^{(1)}(-2\omega; 2\omega)T_{jk}\alpha_{kl}^{(2)}(-2\omega; 2\omega)T_{lm}\gamma_{mvwa}^{(1)}T_{ab}\alpha_{bc}^{(2)}(0; 0)T_{cd}\alpha_{dh}^{(1)}(0; 0) \\
& + \alpha_{ij}^{(1)}(-2\omega; 2\omega)T_{jk}\gamma_{kvwa}^{(2)}T_{ab}\alpha_{bc}^{(1)}(0; 0)T_{cd}\alpha_{de}^{(2)}(0; 0)T_{ef}\alpha_{fh}^{(1)}(0; 0) + \dots \Big) \mathcal{E}_z^2 E_z a_i^z a_v^z a_w^z a_h^z \\
& - \frac{1}{12} \left(\gamma_{iuvw}^{(1)}(-2\omega; \omega, \omega, 0)T_{jqr}\Theta_{0qr}^{(2)} + 2\gamma_{iuvj}^{(1)}T_{jk}\alpha_{kw}^{(2)}(-\omega; \omega)T_{lqr}\Theta_{0qr}^{(2)} - \alpha_{ij}^{(1)}(-2\omega; 2\omega)T_{jk}\gamma_{kvwl}^{(2)}T_{lqr}\Theta_{0qr}^{(1)} - \gamma_{iuvw}^{(1)}T_{jk}\alpha_{kl}^{(2)}(0; 0)T_{lqr}\Theta_{0qr}^{(1)} \right. \\
& \quad + 2\gamma_{iujp}^{(1)}T_{jk}\alpha_{kl}^{(2)}(-\omega; \omega)T_{lm}\alpha_{mw}^{(1)}(-\omega; \omega)T_{pqr}\Theta_{0qr}^{(2)} + \gamma_{ijlp}^{(1)}T_{jk}\alpha_{kv}^{(2)}(-\omega; \omega)T_{lm}\alpha_{mw}^{(2)}(-\omega; \omega)T_{pqr}\Theta_{0qr}^{(2)} - 2\alpha_{ij}^{(1)}(-2\omega; 2\omega)T_{jk}\gamma_{kvlp}^{(2)}T_{lm}\alpha_{mw}^{(1)}(-\omega; \omega)T_{pqr}\Theta_{0qr}^{(1)} \\
& \quad + \alpha_{ij}^{(1)}(-2\omega; 2\omega)T_{jk}\alpha_{kl}^{(2)}(-2\omega; 2\omega)T_{lm}\gamma_{mvwp}^{(1)}T_{pqr}\Theta_{0qr}^{(2)} + \alpha_{ij}^{(1)}(-2\omega; 2\omega)T_{jk}\gamma_{kvwl}^{(2)}T_{lm}\alpha_{mp}^{(1)}(0; 0)T_{pqr}\Theta_{0qr}^{(2)} - 2\gamma_{iuvj}^{(1)}T_{jk}\alpha_{kw}^{(2)}(-\omega; \omega)T_{lm}\alpha_{mp}^{(2)}(0; 0)T_{pqr}\Theta_{0qr}^{(1)} \\
& \quad \left. + \gamma_{iuvw}^{(1)}T_{jk}\alpha_{kl}^{(2)}(0; 0)T_{lm}\alpha_{mp}^{(1)}(0; 0)T_{pqr}\Theta_{0qr}^{(2)} + \dots \right) \mathcal{E}_z^2 a_i^z a_v^z a_w^z \\
& + \frac{1}{6} \left(B_{ijjk}^{(1)}(-2\omega; \omega, \omega)T_{jkl}\alpha_{lw}^{(2)}(-\omega; \omega) - \alpha_{ij}^{(1)}(-2\omega; 2\omega)T_{jk}B_{kvlm}^{(2)}T_{lmn}\alpha_{nw}^{(1)}(-\omega; \omega) + B_{ijjk}^{(1)}T_{jkl}\alpha_{lm}^{(2)}(-\omega; \omega)T_{mn}\alpha_{nw}^{(1)}(-\omega; \omega) \right. \\
& \quad \left. + B_{ijlm}^{(1)}T_{jk}\alpha_{kv}^{(2)}(-\omega; \omega)T_{lmn}\alpha_{nw}^{(2)}(-\omega; \omega) + \dots \right) \mathcal{E}_z^2 a_i^z a_v^z a_w^z \\
& - \frac{1}{12} \left(\alpha_{ij}^{(1)}(-2\omega; 2\omega)T_{jkl}D_{klvw}^{(2)}(-2\omega; \omega, \omega) - \alpha_{ij}^{(1)}(-2\omega; 2\omega)T_{jk}\alpha_{kl}^{(2)}(-2\omega; 2\omega)T_{lmn}D_{mnvw}^{(1)} + 2\alpha_{ij}^{(1)}(-2\omega; 2\omega)T_{jkl}D_{klvm}^{(2)}T_{mn}\alpha_{nw}^{(1)}(-\omega; \omega) + \dots \right) \mathcal{E}_z^2 a_i^z a_v^z a_w^z .
\end{aligned}$$

(4.58)

The groundwork permitting evaluation of the term $\frac{1}{2} \left(\overline{\partial \mu_z^{(12)}(2\omega, \tau, \mathbf{E}) / \partial E_z} \right)_{E_z=0}$ in the expression for B_γ in equation (4.23) has successfully been laid. Using equation (4.25) in equation (4.16) yields

$$\left\langle \frac{\partial \mu_z^{(12)}(2\omega)}{\partial E_z} \right\rangle = \left\langle \frac{\partial \mu_z^{(1)}(2\omega)}{\partial E_z} \right\rangle + \left\langle \frac{\partial \mu_z^{(2)}(2\omega)}{\partial E_z} \right\rangle, \quad (4.59)$$

and since molecules 1 and 2 are identical, the isotropic averages of their molecular properties must be the same, so that

$$\left\langle \frac{\partial \mu_z^{(12)}(2\omega)}{\partial E_z} \right\rangle = 2 \left\langle \frac{\partial \mu_z^{(1)}(2\omega)}{\partial E_z} \right\rangle. \quad (4.60)$$

Similarly, using equations (4.25) and (4.41) in equation (4.16) yields

$$-\frac{1}{kT} \left\langle \mu_z^{(12)}(2\omega) \frac{\partial U^{(12)}}{\partial E_z} \right\rangle = -\frac{2}{kT} \left\{ \left\langle \mu_z^{(1)}(2\omega) \frac{\partial U^{(1)}}{\partial E_z} \right\rangle + \left\langle \mu_z^{(1)}(2\omega) \frac{\partial U^{(2)}}{\partial E_z} \right\rangle \right\}. \quad (4.61)$$

Hence,

$$\begin{aligned} \frac{1}{2} \left(\overline{\frac{\partial \mu_z^{(12)}(2\omega, \tau, \mathbf{E})}{\partial E_z}} \right)_{E_z=0} &= \left\langle \frac{\partial \mu_z^{(1)}(2\omega)}{\partial E_z} \right\rangle - \frac{1}{kT} \left\{ \left\langle \mu_z^{(1)}(2\omega) \frac{\partial U^{(1)}}{\partial E_z} \right\rangle \right. \\ &\quad \left. + \left\langle \mu_z^{(1)}(2\omega) \frac{\partial U^{(2)}}{\partial E_z} \right\rangle \right\}. \end{aligned} \quad (4.62)$$

Evaluation of these isotropic averages requires expressions for $\left(\mu_z^{(1)}(2\omega, \tau, \mathbf{E}) \right)_{E_z=0}$, $\left(\partial \mu_z^{(1)}(2\omega, \tau, \mathbf{E}) / \partial E_z \right)_{E_z=0}$, $\left(\partial U^{(1)}(\tau, \mathbf{E}) / \partial E_z \right)_{E_z=0}$ and $\left(\partial U^{(2)}(\tau, \mathbf{E}) / \partial E_z \right)_{E_z=0}$, which are readily obtained from equations (4.58), (4.43) and (4.44). These are as follows:

$$\begin{aligned}
\left(\mu_z^{(1)}(2\omega)\right)_{E_z=0} &= -\frac{1}{12} \left(\gamma_{i\bar{w}j}^{(1)}(-2\omega; \omega, \omega, 0) T_{jqr} \Theta_{0qr}^{(2)} \right. \\
&\quad + 2\gamma_{i\bar{v}j}^{(1)} T_{jk} \alpha_{k\bar{w}}^{(2)}(-\omega; \omega) T_{lqr} \Theta_{0qr}^{(2)} - \alpha_{ij}^{(1)}(-2\omega; 2\omega) T_{jk} \gamma_{k\bar{v}l}^{(2)} T_{lqr} \Theta_{0qr}^{(1)} - \gamma_{i\bar{v}w}^{(1)} T_{jk} \alpha_{kl}^{(2)}(0; 0) T_{lqr} \Theta_{0qr}^{(1)} \\
&\quad + 2\gamma_{i\bar{v}j}^{(1)} T_{jk} \alpha_{kl}^{(2)}(-\omega; \omega) T_{lm} \alpha_{m\bar{w}}^{(1)}(-\omega; \omega) T_{pqr} \Theta_{0qr}^{(2)} + \gamma_{i\bar{v}l}^{(1)} T_{jk} \alpha_{k\bar{v}}^{(2)}(-\omega; \omega) T_{lm} \alpha_{m\bar{w}}^{(2)}(-\omega; \omega) T_{pqr} \Theta_{0qr}^{(2)} \\
&\quad - 2\alpha_{ij}^{(1)}(-2\omega; 2\omega) T_{jk} \gamma_{k\bar{v}l}^{(2)} T_{lm} \alpha_{m\bar{w}}^{(1)}(-\omega; \omega) T_{pqr} \Theta_{0qr}^{(1)} + \alpha_{ij}^{(1)}(-2\omega; 2\omega) T_{jk} \alpha_{kl}^{(2)}(-2\omega; 2\omega) T_{lm} \gamma_{m\bar{v}w}^{(1)} T_{pqr} \Theta_{0qr}^{(2)} \\
&\quad + \alpha_{ij}^{(1)}(-2\omega; 2\omega) T_{jk} \gamma_{k\bar{v}l}^{(2)} T_{lm} \alpha_{m\bar{p}}^{(1)}(0; 0) T_{pqr} \Theta_{0qr}^{(2)} - 2\gamma_{i\bar{v}j}^{(1)} T_{jk} \alpha_{k\bar{w}}^{(2)}(-\omega; \omega) T_{lm} \alpha_{m\bar{p}}^{(2)}(0; 0) T_{pqr} \Theta_{0qr}^{(1)} \\
&\quad \left. + \gamma_{i\bar{v}w}^{(1)} T_{jk} \alpha_{kl}^{(2)}(0; 0) T_{lm} \alpha_{m\bar{p}}^{(1)}(0; 0) T_{pqr} \Theta_{0qr}^{(2)} + \dots \right) \mathcal{E}_z^2 a_i^z a_{\bar{v}}^z a_{\bar{w}}^z \\
&\quad + \frac{1}{6} \left(B_{i\bar{v}jk}^{(1)}(-2\omega; \omega, \omega) T_{jkl} \alpha_{l\bar{w}}^{(2)}(-\omega; \omega) - \alpha_{ij}^{(1)}(-2\omega; 2\omega) T_{jk} B_{k\bar{v}lm}^{(2)} T_{lmn} \alpha_{n\bar{w}}^{(1)}(-\omega; \omega) \right. \\
&\quad \left. + B_{i\bar{v}jk}^{(1)} T_{jkl} \alpha_{lm}^{(2)}(-\omega; \omega) T_{mn} \alpha_{n\bar{w}}^{(1)}(-\omega; \omega) + B_{i\bar{v}lm}^{(1)} T_{jk} \alpha_{k\bar{v}}^{(2)}(-\omega; \omega) T_{lmn} \alpha_{n\bar{w}}^{(2)}(-\omega; \omega) + \dots \right) \mathcal{E}_z^2 a_i^z a_{\bar{v}}^z a_{\bar{w}}^z \\
&\quad - \frac{1}{12} \left(\alpha_{ij}^{(1)}(-2\omega; 2\omega) T_{jkl} D_{k\bar{v}w}^{(2)}(-2\omega; \omega, \omega) - \alpha_{ij}^{(1)}(-2\omega; 2\omega) T_{jk} \alpha_{kl}^{(2)}(-2\omega; 2\omega) T_{lmn} D_{m\bar{v}w}^{(1)} \right. \\
&\quad \left. + 2\alpha_{ij}^{(1)}(-2\omega; 2\omega) T_{jkl} D_{k\bar{v}m}^{(2)} T_{mn} \alpha_{n\bar{w}}^{(1)}(-\omega; \omega) + \dots \right) \mathcal{E}_z^2 a_i^z a_{\bar{v}}^z a_{\bar{w}}^z, \tag{4.63}
\end{aligned}$$

$$\begin{aligned}
\left(\frac{\partial \mu_z^{(1)}(2\omega)}{\partial E_z} \right)_{E_z=0} &= \frac{1}{4} \left(\gamma_{iwvh}^{(1)}(-2\omega; \omega, \omega, 0) + 2\gamma_{ivjh}^{(1)} T_{jk} \alpha_{kw}^{(2)}(-\omega; \omega) + \alpha_{ij}^{(1)}(-2\omega; 2\omega) T_{jk} \gamma_{kvwh}^{(2)} + \gamma_{ivwa}^{(1)} T_{ab} \alpha_{bh}^{(2)}(0; 0) + 2\gamma_{ivjh}^{(1)} T_{jk} \alpha_{kl}^{(2)}(-\omega; \omega) T_{lm} \alpha_{mw}^{(1)}(-\omega; \omega) \right. \\
&+ \gamma_{ijph}^{(1)} T_{jk} \alpha_{kv}^{(2)}(-\omega; \omega) T_{pq} \alpha_{qw}^{(2)}(-\omega; \omega) + 2\alpha_{ij}^{(1)}(-2\omega; 2\omega) T_{jk} \gamma_{kvwh}^{(2)} T_{lm} \alpha_{mw}^{(1)}(-\omega; \omega) + \alpha_{ij}^{(1)}(-2\omega; 2\omega) T_{jk} \alpha_{kl}^{(2)}(-2\omega; 2\omega) T_{lm} \gamma_{mvwh}^{(1)} \\
&+ \alpha_{ij}^{(1)}(-2\omega; 2\omega) T_{jk} \gamma_{kvwa}^{(2)} T_{ab} \alpha_{bh}^{(1)}(0; 0) + 2\gamma_{ivja}^{(1)} T_{jk} \alpha_{kw}^{(2)}(-\omega; \omega) T_{ab} \alpha_{bh}^{(2)}(0; 0) + \gamma_{ivwa}^{(1)} T_{ab} \alpha_{bc}^{(2)}(0; 0) T_{cd} \alpha_{dh}^{(1)}(0; 0) \\
&+ 2\gamma_{ivjh}^{(1)} T_{jk} \alpha_{kl}^{(2)}(-\omega; \omega) T_{lm} \alpha_{mn}^{(1)}(-\omega; \omega) T_{np} \alpha_{pw}^{(2)}(-\omega; \omega) + 2\gamma_{ijph}^{(1)} T_{jk} \alpha_{kv}^{(2)}(-\omega; \omega) T_{pq} \alpha_{qr}^{(2)}(-\omega; \omega) T_{rs} \alpha_{sw}^{(1)}(-\omega; \omega) \\
&+ 2\alpha_{ij}^{(1)}(-2\omega; 2\omega) T_{jk} \gamma_{kvwh}^{(2)} T_{lm} \alpha_{mn}^{(1)}(-\omega; \omega) T_{np} \alpha_{pw}^{(2)}(-\omega; \omega) + \alpha_{ij}^{(1)}(-2\omega; 2\omega) T_{jk} \gamma_{klph}^{(2)} T_{lm} \alpha_{mv}^{(1)}(-\omega; \omega) T_{pq} \alpha_{qw}^{(1)}(-\omega; \omega) \\
&+ 2\alpha_{ij}^{(1)}(-2\omega; 2\omega) T_{jk} \alpha_{kl}^{(2)}(-2\omega; 2\omega) T_{lm} \gamma_{mvnh}^{(1)} T_{np} \alpha_{pw}^{(2)}(-\omega; \omega) + \alpha_{ij}^{(1)}(-2\omega; 2\omega) T_{jk} \alpha_{kl}^{(2)}(-2\omega; 2\omega) T_{lm} \alpha_{mn}^{(1)}(-2\omega; 2\omega) T_{np} \gamma_{pvwh}^{(2)} \\
&+ \alpha_{ij}^{(1)}(-2\omega; 2\omega) T_{jk} \alpha_{kl}^{(2)}(-2\omega; 2\omega) T_{lm} \gamma_{mvwn}^{(1)} T_{np} \alpha_{ph}^{(2)}(0; 0) + 2\alpha_{ij}^{(1)}(-2\omega; 2\omega) T_{jk} \gamma_{kvma}^{(2)} T_{mn} \alpha_{nw}^{(1)}(-\omega; \omega) T_{ab} \alpha_{bh}^{(1)}(0; 0) \\
&+ \alpha_{ij}^{(1)}(-2\omega; 2\omega) T_{jk} \gamma_{kvwa}^{(2)} T_{ab} \alpha_{bc}^{(1)}(0; 0) T_{cd} \alpha_{dh}^{(2)}(0; 0) + \gamma_{ijpa}^{(1)} T_{jk} \alpha_{kv}^{(2)}(-\omega; \omega) T_{pq} \alpha_{qw}^{(2)}(-\omega; \omega) T_{ab} \alpha_{bh}^{(2)}(0; 0) \\
&+ 2\gamma_{ivja}^{(1)} T_{jk} \alpha_{kl}^{(2)}(-\omega; \omega) T_{lm} \alpha_{mw}^{(1)}(-\omega; \omega) T_{ab} \alpha_{bh}^{(2)}(0; 0) + 2\gamma_{ivja}^{(1)} T_{jk} \alpha_{kw}^{(2)}(-\omega; \omega) T_{ab} \alpha_{bc}^{(2)}(0; 0) T_{cd} \alpha_{dh}^{(1)}(0; 0) \\
&+ \gamma_{ivwa}^{(1)} T_{ab} \alpha_{bc}^{(2)}(0; 0) T_{cd} \alpha_{de}^{(1)}(0; 0) T_{ef} \alpha_{fh}^{(2)}(0; 0) + 2\gamma_{ivjh}^{(1)} T_{jk} \alpha_{kl}^{(2)}(-\omega; \omega) T_{lm} \alpha_{mn}^{(1)}(-\omega; \omega) T_{np} \alpha_{pq}^{(2)}(-\omega; \omega) T_{qr} \alpha_{rw}^{(1)}(-\omega; \omega) \\
&+ 2\gamma_{ijph}^{(1)} T_{jk} \alpha_{kv}^{(2)}(-\omega; \omega) T_{pq} \alpha_{qr}^{(2)}(-\omega; \omega) T_{rs} \alpha_{st}^{(1)}(-\omega; \omega) T_{tu} \alpha_{uw}^{(2)}(-\omega; \omega) + \gamma_{ijph}^{(1)} T_{jk} \alpha_{kl}^{(2)}(-\omega; \omega) T_{lm} \alpha_{mv}^{(1)}(-\omega; \omega) T_{pq} \alpha_{qr}^{(2)}(-\omega; \omega) T_{rs} \alpha_{sw}^{(1)}(-\omega; \omega) \\
&+ 2\gamma_{ivja}^{(1)} T_{jk} \alpha_{kl}^{(2)}(-\omega; \omega) T_{lm} \alpha_{mn}^{(1)}(-\omega; \omega) T_{np} \alpha_{pw}^{(2)}(-\omega; \omega) T_{ab} \alpha_{bh}^{(2)}(0; 0) + 2\gamma_{ijpa}^{(1)} T_{jk} \alpha_{kv}^{(2)}(-\omega; \omega) T_{pq} \alpha_{qr}^{(2)}(-\omega; \omega) T_{rs} \alpha_{sw}^{(1)}(-\omega; \omega) T_{ab} \alpha_{bh}^{(2)}(0; 0) \\
&+ 2\gamma_{ivja}^{(1)} T_{jk} \alpha_{kl}^{(2)}(-\omega; \omega) T_{lm} \alpha_{mw}^{(1)}(-\omega; \omega) T_{ab} \alpha_{bc}^{(2)}(0; 0) T_{cd} \alpha_{dh}^{(1)}(0; 0) + \gamma_{ijpa}^{(1)} T_{jk} \alpha_{kv}^{(2)}(-\omega; \omega) T_{pq} \alpha_{qw}^{(2)}(-\omega; \omega) T_{ab} \alpha_{bc}^{(2)}(0; 0) T_{cd} \alpha_{dh}^{(1)}(0; 0) \\
&+ 2\gamma_{ivja}^{(1)} T_{jk} \alpha_{kw}^{(2)}(-\omega; \omega) T_{ab} \alpha_{bc}^{(2)}(0; 0) T_{cd} \alpha_{de}^{(1)}(0; 0) T_{ef} \alpha_{fh}^{(2)}(0; 0) + \gamma_{ivwa}^{(1)} T_{ab} \alpha_{bc}^{(2)}(0; 0) T_{cd} \alpha_{de}^{(1)}(0; 0) T_{ef} \alpha_{fg}^{(2)}(0; 0) T_{gj} \alpha_{jh}^{(1)}(0; 0)
\end{aligned}$$

(continued over the page ...)

$$\begin{aligned}
& + 2\alpha_{ij}^{(1)}(-2\omega; 2\omega)T_{jk}\gamma_{kvlh}^{(2)}T_{lm}\alpha_{mn}^{(1)}(-\omega; \omega)T_{np}\alpha_{pq}^{(2)}(-\omega; \omega)T_{qr}\alpha_{rw}^{(1)}(-\omega; \omega) \\
& + \alpha_{ij}^{(1)}(-2\omega; 2\omega)T_{jk}\gamma_{klph}^{(2)}T_{lm}\alpha_{mv}^{(1)}(-\omega; \omega)T_{pq}\alpha_{qr}^{(1)}(-\omega; \omega)T_{rs}\alpha_{sw}^{(2)}(-\omega; \omega) \\
& + 2\alpha_{ij}^{(1)}(-2\omega; 2\omega)T_{jk}\alpha_{kl}^{(2)}(-2\omega; 2\omega)T_{lm}\gamma_{mnh}^{(1)}T_{np}\alpha_{pq}^{(2)}(-\omega; \omega)T_{qr}\alpha_{rw}^{(1)}(-\omega; \omega) \\
& + \alpha_{ij}^{(1)}(-2\omega; 2\omega)T_{jk}\alpha_{kl}^{(2)}(-2\omega; 2\omega)T_{lm}\gamma_{mnqh}^{(1)}T_{np}\alpha_{pv}^{(2)}(-\omega; \omega)T_{qr}\alpha_{rw}^{(2)}(-\omega; \omega) \\
& + 2\alpha_{ij}^{(1)}(-2\omega; 2\omega)T_{jk}\alpha_{kl}^{(2)}(-2\omega; 2\omega)T_{lm}\alpha_{mn}^{(1)}(-2\omega; 2\omega)T_{np}\gamma_{pqh}^{(2)}T_{qr}\alpha_{rw}^{(1)}(-\omega; \omega) \\
& + \alpha_{ij}^{(1)}(-2\omega; 2\omega)T_{jk}\alpha_{kl}^{(2)}(-2\omega; 2\omega)T_{lm}\alpha_{mn}^{(1)}(-2\omega; 2\omega)T_{np}\alpha_{pq}^{(2)}(-2\omega; 2\omega)T_{qr}\gamma_{rvwh}^{(1)} \\
& + 2\alpha_{ij}^{(1)}(-2\omega; 2\omega)T_{jk}\gamma_{kvla}^{(2)}T_{lm}\alpha_{mn}^{(1)}(-\omega; \omega)T_{np}\alpha_{pw}^{(2)}(-2\omega; 2\omega)T_{ab}\alpha_{bh}^{(1)}(0; 0) \\
& + \alpha_{ij}^{(1)}(-2\omega; 2\omega)T_{jk}\gamma_{klpa}^{(2)}T_{lm}\alpha_{mv}^{(1)}(-\omega; \omega)T_{pq}\alpha_{qw}^{(1)}(-2\omega; 2\omega)T_{ab}\alpha_{bh}^{(1)}(0; 0) \\
& + 2\alpha_{ij}^{(1)}(-2\omega; 2\omega)T_{jk}\alpha_{kl}^{(2)}(-2\omega; 2\omega)T_{lm}\gamma_{mvna}^{(1)}T_{np}\alpha_{pw}^{(2)}(-\omega; \omega)T_{ab}\alpha_{bh}^{(2)}(0; 0) \\
& + \alpha_{ij}^{(1)}(-2\omega; 2\omega)T_{jk}\alpha_{kl}^{(2)}(-2\omega; 2\omega)T_{lm}\alpha_{mn}^{(1)}(-2\omega; 2\omega)T_{np}\gamma_{pvwa}^{(2)}T_{ab}\alpha_{bh}^{(1)}(0; 0) \\
& + 2\alpha_{ij}^{(1)}(-2\omega; 2\omega)T_{jk}\gamma_{kvla}^{(2)}T_{lm}\alpha_{mw}^{(1)}(-\omega; \omega)T_{ab}\alpha_{bc}^{(1)}(0; 0)T_{cd}\alpha_{dh}^{(2)}(0; 0) \\
& + \alpha_{ij}^{(1)}(-2\omega; 2\omega)T_{jk}\alpha_{kl}^{(2)}(-2\omega; 2\omega)T_{lm}\gamma_{mvwa}^{(1)}T_{ab}\alpha_{bc}^{(2)}(0; 0)T_{cd}\alpha_{dh}^{(1)}(0; 0) \\
& + \alpha_{ij}^{(1)}(-2\omega; 2\omega)T_{jk}\gamma_{kvwa}^{(2)}T_{ab}\alpha_{bc}^{(1)}(0; 0)T_{cd}\alpha_{de}^{(2)}(0; 0)T_{ef}\alpha_{fh}^{(1)}(0; 0) + \cdots \Big) \mathcal{E}_z^2 a_i^z a_v^z a_w^z a_h^z, \tag{4.64}
\end{aligned}$$

$$\begin{aligned}
\left(\frac{\partial U^{(1)}(\tau, \mathbf{E})}{\partial E_z} \right)_{E_z=0} &= \frac{1}{3} \left(\alpha_{ab}^{(1)}(0; 0) T_{bgh} \Theta_{0gh}^{(2)} - \alpha_{ab}^{(1)}(0; 0) T_{bc} \alpha_{cd}^{(2)}(0; 0) T_{dgh} \Theta_{0gh}^{(1)} \right. \\
&\quad + \alpha_{ab}^{(1)}(0; 0) T_{bc} \alpha_{cd}^{(2)}(0; 0) T_{de} \alpha_{ef}^{(1)}(0; 0) T_{fgh} \Theta_{0gh}^{(2)} \\
&\quad - \alpha_{ab}^{(1)}(0; 0) T_{bc} \alpha_{cd}^{(2)}(0; 0) T_{de} \alpha_{ef}^{(1)}(0; 0) T_{fs} \alpha_{st}^{(2)}(0; 0) T_{tgh} \Theta_{0gh}^{(1)} \\
&\quad \left. + \dots \right) a_a^z
\end{aligned} \tag{4.65}$$

and

$$\begin{aligned}
\left(\frac{\partial U^{(2)}(\tau, \mathbf{E})}{\partial E_z} \right)_{E_z=0} &= \frac{1}{3} \left(-\alpha_{ab}^{(2)}(0; 0) T_{bgh} \Theta_{0gh}^{(1)} + \alpha_{ab}^{(2)}(0; 0) T_{bc} \alpha_{cd}^{(1)}(0; 0) T_{dgh} \Theta_{0gh}^{(2)} \right. \\
&\quad - \alpha_{ab}^{(2)}(0; 0) T_{bc} \alpha_{cd}^{(1)}(0; 0) T_{de} \alpha_{ef}^{(2)}(0; 0) T_{fgh} \Theta_{0gh}^{(1)} \\
&\quad + \alpha_{ab}^{(2)}(0; 0) T_{bc} \alpha_{cd}^{(1)}(0; 0) T_{de} \alpha_{ef}^{(2)}(0; 0) T_{fs} \alpha_{st}^{(1)}(0; 0) T_{tgh} \Theta_{0gh}^{(2)} \\
&\quad \left. + \dots \right) a_a^z.
\end{aligned} \tag{4.66}$$

Substituting equations (4.63) to (4.66) into equation (4.62) yields the contributions to B_γ in equation (4.23). These are

$$\begin{aligned}
& \left\{ \frac{1}{2} \left(\frac{\overline{\partial \mu_z^{(12)}(2\omega, \tau, \mathbf{E})}}{\partial E_z} \right)_{E_z=0} - \left(\frac{\overline{\partial \mu_z(2\omega)}}{\partial E_z} \right)_{E_z=0} \right\} \\
& = \gamma_1 \alpha_1 + \gamma_1 \alpha_2 + \gamma_1 \alpha_3 + \gamma_1 \alpha_4 + \dots \\
& \quad + \gamma_1 \alpha_1 \Theta_2 + \gamma_1 \alpha_2 \Theta_2 + \gamma_1 \alpha_3 \Theta_2 + \dots \tag{4.67} \\
& \quad + B_1 \alpha_2 \Theta_1 + B_1 \alpha_3 \Theta_1 + \dots \\
& \quad + D_1 \alpha_2 \Theta_1 + D_1 \alpha_3 \Theta_1 + \dots,
\end{aligned}$$

where

$$\begin{aligned}
\gamma_1 \alpha_1 = \frac{\mathcal{E}_z^2}{4} & \left\{ 2\gamma_{ivjh}^{(1)}(-2\omega; \omega, \omega, 0) T_{jk} \alpha_{kw}^{(2)}(-\omega; \omega) \right. \\
& + \alpha_{ij}^{(1)}(-2\omega; 2\omega) T_{jk} \gamma_{kvwh}^{(2)}(-2\omega; \omega, \omega, 0) \\
& \left. + \gamma_{ivwa}^{(1)}(-2\omega; \omega, \omega, 0) T_{ab} \alpha_{bh}^{(2)}(0; 0) \right\} \langle a_i^z a_v^z a_w^z a_h^z \rangle, \tag{4.68}
\end{aligned}$$

$$\begin{aligned}
\gamma_1 \alpha_2 = \frac{\mathcal{E}_z^2}{4} & \left\{ 2\gamma_{ivjh}^{(1)}(-2\omega; \omega, \omega, 0) T_{jk} \alpha_{kl}^{(2)}(-\omega; \omega) T_{lm} \alpha_{mw}^{(1)}(-\omega; \omega) \right. \\
& + \gamma_{ijph}^{(1)}(-2\omega; \omega, \omega, 0) T_{jk} \alpha_{kv}^{(2)}(-\omega; \omega) T_{pq} \alpha_{qw}^{(2)}(-\omega; \omega) \\
& + 2\alpha_{ij}^{(1)}(-2\omega; 2\omega) T_{jk} \gamma_{kvlh}^{(2)}(-2\omega; \omega, \omega, 0) T_{lm} \alpha_{mw}^{(1)}(-\omega; \omega) \\
& + \alpha_{ij}^{(1)}(-2\omega; 2\omega) T_{jk} \alpha_{kl}^{(2)}(-2\omega; 2\omega) T_{lm} \gamma_{mvwh}^{(1)}(-2\omega; \omega, \omega, 0) \quad (4.69) \\
& + \alpha_{ij}^{(1)}(-2\omega; 2\omega) T_{jk} \gamma_{kvwa}^{(2)}(-2\omega; \omega, \omega, 0) T_{ab} \alpha_{bh}^{(1)}(0; 0) \\
& + 2\gamma_{ivja}^{(1)}(-2\omega; \omega, \omega, 0) T_{jk} \alpha_{kw}^{(2)}(-\omega; \omega) T_{ab} \alpha_{bh}^{(2)}(0; 0) \\
& \left. + \gamma_{ivwa}^{(1)}(-2\omega; \omega, \omega, 0) T_{ab} \alpha_{bc}^{(2)}(0; 0) T_{cd} \alpha_{dh}^{(1)}(0; 0) \right\} \left\langle a_i^z a_v^z a_w^z a_h^z \right\rangle,
\end{aligned}$$

$$\begin{aligned}
\gamma_1 \alpha_3 = \frac{\mathcal{E}_z^2}{4} \left\{ & 2\gamma_{ivjh}^{(1)}(-2\omega; \omega, \omega, 0) T_{jk} \alpha_{kl}^{(2)}(-\omega; \omega) T_{lm} \alpha_{mn}^{(1)}(-\omega; \omega) T_{np} \alpha_{pw}^{(2)}(-\omega; \omega) \right. \\
& + 2\gamma_{ijph}^{(1)}(-2\omega; \omega, \omega, 0) T_{jk} \alpha_{kv}^{(2)}(-\omega; \omega) T_{pq} \alpha_{qr}^{(2)}(-\omega; \omega) T_{rs} \alpha_{sw}^{(1)}(-\omega; \omega) \\
& + 2\alpha_{ij}^{(1)}(-2\omega; 2\omega) T_{jk} \gamma_{klvh}^{(2)}(-2\omega; \omega, \omega, 0) T_{lm} \alpha_{mn}^{(1)}(-\omega; \omega) T_{np} \alpha_{pw}^{(2)}(-\omega; \omega) \\
& + \alpha_{ij}^{(1)}(-2\omega; 2\omega) T_{jk} \gamma_{klph}^{(2)}(-2\omega; \omega, \omega, 0) T_{lm} \alpha_{mv}^{(1)}(-\omega; \omega) T_{pq} \alpha_{qw}^{(1)}(-\omega; \omega) \\
& + 2\alpha_{ij}^{(1)}(-2\omega; 2\omega) T_{jk} \alpha_{kl}^{(2)}(-2\omega; 2\omega) T_{lm} \gamma_{mvnh}^{(1)}(-2\omega; \omega, \omega, 0) T_{np} \alpha_{pw}^{(2)}(-\omega; \omega) \\
& + \alpha_{ij}^{(1)}(-2\omega; 2\omega) T_{jk} \alpha_{kl}^{(2)}(-2\omega; 2\omega) T_{lm} \alpha_{mn}^{(1)}(-2\omega; 2\omega) T_{np} \gamma_{pvwh}^{(2)}(-2\omega; \omega, \omega, 0) \\
& + \alpha_{ij}^{(1)}(-2\omega; 2\omega) T_{jk} \alpha_{kl}^{(2)}(-2\omega; 2\omega) T_{lm} \gamma_{mvwn}^{(1)}(-2\omega; \omega, \omega, 0) T_{np} \alpha_{ph}^{(2)}(0; 0) \\
& + 2\alpha_{ij}^{(1)}(-2\omega; 2\omega) T_{jk} \gamma_{kvma}^{(2)}(-2\omega; \omega, \omega, 0) T_{mn} \alpha_{nw}^{(1)}(-\omega; \omega) T_{ab} \alpha_{bh}^{(1)}(0; 0) \\
& + \alpha_{ij}^{(1)}(-2\omega; 2\omega) T_{jk} \gamma_{kvwa}^{(2)}(-2\omega; \omega, \omega, 0) T_{ab} \alpha_{bc}^{(1)}(0; 0) T_{cd} \alpha_{dh}^{(2)}(0; 0) \\
& + \gamma_{ijpa}^{(1)}(-2\omega; \omega, \omega, 0) T_{jk} \alpha_{kv}^{(2)}(-\omega; \omega) T_{pq} \alpha_{qw}^{(2)}(-\omega; \omega) T_{ab} \alpha_{bh}^{(2)}(0; 0) \\
& + 2\gamma_{ivja}^{(1)}(-2\omega; \omega, \omega, 0) T_{jk} \alpha_{kl}^{(2)}(-\omega; \omega) T_{lm} \alpha_{mw}^{(1)}(-\omega; \omega) T_{ab} \alpha_{bh}^{(2)}(0; 0) \\
& + 2\gamma_{ivja}^{(1)}(-2\omega; \omega, \omega, 0) T_{jk} \alpha_{kw}^{(2)}(-\omega; \omega) T_{ab} \alpha_{bc}^{(2)}(0; 0) T_{cd} \alpha_{dh}^{(1)}(0; 0) \\
& \left. + \gamma_{ivwa}^{(1)}(-2\omega; \omega, \omega, 0) T_{ab} \alpha_{bc}^{(2)}(0; 0) T_{cd} \alpha_{de}^{(1)}(0; 0) T_{ef} \alpha_{fh}^{(2)}(0; 0) \right\} \left\langle a_i^z a_v^z a_w^z a_h^z \right\rangle,
\end{aligned} \tag{4.70}$$

$$\begin{aligned}
\gamma_1 \alpha_4 = \frac{\mathcal{E}_z^2}{4} & \left\{ 2\gamma_{ivjh}^{(1)}(-2\omega; \omega, \omega, 0) T_{jk} \alpha_{kl}^{(2)}(-\omega; \omega) T_{lm} \alpha_{mn}^{(1)}(-\omega; \omega) T_{np} \alpha_{pq}^{(2)}(-\omega; \omega) T_{qr} \alpha_{rw}^{(1)}(-\omega; \omega) \right. \\
& + 2\gamma_{ijph}^{(1)}(-2\omega; \omega, \omega, 0) T_{jk} \alpha_{kv}^{(2)}(-\omega; \omega) T_{pq} \alpha_{qr}^{(2)}(-\omega; \omega) T_{rs} \alpha_{st}^{(1)}(-\omega; \omega) T_{tu} \alpha_{uw}^{(2)}(-\omega; \omega) \\
& + \gamma_{ijph}^{(1)}(-2\omega; \omega, \omega, 0) T_{jk} \alpha_{kl}^{(2)}(-\omega; \omega) T_{lm} \alpha_{mv}^{(1)}(-\omega; \omega) T_{pq} \alpha_{qr}^{(2)}(-\omega; \omega) T_{rs} \alpha_{sw}^{(1)}(-\omega; \omega) \\
& + 2\gamma_{ivja}^{(1)}(-2\omega; \omega, \omega, 0) T_{jk} \alpha_{kl}^{(2)}(-\omega; \omega) T_{lm} \alpha_{mn}^{(1)}(-\omega; \omega) T_{np} \alpha_{pw}^{(2)}(-\omega; \omega) T_{ab} \alpha_{bh}^{(2)}(0; 0) \\
& + 2\gamma_{ijpa}^{(1)}(-2\omega; \omega, \omega, 0) T_{jk} \alpha_{kv}^{(2)}(-\omega; \omega) T_{pq} \alpha_{qr}^{(2)}(-\omega; \omega) T_{rs} \alpha_{sw}^{(1)}(-\omega; \omega) T_{ab} \alpha_{bh}^{(2)}(0; 0) \\
& + 2\gamma_{ivja}^{(1)}(-2\omega; \omega, \omega, 0) T_{jk} \alpha_{kl}^{(2)}(-\omega; \omega) T_{lm} \alpha_{mv}^{(1)}(-\omega; \omega) T_{ab} \alpha_{bc}^{(2)}(0; 0) T_{cd} \alpha_{dh}^{(1)}(0; 0) \\
& + \gamma_{ijpa}^{(1)}(-2\omega; \omega, \omega, 0) T_{jk} \alpha_{kv}^{(2)}(-\omega; \omega) T_{pq} \alpha_{qw}^{(2)}(-\omega; \omega) T_{ab} \alpha_{bc}^{(2)}(0; 0) T_{cd} \alpha_{dh}^{(1)}(0; 0) \\
& + 2\gamma_{ivja}^{(1)}(-2\omega; \omega, \omega, 0) T_{jk} \alpha_{kw}^{(2)}(-\omega; \omega) T_{ab} \alpha_{bc}^{(2)}(0; 0) T_{cd} \alpha_{de}^{(1)}(0; 0) T_{ef} \alpha_{fh}^{(2)}(0; 0) \\
& + \gamma_{ivva}^{(1)}(-2\omega; \omega, \omega, 0) T_{ab} \alpha_{bc}^{(2)}(0; 0) T_{cd} \alpha_{de}^{(1)}(0; 0) T_{ef} \alpha_{fg}^{(2)}(0; 0) T_{gj} \alpha_{jh}^{(1)}(0; 0) \\
& + 2\alpha_{ij}^{(1)}(-2\omega; 2\omega) T_{jk} \gamma_{kvlh}^{(2)}(-2\omega; \omega, \omega, 0) T_{lm} \alpha_{mn}^{(1)}(-\omega; \omega) T_{np} \alpha_{pq}^{(2)}(-\omega; \omega) T_{qr} \alpha_{rw}^{(1)}(-\omega; \omega) \\
& + \alpha_{ij}^{(1)}(-2\omega; 2\omega) T_{jk} \gamma_{klph}^{(2)}(-2\omega; \omega, \omega, 0) T_{lm} \alpha_{mv}^{(1)}(-\omega; \omega) T_{pq} \alpha_{qr}^{(1)}(-\omega; \omega) T_{rs} \alpha_{sw}^{(2)}(-\omega; \omega) \\
& + 2\alpha_{ij}^{(1)}(-2\omega; 2\omega) T_{jk} \alpha_{kl}^{(2)}(-2\omega; 2\omega) T_{lm} \gamma_{mnh}^{(1)}(-2\omega; \omega, \omega, 0) T_{np} \alpha_{pq}^{(2)}(-\omega; \omega) T_{qr} \alpha_{rw}^{(1)}(-\omega; \omega) \\
& + \alpha_{ij}^{(1)}(-2\omega; 2\omega) T_{jk} \alpha_{kl}^{(2)}(-2\omega; 2\omega) T_{lm} \gamma_{mnqh}^{(1)}(-2\omega; \omega, \omega, 0) T_{np} \alpha_{pw}^{(2)}(-\omega; \omega) T_{qr} \alpha_{rw}^{(2)}(-\omega; \omega) \\
& + 2\alpha_{ij}^{(1)}(-2\omega; 2\omega) T_{jk} \alpha_{kl}^{(2)}(-2\omega; 2\omega) T_{lm} \alpha_{mn}^{(1)}(-2\omega; 2\omega) T_{np} \gamma_{pvqh}^{(2)}(-2\omega; \omega, \omega, 0) T_{qr} \alpha_{rw}^{(1)}(-\omega; \omega) \\
& + \alpha_{ij}^{(1)}(-2\omega; 2\omega) T_{jk} \alpha_{kl}^{(2)}(-2\omega; 2\omega) T_{lm} \alpha_{mn}^{(1)}(-2\omega; 2\omega) T_{np} \alpha_{pq}^{(2)}(-2\omega; 2\omega) T_{qr} \gamma_{rvwh}^{(1)}(-2\omega; \omega, \omega, 0) \\
& + 2\alpha_{ij}^{(1)}(-2\omega; 2\omega) T_{jk} \gamma_{kvla}^{(2)}(-2\omega; \omega, \omega, 0) T_{lm} \alpha_{mn}^{(1)}(-\omega; \omega) T_{np} \alpha_{pw}^{(2)}(-2\omega; 2\omega) T_{ab} \alpha_{bh}^{(1)}(0; 0) \\
& + \alpha_{ij}^{(1)}(-2\omega; 2\omega) T_{jk} \gamma_{klpa}^{(2)}(-2\omega; \omega, \omega, 0) T_{lm} \alpha_{mv}^{(1)}(-\omega; \omega) T_{pq} \alpha_{qw}^{(1)}(-2\omega; 2\omega) T_{ab} \alpha_{bh}^{(1)}(0; 0) \\
& + 2\alpha_{ij}^{(1)}(-2\omega; 2\omega) T_{jk} \alpha_{kl}^{(2)}(-2\omega; 2\omega) T_{lm} \gamma_{mvna}^{(1)}(-2\omega; \omega, \omega, 0) T_{np} \alpha_{pw}^{(2)}(-\omega; \omega) T_{ab} \alpha_{bh}^{(2)}(0; 0) \\
& + \alpha_{ij}^{(1)}(-2\omega; 2\omega) T_{jk} \alpha_{kl}^{(2)}(-2\omega; 2\omega) T_{lm} \alpha_{mn}^{(1)}(-2\omega; 2\omega) T_{np} \gamma_{pvwa}^{(2)}(-2\omega; \omega, \omega, 0) T_{ab} \alpha_{bh}^{(1)}(0; 0) \\
& + 2\alpha_{ij}^{(1)}(-2\omega; 2\omega) T_{jk} \gamma_{kvla}^{(2)}(-2\omega; \omega, \omega, 0) T_{lm} \alpha_{mw}^{(1)}(-\omega; \omega) T_{ab} \alpha_{bc}^{(1)}(0; 0) T_{cd} \alpha_{dh}^{(2)}(0; 0) \\
& + \alpha_{ij}^{(1)}(-2\omega; 2\omega) T_{jk} \alpha_{kl}^{(2)}(-2\omega; 2\omega) T_{lm} \gamma_{mvwa}^{(1)}(-2\omega; \omega, \omega, 0) T_{ab} \alpha_{bc}^{(2)}(0; 0) T_{cd} \alpha_{dh}^{(1)}(0; 0) \\
& \left. + \alpha_{ij}^{(1)}(-2\omega; 2\omega) T_{jk} \gamma_{kvwa}^{(2)}(-2\omega; \omega, \omega, 0) T_{ab} \alpha_{bc}^{(1)}(0; 0) T_{cd} \alpha_{de}^{(2)}(0; 0) T_{ef} \alpha_{fh}^{(1)}(0; 0) \right\} \left\langle a_i^z a_v^z a_w^z a_h^z \right\rangle,
\end{aligned}
\tag{4.71}$$

$$\begin{aligned}
\gamma_1 \alpha_1 \Theta_2 = \frac{\mathcal{E}_z^2}{36kT} & \left\{ \gamma_{i v w j}^{(1)}(-2\omega; \omega, \omega, 0) T_{j q r} \Theta_{0 q r}^{(2)} \alpha_{a b}^{(1)}(0; 0) T_{b g h} \Theta_{0 g h}^{(2)} \right. \\
& \left. - \gamma_{i v w j}^{(1)}(-2\omega; \omega, \omega, 0) T_{j q r} \Theta_{0 q r}^{(2)} \alpha_{a b}^{(2)}(0; 0) T_{b g h} \Theta_{0 g h}^{(1)} \right\} \left\langle a_i^z a_v^z a_w^z a_a^z \right\rangle,
\end{aligned} \tag{4.72}$$

$$\begin{aligned}
\gamma_1 \alpha_2 \Theta_2 = \frac{\mathcal{E}_z^2}{36kT} & \left\{ 2\gamma_{i v j l}^{(1)}(-2\omega; \omega, \omega, 0) T_{j k} \alpha_{k w}^{(2)}(-\omega; \omega) T_{l q r} \Theta_{0 q r}^{(2)} \alpha_{a b}^{(1)}(0; 0) T_{b g h} \Theta_{0 g h}^{(2)} \right. \\
& - 2\gamma_{i v j l}^{(1)}(-2\omega; \omega, \omega, 0) T_{j k} \alpha_{k w}^{(2)}(-\omega; \omega) T_{l q r} \Theta_{0 q r}^{(2)} \alpha_{a b}^{(2)}(0; 0) T_{b g h} \Theta_{0 g h}^{(1)} \\
& - \alpha_{i j}^{(1)}(-2\omega; 2\omega) T_{j k} \gamma_{k v w l}^{(2)}(-2\omega; \omega, \omega, 0) T_{l q r} \Theta_{0 q r}^{(1)} \alpha_{a b}^{(1)}(0; 0) T_{b g h} \Theta_{0 g h}^{(2)} \\
& + \alpha_{i j}^{(1)}(-2\omega; 2\omega) T_{j k} \gamma_{k v w l}^{(2)}(-2\omega; \omega, \omega, 0) T_{l q r} \Theta_{0 q r}^{(1)} \alpha_{a b}^{(2)}(0; 0) T_{b g h} \Theta_{0 g h}^{(1)} \\
& - \gamma_{i v w j}^{(1)}(-2\omega; \omega, \omega, 0) T_{j k} \alpha_{k l}^{(2)}(0; 0) T_{l q r} \Theta_{0 q r}^{(1)} \alpha_{a b}^{(1)}(0; 0) T_{b g h} \Theta_{0 g h}^{(2)} \\
& + \gamma_{i v w j}^{(1)}(-2\omega; \omega, \omega, 0) T_{j k} \alpha_{k l}^{(2)}(0; 0) T_{l q r} \Theta_{0 q r}^{(1)} \alpha_{a b}^{(2)}(0; 0) T_{b g h} \Theta_{0 g h}^{(1)} \\
& - \gamma_{i v w j}^{(1)}(-2\omega; \omega, \omega, 0) T_{j q r} \Theta_{0 q r}^{(2)} \alpha_{a b}^{(1)}(0; 0) T_{b c} \alpha_{c d}^{(2)}(0; 0) T_{d g h} \Theta_{0 g h}^{(1)} \\
& \left. + \gamma_{i v w j}^{(1)}(-2\omega; \omega, \omega, 0) T_{j q r} \Theta_{0 q r}^{(2)} \alpha_{a b}^{(2)}(0; 0) T_{b c} \alpha_{c d}^{(1)}(0; 0) T_{d g h} \Theta_{0 g h}^{(2)} \right\} \left\langle a_i^z a_v^z a_w^z a_a^z \right\rangle,
\end{aligned} \tag{4.73}$$

$$\begin{aligned}
\gamma_1 \alpha_3 \Theta_2 = \frac{\mathcal{E}_z^2}{36kT} \left\{ 2\gamma_{ivjp}^{(1)} T_{jk} \alpha_{kl}^{(2)}(-\omega; \omega) T_{lm} \alpha_{mw}^{(1)}(-\omega; \omega) T_{pqr} \Theta_{0qr}^{(2)} \alpha_{ab}^{(1)}(0; 0) T_{bgh} \Theta_{0gh}^{(2)} \right. \\
+ 2\gamma_{ivjp}^{(1)} T_{jk} \alpha_{kl}^{(2)}(-\omega; \omega) T_{lm} \alpha_{mw}^{(1)}(-\omega; \omega) T_{pqr} \Theta_{0qr}^{(2)} \alpha_{ab}^{(2)}(0; 0) T_{bgh} \Theta_{0gh}^{(1)} \\
+ \gamma_{ijlp}^{(1)} T_{jk} \alpha_{kv}^{(2)}(-\omega; \omega) T_{lm} \alpha_{mw}^{(2)}(-\omega; \omega) T_{pqr} \Theta_{0qr}^{(2)} \alpha_{ab}^{(1)}(0; 0) T_{bgh} \Theta_{0gh}^{(2)} \\
+ \gamma_{ijlp}^{(1)} T_{jk} \alpha_{kv}^{(2)}(-\omega; \omega) T_{lm} \alpha_{mw}^{(2)}(-\omega; \omega) T_{pqr} \Theta_{0qr}^{(2)} \alpha_{ab}^{(2)}(0; 0) T_{bgh} \Theta_{0gh}^{(1)} \\
- 2\alpha_{ij}^{(1)}(-2\omega; 2\omega) T_{jk} \gamma_{kvlp}^{(2)} T_{lm} \alpha_{mw}^{(1)}(-\omega; \omega) T_{pqr} \Theta_{0qr}^{(1)} \alpha_{ab}^{(1)}(0; 0) T_{bgh} \Theta_{0gh}^{(2)} \\
- 2\alpha_{ij}^{(1)}(-2\omega; 2\omega) T_{jk} \gamma_{kvlp}^{(2)} T_{lm} \alpha_{mw}^{(1)}(-\omega; \omega) T_{pqr} \Theta_{0qr}^{(1)} \alpha_{ab}^{(2)}(0; 0) T_{bgh} \Theta_{0gh}^{(1)} \\
+ \alpha_{ij}^{(1)}(-2\omega; 2\omega) T_{jk} \alpha_{kl}^{(2)}(-2\omega; 2\omega) T_{lm} \gamma_{mvwp}^{(1)} T_{pqr} \Theta_{0qr}^{(2)} \alpha_{ab}^{(1)}(0; 0) T_{bgh} \Theta_{0gh}^{(2)} \\
+ \alpha_{ij}^{(1)}(-2\omega; 2\omega) T_{jk} \alpha_{kl}^{(2)}(-2\omega; 2\omega) T_{lm} \gamma_{mvwp}^{(1)} T_{pqr} \Theta_{0qr}^{(2)} \alpha_{ab}^{(2)}(0; 0) T_{bgh} \Theta_{0gh}^{(1)} \\
- \alpha_{ij}^{(1)}(-2\omega; 2\omega) T_{jk} \gamma_{kvwl}^{(2)} T_{lm} \alpha_{mp}^{(1)}(0; 0) T_{pqr} \Theta_{0qr}^{(2)} \alpha_{ab}^{(1)}(0; 0) T_{bgh} \Theta_{0gh}^{(2)} \\
- \alpha_{ij}^{(1)}(-2\omega; 2\omega) T_{jk} \gamma_{kvwl}^{(2)} T_{lm} \alpha_{mp}^{(1)}(0; 0) T_{pqr} \Theta_{0qr}^{(2)} \alpha_{ab}^{(2)}(0; 0) T_{bgh} \Theta_{0gh}^{(1)} \\
- 2\gamma_{ivjl}^{(1)} T_{jk} \alpha_{kw}^{(2)}(-\omega; \omega) T_{lm} \alpha_{mp}^{(2)}(0; 0) T_{pqr} \Theta_{0qr}^{(1)} \alpha_{ab}^{(1)}(0; 0) T_{bgh} \Theta_{0gh}^{(2)} \\
- 2\gamma_{ivjl}^{(1)} T_{jk} \alpha_{kw}^{(2)}(-\omega; \omega) T_{lm} \alpha_{mp}^{(2)}(0; 0) T_{pqr} \Theta_{0qr}^{(1)} \alpha_{ab}^{(2)}(0; 0) T_{bgh} \Theta_{0gh}^{(1)} \\
+ \gamma_{ivwj}^{(1)} T_{jk} \alpha_{kl}^{(2)}(0; 0) T_{lm} \alpha_{mp}^{(1)}(0; 0) T_{pqr} \Theta_{0qr}^{(2)} \alpha_{ab}^{(1)}(0; 0) T_{bgh} \Theta_{0gh}^{(2)} \\
+ \gamma_{ivwj}^{(1)} T_{jk} \alpha_{kl}^{(2)}(0; 0) T_{lm} \alpha_{mp}^{(1)}(0; 0) T_{pqr} \Theta_{0qr}^{(2)} \alpha_{ab}^{(2)}(0; 0) T_{bgh} \Theta_{0gh}^{(1)} \\
+ 2\gamma_{ivjl}^{(1)}(-2\omega; \omega, \omega, 0) T_{jk} \alpha_{kw}^{(2)}(-\omega; \omega) T_{lqr} \Theta_{0qr}^{(2)} \alpha_{ab}^{(1)}(0; 0) T_{bc} \alpha_{cd}^{(2)}(0; 0) T_{dgh} \Theta_{0gh}^{(1)} \\
- 2\gamma_{ivjl}^{(1)}(-2\omega; \omega, \omega, 0) T_{jk} \alpha_{kw}^{(2)}(-\omega; \omega) T_{lqr} \Theta_{0qr}^{(2)} \alpha_{ab}^{(2)}(0; 0) T_{bc} \alpha_{cd}^{(1)}(0; 0) T_{dgh} \Theta_{0gh}^{(2)} \\
- \alpha_{ij}^{(1)}(-2\omega; 2\omega) T_{jk} \gamma_{kvwl}^{(2)}(-2\omega; \omega, \omega, 0) T_{lqr} \Theta_{0qr}^{(1)} \alpha_{ab}^{(1)}(0; 0) T_{bc} \alpha_{cd}^{(2)}(0; 0) T_{dgh} \Theta_{0gh}^{(1)} \\
+ \alpha_{ij}^{(1)}(-2\omega; 2\omega) T_{jk} \gamma_{kvwl}^{(2)}(-2\omega; \omega, \omega, 0) T_{lqr} \Theta_{0qr}^{(1)} \alpha_{ab}^{(2)}(0; 0) T_{bc} \alpha_{cd}^{(1)}(0; 0) T_{dgh} \Theta_{0gh}^{(2)} \\
- \gamma_{ivwj}^{(1)}(-2\omega; \omega, \omega, 0) T_{jk} \alpha_{kl}^{(2)}(0; 0) T_{lqr} \Theta_{0qr}^{(1)} \alpha_{ab}^{(1)}(0; 0) T_{bc} \alpha_{cd}^{(2)}(0; 0) T_{dgh} \Theta_{0gh}^{(1)} \\
+ \gamma_{ivwj}^{(1)}(-2\omega; \omega, \omega, 0) T_{jk} \alpha_{kl}^{(2)}(0; 0) T_{lqr} \Theta_{0qr}^{(1)} \alpha_{ab}^{(2)}(0; 0) T_{bc} \alpha_{cd}^{(1)}(0; 0) T_{dgh} \Theta_{0gh}^{(2)} \\
- \gamma_{ivwj}^{(1)}(-2\omega; \omega, \omega, 0) T_{jqr} \Theta_{0qr}^{(2)} \alpha_{ab}^{(1)}(0; 0) T_{bc} \alpha_{cd}^{(2)}(0; 0) T_{de} \alpha_{ef}^{(1)}(0; 0) T_{fgh} \Theta_{0gh}^{(2)} \\
+ \gamma_{ivwj}^{(1)}(-2\omega; \omega, \omega, 0) T_{jqr} \Theta_{0qr}^{(2)} \alpha_{ab}^{(2)}(0; 0) T_{bc} \alpha_{cd}^{(1)}(0; 0) T_{de} \alpha_{ef}^{(2)}(0; 0) T_{fgh} \Theta_{0gh}^{(1)} \left. \right\} \langle a_i^z a_v^z a_w^z a_a^z \rangle,
\end{aligned} \tag{4.74}$$

$$\begin{aligned}
B_1\alpha_2\Theta_1 = & -\frac{\mathcal{E}_z^2}{18kT} \left\{ B_{ivjk}^{(1)}(-2\omega; \omega, \omega) T_{jkl} \alpha_{lw}^{(2)}(-\omega; \omega) \alpha_{ab}^{(1)}(0; 0) T_{bgh} \Theta_{0gh}^{(2)} \right. \\
& \left. - B_{ivjk}^{(1)}(-2\omega; \omega, \omega) T_{jkl} \alpha_{lw}^{(2)}(-\omega; \omega) \alpha_{ab}^{(2)}(0; 0) T_{bgh} \Theta_{0gh}^{(1)} \right\} \left\langle a_i^z a_v^z a_w^z a_a^z \right\rangle,
\end{aligned} \tag{4.75}$$

$$\begin{aligned}
B_1\alpha_3\Theta_1 = & -\frac{\mathcal{E}_z^2}{18kT} \left\{ -\alpha_{ij}^{(1)}(-2\omega; 2\omega) T_{jk} B_{klm}^{(2)} T_{lmn} \alpha_{nw}^{(1)}(-\omega; \omega) \alpha_{ab}^{(1)}(0; 0) T_{bgh} \Theta_{0gh}^{(2)} \right. \\
& + \alpha_{ij}^{(1)}(-2\omega; 2\omega) T_{jk} B_{klm}^{(2)} T_{lmn} \alpha_{nw}^{(1)}(-\omega; \omega) \alpha_{ab}^{(2)}(0; 0) T_{bgh} \Theta_{0gh}^{(1)} \\
& + B_{ivjk}^{(1)} T_{jkl} \alpha_{lm}^{(2)}(-\omega; \omega) T_{mn} \alpha_{nw}^{(1)}(-\omega; \omega) \alpha_{ab}^{(1)}(0; 0) T_{bgh} \Theta_{0gh}^{(2)} \\
& - B_{ivjk}^{(1)} T_{jkl} \alpha_{lm}^{(2)}(-\omega; \omega) T_{mn} \alpha_{nw}^{(1)}(-\omega; \omega) \alpha_{ab}^{(2)}(0; 0) T_{bgh} \Theta_{0gh}^{(1)} \\
& + B_{ijlm}^{(1)} T_{jk} \alpha_{kv}^{(2)}(-\omega; \omega) T_{lmn} \alpha_{nw}^{(2)}(-\omega; \omega) \alpha_{ab}^{(1)}(0; 0) T_{bgh} \Theta_{0gh}^{(2)} \\
& - B_{ijlm}^{(1)} T_{jk} \alpha_{kv}^{(2)}(-\omega; \omega) T_{lmn} \alpha_{nw}^{(2)}(-\omega; \omega) \alpha_{ab}^{(2)}(0; 0) T_{bgh} \Theta_{0gh}^{(1)} \\
& - B_{ivjk}^{(1)}(-2\omega; \omega, \omega) T_{jkl} \alpha_{lw}^{(2)}(-\omega; \omega) \alpha_{ab}^{(1)}(0; 0) T_{bc} \alpha_{cd}^{(2)}(0; 0) T_{dgh} \Theta_{0gh}^{(1)} \\
& \left. + B_{ivjk}^{(1)}(-2\omega; \omega, \omega) T_{jkl} \alpha_{lw}^{(2)}(-\omega; \omega) \alpha_{ab}^{(2)}(0; 0) T_{bc} \alpha_{cd}^{(1)}(0; 0) T_{dgh} \Theta_{0gh}^{(2)} \right\} \left\langle a_i^z a_v^z a_w^z a_a^z \right\rangle,
\end{aligned} \tag{4.76}$$

$$\begin{aligned}
D_1\alpha_2\Theta_1 = & \frac{\mathcal{E}_z^2}{36kT} \left\{ \alpha_{ij}^{(1)}(-2\omega; 2\omega) T_{jkl} D_{klvw}^{(2)}(-2\omega; \omega, \omega) \alpha_{ab}^{(1)}(0; 0) T_{bgh} \Theta_{0gh}^{(2)} \right. \\
& \left. - \alpha_{ij}^{(1)}(-2\omega; 2\omega) T_{jkl} D_{klvw}^{(2)}(-2\omega; \omega, \omega) \alpha_{ab}^{(2)}(0; 0) T_{bgh} \Theta_{0gh}^{(1)} \right\} \left\langle a_i^z a_v^z a_w^z a_a^z \right\rangle,
\end{aligned} \tag{4.77}$$

and

$$\begin{aligned}
D_1\alpha_3\Theta_1 = \frac{\mathcal{E}_z^2}{36kT} \left\{ -\alpha_{ij}^{(1)}(-2\omega; 2\omega)T_{jk}\alpha_{kl}^{(2)}(-2\omega; 2\omega)T_{lmn}D_{mnvw}^{(1)}\alpha_{ab}^{(1)}(0; 0)T_{bgh}\Theta_{0gh}^{(2)} \right. \\
+ \alpha_{ij}^{(1)}(-2\omega; 2\omega)T_{jk}\alpha_{kl}^{(2)}(-2\omega; 2\omega)T_{lmn}D_{mnvw}^{(1)}\alpha_{ab}^{(2)}(0; 0)T_{bgh}\Theta_{0gh}^{(1)} \\
+ 2\alpha_{ij}^{(1)}(-2\omega; 2\omega)T_{jkl}D_{klvm}^{(2)}T_{mn}\alpha_{nw}^{(1)}(-\omega; \omega)\alpha_{ab}^{(1)}(0; 0)T_{bgh}\Theta_{0gh}^{(2)} \\
- 2\alpha_{ij}^{(1)}(-2\omega; 2\omega)T_{jkl}D_{klvm}^{(2)}T_{mn}\alpha_{nw}^{(1)}(-\omega; \omega)\alpha_{ab}^{(2)}(0; 0)T_{bgh}\Theta_{0gh}^{(1)} \\
- \alpha_{ij}^{(1)}(-2\omega; 2\omega)T_{jkl}D_{klvw}^{(2)}(-2\omega; \omega, \omega)\alpha_{ab}^{(1)}(0; 0)T_{bc}\alpha_{cd}^{(2)}(0; 0)T_{dgh}\Theta_{0gh}^{(1)} \\
\left. + \alpha_{ij}^{(1)}(-2\omega; 2\omega)T_{jkl}D_{klvw}^{(2)}(-2\omega; \omega, \omega)\alpha_{ab}^{(2)}(0; 0)T_{bc}\alpha_{cd}^{(1)}(0; 0)T_{dgh}\Theta_{0gh}^{(2)} \right\} \left\langle a_i^z a_v^z a_w^z a_a^z \right\rangle. \tag{4.78}
\end{aligned}$$

The isotropic averages in equations (4.68) to (4.78) are carried out using equation (3.35), and the procedure will now be demonstrated by evaluating the term for $\gamma_1\alpha_1$.

$$\begin{aligned}
\gamma_1\alpha_1 = \frac{\mathcal{E}_z^2}{4} \left\{ 2\gamma_{ivjh}^{(1)}(-2\omega; \omega, \omega, 0)T_{jk}\alpha_{kw}^{(2)}(-\omega; \omega) + \alpha_{ij}^{(1)}(-2\omega; 2\omega)T_{jk}\gamma_{kvvwh}^{(2)}(-2\omega; \omega, \omega, 0) \right. \\
\left. + \gamma_{ivva}^{(1)}(-2\omega; \omega, \omega, 0)T_{ab}\alpha_{bh}^{(2)}(0; 0) \right\} \left\langle a_i^z a_v^z a_w^z a_h^z \right\rangle \\
= \frac{\mathcal{E}_z^2}{4 \cdot 15} \left\{ 2\gamma_{ivjh}^{(1)}(-2\omega; \omega, \omega, 0)T_{jk}\alpha_{kw}^{(2)}(-\omega; \omega) + \alpha_{ij}^{(1)}(-2\omega; 2\omega)T_{jk}\gamma_{kvvwh}^{(2)}(-2\omega; \omega, \omega, 0) \right. \\
\left. + \gamma_{ivva}^{(1)}(-2\omega; \omega, \omega, 0)T_{ab}\alpha_{bh}^{(2)}(0; 0) \right\} \left(\delta_{iv}\delta_{wh} + \delta_{iv}\delta_{vh} + \delta_{ih}\delta_{vw} \right) \\
= \frac{\mathcal{E}_z^2}{60} \left\{ 2\gamma_{iijh}^{(1)}(-2\omega; \omega, \omega, 0)T_{jk}\alpha_{kh}^{(2)}(-\omega; \omega) + 2\gamma_{ivjv}^{(1)}(-2\omega; \omega, \omega, 0)T_{jk}\alpha_{ki}^{(2)}(-\omega; \omega) \right. \\
+ 2\gamma_{ivji}^{(1)}(-2\omega; \omega, \omega, 0)T_{jk}\alpha_{kv}^{(2)}(-\omega; \omega) \\
+ 2\alpha_{ij}^{(1)}(-2\omega; 2\omega)T_{jk}\gamma_{kiww}^{(2)}(-2\omega; \omega, \omega, 0) + \alpha_{ij}^{(1)}(-2\omega; 2\omega)T_{jk}\gamma_{kvvvi}^{(2)}(-2\omega; \omega, \omega, 0) \\
\left. + 2\gamma_{iiva}^{(1)}(-2\omega; \omega, \omega, 0)T_{ab}\alpha_{bv}^{(2)}(0; 0) + \gamma_{ivva}^{(1)}(-2\omega; \omega, \omega, 0)T_{ab}\alpha_{bi}^{(2)}(0; 0) \right\}. \tag{4.79}
\end{aligned}$$

The final scalar expression for $\gamma_1\alpha_1$ in equation (4.79) is obtained through summation

over the tensor indices, which is conveniently done using the Macsyma algebraic-manipulation software package. Macsyma has a facility to translate the final expression into Fortran code for direct insertion into the program which performs the numerical integration by the Gaussian quadrature method. This procedure is carried out on all of the terms in equation (4.67), and the final expressions will not be provided in this thesis since they are generally too large to reproduce here. An example of the Fortran code is however given in Appendix A.1. The ranges of the angular variables α_1 , α_2 , β_1 , β_2 , γ_1 and γ_2 were divided into sixteen intervals each, while R was given a range of 0.1 nm to 3.0 nm divided into 64 intervals. Increasing the number of intervals beyond these yields negligible change in the integral (to within the 6th significant figure). Fortran programs were all run in double precision. Substituting the final expressions for the terms into equation (4.23), followed by numerical integration over the pair-interaction coordinates, will yield their numerical contributions to the second ESHG virial coefficient B_γ for a particular molecule. This requires knowledge of the numerical values of the tensor components of the molecular-property tensors for the particular molecule under investigation. Where possible, the best experimentally measured data available in the literature are used. Otherwise, the highest-quality *ab initio* quantum-mechanical calculations have been sought in the literature. In the absence of available data, the DALTON molecular electronic-structure program has been used to calculate the molecular-property tensor components as part of this project.

The molecules which have been investigated are the axially-symmetric non-dipolar molecules H_2 , N_2 and CO_2 (all of which are of $D_{\infty h}$ symmetry), and the planar non-dipolar molecule C_2H_4 (which is of D_{2h} symmetry). The independent components of the various molecular-property tensors in equations (4.68) to (4.78) for the symmetry point groups $D_{\infty h}$ and D_{2h} are now explicitly listed.

4.2 The molecular-property tensors

It is perhaps best to begin with the more general case of the lower-symmetry D_{2h} point group, since the higher symmetry of the $D_{\infty h}$ point group will result in the same number of components for any given molecular-property tensor as for the D_{2h} point group, but in a reduction in the number of independent components.

4.2.1 Molecules of D_{2h} symmetry

For the D_{2h} point group, if the molecule-fixed axes $O(1, 2, 3)$ are oriented such that the 1- and 3-axes lie in the molecular plane, with the 3-axis along the principal molecular axis (*e.g.* along the double bond of the C_2H_4 molecule) and the 2-axis perpendicular to the molecular plane, then the polarizability tensor $\alpha_{ij}^{(1)}(-\omega; \omega)$ is diagonal and has three independent components [83], namely

$$\alpha_{ij}^{(1)}(-\omega; \omega) = \alpha_{ij}^{(2)}(-\omega; \omega) = \begin{bmatrix} \alpha_{11} & 0 & 0 \\ 0 & \alpha_{22} & 0 \\ 0 & 0 & \alpha_{33} \end{bmatrix}. \quad (4.80)$$

The mean polarizability $\alpha(-\omega; \omega)$ is

$$\alpha(-\omega; \omega) = \frac{1}{3}\alpha_{ii}(-\omega; \omega) = \frac{1}{3}(\alpha_{11} + \alpha_{22} + \alpha_{33}), \quad (4.81)$$

while the anisotropy in the polarizability $\Delta\alpha(-\omega; \omega)$ is

$$\Delta\alpha(-\omega; \omega) = \frac{1}{\sqrt{2}} \left\{ (\alpha_{11} - \alpha_{22})^2 + (\alpha_{22} - \alpha_{33})^2 + (\alpha_{33} - \alpha_{11})^2 \right\}^{1/2}. \quad (4.82)$$

In these expressions, ω is zero for the static polarizability, while for a dynamic polarizability, ω is the vacuum frequency of the incident photon. In addition, $\alpha_{ij}^{(2)}(-\omega; \omega)$ is the polarizability tensor of molecule 2 expressed in the molecule-fixed axes of

molecule 1, which is provided by

$$\alpha_{ij}^{(2)}(-\omega; \omega) = a_{\alpha}^i a_{\beta}^j a_{i'}^{\alpha} a_{j'}^{\beta} \alpha_{i'j'}^{(2)}(-\omega; \omega) . \quad (4.83)$$

The ESHG optical-frequency second hyperpolarizability $\gamma_{ijkl}(-2\omega; \omega, \omega, 0)$ is symmetric in the suffices jk alone. Using standard group-theory methods [129, 130], it can be shown that for molecules of D_{2h} symmetry, the tensors $\gamma_{ijkl}^{(1)}(-2\omega; \omega, \omega, 0) = \gamma_{i'j'k'l'}^{(2)}(-2\omega; \omega, \omega, 0)$ have a total of 21 non-zero components, of which 15 are independent:

$$\begin{aligned} & \gamma_{1111} \\ & \gamma_{2222} \\ & \gamma_{3333} \\ & \gamma_{1122} = \gamma_{1212} \\ & \gamma_{2211} = \gamma_{2121} \\ & \gamma_{1221} \\ & \gamma_{2112} \\ & \gamma_{1133} = \gamma_{1313} \\ & \gamma_{3311} = \gamma_{3131} \\ & \gamma_{1331} \\ & \gamma_{3113} \\ & \gamma_{2233} = \gamma_{2323} \\ & \gamma_{3322} = \gamma_{3232} \\ & \gamma_{2332} \\ & \gamma_{3223} . \end{aligned} \quad (4.84)$$

The ESHG dynamic second hyperpolarizability tensor of molecule 2 expressed in the molecule-fixed axes of molecule 1 is

$$\gamma_{ijkl}^{(2)}(-2\omega; \omega, \omega, 0) = a_{\alpha}^i a_{\beta}^j a_{\gamma}^k a_{\delta}^l a_{i'}^{\alpha} a_{j'}^{\beta} a_{k'}^{\gamma} a_{l'}^{\delta} \gamma_{i'j'k'l'}^{(2)}(-2\omega; \omega, \omega, 0) . \quad (4.85)$$

From equation (3.110), the experimentally measurable hyperpolarizability $\gamma_{\parallel}^{\text{ESHG}}$ is

$$\gamma_{\parallel}^{\text{ESHG}}(-2\omega; \omega, \omega, 0) = \frac{1}{15} \left(2\gamma_{iijj}(-2\omega; \omega, \omega, 0) + \gamma_{ijji}(-2\omega; \omega, \omega, 0) \right) , \quad (4.86)$$

which for molecules of D_{2h} symmetry becomes

$$\begin{aligned} \gamma_{\parallel}^{\text{ESHG}}(-2\omega; \omega, \omega, 0) = \frac{1}{15} \left(3\gamma_{1111} + 2\gamma_{1122} + \gamma_{1221} + 2\gamma_{1133} + \gamma_{1331} + 2\gamma_{2211} \right. \\ \left. + \gamma_{2112} + 3\gamma_{2222} + 2\gamma_{2233} + \gamma_{2332} + 2\gamma_{3311} \right. \\ \left. + \gamma_{3113} + 2\gamma_{3322} + \gamma_{3223} + 3\gamma_{3333} \right) . \end{aligned} \quad (4.87)$$

The static second hyperpolarizability $\gamma_{ijkl}(0; 0, 0, 0)$ has full permutation symmetry, and has the 6 independent components

$$\begin{aligned} \gamma_{1111} \\ \gamma_{2222} \\ \gamma_{3333} \\ \gamma_{1122} = \gamma_{1212} = \gamma_{1221} = \gamma_{2112} = \gamma_{2121} = \gamma_{2211} \\ \gamma_{1133} = \gamma_{1313} = \gamma_{1331} = \gamma_{3113} = \gamma_{3131} = \gamma_{3311} \\ \gamma_{2233} = \gamma_{2323} = \gamma_{2332} = \gamma_{3223} = \gamma_{3232} = \gamma_{3322} . \end{aligned} \quad (4.88)$$

Hence,

$$\gamma_{\parallel}^{\text{ESHG}}(0; 0, 0, 0) = \frac{1}{15} \left(3\gamma_{1111} + 6\gamma_{1122} + 6\gamma_{1133} + 6\gamma_{2233} + 3\gamma_{2222} + 3\gamma_{3333} \right) . \quad (4.89)$$

The SHG optical-frequency dipole-dipole-quadrupole hyperpolarizability $B_{ijkl}(-2\omega; \omega, \omega)$ is symmetric in the suffices kl only, so that for molecules of D_{2h} symmetry this tensor has 21 non-zero components, of which 12 are independent:

$$\begin{aligned}
& B_{1111} \\
& B_{2222} \\
& B_{3333} \\
& B_{1122} \\
& B_{2211} \\
& B_{3322} \\
& B_{1212} = B_{1221} \\
& B_{2121} = B_{2112} \\
& B_{1313} = B_{1331} \\
& B_{2323} = B_{2332} \\
& B_{3131} = B_{3113} \\
& B_{3232} = B_{3223} .
\end{aligned} \tag{4.90}$$

The following are the remaining non-zero dependent components:

$$\begin{aligned}
& B_{1133} = -(B_{1111} + B_{1122}) \\
& B_{2233} = -(B_{2222} + B_{2211}) \\
& B_{3311} = -(B_{3333} + B_{3322}) .
\end{aligned} \tag{4.91}$$

The $B_{ijkl}(-2\omega; \omega, \omega)$ tensor of molecule 2 expressed in the molecule-fixed axes of molecule 1 is

$$B_{ijkl}^{(2)}(-2\omega; \omega, \omega) = a_{\alpha}^i a_{\beta}^j a_{\gamma}^k a_{\delta}^l a_{i'}^{\alpha} a_{j'}^{\beta} a_{k'}^{\gamma} a_{l'}^{\delta} B_{i'j'k'l'}^{(2)}(-2\omega; \omega, \omega) . \tag{4.92}$$

The static dipole-dipole-quadrupole hyperpolarizability $B_{ijkl}(0; 0, 0)$ is symmetric in ij and in kl , and has 9 independent components:

$$\begin{aligned}
 & B_{1111} \\
 & B_{2222} \\
 & B_{3333} \\
 & B_{1122} \\
 & B_{2211} \\
 & B_{3322} \\
 & B_{1212} = B_{1221} = B_{2112} = B_{2121} \\
 & B_{1313} = B_{1331} = B_{3113} = B_{3131} \\
 & B_{2323} = B_{2332} = B_{3223} = B_{3232} ,
 \end{aligned} \tag{4.93}$$

with the additional non-zero dependent components

$$\begin{aligned}
 B_{1133} &= - (B_{1111} + B_{1122}) \\
 B_{2233} &= - (B_{2222} + B_{2211}) \\
 B_{3311} &= - (B_{3333} + B_{3322}) .
 \end{aligned} \tag{4.94}$$

The SHG optical-frequency dipole-dipole-quadrupole hyperpolarizability $D_{ijkl}(-2\omega; \omega, \omega)$ is symmetric in the suffices ij and in the suffices kl , so that for molecules of D_{2h}

symmetry this tensor has 21 non-zero components, of which 9 are independent:

$$\begin{aligned}
& D_{1111} \\
& D_{2222} \\
& D_{3333} \\
& D_{1122} \\
& D_{2211} \tag{4.95} \\
& D_{2233} \\
& D_{1212} = D_{1221} = D_{2112} = D_{2121} \\
& D_{1313} = D_{1331} = D_{3113} = D_{3131} \\
& D_{2323} = D_{2332} = D_{3223} = D_{3232} .
\end{aligned}$$

The following are the remaining non-zero dependent components:

$$\begin{aligned}
D_{3311} &= -(D_{1111} + D_{2211}) \\
D_{3322} &= -(D_{2222} + D_{1122}) \tag{4.96} \\
D_{1133} &= -(D_{3333} + D_{2233}) .
\end{aligned}$$

The $D_{ijkl}(-2\omega; \omega, \omega)$ tensor of molecule 2 expressed in the molecule-fixed axes of molecule 1 is

$$D_{ijkl}^{(2)}(-2\omega; \omega, \omega) = a_{\alpha}^i a_{\beta}^j a_{\gamma}^k a_{\delta}^l a_{i'}^{\alpha} a_{j'}^{\beta} a_{k'}^{\gamma} a_{l'}^{\delta} D_{i'j'k'l'}^{(2)}(-2\omega; \omega, \omega) . \tag{4.97}$$

The static dipole-dipole-quadrupole hyperpolarizability $D_{ijkl}(0; 0, 0)$ is also symmetric in ij and in kl , so there is no further simplification, this tensor having the same 9 independent components as in equation (4.95). In addition, $D_{ijkl}(0; 0, 0) = B_{klij}(0; 0, 0)$.

The traceless permanent electric quadrupole moment for molecules of D_{2h} symmetry

has two independent components [83], giving

$$\Theta_{0ij}^{(1)} = \Theta_{0i'j'}^{(2)} = \begin{bmatrix} \Theta_{11} & 0 & 0 \\ 0 & \Theta_{22} & 0 \\ 0 & 0 & \Theta_{33} = -\Theta_{11} - \Theta_{22} \end{bmatrix}. \quad (4.98)$$

Similarly,

$$\Theta_{0ij}^{(2)} = a_{\alpha}^i a_{\beta}^j a_{i'}^{\alpha} a_{j'}^{\beta} \Theta_{0i'j'}^{(2)}. \quad (4.99)$$

4.2.2 Molecules of $D_{\infty h}$ symmetry

For axially-symmetric molecules, if the molecule-fixed axes $O(1, 2, 3)$ are oriented such that the 3-axis co-incides with the rotation axis of the molecule, then the polarizability tensor $\alpha_{ij}(-\omega; \omega)$ has the two independent components $\alpha_{11} = \alpha_{22} = \alpha_{\perp}$ and $\alpha_{33} = \alpha_{\parallel}$ [83] so that equation (4.80) reduces to

$$\alpha_{ij}^{(1)}(-\omega; \omega) = \alpha_{i'j'}^{(2)}(-\omega; \omega) = \begin{bmatrix} \alpha_{\perp} & 0 & 0 \\ 0 & \alpha_{\perp} & 0 \\ 0 & 0 & \alpha_{\parallel} \end{bmatrix}. \quad (4.100)$$

These two independent components can be deduced from measured values of the mean polarizability

$$\alpha(-\omega; \omega) = \frac{1}{3} \alpha_{ii}(-\omega; \omega) = \frac{1}{3} (2\alpha_{\perp} + \alpha_{\parallel}) \quad (4.101)$$

and the polarizability anisotropy

$$\Delta\alpha(-\omega; \omega) = (\alpha_{\parallel} - \alpha_{\perp}), \quad (4.102)$$

so that

$$\alpha_{\perp} = \alpha(-\omega; \omega) - \frac{1}{3} \Delta \alpha(-\omega; \omega) \quad (4.103)$$

and

$$\alpha_{\parallel} = \alpha(-\omega; \omega) + \frac{2}{3} \Delta \alpha(-\omega; \omega). \quad (4.104)$$

For axially-symmetric molecules, the ESHG optical-frequency second hyperpolarizability tensor $\gamma_{ijkl}(-2\omega; \omega, \omega, 0)$ reduces to 7 independent components:

$$\begin{aligned} \gamma_{1111} &= \gamma_{2222} \\ \gamma_{3333} \\ \gamma_{1133} &= \gamma_{1313} = \gamma_{2233} = \gamma_{2323} \\ \gamma_{3311} &= \gamma_{3131} = \gamma_{3322} = \gamma_{3232} \\ \gamma_{1331} &= \gamma_{2332} \\ \gamma_{3113} &= \gamma_{3223} \\ \gamma_{1122} &= \gamma_{1212} = \gamma_{2211} = \gamma_{2121} = \frac{1}{2} (\gamma_{1111} - \gamma_{1221}) = \frac{1}{2} (\gamma_{1111} - \gamma_{2112}) . \end{aligned} \quad (4.105)$$

The expression in equation (4.86) for $\gamma_{\parallel}^{\text{ESHG}}$ becomes

$$\gamma_{\parallel}^{\text{ESHG}}(-2\omega; \omega, \omega, 0) = \frac{1}{15} \left(8\gamma_{1111} + 4(\gamma_{1133} + \gamma_{3311}) + 2(\gamma_{1331} + \gamma_{3113}) + 3\gamma_{3333} \right) . \quad (4.106)$$

The static second hyperpolarizability $\gamma_{ijkl}(0; 0, 0, 0)$ has the 3 independent components

$$\begin{aligned} \gamma_{1111} &= \gamma_{2222} = 3\gamma_{1122} = 3\gamma_{1212} = 3\gamma_{1221} = 3\gamma_{2112} = 3\gamma_{2121} = 3\gamma_{2211} \\ \gamma_{3333} \\ \gamma_{1133} &= \gamma_{1313} = \gamma_{1331} = \gamma_{3113} = \gamma_{3131} = \gamma_{3311} = \gamma_{2233} = \gamma_{2323} = \gamma_{2332} = \gamma_{3223} = \gamma_{3232} = \gamma_{3322} \end{aligned} \quad (4.107)$$

with

$$\gamma_{\parallel}^{\text{ESHG}}(0; 0, 0, 0) = \frac{1}{15} \left(8\gamma_{1111} + 12\gamma_{1133} + 3\gamma_{3333} \right). \quad (4.108)$$

The SHG optical-frequency dipole-dipole-quadrupole hyperpolarizability $B_{ijkl}(-2\omega; \omega, \omega)$ has the 5 independent components

$$\begin{aligned} B_{1111} &= B_{2222} \\ B_{3333} \\ B_{1313} &= B_{1331} = B_{2323} = B_{2332} \\ B_{3131} &= B_{3113} = B_{3232} = B_{3223} \\ B_{1122} &= B_{2211} = B_{1111} - 2B_{1212}, \end{aligned} \quad (4.109)$$

with the additional non-zero dependent components

$$\begin{aligned} B_{1212} &= B_{1221} = B_{2121} = B_{2112} = \frac{1}{2} (B_{1111} - B_{1122}) \\ B_{1133} &= B_{2233} = -(B_{1111} + B_{1122}) \\ B_{3311} &= B_{3322} = -\frac{1}{2} B_{3333}. \end{aligned} \quad (4.110)$$

The static dipole-dipole-quadrupole hyperpolarizability $B_{ijkl}(0; 0, 0)$ has 4 independent components:

$$\begin{aligned}
 B_{1111} &= B_{2222} \\
 B_{3333} \\
 B_{1313} &= B_{1331} = B_{2323} = B_{2332} = B_{3131} = B_{3113} = B_{3232} = B_{3223} \\
 B_{1122} &= B_{2211} = B_{1111} - 2B_{1212} .
 \end{aligned} \tag{4.111}$$

The SHG optical-frequency dipole-dipole-quadrupole hyperpolarizability $D_{ijkl}(-2\omega; \omega, \omega)$ has 4 independent components:

$$\begin{aligned}
 D_{1111} &= D_{2222} \\
 D_{3333} \\
 D_{1313} &= D_{1331} = D_{2323} = D_{2332} = D_{3131} = D_{3113} = D_{3232} = D_{3223} \\
 D_{1122} &= D_{2211} = D_{1111} - 2D_{1212} .
 \end{aligned} \tag{4.112}$$

The additional non-zero dependent components are

$$\begin{aligned}
 D_{1212} &= D_{1221} = D_{2121} = D_{2112} = \frac{1}{2}(D_{1111} - D_{1122}) \\
 D_{1133} &= D_{2233} = -\frac{1}{2}D_{3333} \\
 D_{3311} &= D_{3322} = -(D_{1111} + D_{1122}) .
 \end{aligned} \tag{4.113}$$

The static dipole-dipole-quadrupole hyperpolarizability $D_{ijkl}(0; 0, 0)$ has no further simplification, this tensor having the same 4 independent components as in equation (4.113).

For axially-symmetric molecules, the traceless permanent quadrupole moment now

has one independent component [83], given by

$$\Theta_{0ij}^{(1)} = \Theta_{0i'j'}^{(2)} = \begin{bmatrix} \Theta_{11} = -\frac{1}{2}\Theta_{33} & 0 & 0 \\ 0 & \Theta_{22} = -\frac{1}{2}\Theta_{33} & 0 \\ 0 & 0 & \Theta_{33} \end{bmatrix}. \quad (4.114)$$

All molecular-property tensors in equations (4.68) to (4.78) for symmetry point groups $D_{\infty h}$ and D_{2h} have now been considered. The only remaining tensors in these equations are the second- and third-rank T -tensors. In the laboratory frame $O(x, y, z)$ the second-rank T -tensor is [83]

$$T_{\alpha\beta} = \frac{1}{4\pi\epsilon_0} \nabla_{\alpha} \nabla_{\beta} R^{-1} = \frac{1}{4\pi\epsilon_0} (3R_{\alpha}R_{\beta} - R^2\delta_{\alpha\beta}) R^{-5}, \quad (4.115)$$

while in the molecule-fixed axes of molecule 1, $T_{ij} = a_{\alpha}^i a_{\beta}^j T_{\alpha\beta}$. The third-rank T -tensor in space-fixed axes is [83]

$$\begin{aligned} T_{\alpha\beta\gamma} &= \frac{1}{4\pi\epsilon_0} \nabla_{\alpha} \nabla_{\beta} \nabla_{\gamma} R^{-1} \\ &= \frac{-3}{4\pi\epsilon_0} \left[5R_{\alpha}R_{\beta}R_{\gamma} - R^2(R_{\alpha}\delta_{\beta\gamma} + R_{\beta}\delta_{\gamma\alpha} + R_{\gamma}\delta_{\alpha\beta}) \right] R^{-7}, \end{aligned} \quad (4.116)$$

while in the molecule-fixed axes of molecule 1, $T_{ijk} = a_{\alpha}^i a_{\beta}^j a_{\gamma}^k T_{\alpha\beta\gamma}$.

The tensor-manipulation package of the Macsyma algebraic manipulation program was used to evaluate the expressions for the terms in equations (4.68) to (4.78), and proved to be an invaluable aid especially for the more complex expressions. These final expressions are often extremely large, and so they are not presented here, but the Macsyma program translates them directly into Fortran code, hence minimizing the introduction of spurious typographical errors. The integration of the final

expressions over the pair-interaction coordinates as per equation (4.23) enumerates the contributions to B_γ of each of the terms in equation (4.67).

The integral in equation (4.23) requires the intermolecular potential $U_{12}(\tau)$. As in previous work [77, 125], the classical potential

$$U_{12}(\tau) = U_{LJ} + U_{\Theta,\Theta} + U_{\Theta, \text{ind } \mu} + U_{\text{shape}} \quad (4.117)$$

is used, where U_{LJ} is the Lennard-Jones 6:12 potential, $U_{\Theta,\Theta}$ is the electrostatic quadrupole-quadrupole interaction energy of the two molecules, and $U_{\Theta, \text{ind } \mu}$ is the quadrupole-induced dipole interaction energy. The angular dependence of short range repulsive forces for non-spherical molecules is accounted for by U_{shape} . Explicit expressions for each of these contributions to $U_{12}(\tau)$ for molecules of D_{2h} symmetry and higher have already been provided [77, 125]. In order to compute the induction energy $U_{\Theta, \text{ind } \mu}$, the static molecular polarizability $\alpha_{ij}(0;0)$ is required.

The integrals were evaluated by numerical integration using Gaussian quadrature. The ranges of the orientation angles were divided into 16 intervals each, while the intermolecular separation R was given the range of 0.1 to 3.0 nm divided into 64 intervals. A sample of the Fortran programs used to compute the contributions to B_γ is provided in Appendix A.1 (it is the program to evaluate $\gamma_1\alpha_1$ for the C_2H_4 molecule). All programs were run in double precision using the Salford F90 compiler.

Chapter 5 presents the results of the computations of B_γ for the molecules H_2 , N_2 , CO_2 and C_2H_4 .

Chapter 5

Results

5.1 Hydrogen

Hydrogen is a homonuclear diatomic molecule, and so is non-dipolar, its leading electric moment being the quadrupole moment. H_2 has axial symmetry, belonging to the $D_{\infty h}$ symmetry point group. The molecular data required in the calculation of B_γ are provided in Tables 5.1 to 5.5. The force constants R_0 and ε/k used in the Lennard-Jones 6:12 potential are taken from Hirschfelder *et al.* [131], and together with the shape parameter D have been optimized by fitting calculated values of the second pressure virial coefficient

$$B(T) = \frac{N_A}{2\Omega} \int_{\tau} \left[1 - e^{-U_{12}(\tau)/kT} \right] d\tau \quad (5.1)$$

to the tabulated measured data over a wide temperature range. These are presented in Table 5.1 together with the molecular electric quadrupole moment.

Table 5.1: The intermolecular potential parameters and quadrupole moment of H₂ used in the calculation of B_γ .

Property	Value	Reference
R_0 (nm)	0.300	[131]
ε/k (K)	30.0	[131]
D_1	0.050 ^a	
D_2	0.000	
$10^{40} \Theta_{33}$ (C m ²)	2.166	[132]

^aObtained by fitting to pressure virial coefficients reported in Ref. [133]

Donley and Shelton’s ESHG experiments to measure pair-interaction contributions to hyperpolarizabilities were undertaken using the argon-ion laser line at $\lambda = 514.5$ nm [48]. We focus on calculations at this wavelength, and so require the optical polarizability tensor components at this wavelength and at half of this wavelength. The static polarizability tensor components are also required. Table 5.2 provides these polarizabilities and polarizability anisotropies for H₂, all deduced from the constrained anisotropic dipole oscillator strength distribution (DOSD) study of Kumar and Meath [134].

Bishop and co-workers have, in a series of studies, obtained accurate *ab initio* calculations of the static and dynamic polarizabilities and hyperpolarizabilities of H₂ [96, 135–137]. Their fourth paper in this series utilized James-Coolidge type wave functions with an extended basis set [96], yielding excellent agreement with ESHG experimental data. Their calculations of the dipole-dipole-quadrupole hyperpolarizability $B_{ijkl}(-\omega_\sigma; \omega_1, \omega_2)$ are for $\omega_\sigma = \omega_1$ and $\omega_2 = 0$, which is encountered in the electric-field-gradient-induced birefringence of molecules [138, 139]. To obtain values of $B_{ijkl}(-2\omega; \omega, \omega)$ and $D_{ijkl}(-2\omega; \omega, \omega)$ for H₂, we have used DALTON to

Table 5.2: H₂ mean polarizabilities, polarizability anisotropies, and deduced polarizability tensor components for zero frequency and relevant optical frequencies.[†] All values are in SI units.^a

λ (nm)	$10^{40} \alpha$ (C ² m ² J ⁻¹)	$10^{40} \Delta\alpha$ (C ² m ² J ⁻¹)	$10^{40} \alpha_{\perp}$ (C ² m ² J ⁻¹)	$10^{40} \alpha_{\parallel}$ (C ² m ² J ⁻¹)
∞	0.8957	0.3367	0.7835	1.1201
514.5	0.9223	0.3530	0.8046	1.1577
257.25	1.0148	0.4126	0.8772	1.2899

[†]*i.e.* for Donley and Shelton’s experimental wavelength $\lambda = 514.5$ nm and the frequency-doubled wavelength $\lambda = 257.25$ nm; the data are extracted from the DOSD [134].

^aThe relationship between SI units and atomic units is:

$$1 \text{ e}^2 \text{a}_0^2 \text{E}_h^{-1} = 1.648778 \times 10^{-41} \text{ C}^2 \text{m}^2 \text{J}^{-1}.$$

perform calculations with a CCSD wavefunction and with Woon and Dunning’s triply-augmented correlation consistent polarized valence quadruple zeta (t-aug-cc-pVQZ) basis [140]. As a cross-check of the reliability of the calculated values, we have also undertaken CCSD calculations of the second hyperpolarizability over a range of wavelengths (presented in Table 5.3), allowing direct comparison with the accurate data of Bishop *et al.* (reproduced for ease of comparison in Table 5.4). All tabulations of *ab initio* calculated hyperpolarizability data are in atomic units, allowing for ease of comparison with results in the literature. Conversion factors to SI units are provided in the tables. Our calculated hyperpolarizabilities for all components save for γ_{3333} agree with the data of Bishop *et al.* to better than 0.3%. For γ_{3333} , agreement is within 1.5%. Our calculated dipole-dipole-quadrupole hyperpolarizabilities are presented in Table 5.5 for a range of wavelengths. Note that the static hyperpolarizabilities $B_{ijkl}(0; 0, 0) = D_{klij}(0; 0, 0)$ can be compared directly with those of Bishop *et al.* [96], and here, agreement is to within 1%. The recent study of the static hyperpolarizabilities of H₂ by Miliordos and Hunt [141] confirms

this level of agreement.

Table 5.3: Components of the ESHG second hyperpolarizability $\gamma_{ijkl}(-2\omega; \omega, \omega, 0)$ for H_2 calculated in this work using a CCSD wavefunction and a t-aug-cc-pVQZ basis set. All values are in atomic units.^a

Property	$\lambda(\text{nm})$				
	400.0	514.5	694.3	1064	∞
γ_{1111}	959.3	774.1	675.3	616.6	577.8
γ_{1122}	308.9	253.2	222.9	204.7	192.6
γ_{1133}	344.3	282.0	248.1	227.7	214.1
γ_{1331}	382.7	299.0	255.7	230.6	214.1
γ_{3113}	393.5	303.5	257.7	231.3	214.1
γ_{3311}	362.2	290.1	251.8	229.1	214.1
γ_{3333}	1216.3	957.0	821.8	742.8	691.0

^aConversion to SI units: $1 \text{ e}^4 \text{ a}_0^4 \text{ E}_\text{h}^{-3} = 6.235378 \times 10^{-65} \text{ C}^4 \text{ m}^4 \text{ J}^{-3}$.

Table 5.4: Components of the ESHG second hyperpolarizability $\gamma_{ijkl}(-2\omega; \omega, \omega, 0)$ for H_2 calculated by Bishop *et al.* using accurate James-Coolidge type wavefunctions and an extended basis set.[†] All values are in atomic units.^a

Property	$\lambda(\text{nm})$			
	514.5	694.3	1064	∞
γ_{1111}	772.2	673.4	614.8	575.9
γ_{1122}	252.6	222.3	204.1	192.0
γ_{1133}	279.4	245.6	225.4	211.9
γ_{1331}	297.0	253.6	228.3	211.9
γ_{3113}	301.5	255.5	229.1	211.9
γ_{3311}	287.6	249.4	226.8	211.9
γ_{3333}	942.8	810.7	733.3	682.5

[†]Note that Bishop *et al.* have quoted values for $\gamma_{ijkl}(-2\omega; 0, \omega, \omega)$ in their paper [96]. These are related to $\gamma_{ijkl}(-2\omega; \omega, \omega, 0)$ via $\gamma_{ijkl}(-2\omega; \omega, \omega, 0) = \gamma_{iljk}(-2\omega; 0, \omega, \omega)$.

^aConversion to SI units: $1 \text{ e}^4 \text{ a}_0^4 \text{ E}_h^{-3} = 6.235378 \times 10^{-65} \text{ C}^4 \text{ m}^4 \text{ J}^{-3}$.

Table 5.5: Components of the SHG dipole-dipole-quadrupole hyperpolarizabilities $B_{ijkl}(-2\omega; \omega, \omega)$ and $D_{ijkl}(-2\omega; \omega, \omega)$ for H_2 calculated *ab initio* in this work using a CCSD wavefunction and a t-aug-cc-pVQZ basis set. All values are in atomic units.^a

Property	$\lambda(\text{nm})$				
	400.0	514.5	694.3	1064	∞
B_{1111}	-92.04	-80.50	-73.88	-69.77	-66.97
B_{1122}	45.01	39.34	36.09	34.07	32.70
B_{1313}	-81.76	-71.48	-65.59	-61.93	-59.43
B_{3131}	-85.03	-73.05	-66.33	-62.22	-59.43
B_{3333}	-131.05	-112.43	-102.00	-95.61	-91.29
D_{1111}	-80.11	-74.41	-70.88	-68.59	-66.97
D_{1122}	39.25	36.40	34.64	33.50	32.70
D_{1313}	-71.71	-66.37	-63.08	-60.94	-59.43
D_{3333}	-111.12	-102.45	-97.14	-93.70	-91.29

^aConversion to SI units: $1 \text{ e}^3 \text{ a}_0^4 \text{ E}_h^{-2} = 1.696733 \times 10^{-63} \text{ C}^3 \text{ m}^4 \text{ J}^{-2}$.

Our calculations of B_γ are summarized in tables 5.6 to 5.9. The relative magnitudes of the contributing terms are listed over the experimentally-accessible temperature range 200 K to 500 K. Contributions from the series in the second hyperpolarizability ($\gamma_1\alpha_n$), the quadrupole-induced series ($\gamma_1\alpha_n\Theta_2$) and the series in the dipole-dipole-quadrupole hyperpolarizabilities ($B_1\alpha_n\Theta_1$ and $D_1\alpha_n\Theta_1$) are each summed separately to allow for quick assessment of their relative contributions to B_γ . At $T = 200$ K, $\sum \gamma_1\alpha_n$ contributes 90.4% to B_γ , $\sum \gamma_1\alpha_n\Theta_2$ contributes 8.8% and $\sum (B_1\alpha_n\Theta_1 + D_1\alpha_n\Theta_1)$ only 0.8%. At $T = 500$ K, $\sum \gamma_1\alpha_n$ contributes 95.6% to B_γ , $\sum \gamma_1\alpha_n\Theta_2$ contributes 4.1% and $\sum (B_1\alpha_n\Theta_1 + D_1\alpha_n\Theta_1)$ 0.4%.

For the $\gamma_1\alpha_n$ series, the term in $\gamma_1\alpha_2$ is dominant, contributing around 90% to B_γ over all temperatures in the range 200 to 500 K. The series then rapidly converges. For the $\gamma_1\alpha_n\Theta_2$ series, the leading $\gamma_1\alpha_1\Theta_2$ term is dominant, after which the series rapidly converges. With the dipole-dipole-quadrupole hyperpolarizability series, the terms in $B_1\alpha_2\Theta_1$ and $D_1\alpha_2\Theta_1$ make the dominant contribution, the series then also rapidly converging.

Calculations have been performed at Donley and Shelton's experimental temperature of 298 K [48], but since ESHG measurements are not absolute, giving instead the ratio of hyperpolarizabilities for two gases, comparison with experiment (where the ratio of hyperpolarizabilities for N_2 and H_2 were obtained) will first require the presentation of B_γ calculations for N_2 . These are given in the next section.

Table 5.6: The relative magnitudes of the contributions to B_γ for H_2 at $T = 200$ K

Contributing Term	$10^{67} \times \text{value}$ ($\text{C}^4\text{m}^7\text{J}^{-3}\text{mol}^{-1}$)	% contribution to B_γ
$\gamma_1\alpha_1$	-0.01496	-1.55
$\gamma_1\alpha_2$	0.85449	88.41
$\gamma_1\alpha_3$	0.02970	3.07
$\gamma_1\alpha_4$	0.00491	0.51
$\gamma_1\alpha_1\Theta_2$	0.07805	8.08
$\gamma_1\alpha_2\Theta_2$	0.00710	0.73
$B_1\alpha_2\Theta_1$	0.00320	0.33
$B_1\alpha_3\Theta_1$	0.00057	0.06
$D_1\alpha_2\Theta_1$	0.00298	0.31
$D_1\alpha_3\Theta_1$	0.00052	0.05
$\sum_{n=1}^4 \gamma_1\alpha_n$	0.87414	90.44
$\sum_{n=1}^2 \gamma_1\alpha_n\Theta_2$	0.08515	8.81
$\sum_{n=2}^3 (B_1\alpha_n\Theta_1 + D_1\alpha_n\Theta_1)$	0.00727	0.75
B_γ	0.96656	

Table 5.7: The relative magnitudes of the contributions to B_γ for H_2 at $T = 298 \text{ K}$

Contributing Term	$10^{67} \times \text{value}$ ($\text{C}^4\text{m}^7\text{J}^{-3}\text{mol}^{-1}$)	% contribution to B_γ
$\gamma_1\alpha_1$	-0.01394	-1.42
$\gamma_1\alpha_2$	0.88752	90.57
$\gamma_1\alpha_3$	0.03304	3.37
$\gamma_1\alpha_4$	0.00590	0.60
$\gamma_1\alpha_1\Theta_2$	0.05665	5.78
$\gamma_1\alpha_2\Theta_2$	0.00541	0.55
$B_1\alpha_2\Theta_1$	0.00232	0.24
$B_1\alpha_3\Theta_1$	0.00044	0.05
$D_1\alpha_2\Theta_1$	0.00217	0.22
$D_1\alpha_3\Theta_1$	0.00040	0.04
$\sum_{n=1}^4 \gamma_1\alpha_n$	0.91252	93.12
$\sum_{n=1}^2 \gamma_1\alpha_n\Theta_2$	0.06206	6.33
$\sum_{n=2}^3 (B_1\alpha_n\Theta_1 + D_1\alpha_n\Theta_1)$	0.00533	0.55
B_γ	0.97991	

Table 5.8: The relative magnitudes of the contributions to B_γ for H_2 at $T = 400$ K

Contributing Term	$10^{67} \times \text{value}$ ($\text{C}^4\text{m}^7\text{J}^{-3}\text{mol}^{-1}$)	% contribution to B_γ
$\gamma_1\alpha_1$	-0.01297	-1.29
$\gamma_1\alpha_2$	0.91978	91.66
$\gamma_1\alpha_3$	0.03601	3.59
$\gamma_1\alpha_4$	0.00677	0.67
$\gamma_1\alpha_1\Theta_2$	0.04511	4.50
$\gamma_1\alpha_2\Theta_2$	0.00446	0.44
$B_1\alpha_2\Theta_1$	0.00185	0.19
$B_1\alpha_3\Theta_1$	0.00037	0.04
$D_1\alpha_2\Theta_1$	0.00172	0.17
$D_1\alpha_3\Theta_1$	0.00033	0.03
$\sum_{n=1}^4 \gamma_1\alpha_n$	0.94959	94.63
$\sum_{n=1}^2 \gamma_1\alpha_n\Theta_2$	0.04957	4.94
$\sum_{n=2}^3 (B_1\alpha_n\Theta_1 + D_1\alpha_n\Theta_1)$	0.00427	0.43
B_γ	1.00343	

Table 5.9: The relative magnitudes of the contributions to B_γ for H₂ at $T = 500$ K

Contributing Term	$10^{67} \times \text{value}$ (C ⁴ m ⁷ J ⁻³ mol ⁻¹)	% contribution to B_γ
$\gamma_1\alpha_1$	-0.01227	-1.19
$\gamma_1\alpha_2$	0.94746	92.27
$\gamma_1\alpha_3$	0.03854	3.75
$\gamma_1\alpha_4$	0.00754	0.74
$\gamma_1\alpha_1\Theta_2$	0.03806	3.70
$\gamma_1\alpha_2\Theta_2$	0.00387	0.38
$B_1\alpha_2\Theta_1$	0.00156	0.15
$B_1\alpha_3\Theta_1$	0.00032	0.03
$D_1\alpha_2\Theta_1$	0.00146	0.14
$D_1\alpha_3\Theta_1$	0.00029	0.03
$\sum_{n=1}^4 \gamma_1\alpha_n$	0.98127	95.57
$\sum_{n=1}^2 \gamma_1\alpha_n\Theta_2$	0.04193	4.08
$\sum_{n=2}^3 (B_1\alpha_n\Theta_1 + D_1\alpha_n\Theta_1)$	0.00363	0.35
B_γ	1.02683	

Table 5.10: A summary of the calculated B_γ values for H_2

T (K)	$10^{67} B_\gamma$ ($\text{C}^4\text{m}^7\text{J}^{-3}\text{mol}^{-1}$)
200	0.96656
250	0.97075
300	0.98035
350	0.99168
400	1.00343
450	1.01519
500	1.02683

Table 5.10 provides a summary of the temperature dependence for B_γ calculated in this work. Donley and Shelton’s density-dependent hyperpolarizability measurements were conducted at the experimental temperature of 298 K, and for a pressure range of 1 to 8 atm. It is instructive to calculate the pair-interaction contribution arising from our ESHG second virial coefficient $B_\gamma = 0.97991 \times 10^{-67} \text{C}^4\text{m}^7\text{J}^{-3}\text{mol}^{-1}$ at this temperature and at the upper end of the experimental pressure range, namely 0.8 MPa, where H_2 has an inverse molar volume of $V_m^{-1} = 321.4 \text{mol m}^{-3}$ as calculated using the NIST Chemistry WebBook [142]. Recall equation (4.9)

$$\Gamma(V_m) = A_\gamma + \frac{B_\gamma}{V_m}, \quad (5.2)$$

where A_γ is the ideal-gas density-independent molecular hyperpolarizability $\gamma_{\parallel}^{\text{ESHG}}$, which for H_2 at $\lambda = 514.5 \text{nm}$ is $\gamma_{\parallel}^{\text{ESHG}} = (59.22 \pm 0.24) \times 10^{-63} \text{C}^4\text{m}^4\text{J}^{-3}$ [45]. Here, $B_\gamma/V_m = 0.031 \times 10^{-63} \text{C}^4\text{m}^4\text{J}^{-3}$, which is 0.052% of $\gamma_{\parallel}^{\text{ESHG}}$. Donley and Shelton had implemented refinements of the ESHG measurement technique and analysis to ensure accuracy at the 0.1% level for their density-dependent measurements of

hyperpolarizability ratios [48], and the B_γ calculated here indicates that even at the upper pressure limit of the measurements, the pair-interaction contributions for H_2 are hovering at the threshold of what is detectable.

At a pressure of 10 MPa and a temperature of 298 K the gas density increases to $V_m^{-1} = 3807.1 \text{ mol m}^{-3}$, for which $B_\gamma/V_m = 0.37 \times 10^{-63} \text{ C}^4\text{m}^4\text{J}^{-3}$. While this contribution would be measurable, it needs to be remembered that to achieve phase matching at a particular gas density requires specific electrode array parameters, including for the electrode spacing and the cylindrical electrode diameter. There are practical limits to the electrode arrays that can be manufactured, for example the laser beam needs to be able to pass through the narrow gap between electrodes. For H_2 gas at a density of $V_m^{-1} = 3807.1 \text{ mol m}^{-3}$, the electrodes would need to be spaced by around a tenth of a millimeter, which is completely impractical.

The results for the N_2 molecule are considered next.

5.2 Nitrogen

The molecular data required to calculate B_γ for the axially-symmetric N_2 molecule are contained in Tables 5.11 to 5.14.

Table 5.11: The intermolecular potential parameters and quadrupole moment of N_2 used in the calculation of B_γ .

Property	Value	Reference
R_0 (nm)	0.368	[131]
ε/k (K)	91.50	[131]
D_1	0.112 ^a	[143]
D_2	0.000	
$10^{40} \Theta_{33}$ (C m ²)	-4.97 ± 0.16	[144]

^aObtained by fitting to pressure virial coefficients reported in Ref. [133]

Table 5.12: N₂ mean polarizabilities, polarizability anisotropies, and deduced polarizability tensor components for zero frequency and relevant optical frequencies.[†] All values are in SI units.^a

λ (nm)	$10^{40} \alpha$ (C ² m ² J ⁻¹)	$10^{40} \Delta\alpha$ (C ² m ² J ⁻¹)	$10^{40} \alpha_{\perp}$ (C ² m ² J ⁻¹)	$10^{40} \alpha_{\parallel}$ (C ² m ² J ⁻¹)
∞	1.936	0.7573	1.6836	2.4409
514.5	1.975	0.7794	1.7152	2.4946
257.25	2.107	0.8541	1.8223	2.6764

[†]The data are extracted from the DOSD [134].

^aThe relationship between SI units and atomic units is:

$$1 \text{ e}^2 \text{a}_0^2 \text{E}_h^{-1} = 1.648778 \times 10^{-41} \text{ C}^2 \text{m}^2 \text{J}^{-1}.$$

Hättig, Christiansen and Jørgensen have calculated the optical-frequency ESHG second hyperpolarizability for N₂ over a range of wavelengths using coupled cluster cubic response theory and a CCSD wavefunction together with a t-aug-cc-pVTZ basis set [145]. Their calculations were performed at the N₂ equilibrium bond length $r_e = 1.098 \text{ \AA}$. This level of theory gives results of $\gamma_{ijkl}(-2\omega; \omega, \omega, 0)$ which are in good agreement (2.5% at $\lambda = 514.5 \text{ nm}$) with measured ESHG values of $\gamma_{\parallel}^{\text{ESHG}}$ [33, 34, 145]. Subsequent calculations at the CC3 level of theory brought the agreement between experiment and theory for $\gamma_{\parallel}^{\text{ESHG}}$ for N₂ to 0.7% at $\lambda = 514.5 \text{ nm}$ [146]. Since the computational time for calculations at the CC3 level of theory rises significantly, all of the DALTON calculations undertaken in his project have been implemented with CCSD wavefunctions. These calculated values have a precision of 3% or better for all molecules.

Since $\gamma_{\parallel}^{\text{ESHG}}$ in equation (4.106) does not require the γ_{1122} tensor component of $\gamma_{ijkl}(-2\omega; \omega, \omega, 0)$, Hättig *et al.* did not compute this component [145]. We have reproduced the $\gamma_{ijkl}(-2\omega; \omega, \omega, 0)$ tensor-component calculations of Hättig *et al.*

for a range of wavelengths, as reported in Table 5.13, and have also evaluated the γ_{1122} independent component required in this work. The tensor components of $B_{ijkl}(-2\omega; \omega, \omega)$ and $D_{ijkl}(-2\omega; \omega, \omega)$ for N_2 have also been computed at the CCSD level of theory with a t-aug-cc-pVTZ basis set, the results being listed in Table 5.14. We are unaware of any calculations or measurements of the SHG dipole-dipole-quadrupole hyperpolarizabilities appearing in the literature against which to compare our results. Maroulis has undertaken second-order Møller-Plesset perturbation theory (MP2) computation of the static (hyper)polarizabilities of N_2 using Utrecht basis sets [147]. For $B_{ijkl}(0; 0, 0)$ he obtained the components $B_{1111} = -126$, $B_{1122} = 61$, $B_{1313} = -124$ and $B_{3333} = -216 e^3 a_0^4 E_h^{-2}$. These values are in good agreement with the static values reported in Table 5.14.

Table 5.13: Components of the ESHG second hyperpolarizability $\gamma_{ijkl}(-2\omega; \omega, \omega, 0)$ for N_2 calculated in this work using a CCSD wavefunction and a t-aug-cc-pVTZ basis set. All values are in atomic units.^a

Property	$\lambda(\text{nm})$				
	400.0	514.5	694.3	1064	∞
γ_{1111}	1226.0	1013.4	897.7	828.3	781.8
γ_{1122}	402.9	335.2	298.1	275.7	260.6
γ_{1133}	480.9	401.2	357.3	330.7	312.8
γ_{1331}	511.5	414.8	363.4	333.0	312.8
γ_{3113}	523.5	420.3	366.0	334.0	312.8
γ_{3311}	503.9	412.0	362.4	332.6	312.8
γ_{3333}	1909.0	1556.7	1367.5	1254.8	1179.9
$\gamma_{\parallel}^{\text{ESHG}} = \gamma_{\parallel}$	1436.3	1180.0	1041.4	958.5	903.2
$\gamma_{\parallel}^{\text{exp}}$ [45]	1500.8 [†]	1210.2 \pm 5.3	1058.6 \pm 6.4	964.5 \pm 3.1	917.3 [†]

^aConversion to SI units: $1 \text{ e}^4 \text{ a}_0^4 \text{ E}_h^{-3} = 6.235378 \times 10^{-65} \text{ C}^4 \text{ m}^4 \text{ J}^{-3}$.

[†]Extrapolated from the measured data in Reference [45].

Table 5.14: Components of the SHG dipole-dipole-quadrupole hyperpolarizabilities $B_{ijkl}(-2\omega; \omega, \omega)$ and $D_{ijkl}(-2\omega; \omega, \omega)$ for N_2 calculated *ab initio* in this work using a CCSD wavefunction and a t-aug-cc-pVTZ basis set. All values are in atomic units.^a

Property	$\lambda(\text{nm})$				
	400.0	514.5	694.3	1064	∞
B_{1111}	-161.14	-144.14	-134.19	-127.94	-123.62
B_{1122}	76.51	68.58	63.94	61.03	59.01
B_{1313}	-151.55	-136.45	-127.61	-122.03	-118.18
B_{3131}	-162.41	-142.03	-130.36	-123.12	-118.18
B_{3333}	-268.60	-239.24	-222.18	-211.48	-204.12
D_{1111}	-149.33	-137.99	-131.12	-126.71	-123.62
D_{1122}	70.58	65.52	62.42	60.42	59.01
D_{1313}	-143.56	-132.14	-125.43	-121.15	-118.18
D_{3333}	-247.89	-228.61	-216.92	-209.39	-204.12

^aConversion to SI units: $1 \text{ e}^3 \text{ a}_0^4 \text{ E}_h^{-2} = 1.696733 \times 10^{-63} \text{ C}^3 \text{ m}^4 \text{ J}^{-2}$.

Tables 5.15 to 5.18 give the relative magnitudes of the contributing terms to B_γ calculated over the temperature range 200 K to 500 K. At $T = 200$ K, $\sum \gamma_1 \alpha_n$ contributes 83.9% to B_γ , $\sum \gamma_1 \alpha_n \Theta_2$ contributes 13.2% and $\sum (B_1 \alpha_n \Theta_1 + D_1 \alpha_n \Theta_1)$ 2.8%. At $T = 500$ K, $\sum \gamma_1 \alpha_n$ contributes 92.7% to B_γ , $\sum \gamma_1 \alpha_n \Theta_2$ contributes 6.0% and $\sum (B_1 \alpha_n \Theta_1 + D_1 \alpha_n \Theta_1)$ 1.3%. As was observed for H_2 , the $\gamma_1 \alpha_2$ term is dominant in the $\gamma_1 \alpha_n$ series, contributing between 88% and 94% to B_γ over the temperature range 200 to 500 K. The series then quickly converges. Again, for the $\gamma_1 \alpha_n \Theta_2$ series, the leading $\gamma_1 \alpha_1 \Theta_2$ term is dominant, after which the series rapidly converges; while for the dipole-dipole-quadrupole hyperpolarizability series, the terms in $B_1 \alpha_2 \Theta_1$ and $D_1 \alpha_2 \Theta_1$ make the dominant contribution, the series then also rapidly converging.

Table 5.15: The relative magnitudes of the contributions to B_γ for N_2 at $T = 200$ K

Contributing Term	$10^{67} \times$ value ($\text{C}^4\text{m}^7\text{J}^{-3}\text{mol}^{-1}$)	% contribution to B_γ
$\gamma_1\alpha_1$	-0.2379	-7.62
$\gamma_1\alpha_2$	2.7482	88.07
$\gamma_1\alpha_3$	0.0933	2.99
$\gamma_1\alpha_4$	0.0155	0.50
$\gamma_1\alpha_1\Theta_2$	0.3789	12.14
$\gamma_1\alpha_2\Theta_2$	0.0340	1.09
$B_1\alpha_2\Theta_1$	0.0583	1.87
$B_1\alpha_3\Theta_1$	0.0029	0.09
$D_1\alpha_2\Theta_1$	0.0264	0.85
$D_1\alpha_3\Theta_1$	0.0007	0.02
$\sum_{n=1}^4 \gamma_1\alpha_n$	2.6191	83.94
$\sum_{n=1}^2 \gamma_1\alpha_n\Theta_2$	0.4129	13.23
$\sum_{n=2}^3 (B_1\alpha_n\Theta_1 + D_1\alpha_n\Theta_1)$	0.0883	2.83
B_γ	3.1203	

Table 5.16: The relative magnitudes of the contributions to B_γ for N_2 at $T = 298$ K

Contributing Term	$10^{67} \times \text{value}$ ($\text{C}^4\text{m}^7\text{J}^{-3}\text{mol}^{-1}$)	% contribution to B_γ
$\gamma_1\alpha_1$	-0.1873	-6.54
$\gamma_1\alpha_2$	2.6193	91.40
$\gamma_1\alpha_3$	0.0921	3.22
$\gamma_1\alpha_4$	0.0161	0.56
$\gamma_1\alpha_1\Theta_2$	0.2462	8.59
$\gamma_1\alpha_2\Theta_2$	0.0223	0.78
$B_1\alpha_2\Theta_1$	0.0378	1.32
$B_1\alpha_3\Theta_1$	0.0018	0.06
$D_1\alpha_2\Theta_1$	0.0171	0.60
$D_1\alpha_3\Theta_1$	0.0004	0.01
$\sum_{n=1}^4 \gamma_1\alpha_n$	2.5402	88.64
$\sum_{n=1}^2 \gamma_1\alpha_n\Theta_2$	0.2685	9.37
$\sum_{n=2}^3 (B_1\alpha_n\Theta_1 + D_1\alpha_n\Theta_1)$	0.0571	1.99
B_γ	2.8658	

Table 5.17: The relative magnitudes of the contributions to B_γ for N_2 at $T = 400$ K

Contributing Term	$10^{67} \times$ value ($C^4 m^7 J^{-3} mol^{-1}$)	% contribution to B_γ
$\gamma_1 \alpha_1$	-0.1639	-5.86
$\gamma_1 \alpha_2$	2.6014	93.03
$\gamma_1 \alpha_3$	0.0950	.40
$\gamma_1 \alpha_4$	0.0174	0.62
$\gamma_1 \alpha_1 \Theta_2$	0.1860	6.65
$\gamma_1 \alpha_2 \Theta_2$	0.0173	0.62
$B_1 \alpha_2 \Theta_1$	0.0286	1.02
$B_1 \alpha_3 \Theta_1$	0.0014	0.05
$D_1 \alpha_2 \Theta_1$	0.0129	0.46
$D_1 \alpha_3 \Theta_1$	0.0003	0.01
$\sum_{n=1}^4 \gamma_1 \alpha_n$	2.5499	91.19
$\sum_{n=1}^2 \gamma_1 \alpha_n \Theta_2$	0.2033	7.27
$\sum_{n=2}^3 (B_1 \alpha_n \Theta_1 + D_1 \alpha_n \Theta_1)$	0.0432	1.54
B_γ	2.7964	

Table 5.18: The relative magnitudes of the contributions to B_γ for N_2 at $T = 500$ K

Contributing Term	$10^{67} \times \text{value}$ ($\text{C}^4\text{m}^7\text{J}^{-3}\text{mol}^{-1}$)	% contribution to B_γ
$\gamma_1\alpha_1$	-0.1493	-5.36
$\gamma_1\alpha_2$	2.6165	93.87
$\gamma_1\alpha_3$	0.0987	3.54
$\gamma_1\alpha_4$	0.0188	0.68
$\gamma_1\alpha_1\Theta_2$	0.1527	5.48
$\gamma_1\alpha_2\Theta_2$	0.0146	0.52
$B_1\alpha_2\Theta_1$	0.0234	0.84
$B_1\alpha_3\Theta_1$	0.0012	0.04
$D_1\alpha_2\Theta_1$	0.0106	0.38
$D_1\alpha_3\Theta_1$	0.0003	0.01
$\sum_{n=1}^4 \gamma_1\alpha_n$	2.5847	92.73
$\sum_{n=1}^2 \gamma_1\alpha_n\Theta_2$	0.1673	6.00
$\sum_{n=2}^3 (B_1\alpha_n\Theta_1 + D_1\alpha_n\Theta_1)$	0.0355	1.27
B_γ	2.7875	

Table 5.19: A summary of the calculated B_γ values for N_2

T (K)	$10^{67} B_\gamma$ ($C^4 m^7 J^{-3} mol^{-1}$)
200	3.1203
250	2.9500
300	2.8633
350	2.8187
400	2.7964
450	2.7879
500	2.7875

Table 5.19 provides a summary of the temperature dependence for B_γ calculated in this work. Donley and Shelton’s density-dependent hyperpolarizability measurements for both H_2 and N_2 were undertaken at room temperature (298 K), and over the pressure range of 1 to 8 atm. Using the methodology applied to the analysis of H_2 in the previous section, the pair-interaction contribution arising from the N_2 second virial coefficient $B_\gamma = 2.8658 \times 10^{-67} C^4 m^7 J^{-3} mol^{-1}$ at 298 K and 0.8 MPa is evaluated. At this temperature and pressure, the gas density is $V_m^{-1} = 323.4 mol m^{-3}$ [142]. In equation (4.9), A_γ is the ideal-gas molecular hyperpolarizability $\gamma_{\parallel}^{ESHG}$, which for N_2 at $\lambda = 514.5 nm$ is $\gamma_{\parallel}^{ESHG} = (75.46 \pm 0.33) \times 10^{-63} C^4 m^4 J^{-3}$ [45]. The second term in the equation is the pair-interaction contribution $B_\gamma/V_m = 0.093 \times 10^{-63} C^4 m^4 J^{-3}$, which is seen to be 0.12% of $\gamma_{\parallel}^{ESHG}$. The refinements in Donley and Shelton’s ESHG measurement and analysis of the density-dependent hyperpolarizability ratios of $\gamma_{N_2}/\gamma_{H_2}$ ensure accuracy at the 0.1% level [48]. As was found in the case of H_2 , our calculated estimate of B_γ suggests that even at the high-

est experimental pressure, the pair-interaction contribution for N_2 is at the limit of detectability.

In ESHG experiments, accurate hyperpolarizability *ratios* γ_A/γ_B of sample molecule A and reference molecule B are measured by comparing the second-harmonic signals generated in gases A and B under identical phase-matching conditions [30, 45, 148]. Absolute measurements of hyperpolarizabilities are extraordinarily difficult [148], and extracting molecular hyperpolarizabilities from measurements of ratios ultimately requires a molecule with a known hyperpolarizability. Helium is used as this ultimate standard reference since the accurate CI-Hylleraas *ab initio* calculations of Bishop and Pipin for helium are accurate to within 0.1% [90]. For these reasons, Donley and Shelton measured the density dependence of $\gamma_{N_2}/\gamma_{H_2}$ (rather than for γ_{N_2} and γ_{H_2} individually). They recast equation (4.9) into the form

$$\Gamma(V_m) = A_\gamma + \frac{B_\gamma}{V_m} = \gamma \left(1 + \frac{b}{V_m} \right) \quad (5.3)$$

where

$$b = \frac{B_\gamma}{\gamma}, \quad (5.4)$$

and where the symbol γ is the macroscopic scalar hyperpolarizability $\gamma_{\parallel}^{\text{ESHG}}$ in our notation. The least-squares straight-line fit to the experimental measurements of density-dependent hyperpolarizability ratios $\gamma_{N_2}/\gamma_{H_2}$ as a function of hydrogen gas density ρ_{H_2} (or inverse molar volume V_m^{-1}) has the form

$$\frac{\gamma_{N_2}}{\gamma_{H_2}} = \left(\frac{\gamma_{N_2}}{\gamma_{H_2}} \right)_{\rho=0} \left[1 + b(N_2H_2)\rho_{H_2} \right] \quad (5.5)$$

where [48]

$$b(\text{N}_2\text{H}_2) = \left(b_{\text{N}_2} - b_{\text{H}_2} \cdot \frac{\rho_{\text{H}_2}}{\rho_{\text{N}_2}} \right) \left(\frac{\rho_{\text{N}_2}}{\rho_{\text{H}_2}} \right). \quad (5.6)$$

Equation (5.6) is equivalent to

$$b(\text{N}_2\text{H}_2) = \frac{1}{\gamma_{\text{He}}} \cdot \frac{\gamma_{\text{He}}}{\gamma_{\text{H}_2}} \left(\frac{\gamma_{\text{H}_2}}{\gamma_{\text{N}_2}} B_{\gamma}^{\text{N}_2} - B_{\gamma}^{\text{H}_2} \cdot \frac{\rho_{\text{H}_2}}{\rho_{\text{N}_2}} \right) \frac{\rho_{\text{N}_2}}{\rho_{\text{H}_2}}. \quad (5.7)$$

Donley and Shelton's experiment yields the following high-accuracy data [48]:

$\gamma_{\text{H}_2}/\gamma_{\text{He}} = (19.551 \pm 0.029)$, $\gamma_{\text{N}_2}/\gamma_{\text{H}_2} = (1.2828 \pm 0.0013)$, $\rho_{\text{He}}/\rho_{\text{H}_2} = (14.574 \pm 0.006)$ and $\rho_{\text{H}_2}/\rho_{\text{N}_2} = (1.4611 \pm 0.0003)$. Bishop and Pipin provide the standard reference of $\gamma_{\text{He}} = (2.9869 \pm 0.0030) \times 10^{-63} \text{ C}^4\text{m}^4\text{J}^{-3}$ at $\lambda = 514.5 \text{ nm}$ from their CI-Hylleraas calculation [90]. Using these data together with our calculated virial coefficients B_{γ} for H_2 and N_2 in equation (5.7) yields a calculated $b(\text{N}_2\text{H}_2) = 0.940 \times 10^{-6} \text{ m}^3\text{mol}^{-1}$. Their measured value is $b(\text{N}_2\text{H}_2) = (-6.9 \pm 4.6) \times 10^{-6} \text{ m}^3\text{mol}^{-1}$, while their (corrected [49]) calculated value is $b(\text{N}_2\text{H}_2) = 1.078 \times 10^{-6} \text{ m}^3\text{mol}^{-1}$. Our calculated value for $b(\text{N}_2\text{H}_2)$ is 15% smaller than Donley and Shelton's calculated value. Both H_2 and N_2 have relatively small permanent quadrupole moments, and the contributing terms arising from the quadrupoles contribute around 10% to B_{γ} for N_2 and around 5% for H_2 , so it is not surprising that for these molecules, the change in the DID model brought about by including quadrupole moment contributions is not so dramatic.

To investigate whether other molecules might present more favourably large pair-interaction contributions, which would be more accessible to measurement, the second ESHG virial coefficients for the CO_2 and C_2H_4 molecules are now considered.

5.3 Carbon Dioxide

The molecular data required to calculate B_γ for the axially-symmetric CO_2 molecule are contained in Tables 5.20 to 5.23.

Table 5.20: The intermolecular potential parameters and quadrupole moment of CO_2 used in the calculation of B_γ .

Property	Value	Reference
R_0 (nm)	0.400	[131]
ε/k (K)	190.0	[131]
D_1	0.250 ^a	[143]
D_2	0.000	
$10^{40} \Theta_{33}(\text{C m}^2)$	-14.27 ± 0.33	[149, 150]

^aObtained by fitting to pressure virial coefficients reported in Ref. [133]

Table 5.21: CO₂ mean polarizabilities, polarizability anisotropies, and deduced polarizability tensor components for zero frequency and relevant optical frequencies.[†] All values are in SI units.^a

λ (nm)	$10^{40} \alpha$ (C ² m ² J ⁻¹)	$10^{40} \Delta\alpha$ (C ² m ² J ⁻¹)	$10^{40} \alpha_{\perp}$ (C ² m ² J ⁻¹)	$10^{40} \alpha_{\parallel}$ (C ² m ² J ⁻¹)
∞	3.2402	2.530	2.397	4.927
514.5	2.9570	2.386	2.162	4.548
257.25	3.1812	2.665	2.293	4.958

^aThe relationship between SI units and atomic units is:

$$1 \text{ e}^2 \text{ a}_0^2 \text{ E}_h^{-1} = 1.648778 \times 10^{-41} \text{ C}^2 \text{ m}^2 \text{ J}^{-1}.$$

[†]Extracted from the measured dispersion data in References [120, 150].

The frequency dependence of the ESHG second hyperpolarizability and of the SHG dipole-dipole-quadrupole hyperpolarizability tensors for the CO₂ molecule have all been calculated using CCSD wavefunctions and t-aug-cc-pVTZ basis sets. The calculations were performed at the C–O equilibrium bond length of $r_{\text{C-O}} = 1.161\,226 \text{ \AA}$ [151]. The $\gamma_{ijkl}(-2\omega; \omega, \omega, 0)$ tensor components are listed in Table 5.22, yielding an electronic contribution of γ_{\parallel}^e which is in reasonable agreement with the measured γ_{\parallel} data over the full range of wavelengths. Bishop and Dalskov have computed the vibrational contribution γ_{\parallel}^v , obtaining -81.89 a.u. at a wavelength of 632.8 nm, and -81.50 a.u. in the static limit [152], which when combined with the electronic contribution yields excellent agreement with the measured data (1% or better over the range of wavelengths considered). The electronic contributions to the tensor components of $B_{ijkl}(-2\omega; \omega, \omega)$ and $D_{ijkl}(-2\omega; \omega, \omega)$ are presented in Table 5.23. The vibrational contributions are not expected to be overly significant. There have been neither measurements nor calculations of these second-harmonic tensors previously reported in the literature. Maroulis has reported on fourth-order many-body perturbation theory (MP4) computation of the static (hyper)polarizabilities for CO₂,

where he obtained for $B_{ijkl}(0;0,0)$ the components $B_{1111} = -140$, $B_{1122} = 61$, $B_{1313} = -205$ and $B_{3333} = -305 e^3 a_0^4 E_h^{-2}$. [153] His values are in reasonable agreement with the static values reported in Table 5.23.

Table 5.22: Components of the ESHG second hyperpolarizability $\gamma_{ijkl}(-2\omega; \omega, \omega, 0)$ for CO₂ calculated in this work using a CCSD wavefunction and a t-aug-cc-pVTZ basis set. All values are in atomic units.^a

Property	$\lambda(\text{nm})$				
	400.0	514.5	694.3	1064	∞
γ_{1111}	1678.8	1383.3	1225.0	1130.5	1067.6
γ_{1122}	561.9	461.9	408.6	376.9	355.9
γ_{1133}	953.0	743.5	640.4	581.5	543.3
γ_{1331}	942.5	743.3	641.2	582.0	543.3
γ_{3113}	1007.9	769.9	652.6	586.1	543.3
γ_{3311}	1076.7	794.3	662.6	589.7	543.3
γ_{3333}	2177.2	1671.0	1418.2	1273.7	1180.1
γ_{\parallel}^e	2132.1	1683.8	1456.9	1325.7	1240.0
γ_{\parallel}^v	-81.89	-81.89	-81.89	-81.89	-81.50
$\gamma_{\parallel}^{\text{calc}\dagger}$	2050.2	1601.9	1375.0	1243.8	1158.5
$\gamma_{\parallel}^{\text{exp}} [45]$	2072.9 [‡]	1613.7 \pm 3.7	1365.8 [†]	1240.2 \pm 7.7	1146.7 [‡]

^aConversion to SI units: $1 \text{ e}^4 \text{ a}_0^4 \text{ E}_h^{-3} = 6.235378 \times 10^{-65} \text{ C}^4 \text{ m}^4 \text{ J}^{-3}$.

[†] $\gamma_{\parallel}^{\text{calc}} = \gamma_{\parallel}^e + \gamma_{\parallel}^v$, using the vibrational value obtained at 632.8 nm for all optical wavelengths

[‡]Extrapolated from measured data [45].

Table 5.23: Components of the SHG dipole-dipole-quadrupole hyperpolarizabilities $B_{ijkl}(-2\omega; \omega, \omega)$ and $D_{ijkl}(-2\omega; \omega, \omega)$ for CO₂ calculated *ab initio* in this work using a CCSD wavefunction and a t-aug-cc-pVTZ basis set. All values are in atomic units.^a

Property	$\lambda(\text{nm})$				
	400.0	514.5	694.3	1064	∞
B_{1111}	-192.50	-173.71	-162.67	-155.70	-150.87
B_{1122}	97.54	86.82	80.73	76.95	74.36
B_{1313}	-283.46	-248.96	-229.61	-217.71	-209.62
B_{3131}	-318.11	-265.24	-237.25	-220.65	-209.62
B_{3333}	-397.83	-348.92	-321.23	-304.13	-292.48
D_{1111}	-180.52	-167.50	-159.58	-154.46	-150.87
D_{1122}	92.07	84.07	79.37	76.41	74.36
D_{1313}	-281.41	-245.89	-227.68	-216.86	-209.62
D_{3333}	-351.74	-325.71	-309.87	-299.65	-292.48

^aConversion to SI units: $1 \text{ e}^3 \text{ a}_0^4 \text{ E}_h^{-2} = 1.696733 \times 10^{-63} \text{ C}^3 \text{ m}^4 \text{ J}^{-2}$.

The quadrupole moment and the polarizability anisotropy of the CO₂ molecule are both around three times larger in magnitude than those of N₂. This will account for much of the behaviour observed in the calculated B_γ virial coefficients in tables 5.24 to 5.27. These tables record the relative magnitudes of the terms contributing to B_γ calculated at intervals of temperature spanning $T = 200$ K to 500 K.

At $T = 200$ K, $\sum \gamma_1 \alpha_n$ contributes 53.8% to B_γ , while $\sum \gamma_1 \alpha_n \Theta_2$ contributes 52.1%, up from the 8.8% for N₂ at this temperature. $\sum (B_1 \alpha_n \Theta_1 + D_1 \alpha_n \Theta_1)$ contributes -6.0%. Even at $T = 500$ K, the quadrupole series of terms make a significant contribution to B_γ , $\sum \gamma_1 \alpha_n \Theta_2$ providing 26.3% and $\sum (B_1 \alpha_n \Theta_1 + D_1 \alpha_n \Theta_1)$ -3.4%. As was observed for H₂ and N₂, the $\gamma_1 \alpha_2$ term is still dominant in the $\gamma_1 \alpha_n$ series, after which the series rapidly converges. Also, for the $\gamma_1 \alpha_n \Theta_2$ series, the leading $\gamma_1 \alpha_1 \Theta_2$ term remains dominant.

Table 5.24: The relative magnitudes of the contributions to B_γ for CO_2 at $T = 200$ K

Contributing Term	$10^{67} \times \text{value}$ ($\text{C}^4\text{m}^7\text{J}^{-3}\text{mol}^{-1}$)	% contribution to B_γ
$\gamma_1\alpha_1$	-2.7117	-15.27
$\gamma_1\alpha_2$	11.7342	66.10
$\gamma_1\alpha_3$	0.4283	2.41
$\gamma_1\alpha_4$	0.1024	0.57
$\gamma_1\alpha_1\Theta_2$	7.9992	45.06
$\gamma_1\alpha_2\Theta_2$	1.2577	7.08
$B_1\alpha_2\Theta_1$	-0.4734	-2.67
$B_1\alpha_3\Theta_1$	-0.0692	-0.39
$D_1\alpha_2\Theta_1$	-0.4243	-2.39
$D_1\alpha_3\Theta_1$	-0.0901	-0.50
$\sum_{n=1}^4 \gamma_1\alpha_n$	9.5532	53.81
$\sum_{n=1}^2 \gamma_1\alpha_n\Theta_2$	9.2569	52.14
$\sum_{n=2}^3 (B_1\alpha_n\Theta_1 + D_1\alpha_n\Theta_1)$	-1.0570	-5.95
B_γ	17.7531	

Table 5.25: The relative magnitudes of the contributions to B_γ for CO_2 at $T = 298$ K

Contributing Term	$10^{67} \times \text{value}$ ($\text{C}^4\text{m}^7\text{J}^{-3}\text{mol}^{-1}$)	% contribution to B_γ
$\gamma_1\alpha_1$	-1.9169	-16.57
$\gamma_1\alpha_2$	9.0768	78.45
$\gamma_1\alpha_3$	0.3248	2.81
$\gamma_1\alpha_4$	0.0797	0.69
$\gamma_1\alpha_1\Theta_2$	3.9980	34.55
$\gamma_1\alpha_2\Theta_2$	0.5689	4.92
$B_1\alpha_2\Theta_1$	-0.2577	-2.23
$B_1\alpha_3\Theta_1$	-0.0365	-0.31
$D_1\alpha_2\Theta_1$	-0.2233	-1.93
$D_1\alpha_3\Theta_1$	-0.0439	-0.38
$\sum_{n=1}^4 \gamma_1\alpha_n$	7.5644	65.38
$\sum_{n=1}^2 \gamma_1\alpha_n\Theta_2$	4.5669	39.47
$\sum_{n=2}^3 (B_1\alpha_n\Theta_1 + D_1\alpha_n\Theta_1)$	-0.5614	-4.85
B_γ	11.5699	

Table 5.26: The relative magnitudes of the contributions to B_γ for CO_2 at $T = 400$ K

Contributing Term	$10^{67} \times \text{value}$ ($\text{C}^4\text{m}^7\text{J}^{-3}\text{mol}^{-1}$)	% contribution to B_γ
$\gamma_1\alpha_1$	-1.5706	-16.36
$\gamma_1\alpha_2$	8.1647	85.07
$\gamma_1\alpha_3$	0.2949	3.07
$\gamma_1\alpha_4$	0.0741	0.77
$\gamma_1\alpha_1\Theta_2$	2.6582	27.70
$\gamma_1\alpha_2\Theta_2$	0.3615	3.76
$B_1\alpha_2\Theta_1$	-0.1784	-1.86
$B_1\alpha_3\Theta_1$	-0.0254	-0.26
$D_1\alpha_2\Theta_1$	-0.1522	-1.59
$D_1\alpha_3\Theta_1$	-0.0292	-0.30
$\sum_{n=1}^4 \gamma_1\alpha_n$	6.9631	72.55
$\sum_{n=1}^2 \gamma_1\alpha_n\Theta_2$	3.0197	31.46
$\sum_{n=2}^3 (B_1\alpha_n\Theta_1 + D_1\alpha_n\Theta_1)$	-0.3852	-4.01
B_γ	9.5976	

Table 5.27: The relative magnitudes of the contributions to B_γ for CO_2 at $T = 500$ K

Contributing Term	$10^{67} \times \text{value}$ ($\text{C}^4\text{m}^7\text{J}^{-3}\text{mol}^{-1}$)	% contribution to B_γ
$\gamma_1\alpha_1$	-1.3781	-15.75
$\gamma_1\alpha_2$	7.7697	88.79
$\gamma_1\alpha_3$	0.2856	3.26
$\gamma_1\alpha_4$	0.0732	0.84
$\gamma_1\alpha_1\Theta_2$	2.0298	23.20
$\gamma_1\alpha_2\Theta_2$	0.2706	3.09
$B_1\alpha_2\Theta_1$	-0.1396	-1.59
$B_1\alpha_3\Theta_1$	-0.0202	-0.23
$D_1\alpha_2\Theta_1$	-0.1180	-1.35
$D_1\alpha_3\Theta_1$	-0.0225	-0.26
$\sum_{n=1}^4 \gamma_1\alpha_n$	6.7504	77.14
$\sum_{n=1}^2 \gamma_1\alpha_n\Theta_2$	2.3004	26.29
$\sum_{n=2}^3 (B_1\alpha_n\Theta_1 + D_1\alpha_n\Theta_1)$	-0.3003	-3.43
B_γ	8.7505	

Table 5.28: A summary of the calculated B_γ values for CO₂

T (K)	$10^{67} B_\gamma$ (C ⁴ m ⁷ J ⁻³ mol ⁻¹)
200	17.753
250	13.561
300	11.509
350	10.337
400	9.598
450	9.101
500	8.751

Table 5.28 summarizes the temperature dependence of B_γ as calculated in this work. As was done for H₂ and N₂, the pair-interaction contribution arising from the CO₂ second virial coefficient $B_\gamma = 11.570 \times 10^{-67} \text{ C}^4\text{m}^7\text{J}^{-3}\text{mol}^{-1}$ at 298 K and 0.8 MPa is evaluated. At this temperature and pressure, the gas density is $V_m^{-1} = 336.7 \text{ mol m}^{-3}$ [142]. In equation (4.9), $A_\gamma = \gamma_{\parallel}^{\text{ESHG}}$, which for CO₂ at $\lambda = 514.5 \text{ nm}$ is $\gamma_{\parallel}^{\text{ESHG}} = (100.58 \pm 0.23) \times 10^{-63} \text{ C}^4\text{m}^4\text{J}^{-3}$ [45]. The pair-interaction contribution in this equation is $B_\gamma/V_m = 0.39 \times 10^{-63} \text{ C}^4\text{m}^4\text{J}^{-3}$, which is 0.4% of $\gamma_{\parallel}^{\text{ESHG}}$. Donley and Shelton's ESHG experiment to measure the density-dependent hyperpolarizabilities of gases achieves accuracy at the 0.1% level [48], so that the effect should be readily discernible with this apparatus. The experimental results for H₂ and N₂ suggest that our calculations of B_γ underestimate (in magnitude) the true virial coefficients by up to a factor of 7, which if true for CO₂ would mean that the interaction-induced contribution to the measured hyperpolarizability ratio would be easily detectable.

5.4 Ethene

The C_2H_4 molecule possesses D_{2h} symmetry. Previous studies have revealed that approximating this molecule to be of axial symmetry yields disagreement between calculated and measured second light-scattering virial coefficients B_ρ [143, 154] and second Kerr-effect virial coefficients B_K [155] of up to 40%. If the full symmetry of the molecule is utilized, the calculated B_ρ is within 3% of the measured value [125], and the measured and calculated B_K values over the experimental temperature range of 202 to 364 K come into satisfactory agreement [80]. The full symmetry of the molecule will be taken into account in evaluating B_γ . The molecular data required in the calculations are contained in Tables 5.29 to 5.33.

Table 5.29: The intermolecular potential parameters and quadrupole moment of C_2H_4 used in the calculation of B_γ .

Property	Value	Reference
R_0 (nm)	0.4232	[125, 156]
ε/k (K)	190.0	[125, 156]
D_1	0.22965 ^a	[125]
D_2	0.21383	
$10^{40} \Theta_{11}(\text{C m}^2)$	5.57 ± 0.63	[157]
$10^{40} \Theta_{22}(\text{C m}^2)$	-10.54 ± 0.63	
$10^{40} \Theta_{33}(\text{C m}^2)$	4.94 ± 0.33	

^aObtained by fitting to pressure virial coefficients reported in Ref. [133]

Table 5.30: C₂H₄ mean polarizabilities, polarizability anisotropies, and polarizability tensor components for zero frequency and relevant optical frequencies. The data are calculated in this work using a CCSD wavefunction and a t-aug-cc-pVTZ basis set. All values are in SI units.^a

λ (nm)	$10^{40} \alpha$ (C ² m ² J ⁻¹)	$10^{40} \Delta\alpha$ (C ² m ² J ⁻¹)	$10^{40} \alpha_{11}$ (C ² m ² J ⁻¹)	$10^{40} \alpha_{22}$ (C ² m ² J ⁻¹)	$10^{40} \alpha_{33}$ (C ² m ² J ⁻¹)
∞	4.489	1.856	4.138	3.637	5.692
632.8	4.557	1.954	4.214	3.736	5.720
514.5	4.678	2.009	4.255	3.789	5.990
257.25	5.465	2.741	4.669	4.439	7.288

^aThe relationship between SI units and atomic units is:
 $1 \text{ e}^2 \text{ a}_0^2 \text{ E}_\text{h}^{-1} = 1.648778 \times 10^{-41} \text{ C}^2 \text{ m}^2 \text{ J}^{-1}$.

Table 5.31: Experimentally deduced mean polarizabilities, polarizability anisotropies, and polarizability tensor components for C₂H₄ for zero frequency and relevant optical frequencies. All values are in SI units.

λ (nm)	$10^{40} \alpha$ (C ² m ² J ⁻¹)	$10^{40} \Delta\alpha$ (C ² m ² J ⁻¹)	$10^{40} \alpha_{11}$ (C ² m ² J ⁻¹)	$10^{40} \alpha_{22}$ (C ² m ² J ⁻¹)	$10^{40} \alpha_{33}$ (C ² m ² J ⁻¹)
∞ [155]	4.73 ± 0.03	1.63 ± 0.05	4.30 ± 0.04	4.09 ± 0.03	5.81 ± 0.02
632.8 [155]	4.71 ± 0.03	1.92 ± 0.04	4.41 ± 0.04	3.79 ± 0.03	5.94 ± 0.02
514.5 [154]	4.787	2.091	4.353	3.857	6.151

The frequency dependence of the polarizability, ESHG second hyperpolarizability and SHG dipole-dipole-quadrupole hyperpolarizability tensors for the C_2H_4 molecule have all been calculated using CCSD wavefunctions and t-aug-cc-pVTZ basis sets. The calculations for the C_2H_4 molecule were performed at the equilibrium geometry of $r_{\text{C-C}} = 1.339 \text{ \AA}$, $r_{\text{C-H}} = 1.085 \text{ \AA}$ and $\Theta_{\text{HCH}} = 117.83^\circ$ [158]. The calculated polarizability tensor components are given in Table 5.30, while Table 5.31 provides the best available experimental data. In the calculations of B_γ we have used the experimental polarizability values at zero frequency and for $\lambda = 514.5 \text{ nm}$. In the absence of experimental data at $\lambda = 257.25 \text{ nm}$, the *ab initio* calculated values have been used for this wavelength. This can be done with confidence, since the calculated and experimental data at the other wavelengths are in reasonable agreement.

The $\gamma_{ijkl}(-2\omega; \omega, \omega, 0)$ tensor components are listed in Table 5.32. The only measurement of $\gamma_{\parallel}^{\text{ESHG}}$ for C_2H_4 is for the ruby laser wavelength $\lambda = 694.3 \text{ nm}$ [27], which gives $\gamma_{\parallel}^{\text{ESHG}} = (9029 \pm 202) e^4 a_0^4 E_h^{-3}$. The *ab initio* calculated value of $\gamma_{\parallel}^{\text{ESHG}} = 9038 e^4 a_0^4 E_h^{-3}$ is in good agreement, which suggests that the vibrational contribution is small. Indeed, *ab initio* calculations of the vibrational second hyperpolarizability for C_2H_4 have already been obtained by Quinet and Champagne, who estimated that the vibrational contribution to $\gamma_{ijkl}(-2\omega; \omega, \omega, 0)$ is only 1% of the electronic contribution [159]. Maroulis has calculated the static (hyper)polarizabilities of C_2H_4 at the fourth-order many-body perturbation theory (MP4) level of theory [158], obtaining the components $\gamma_{1111} = 3644$, $\gamma_{2222} = 8855$, $\gamma_{3333} = 5755$, $\gamma_{1122} = 2119$, $\gamma_{2233} = 2892$ and $\gamma_{1133} = 1850 e^4 a_0^4 E_h^{-3}$. These values agree well with the static values reported in Table 5.32. The tensor components of $B_{ijkl}(-2\omega; \omega, \omega)$ and $D_{ijkl}(-2\omega; \omega, \omega)$ are listed in Table 5.33; we are not aware of any previous calculations of these properties for C_2H_4 , even in the static limit.

Table 5.32: Components of the ESHG second hyperpolarizability $\gamma_{ijkl}(-2\omega; \omega, \omega, 0)$ for C_2H_4 calculated using a CCSD wavefunction and a t-aug-cc-pVTZ basis set. All values are in atomic units.^a

Property	$\lambda(\text{nm})$				
	400.0	514.5	694.3	1064	∞
γ_{1111}	8612.8	5754.2	4595.7	3992.9	3622.4
γ_{1122}	7304.5	4042.1	2953.6	2439.0	2140.5
γ_{2211}	15734.7	5295.6	3299.8	2537.0	2140.5
γ_{1221}	8273.5	4311.2	3047.9	2469.3	2140.5
γ_{2112}	12736.4	4976.7	3227.8	2519.2	2140.5
γ_{2222}	50955.0	20909.9	13696.6	10692.9	9065.3
γ_{1133}	4663.0	3083.2	2424.9	2082.5	1873.1
γ_{3311}	6235.2	3459.2	2550.7	2122.1	1873.1
γ_{1331}	5418.9	3267.0	2486.9	2102.2	1873.1
γ_{3113}	6728.2	3507.7	2557.9	2122.9	1873.1
γ_{2233}	17110.5	6334.1	4092.1	3199.5	2724.5
γ_{3322}	15056.0	6369.4	4152.3	3225.6	2724.5
γ_{2332}	17394.3	6620.6	4209.3	3239.6	2724.5
γ_{3223}	16894.7	6717.6	4253.0	3254.4	2724.5
γ_{3333}	19360.4	10063.1	7321.2	6074.1	5361.5
γ_{\parallel}^e	29095.9	13116.6	9038.0	7279.9	6305.1

^aConversion to SI units: $1 \text{ e}^4 \text{ a}_0^4 \text{ E}_h^{-3} = 6.235378 \times 10^{-65} \text{ C}^4 \text{ m}^4 \text{ J}^{-3}$.

Table 5.33: Components of the SHG dipole-dipole-quadrupole hyperpolarizabilities $B_{ijkl}(-2\omega; \omega, \omega)$ and $D_{ijkl}(-2\omega; \omega, \omega)$ for C_2H_4 calculated *ab initio* in this work using a CCSD wavefunction and a t-aug-cc-pVTZ basis set. All values are in au.^a

Property	$\lambda(\text{nm})$				
	400.0	514.5	694.3	1064	∞
B_{1111}	-624.8	-527.4	-475.7	-444.8	-424.1
B_{1122}	248.2	229.5	214.9	204.8	197.6
B_{2211}	926.4	583.5	464.2	404.8	369.0
B_{1212}	-846.6	-630.6	-533.0	-479.6	-445.8
B_{2121}	-1282.1	-717.1	-559.9	-487.7	-445.8
B_{2222}	-2252.3	-1347.9	-1054.4	-911.9	-827.1
B_{1313}	-1004.3	-798.7	-696.9	-638.5	-600.5
B_{2323}	-1635.9	-944.7	-741.5	-645.9	-589.7
B_{3131}	-1271.9	-876.9	-726.3	-648.5	-600.5
B_{3232}	-1678.8	-988.7	-761.5	-653.2	-589.7
B_{3322}	223.0	266.2	262.2	254.5	247.7
B_{3333}	-1098.5	-827.4	-716.2	-656.0	-617.8
D_{1111}	-509.6	-479.0	-453.9	-436.6	-424.1
D_{1122}	762.4	536.3	445.4	398.1	369.0
D_{2211}	147.1	191.3	198.5	198.8	197.6
D_{2233}	113.8	214.2	238.3	245.5	247.7
D_{1212}	-829.4	-607.0	-519.9	-474.2	-445.8
D_{1313}	-928.4	-764.4	-681.0	-632.5	-600.5
D_{2323}	-1096.5	-808.4	-691.2	-628.9	-589.7
D_{2222}	-1738.7	-1215.2	-1004.4	-894.7	-827.1
D_{3333}	-714.5	-691.4	-659.4	-635.5	-617.8

^aConversion to SI units: $1 \text{ e}^3 \text{ a}_0^4 \text{ E}_h^{-2} = 1.696733 \times 10^{-63} \text{ C}^3 \text{ m}^4 \text{ J}^{-2}$.

The quadrupole moments and polarizability anisotropies of C₂H₄ and CO₂ are comparable, but C₂H₄ has significantly larger ESHG second hyperpolarizability and SHG dipole-dipole-quadrupole hyperpolarizability tensor components. The calculated $\gamma_{\parallel}^{\text{ESHG}}$ for C₂H₄ at $\lambda = 514.5$ nm is 5.4 times that of CO₂ at this wavelength. The expectation is that B_{γ} for C₂H₄ should be considerably larger than that for CO₂, and this is borne out by the calculated data in Tables 5.34 to 5.37. These tables give the relative magnitudes of the terms contributing to B_{γ} calculated at 100 K intervals spanning $T = 200$ K to 500 K, while Table 5.38 summarizes the calculated B_{γ} temperature dependence.

At $T = 200$ K, $\sum \gamma_1 \alpha_n$ contributes 43.7% to B_{γ} , while $\sum \gamma_1 \alpha_n \Theta_2$ contributes 30.4% and $\sum (B_1 \alpha_n \Theta_1 + D_1 \alpha_n \Theta_1)$ contributes 25.9%. At this temperature, $\sum (B_1 \alpha_n \Theta_1 + D_1 \alpha_n \Theta_1)$ contributed only -6.0% for CO₂, 2.8% for N₂ and 0.8% for H₂. For C₂H₄, the dipole-dipole-quadrupole hyperpolarizability has become a significant contributor to the pair-interaction, being of comparable size to the quadrupole-induced second hyperpolarizability effect over the entire temperature range considered here.

Table 5.34: The relative magnitudes of the contributions to B_γ for C_2H_4 at $T = 200$ K

Contributing Term	$10^{67} \times \text{value}$ ($\text{C}^4\text{m}^7\text{J}^{-3}\text{mol}^{-1}$)	% contribution to B_γ
$\gamma_1\alpha_1$	-49.000	-6.88
$\gamma_1\alpha_2$	322.808	45.34
$\gamma_1\alpha_3$	23.063	3.24
$\gamma_1\alpha_4$	13.958	1.96
$\gamma_1\alpha_1\Theta_2$	143.874	20.21
$\gamma_1\alpha_2\Theta_2$	72.611	10.20
$B_1\alpha_2\Theta_1$	73.141	10.27
$B_1\alpha_3\Theta_1$	34.049	4.78
$D_1\alpha_2\Theta_1$	54.590	7.67
$D_1\alpha_3\Theta_1$	22.879	3.21
$\sum_{n=1}^4 \gamma_1\alpha_n$	310.829	43.66
$\sum_{n=1}^2 \gamma_1\alpha_n\Theta_2$	216.485	30.41
$\sum_{n=2}^3 (B_1\alpha_n\Theta_1 + D_1\alpha_n\Theta_1)$	184.659	25.93
B_γ	711.973	

Table 5.35: The relative magnitudes of the contributions to B_γ for C_2H_4 at $T = 298$ K

Contributing Term	$10^{67} \times$ value ($C^4m^7J^{-3}mol^{-1}$)	% contribution to B_γ
$\gamma_1\alpha_1$	-11.864	-5.02
$\gamma_1\alpha_2$	161.747	68.40
$\gamma_1\alpha_3$	10.005	4.23
$\gamma_1\alpha_4$	3.706	1.57
$\gamma_1\alpha_1\Theta_2$	30.034	12.70
$\gamma_1\alpha_2\Theta_2$	8.645	3.66
$B_1\alpha_2\Theta_1$	15.132	6.40
$B_1\alpha_3\Theta_1$	4.050	1.71
$D_1\alpha_2\Theta_1$	12.159	5.14
$D_1\alpha_3\Theta_1$	2.857	1.21
$\sum_{n=1}^4 \gamma_1\alpha_n$	163.594	69.18
$\sum_{n=1}^2 \gamma_1\alpha_n\Theta_2$	38.679	16.36
$\sum_{n=2}^3 (B_1\alpha_n\Theta_1 + D_1\alpha_n\Theta_1)$	34.198	14.46
B_γ	236.471	

Table 5.36: The relative magnitudes of the contributions to B_γ for C_2H_4 at $T = 400$ K

Contributing Term	$10^{67} \times \text{value}$ ($\text{C}^4\text{m}^7\text{J}^{-3}\text{mol}^{-1}$)	% contribution to B_γ
$\gamma_1\alpha_1$	-6.611	-3.72
$\gamma_1\alpha_2$	135.322	76.17
$\gamma_1\alpha_3$	8.197	4.61
$\gamma_1\alpha_4$	2.632	1.48
$\gamma_1\alpha_1\Theta_2$	16.393	9.23
$\gamma_1\alpha_2\Theta_2$	3.660	2.06
$B_1\alpha_2\Theta_1$	8.277	4.66
$B_1\alpha_3\Theta_1$	1.728	0.97
$D_1\alpha_2\Theta_1$	6.803	3.83
$D_1\alpha_3\Theta_1$	1.256	0.71
$\sum_{n=1}^4 \gamma_1\alpha_n$	139.540	78.54
$\sum_{n=1}^2 \gamma_1\alpha_n\Theta_2$	20.053	11.29
$\sum_{n=2}^3 (B_1\alpha_n\Theta_1 + D_1\alpha_n\Theta_1)$	18.064	10.17
B_γ	177.657	

Table 5.37: The relative magnitudes of the contributions to B_γ for C_2H_4 at $T = 500$ K

Contributing Term	$10^{67} \times$ value ($C^4m^7J^{-3}mol^{-1}$)	% contribution to B_γ
$\gamma_1\alpha_1$	-4.823	-3.06
$\gamma_1\alpha_2$	125.817	79.77
$\gamma_1\alpha_3$	7.646	4.85
$\gamma_1\alpha_4$	2.360	1.50
$\gamma_1\alpha_1\Theta_2$	11.649	7.39
$\gamma_1\alpha_2\Theta_2$	2.348	1.49
$B_1\alpha_2\Theta_1$	5.893	3.74
$B_1\alpha_3\Theta_1$	1.117	0.71
$D_1\alpha_2\Theta_1$	4.882	3.09
$D_1\alpha_3\Theta_1$	0.824	0.52
$\sum_{n=1}^4 \gamma_1\alpha_n$	131.000	83.06
$\sum_{n=1}^2 \gamma_1\alpha_n\Theta_2$	13.997	8.88
$\sum_{n=2}^3 (B_1\alpha_n\Theta_1 + D_1\alpha_n\Theta_1)$	12.716	8.06
B_γ	157.713	

Table 5.38: A summary of the calculated B_γ values for C_2H_4

T (K)	$10^{67} B_\gamma$ ($\text{C}^4\text{m}^7\text{J}^{-3}\text{mol}^{-1}$)
200	711.97
250	326.11
300	234.30
350	197.22
400	177.66
450	165.70
500	157.71

The pair-interaction contribution arising from the C_2H_4 second virial coefficient $B_\gamma = 236.47 \times 10^{-67} \text{C}^4\text{m}^7\text{J}^{-3}\text{mol}^{-1}$ at 298 K and 0.8 MPa is now evaluated. At this temperature and pressure, the gas density is $V_m^{-1} = 338.7 \text{ mol m}^{-3}$ [142]. In equation (4.9), $A_\gamma = \gamma_{\parallel}^{\text{ESHG}}$, which for C_2H_4 at $\lambda = 514.5 \text{ nm}$ is calculated here to be $\gamma_{\parallel}^{\text{ESHG}} = (795.7 \pm 0.23) \times 10^{-63} \text{C}^4\text{m}^4\text{J}^{-3}$. The pair-interaction contribution in this equation is $B_\gamma/V_m = 8.0 \times 10^{-63} \text{C}^4\text{m}^4\text{J}^{-3}$, which is 1.0% of $\gamma_{\parallel}^{\text{ESHG}}$. Since the ESHG experiment of Donley and Shelton for measuring the density-dependent hyperpolarizabilities of gases achieves an accuracy at the 0.1% level [48], the pair-interaction contributions for C_2H_4 should be readily measurable with this apparatus.

5.5 Concluding Remarks

Donley and Shelton's experimental study of the density dependence of atomic and molecular hyperpolarizabilities appears to be the only such investigation in the gas

phase [48]. The relative size of the pair-interaction contribution at the experimentally accessible gas densities is extremely small, so that even at the excellent 0.1% level of accuracy achieved by the apparatus, the density dependence of the hyperpolarizability ratio for the H₂ and N₂ molecules is hovering near the very limits of detectability. Using a classical DID model, they obtained calculated pair-interaction second virial coefficients around 6 times smaller than the experimentally-deduced values, and of opposite sign.

Ab initio calculations of the frequency-dependent interaction-induced second hyperpolarizabilities for helium and argon [67] were used by Koch *et al.* to evaluate the ESHG second virial coefficients for these atoms using a semi-classical approach [69]. The computed interaction-induced second hyperpolarizabilities are rather sensitive to the choice of basis set, and so the calculations were performed with extended and diffuse basis sets. The ESHG second virial coefficients obtained for Ar depend quite dramatically on the choice of basis set, and are positive while the virial coefficients for He are negative.

The full extent to which short-range electron overlap effects will affect the collision-induced hyperpolarizability contributions for polyatomic molecules such as CO₂ and C₂H₄ will only be made known when *ab initio* quantum mechanical calculations (employing large basis sets with diffuse basis functions) are realisable. These calculations would inevitably require considerable computational resources.

This investigation has sought to provide some interim insight into the question. Utilizing the classical DID model, and taking note of the suggestions of Donley and Shelton to improve the accuracy of the model, second ESHG virial coefficients have been computed for the H₂, N₂, CO₂ and C₂H₄ molecules. Whereas Donley and Shelton assumed the molecules to be of spherical symmetry, we have taken into account

their true symmetry, using the correct independent tensor components for the (hyper)polarizabilities. The DALTON molecular electronic structure software package has allowed for accurate calculation of the hyperpolarizability tensor components. We are unaware of any previous calculations of the second-harmonic dipole-dipole-quadrupole hyperpolarizabilities for these molecules. The contributions arising from the permanent electric quadrupole moments and the dipole-dipole-quadrupole hyperpolarizabilities of the molecules have been comprehensively accounted for. For H_2 and N_2 , the quadrupole contributions are around 5 to 10% of the ESHG second virial coefficient, while the dipole-dipole-quadrupole hyperpolarizabilities contribute less than 1% for H_2 and no more than 3% for N_2 . In the case of CO_2 , the quadrupole contribution is 52% at $T = 200$ K and 26% at 500 K, while the dipole-dipole-quadrupole hyperpolarizabilities contribute -6% at 200 K and -3.4% at 500 K. For C_2H_4 , the quadrupole contribution is 30% at $T = 200$ K and 9% at 500 K, while the dipole-dipole-quadrupole hyperpolarizabilities now contribute significantly, being 26% of B_γ at 200 K and 8% at 500 K. Indications are that the overall pair-interaction contributions arising for CO_2 and for C_2H_4 are significant enough to be comfortably measurable using the existing ESHG apparatus and electrode arrays.

Appendix A

A.1 Fortran Program to calculate the $\gamma_1\alpha_1$ contribution to B_γ .

```
PROGRAM ESHGG1A1

C
C PROGRAM TO CALCULATE THE G1A1 TERM'S CONTRIBUTION TO B_gamma FOR C2H4
C USING GAUSSIAN INTEGRATION WITH 64 INTERVALS FOR THE RANGE,
C AND 16 INTERVALS FOR ALL ANGULAR VARIABLES
C (I.E. ALPHA1, BETA1, GAMMA1, ALPHA2, BETA2 AND GAMMA2).
C DOUBLE PRECISION IS USED THROUGHOUT.
C

C -----
C SYSTEM INITIALIZATION:
C -----

      IMPLICIT DOUBLE PRECISION (A-H,O-Z)
      COMMON COEF1,DCTC
      DIMENSION COEF2(64,2),COEF1(16,2),SEP(64),AL1(16),BE1(16),GA1(16)
+ ,AL2(16),BE2(16),GA2(16),DCTC(9,16,16,16),FI(16,16,16,16),D1(6
+ 4),E1(16,16,16,16),F1(16,16,16,16),SE3(64),SE4(64),SE5(64),
+ SE6(64),SE8(64),SE12(64),G1(16,16,16),DDP(16,16,16,16),DQP(16,
+ 16,16,16),DIDP(16,16,16,16)
      INTEGER X1,X2,X3,X4,X5,X6,X7

C
C Molecular Data for C2H4 ESHG (514.5 nm)
C

      SS1=0.000000
      SS2=0.000000
      SS3=0.000000
      SS4=0.000000
      SS5=0.000000
      SS6=0.000000
```

SS7=0.000000

DIP=0.000

C dynamic alpha(-omega;omega) {experimental source wavelength = 514.5 nm}
C 514.5 nm

A11=4.353

A22=3.857

A33=6.151

ALDYN=(A11+A22+A33)/3

C dynamic alpha(-2*omega;omega) {frequency doubled lambda = 257.25 nm}
C 257.25 nm

B11=4.669

B22=4.439

B33=7.288

C static alpha(0;0)

V11=4.30

V22=4.09

V33=5.81

ALSTAT=(V11+V22+V33)/3

C dynamic gamma(-2*omega;omega,omega,0)
C general D_{2h} symmetry ... for CO₂ this reduces to D_{∞h} symmetry

G1111=0.358795

G2222=1.303809

G3333=0.627473

G1122=0.252043

G2211=0.330203

G1221=0.268818

G2112=0.310313

G1133=0.192251

G3311=0.215693

G1331=0.203709

G3113=0.218716

G2233=0.228472

G3322=0.397159

G2332=0.412819

G3223=0.418865

C quadrupole

Q1=5.57

Q2=-10.54

A.1. FORTRAN PROGRAM TO CALCULATE THE $\gamma_1\alpha_1$ CONTRIBUTION TO B_γ .183

```
      AMIN1=0.1000
      AMAX1=3.0000

C
C END: Molecular data for C2H4 ESHG (514.5nm)
C
C
C READ THE GAUSSIAN COEFFICIENTS FROM THE DATAFILE GAUSS64.DAT:
C
      OPEN(UNIT=10,FILE='GAUSS64.DAT')
      DO 10 ICTR1=1,64
      DO 20 ICTR2=1,2
      READ(10,1010,END=11)COEF2(ICTR1,ICTR2)
1010      FORMAT(F18.15)
20      CONTINUE
10      CONTINUE
11      CLOSE(UNIT=10)

C
C CALCULATE THE INTEGRATION POINTS FOR THE RANGE:
C
      SEP1=(AMAX1-AMIN1)/2
      SEP2=(AMAX1+AMIN1)/2
      DO 30 INDX=1,64
      SEP(INDX)=SEP1*COEF2(INDX,1)+SEP2
30      CONTINUE

C
C READ THE GAUSSIAN COEFFICIENTS FROM THE DATAFILE GAUSS16.DAT:
C
      OPEN(UNIT=11,FILE='GAUSS16.DAT')
      DO 100 ICTR1=1,16
      DO 110 ICTR2=1,2
      READ(11,6000,END=12)COEF1(ICTR1,ICTR2)
6000      FORMAT(F18.15)
110      CONTINUE
100      CONTINUE
12      CLOSE(UNIT=11)

C
C CALCULATE THE INTEGRATION POINTS FOR ALPHA1:
C
      AMIN=0.0
      AMAX=2.*3.14159265358979323846

      AL11=(AMAX-AMIN)/2.
      AL12=(AMAX+AMIN)/2.
```

```
DO 120 INDX=1,16
  AL1(INDX)=AL11*COEF1(INDX,1)+AL12
120  CONTINUE

C
C CALCULATE THE INTEGRATION POINTS FOR BETA1:
C
  AMIN=0.0
  AMAX=3.14159265358979323846

  BE11=(AMAX-AMIN)/2.
  BE12=(AMAX+AMIN)/2.
  DO 121 INDX=1,16
    BE1(INDX)=BE11*COEF1(INDX,1)+BE12
121  CONTINUE

C
C CALCULATE THE INTEGRATION POINTS FOR GAMMA1:
C
  AMIN=0.0
  AMAX=2.*3.14159265358979323846

  GA11=(AMAX-AMIN)/2.
  GA12=(AMAX+AMIN)/2.
  DO 122 INDX=1,16
    GA1(INDX)=GA11*COEF1(INDX,1)+GA12
122  CONTINUE

C
C CALCULATE THE INTEGRATION POINTS FOR ALPHA2:
C
  AMIN=0.0
  AMAX=2.*3.14159265358979323846

  AL21=(AMAX-AMIN)/2.
  AL22=(AMAX+AMIN)/2.
  DO 123 INDX=1,16
    AL2(INDX)=AL21*COEF1(INDX,1)+AL22
123  CONTINUE

C
C CALCULATE THE INTEGRATION POINTS FOR BETA2:
C
  AMIN=0.0
  AMAX=3.14159265358979323846

  BE21=(AMAX-AMIN)/2.
  BE22=(AMAX+AMIN)/2.
  DO 124 INDX=1,16
```

A.1. FORTRAN PROGRAM TO CALCULATE THE $\gamma_1\alpha_1$ CONTRIBUTION TO B_γ .185

```

      BE2(INDX)=BE21*COEF1(INDX,1)+BE22
124  CONTINUE

C
C CALCULATE THE INTEGRATION POINTS FOR GAMMA2:
C
      AMIN=0.0
      AMAX=2.*3.14159265358979323846

      GA21=(AMAX-AMIN)/2.
      GA22=(AMAX+AMIN)/2.
      DO 125 INDX=1,16
        GA2(INDX)=GA21*COEF1(INDX,1)+GA22
125  CONTINUE

C -----
C MAIN PROGRAM:
C -----

      OPEN(UNIT=4,FILE='ESHGg1a1_D2h_298K')

C
C INPUT MOLECULAR PARAMETERS:
C
      TEMP=298.0
      TEMPK=TEMP*1.380622E-23
      R=0.4232
      PARAM2=190.0
      SHAPE1=0.22965
      SHAPE2=0.21383

C
C CALCULATION OF THE LENNARD-JONES 6:12 POTENTIAL & STORAGE OF THE
C VALUES IN AN ARRAY:
C

      DO 61 X1=1,64

      D1(X1)=4.*PARAM2*1.380622E-23*((R/SEP(X1))**12-(R/SEP(X1))**6)
      SE3(X1)=SEP(X1)**3
      SE4(X1)=SEP(X1)**4
      SE5(X1)=SEP(X1)**5
      SE6(X1)=SEP(X1)**6
      SE8(X1)=SEP(X1)**8
      SE12(X1)=SEP(X1)**12

61  CONTINUE
```

```

C
C THE DIRECTION COSINE TENSOR COMPONENTS ARE STORED IN AN ARRAY:
C

```

```

      DO 66 X4=1,16
        DO 77 X3=1,16
          DO 88 X2=1,16

```

```

C
C DIRECTION COSINE TENSOR COMPONENTS:
C

```

```

      A1=COS(AL1(X2))*COS(BE1(X3))*COS(GA1(X4))-1.*SIN(AL1(X2))*SIN(GA1
+ (X4))
      A2=SIN(AL1(X2))*COS(BE1(X3))*COS(GA1(X4))+COS(AL1(X2))*SIN(GA1(X4
+ ))
      A3=-1.*SIN(BE1(X3))*COS(GA1(X4))
      A4=-1.*COS(AL1(X2))*COS(BE1(X3))*SIN(GA1(X4))-1.*SIN(AL1(X2))*COS
+ (GA1(X4))
      A5=-1.*SIN(AL1(X2))*COS(BE1(X3))*SIN(GA1(X4))+COS(AL1(X2))*COS(GA
+ 1(X4))
      A6=SIN(BE1(X3))*SIN(GA1(X4))
      A7=COS(AL1(X2))*SIN(BE1(X3))
      A8=SIN(AL1(X2))*SIN(BE1(X3))
      A9=COS(BE1(X3))

```

```

      DCTC(1,X2,X3,X4)=A1
      DCTC(2,X2,X3,X4)=A2
      DCTC(3,X2,X3,X4)=A3
      DCTC(4,X2,X3,X4)=A4
      DCTC(5,X2,X3,X4)=A5
      DCTC(6,X2,X3,X4)=A6
      DCTC(7,X2,X3,X4)=A7
      DCTC(8,X2,X3,X4)=A8
      DCTC(9,X2,X3,X4)=A9

```

```

88      CONTINUE
77      CONTINUE
66      CONTINUE

```

```

C
C THE MULTIPOLE INTERACTION ENERGIES ARE CALCULATED AND STORED
C IN ARRAYS:
C

```

```

      DO 939 X7=1,16
        WRITE(4,1000)X7

```

A.1. FORTRAN PROGRAM TO CALCULATE THE $\gamma_1\alpha_1$ CONTRIBUTION TO B_γ .187

```
1000  FORMAT (1X, 'INDEX (IN RANGE 1 TO 16) IS CURRENTLY ',I2 )  
      WRITE(6,1111)X7  
1111  FORMAT (1X, 'Index (in range 1 to 16) is currently ',I2 )  
      DO 40 X6=1,16
```

```
      DO 50 X5=1,16
```

C

C MOLECULE 2'S DIRECTION COSINE TENSOR COMPONENTS:

C

```
B1=DCTC(1,X5,X6,X7)  
B2=DCTC(2,X5,X6,X7)  
B3=DCTC(3,X5,X6,X7)  
B4=DCTC(4,X5,X6,X7)  
B5=DCTC(5,X5,X6,X7)  
B6=DCTC(6,X5,X6,X7)  
B7=DCTC(7,X5,X6,X7)  
B8=DCTC(8,X5,X6,X7)  
B9=DCTC(9,X5,X6,X7)
```

```
      DO 60 X4=1,16  
        DO 70 X3=1,16  
          DO 80 X2=1,16
```

C

C MOLECULE 1'S DIRECTION COSINE TENSOR COMPONENTS:

C

```
A1=DCTC(1,X2,X3,X4)  
A2=DCTC(2,X2,X3,X4)  
A3=DCTC(3,X2,X3,X4)  
A4=DCTC(4,X2,X3,X4)  
A5=DCTC(5,X2,X3,X4)  
A6=DCTC(6,X2,X3,X4)  
A7=DCTC(7,X2,X3,X4)  
A8=DCTC(8,X2,X3,X4)  
A9=DCTC(9,X2,X3,X4)
```

C

C CALCULATION OF THE DIPOLE-DIPOLE POTENTIAL:

C

```
DDP(X2,X3,X4,X5,X6)=8.98758E-24*DIP**2*(-2*A9*B9+A6*B6+A3*B3)
```

C

C CALCULATION OF THE DIPOLE-QUADRUPOLE POTENTIAL:

C

```
DQP(X2,X3,X4,X5,X6)=8.98758E-25*DIP*(Q2*(-2*A9*B9**2+(2*A6*B6+2*A
```

```

+ 3*B3+2*A9**2-2*A8**2-A6**2+A5**2-A3**2+A2**2)*B9+2*A9*B8**2+(-2*A
+ 6*B5-2*A3*B2)*B8+A9*B6**2+(2*A5*A8-2*A6*A9)*B6-A9*B5**2+A9*B3**2+
+ (2*A2*A8-2*A3*A9)*B3-A9*B2**2)+Q1*(-2*A9*B9**2+(2*A6*B6+2*A3*B3+2
+ *A9**2-2*A7**2-A6**2+A4**2-A3**2+A1**2)*B9+2*A9*B7**2+(-2*A6*B4-2
+ *A3*B1)*B7+A9*B6**2+(2*A4*A7-2*A6*A9)*B6-A9*B4**2+A9*B3**2+(2*A1*
+ A7-2*A3*A9)*B3-A9*B1**2))

```

C

C CALCULATION OF THE DIPOLE-INDUCED DIPOLE POTENTIAL:

C

```

DIDP(X2,X3,X4,X5,X6)=-0.50*ALSTAT*8.07765E-27*DIP**2*(3*B9**2
+ +3*A9**2-2)

```

C

C CALCULATION OF THE QUADRUPOLE-QUADRUPOLE POTENTIAL:

C

```

QUAD1=-16.*(A6*A9-A5*A8)*(B6*B9-B5*B8)-16.*(A3*A9-A2*A8)*(B3*B9-B
+ 2*B8)+4.*(2.*A9**2-2.*A8**2-A6**2+A5**2-A3**2+A2**2)*(B9-B8)*(B9+
+ B8)+(-4.*A9**2+4.*A8**2+3.*A6**2-3.*A5**2+A3**2-A2**2)*(B6**2-B5*
+ *2)+4.*(A3*A6-A2*A5)*(B3*B6-B2*B5)+(-4.*A9**2+4.*A8**2+A6**2-A5**
+ 2+3.*A3**2-3.*A2**2)*(B3**2-B2**2)

```

```

QUAD2=-16.*(A6*A9-A4*A7)*(B6*B9-B4*B7)-16.*(A3*A9-A1*A7)*(B3*B9-B
+ 1*B7)+4.*(2.*A9**2-2.*A7**2-A6**2+A4**2-A3**2+A1**2)*(B9-B7)*(B9+
+ B7)+(-4.*A9**2+4.*A7**2+3.*A6**2-3.*A4**2+A3**2-A1**2)*(B6**2-B4*
+ *2)+4.*(A3*A6-A1*A4)*(B3*B6-B1*B4)+(-4.*A9**2+4.*A7**2+A6**2-A4**
+ 2+3.*A3**2-3.*A1**2)*(B3**2-B1**2)

```

```

QUAD3=4.*(4.*A9**2-2.*(A8**2+A7**2+A6**2+A3**2)+A5**2+A4**2+A2**2
+ +A1**2)*B9**2-16.*(2.*A6*A9-A5*A8-A4*A7)*B6*B9-16*(2.*A3*A9-A2*A8
+ -A1*A7)*B3*B9-4.*(2.*A9**2-2.*A7**2-A6**2+A4**2-A3**2+A1**2)*B8**
+ 2+16.*(A6*A9-A4*A7)*B5*B8+16.*(A3*A9-A1*A7)*B2*B8-4.*(2.*A9**2-2.
+ *A8**2-A6**2+A5**2-A3**2+A2**2)*B7**2+16.*(A6*A9-A5*A8)*B4*B7+16.
+ *(A3*A9-A2*A8)*B1*B7+(-8.*A9**2+4.*(A8**2+A7**2)+6.*A6**2-3.*(A5*
+ *2+A4**2)+2*A3**2-A2**2-A1**2)*B6**2+4.*(2.*A3*A6-A2*A5-A1*A4)*B3
+ *B6+(4.*A9**2-4.*A7**2-3.*A6**2+3.*A4**2-A3**2+A1**2)*B5**2-4.*(A
+ 3*A6-A1*A4)*B2*B5+(4.*A9**2-4.*A8**2-3.*A6**2+3.*A5**2-A3**2+A2**
+ 2)*B4**2-4.*(A3*A6-A2*A5)*B1*B4+(-8.*A9**2+4.*(A8**2+A7**2)+2.*A6
+ **2-A5**2-A4**2+6.*A3**2-3.*(A2**2+A1**2))*B3**2+(4.*A9**2-4.*A7*
+ *2-A6**2+A4**2-3.*A3**2+3.*A1**2)*B2**2+(4.*A9**2-4.*A8**2-A6**2+
+ A5**2-3.*A3**2+3.*A2**2)*B1**2

```

```

E1(X2,X3,X4,X5,X6)=8.98758E-26*(1./3.)*(Q2**2*QUAD1+Q1**2*QUAD
+ 2+Q1*Q2*QUAD3)

```

C

C CALCULATION OF THE QUADRUPOLE-INDUCED DIPOLE POTENTIAL:

C

A.1. FORTRAN PROGRAM TO CALCULATE THE $\gamma_1\alpha_1$ CONTRIBUTION TO B_γ .189

```

QID1=Q2**2*(4.*A9**4+(-8.*A8**2+4.*A5**2+4.*A2**2)*A9**2+(-8.*A5*
+ A6-8.*A2*A3)*A8*A9+4.*A8**4+(4.*A6**2+4.*A3**2)*A8**2+A6**4+(-2.*
+ A5**2+2.*A3**2-2.*A2**2)*A6**2+A5**4+(2.*A2**2-2.*A3**2)*A5**2+A3
+ **4-2.*A2**2*A3**2+A2**4)+Q1**2*(4.*A9**4+(-8.*A7**2+4.*A4**2+4.*
+ A1**2)*A9**2+(-8.*A4*A6-8.*A1*A3)*A7*A9+4.*A7**4+(4.*A6**2+4.*A3*
+ *2)*A7**2+A6**4+(-2.*A4**2+2.*A3**2-2.*A1**2)*A6**2+A4**4+(2.*A1*
+ *2-2.*A3**2)*A4**2+A3**4-2.*A1**2*A3**2+A1**4)+Q1*Q2*(8.*A9**4+(-
+ 8.*A8**2-8.*A7**2+4.*A5**2+4.*A4**2+4.*A2**2+4.*A1**2)*A9**2+((-8
+ .*A5*A6-8.*A2*A3)*A8+(-8.*A4*A6-8.*A1*A3)*A7)*A9+(8.*A7**2+4.*A6*
+ *2-4.*A4**2+4.*A3**2-4.*A1**2)*A8**2+(8.*A4*A5+8.*A1*A2)*A7*A8+(4
+ .*A6**2-4.*A5**2+4.*A3**2-4.*A2**2)*A7**2+2.*A6**4+(-2.*A5**2-2.*
+ A4**2+4.*A3**2-2.*A2**2-2.*A1**2)*A6**2+(2.*A4**2-2.*A3**2+2.*A1*
+ *2)*A5**2+(2.*A2**2-2.*A3**2)*A4**2+2.*A3**4+(-2.*A2**2-2.*A1**2)
+ *A3**2+2.*A1**2*A2**2)

```

```

QID2=Q2**2*(4.*B9**4+(-8.*B8**2+4.*B5**2+4.*B2**2)*B9**2+(-8.*B5*
+ B6-8.*B2*B3)*B8*B9+4.*B8**4+(4.*B6**2+4.*B3**2)*B8**2+B6**4+(-2.*
+ B5**2+2.*B3**2-2.*B2**2)*B6**2+B5**4+(2.*B2**2-2.*B3**2)*B5**2+B3
+ **4-2.*B2**2*B3**2+B2**4)+Q1**2*(4.*B9**4+(-8.*B7**2+4.*B4**2+4.*
+ B1**2)*B9**2+(-8.*B4*B6-8.*B1*B3)*B7*B9+4.*B7**4+(4.*B6**2+4.*B3*
+ *2)*B7**2+B6**4+(-2.*B4**2+2.*B3**2-2.*B1**2)*B6**2+B4**4+(2.*B1*
+ *2-2.*B3**2)*B4**2+B3**4-2.*B1**2*B3**2+B1**4)+Q1*Q2*(8.*B9**4+(-
+ 8.*B8**2-8.*B7**2+4.*B5**2+4.*B4**2+4.*B2**2+4.*B1**2)*B9**2+((-8
+ .*B5*B6-8.*B2*B3)*B8+(-8.*B4*B6-8.*B1*B3)*B7)*B9+(8.*B7**2+4.*B6*
+ *2-4.*B4**2+4.*B3**2-4.*B1**2)*B8**2+(8.*B4*B5+8.*B1*B2)*B7*B8+(4
+ .*B6**2-4.*B5**2+4.*B3**2-4.*B2**2)*B7**2+2.*B6**4+(-2.*B5**2-2.*
+ B4**2+4.*B3**2-2.*B2**2-2.*B1**2)*B6**2+(2.*B4**2-2.*B3**2+2.*B1*
+ *2)*B5**2+(2.*B2**2-2.*B3**2)*B4**2+2.*B3**4+(-2.*B2**2-2.*B1**2)
+ *B3**2+2.*B1**2*B2**2)

```

F1(X2,X3,X4,X5,X6)=-0.5*8.07765E-29*ALSTAT*(QID1+QID2)

C

C CALCULATION OF THE INTEGRATION ARGUMENT:

C

```

T11=2.*A7**2-A4**2-A1**2
T22=2.*A8**2-A5**2-A2**2
T33=2.*A9**2-A6**2-A3**2
T12=2.*A7*A8-A4*A5-A1*A2
T13=2.*A7*A9-A4*A6-A1*A3
T23=2.*A8*A9-A5*A6-A2*A3

```

```

Z11 = A33*(A7**2*B9**2+(2*A4*A7*B6+2*A1*A7*B3)*B9+A4**2*B6**2+2*A
+ 1*A4*B3*B6+A1**2*B3**2)+A22*(A7**2*B8**2+(2*A4*A7*B5+2*A1*A7*B2
+ )*B8+A4**2*B5**2+2*A1*A4*B2*B5+A1**2*B2**2)+A11*(A7**2*B7**2+(2
+ *A4*A7*B4+2*A1*A7*B1)*B7+A4**2*B4**2+2*A1*A4*B1*B4+A1**2*B1**2)

```

```

Z22 = A33*(A8**2*B9**2+(2*A5*A8*B6+2*A2*A8*B3)*B9+A5**2*B6**2+2*A

```

$$\begin{aligned}
& + 2*A5*B3*B6+A2**2*B3**2)+A22*(A8**2*B8**2+(2*A5*A8*B5+2*A2*A8*B2 \\
& +)*B8+A5**2*B5**2+2*A2*A5*B2*B5+A2**2*B2**2)+A11*(A8**2*B7**2+(2 \\
& + *A5*A8*B4+2*A2*A8*B1)*B7+A5**2*B4**2+2*A2*A5*B1*B4+A2**2*B1**2)
\end{aligned}$$

$$\begin{aligned}
Z33 = & A33*(A9**2*B9**2+(2*A6*A9*B6+2*A3*A9*B3)*B9+A6**2*B6**2+2*A \\
& + 3*A6*B3*B6+A3**2*B3**2)+A22*(A9**2*B8**2+(2*A6*A9*B5+2*A3*A9*B2 \\
& +)*B8+A6**2*B5**2+2*A3*A6*B2*B5+A3**2*B2**2)+A11*(A9**2*B7**2+(2 \\
& + *A6*A9*B4+2*A3*A9*B1)*B7+A6**2*B4**2+2*A3*A6*B1*B4+A3**2*B1**2)
\end{aligned}$$

$$\begin{aligned}
Z12 = & A33*(A7*A8*B9**2+((A4*A8+A5*A7)*B6+(A1*A8+A2*A7)*B3)*B9+A4* \\
& + A5*B6**2+(A1*A5+A2*A4)*B3*B6+A1*A2*B3**2)+A22*(A7*A8*B8**2+((A4 \\
& + *A8+A5*A7)*B5+(A1*A8+A2*A7)*B2)*B8+A4*A5*B5**2+(A1*A5+A2*A4)*B2 \\
& + *B5+A1*A2*B2**2)+A11*(A7*A8*B7**2+((A4*A8+A5*A7)*B4+(A1*A8+A2*A \\
& + 7)*B1)*B7+A4*A5*B4**2+(A1*A5+A2*A4)*B1*B4+A1*A2*B1**2)
\end{aligned}$$

$$\begin{aligned}
Z13 = & A33*(A7*A9*B9**2+((A4*A9+A6*A7)*B6+(A1*A9+A3*A7)*B3)*B9+A4* \\
& + A6*B6**2+(A1*A6+A3*A4)*B3*B6+A1*A3*B3**2)+A22*(A7*A9*B8**2+((A4 \\
& + *A9+A6*A7)*B5+(A1*A9+A3*A7)*B2)*B8+A4*A6*B5**2+(A1*A6+A3*A4)*B2 \\
& + *B5+A1*A3*B2**2)+A11*(A7*A9*B7**2+((A4*A9+A6*A7)*B4+(A1*A9+A3*A \\
& + 7)*B1)*B7+A4*A6*B4**2+(A1*A6+A3*A4)*B1*B4+A1*A3*B1**2)
\end{aligned}$$

$$\begin{aligned}
Z23 = & A33*(A8*A9*B9**2+((A5*A9+A6*A8)*B6+(A2*A9+A3*A8)*B3)*B9+A5* \\
& + A6*B6**2+(A2*A6+A3*A5)*B3*B6+A2*A3*B3**2)+A22*(A8*A9*B8**2+((A5 \\
& + *A9+A6*A8)*B5+(A2*A9+A3*A8)*B2)*B8+A5*A6*B5**2+(A2*A6+A3*A5)*B2 \\
& + *B5+A2*A3*B2**2)+A11*(A8*A9*B7**2+((A5*A9+A6*A8)*B4+(A2*A9+A3*A \\
& + 8)*B1)*B7+A5*A6*B4**2+(A2*A6+A3*A5)*B1*B4+A2*A3*B1**2)
\end{aligned}$$

$$\begin{aligned}
Y11 = & B33*(A7**2*B9**2+(2*A4*A7*B6+2*A1*A7*B3)*B9+A4**2*B6**2+2*A \\
& + 1*A4*B3*B6+A1**2*B3**2)+B22*(A7**2*B8**2+(2*A4*A7*B5+2*A1*A7*B2 \\
& +)*B8+A4**2*B5**2+2*A1*A4*B2*B5+A1**2*B2**2)+B11*(A7**2*B7**2+(2 \\
& + *A4*A7*B4+2*A1*A7*B1)*B7+A4**2*B4**2+2*A1*A4*B1*B4+A1**2*B1**2)
\end{aligned}$$

$$\begin{aligned}
Y22 = & B33*(A8**2*B9**2+(2*A5*A8*B6+2*A2*A8*B3)*B9+A5**2*B6**2+2*A \\
& + 2*A5*B3*B6+A2**2*B3**2)+B22*(A8**2*B8**2+(2*A5*A8*B5+2*A2*A8*B2 \\
& +)*B8+A5**2*B5**2+2*A2*A5*B2*B5+A2**2*B2**2)+B11*(A8**2*B7**2+(2 \\
& + *A5*A8*B4+2*A2*A8*B1)*B7+A5**2*B4**2+2*A2*A5*B1*B4+A2**2*B1**2)
\end{aligned}$$

$$\begin{aligned}
Y33 = & B33*(A9**2*B9**2+(2*A6*A9*B6+2*A3*A9*B3)*B9+A6**2*B6**2+2*A \\
& + 3*A6*B3*B6+A3**2*B3**2)+B22*(A9**2*B8**2+(2*A6*A9*B5+2*A3*A9*B2 \\
& +)*B8+A6**2*B5**2+2*A3*A6*B2*B5+A3**2*B2**2)+B11*(A9**2*B7**2+(2 \\
& + *A6*A9*B4+2*A3*A9*B1)*B7+A6**2*B4**2+2*A3*A6*B1*B4+A3**2*B1**2)
\end{aligned}$$

$$\begin{aligned}
Y12 = & B33*(A7*A8*B9**2+((A4*A8+A5*A7)*B6+(A1*A8+A2*A7)*B3)*B9+A4* \\
& + A5*B6**2+(A1*A5+A2*A4)*B3*B6+A1*A2*B3**2)+B22*(A7*A8*B8**2+((A4 \\
& + *A8+A5*A7)*B5+(A1*A8+A2*A7)*B2)*B8+A4*A5*B5**2+(A1*A5+A2*A4)*B2 \\
& + *B5+A1*A2*B2**2)+B11*(A7*A8*B7**2+((A4*A8+A5*A7)*B4+(A1*A8+A2*A \\
& + 7)*B1)*B7+A4*A5*B4**2+(A1*A5+A2*A4)*B1*B4+A1*A2*B1**2)
\end{aligned}$$

A.1. FORTRAN PROGRAM TO CALCULATE THE $\gamma_1\alpha_1$ CONTRIBUTION TO B_γ .191

```

Y13 = B33*(A7*A9*B9**2+((A4*A9+A6*A7)*B6+(A1*A9+A3*A7)*B3)*B9+A4*
+ A6*B6**2+(A1*A6+A3*A4)*B3*B6+A1*A3*B3**2)+B22*(A7*A9*B8**2+((A4
+ *A9+A6*A7)*B5+(A1*A9+A3*A7)*B2)*B8+A4*A6*B5**2+(A1*A6+A3*A4)*B2
+ *B5+A1*A3*B2**2)+B11*(A7*A9*B7**2+((A4*A9+A6*A7)*B4+(A1*A9+A3*A
+ 7)*B1)*B7+A4*A6*B4**2+(A1*A6+A3*A4)*B1*B4+A1*A3*B1**2)

```

```

Y23 = B33*(A8*A9*B9**2+((A5*A9+A6*A8)*B6+(A2*A9+A3*A8)*B3)*B9+A5*
+ A6*B6**2+(A2*A6+A3*A5)*B3*B6+A2*A3*B3**2)+B22*(A8*A9*B8**2+((A5
+ *A9+A6*A8)*B5+(A2*A9+A3*A8)*B2)*B8+A5*A6*B5**2+(A2*A6+A3*A5)*B2
+ *B5+A2*A3*B2**2)+B11*(A8*A9*B7**2+((A5*A9+A6*A8)*B4+(A2*A9+A3*A
+ 8)*B1)*B7+A5*A6*B4**2+(A2*A6+A3*A5)*B1*B4+A2*A3*B1**2)

```

```

W11 = V33*(A7**2*B9**2+(2*A4*A7*B6+2*A1*A7*B3)*B9+A4**2*B6**2+2*A
+ 1*A4*B3*B6+A1**2*B3**2)+V22*(A7**2*B8**2+(2*A4*A7*B5+2*A1*A7*B2
+ )*B8+A4**2*B5**2+2*A1*A4*B2*B5+A1**2*B2**2)+V11*(A7**2*B7**2+(2
+ *A4*A7*B4+2*A1*A7*B1)*B7+A4**2*B4**2+2*A1*A4*B1*B4+A1**2*B1**2)

```

```

W22 = V33*(A8**2*B9**2+(2*A5*A8*B6+2*A2*A8*B3)*B9+A5**2*B6**2+2*A
+ 2*A5*B3*B6+A2**2*B3**2)+V22*(A8**2*B8**2+(2*A5*A8*B5+2*A2*A8*B2
+ )*B8+A5**2*B5**2+2*A2*A5*B2*B5+A2**2*B2**2)+V11*(A8**2*B7**2+(2
+ *A5*A8*B4+2*A2*A8*B1)*B7+A5**2*B4**2+2*A2*A5*B1*B4+A2**2*B1**2)

```

```

W33 = V33*(A9**2*B9**2+(2*A6*A9*B6+2*A3*A9*B3)*B9+A6**2*B6**2+2*A
+ 3*A6*B3*B6+A3**2*B3**2)+V22*(A9**2*B8**2+(2*A6*A9*B5+2*A3*A9*B2
+ )*B8+A6**2*B5**2+2*A3*A6*B2*B5+A3**2*B2**2)+V11*(A9**2*B7**2+(2
+ *A6*A9*B4+2*A3*A9*B1)*B7+A6**2*B4**2+2*A3*A6*B1*B4+A3**2*B1**2)

```

```

W12 = V33*(A7*A8*B9**2+((A4*A8+A5*A7)*B6+(A1*A8+A2*A7)*B3)*B9+A4*
+ A5*B6**2+(A1*A5+A2*A4)*B3*B6+A1*A2*B3**2)+V22*(A7*A8*B8**2+((A4
+ *A8+A5*A7)*B5+(A1*A8+A2*A7)*B2)*B8+A4*A5*B5**2+(A1*A5+A2*A4)*B2
+ *B5+A1*A2*B2**2)+V11*(A7*A8*B7**2+((A4*A8+A5*A7)*B4+(A1*A8+A2*A
+ 7)*B1)*B7+A4*A5*B4**2+(A1*A5+A2*A4)*B1*B4+A1*A2*B1**2)

```

```

W13 = V33*(A7*A9*B9**2+((A4*A9+A6*A7)*B6+(A1*A9+A3*A7)*B3)*B9+A4*
+ A6*B6**2+(A1*A6+A3*A4)*B3*B6+A1*A3*B3**2)+V22*(A7*A9*B8**2+((A4
+ *A9+A6*A7)*B5+(A1*A9+A3*A7)*B2)*B8+A4*A6*B5**2+(A1*A6+A3*A4)*B2
+ *B5+A1*A3*B2**2)+V11*(A7*A9*B7**2+((A4*A9+A6*A7)*B4+(A1*A9+A3*A
+ 7)*B1)*B7+A4*A6*B4**2+(A1*A6+A3*A4)*B1*B4+A1*A3*B1**2)

```

```

W23 = V33*(A8*A9*B9**2+((A5*A9+A6*A8)*B6+(A2*A9+A3*A8)*B3)*B9+A5*
+ A6*B6**2+(A2*A6+A3*A5)*B3*B6+A2*A3*B3**2)+V22*(A8*A9*B8**2+((A5
+ *A9+A6*A8)*B5+(A2*A9+A3*A8)*B2)*B8+A5*A6*B5**2+(A2*A6+A3*A5)*B2
+ *B5+A2*A3*B2**2)+V11*(A8*A9*B7**2+((A5*A9+A6*A8)*B4+(A2*A9+A3*A
+ 8)*B1)*B7+A5*A6*B4**2+(A2*A6+A3*A5)*B1*B4+A2*A3*B1**2)

```

C NB ... checked against D_ooH for CO2, passed check!
 C These are the G1A1 terms (tensors evaluated in Macsyma,
 C translated directly into Fortran code):
 C

```
D513 = G3333*T33*W33+G2233*T33*W33+G1133*T33*W33+G3333*T23*W23+G
1  3322*T23*W23+G2233*T23*W23+G2222*T23*W23+G1133*T23*W23+G1122*
2  T23*W23+G3322*T22*W22+G2222*T22*W22+G1122*T22*W22+G3333*T13*W
3  13+G3311*T13*W13+G2233*T13*W13+G2211*T13*W13+G1133*T13*W13+G1
4  111*T13*W13+G3322*T12*W12+G3311*T12*W12+G2222*T12*W12+G2211*T
5  12*W12+G1122*T12*W12+G1111*T12*W12+G3311*T11*W11+G2211*T11*W1
6  1+G1111*T11*W11
```

```
D521 = G3333*T33*W33+G3223*T33*W33+G3113*T33*W33+G3333*T23*W23+G
1  3223*T23*W23+G3113*T23*W23+G2332*T23*W23+G2222*T23*W23+G2112*
2  T23*W23+G2332*T22*W22+G2222*T22*W22+G2112*T22*W22+G3333*T13*W
3  13+G3223*T13*W13+G3113*T13*W13+G1331*T13*W13+G1221*T13*W13+G1
4  111*T13*W13+G2332*T12*W12+G2222*T12*W12+G2112*T12*W12+G1331*T
5  12*W12+G1221*T12*W12+G1111*T12*W12+G1331*T11*W11+G1221*T11*W1
6  1+G1111*T11*W11
```

```
D526 = G3333*T33*Z33+G2233*T33*Z33+G1133*T33*Z33+G3333*T23*Z23+G
1  3322*T23*Z23+G2233*T23*Z23+G2222*T23*Z23+G1133*T23*Z23+G1122*
2  T23*Z23+G3322*T22*Z22+G2222*T22*Z22+G1122*T22*Z22+G3333*T13*Z
3  13+G3311*T13*Z13+G2233*T13*Z13+G2211*T13*Z13+G1133*T13*Z13+G1
4  111*T13*Z13+G3322*T12*Z12+G3311*T12*Z12+G2222*T12*Z12+G2211*T
5  12*Z12+G1122*T12*Z12+G1111*T12*Z12+G3311*T11*Z11+G2211*T11*Z1
6  1+G1111*T11*Z11
```

```
D529 = G3333*T33*Z33+G3322*T33*Z33+G3311*T33*Z33+G3333*T23*Z23+G
1  3322*T23*Z23+G3311*T23*Z23+G2233*T23*Z23+G2222*T23*Z23+G2211*
2  T23*Z23+G2233*T22*Z22+G2222*T22*Z22+G2211*T22*Z22+G3333*T13*Z
3  13+G3322*T13*Z13+G3311*T13*Z13+G1133*T13*Z13+G1122*T13*Z13+G1
4  111*T13*Z13+G2233*T12*Z12+G2222*T12*Z12+G2211*T12*Z12+G1133*T
5  12*Z12+G1122*T12*Z12+G1111*T12*Z12+G1133*T11*Z11+G1122*T11*Z1
6  1+G1111*T11*Z11
```

```
D532 = G3333*T33*Z33+G2332*T33*Z33+G1331*T33*Z33+G3333*T23*Z23+G
1  3223*T23*Z23+G2332*T23*Z23+G2222*T23*Z23+G1331*T23*Z23+G1221*
2  T23*Z23+G3223*T22*Z22+G2222*T22*Z22+G1221*T22*Z22+G3333*T13*Z
3  13+G3113*T13*Z13+G2332*T13*Z13+G2112*T13*Z13+G1331*T13*Z13+G1
4  111*T13*Z13+G3223*T12*Z12+G3113*T12*Z12+G2222*T12*Z12+G2112*T
5  12*Z12+G1221*T12*Z12+G1111*T12*Z12+G3113*T11*Z11+G2112*T11*Z1
6  1+G1111*T11*Z11
```

```
D535 = G3333*T33*Y33+G3322*T33*Y33+G3311*T33*Y33+G3333*T23*Y23+G
1  3322*T23*Y23+G3311*T23*Y23+G2233*T23*Y23+G2222*T23*Y23+G2211*
2  T23*Y23+G2233*T22*Y22+G2222*T22*Y22+G2211*T22*Y22+G3333*T13*Y
3  13+G3322*T13*Y13+G3311*T13*Y13+G1133*T13*Y13+G1122*T13*Y13+G1
```

A.1. FORTRAN PROGRAM TO CALCULATE THE $\gamma_1\alpha_1$ CONTRIBUTION TO B_γ .193

```

4  111*T13*Y13+G2233*T12*Y12+G2222*T12*Y12+G2211*T12*Y12+G1133*T
5  12*Y12+G1122*T12*Y12+G1111*T12*Y12+G1133*T11*Y11+G1122*T11*Y1
6  1+G1111*T11*Y11

```

```

D542 = G3333*T33*Y33+G3223*T33*Y33+G3113*T33*Y33+G3333*T23*Y23+G
1  3223*T23*Y23+G3113*T23*Y23+G2332*T23*Y23+G2222*T23*Y23+G2112*
2  T23*Y23+G2332*T22*Y22+G2222*T22*Y22+G2112*T22*Y22+G3333*T13*Y
3  13+G3223*T13*Y13+G3113*T13*Y13+G1331*T13*Y13+G1221*T13*Y13+G1
4  111*T13*Y13+G2332*T12*Y12+G2222*T12*Y12+G2112*T12*Y12+G1331*T
5  12*Y12+G1221*T12*Y12+G1111*T12*Y12+G1331*T11*Y11+G1221*T11*Y1
6  1+G1111*T11*Y11

```

```

TERM = (d513+d526+d529+d532+d535)+(d521+d542)/2.0

```

C The integration argument:

```

FI(X2,X3,X4,X5,X6)=(1/(120.*3.14159265358979323846**3))*(SI
+ N(BE1(X3))*SIN(BE2(X6)))*TERM

```

C

C CALCULATION OF THE SHAPE POTENTIAL:

C

```

G1(X3,X4,X6)=4.*PARAM2*1.380622E-23*R**12*(SHAPE1*(3.*COS(BE1(X3)
+ )**2+3.*COS(BE2(X6))**2-2.))+SHAPE2*(3.*COS(GA1(X4))**2*SIN(BE1(X3
+ )**2+3.*COS(GA2(X7))**2*SIN(BE2(X6))**2-2.))

```

```

80          CONTINUE

```

```

70          CONTINUE

```

```

60          CONTINUE

```

```

50          CONTINUE

```

```

40          CONTINUE

```

C

C THE INTEGRAL IS CALCULATED:

C

```

SS6=0.00
DO 940 X6=1,16
  SS5=0.00
  DO 950 X5=1,16
    SS4=0.00
    DO 960 X4=1,16
      SS3=0.00
      DO 970 X3=1,16
        SS2=0.00

```

```

DO 980 X2=1,16
  SS1=0.00
DO 990 X1=1,64

```

C

C SUMMATION OF THE ENERGY TERMS WITH SUBSEQUENT DIVISION BY (-kT):

C

```

G3=-1.*(D1(X1)+E1(X2,X3,X4,X5,X6)/SE5(X1)+F1(X2,X3,X4,X5,X6)/SE8(
+ X1)+G1(X3,X4,X6)/SE12(X1)+DDP(X2,X3,X4,X5,X6)/SE3(X1)+DIDP(X2,X3,
+ X4,X5,X6)/SE6(X1)+DQP(X2,X3,X4,X5,X6)/SE4(X1))/TEMPK

```

```

IF(G3.LT.-85) GO TO 5000

```

```

G4=2.71828**G3

```

```

GO TO 5010

```

```

5000 G4=0

```

```

5010 SS1=SS1+(FI(X2,X3,X4,X5,X6)/SEP(X1))*G4*COEF2(X1,2)

```

```

990 CONTINUE

```

```

SS2=SS2+SS1*COEF1(X2,2)

```

```

980 CONTINUE

```

```

SS3=SS3+SS2*COEF1(X3,2)

```

```

970 CONTINUE

```

```

SS4=SS4+SS3*COEF1(X4,2)

```

```

960 CONTINUE

```

```

SS5=SS5+SS4*COEF1(X5,2)

```

```

950 CONTINUE

```

```

SS6=SS6+SS5*COEF1(X6,2)

```

```

940 CONTINUE

```

```

SS7=SS7+SS6*COEF1(X7,2)

```

```

939 CONTINUE

```

```

ANS=SS7*SEP1*AL11*BE11*GA11*AL21*BE21*GA21*1.E-68*6.022141*
+ 8.98755

```

C

C THE INTEGRAL IS PRINTED TOGETHER WITH MOLECULAR DATA USED

C

```

WRITE(4,2266)

```

```

2266 FORMAT(1X,'THE G1A1 TERM CONTRIBUTION TO B(ESHG) FOR C2H4')

```

```

WRITE(4,2268)

```

```

2268 FORMAT(1X,'AT THE WAVELENGTH 514.5 nm')

```

A.1. FORTRAN PROGRAM TO CALCULATE THE $\gamma_1\alpha_1$ CONTRIBUTION TO B_γ .195

```

WRITE(4,2267)
2267  FORMAT(1X,'  ')
WRITE(4,2269)
2269  FORMAT(1X,'  ')
WRITE(4,1140)ANS
1140  FORMAT(1X,'THE INTEGRAL IS',E15.7)
WRITE(4,2150)
2150  FORMAT(1X,'INPUT DATA:  ')
WRITE(4,2155)TEMP
2155  FORMAT(1X,'TEMPERATURE:           ',F10.5)
WRITE(4,2156)DIP
2156  FORMAT(1X,'DIPOLE MOMENT:         ',F10.5)

WRITE(4,2911)ALDYN
2911  FORMAT(1X,'MEAN ALPHA(-w;w):      ',F10.5)
WRITE(4,2912)A11
2912  FORMAT(1X,'ALPHA11(-w;w):        ',F10.5)
WRITE(4,2913)A22
2913  FORMAT(1X,'ALPHA22(-w;w):        ',F10.5)
WRITE(4,2914)A33
2914  FORMAT(1X,'ALPHA33(-w;w):        ',F10.5)

WRITE(4,2921)ALDYN
2921  FORMAT(1X,'MEAN ALPHA(-2w;2w):   ',F10.5)
WRITE(4,2922)A11
2922  FORMAT(1X,'ALPHA11(-2w;2w):       ',F10.5)
WRITE(4,2923)A22
2923  FORMAT(1X,'ALPHA22(-2w;2w):       ',F10.5)
WRITE(4,2924)A33
2924  FORMAT(1X,'ALPHA33(-2w;2w):       ',F10.5)

WRITE(4,2160)ALSTAT
2160  FORMAT(1X,'MEAN ALPHA(0;0):       ',F10.5)
WRITE(4,2161)V11
2161  FORMAT(1X,'ALPHA11(0;0):          ',F10.5)
WRITE(4,2162)V22
2162  FORMAT(1X,'ALPHA22(0;0):          ',F10.5)
WRITE(4,2163)V33
2163  FORMAT(1X,'ALPHA33(0;0):          ',F10.5)

WRITE(4,2992)G1111
2992  FORMAT(1X,'DYNAMIC GAMMA1111(-2w;w,w,0): ',F10.5)
WRITE(4,2993)G2222
2993  FORMAT(1X,'DYNAMIC GAMMA2222(-2w;w,w,0): ',F10.5)
WRITE(4,2994)G3333
2994  FORMAT(1X,'DYNAMIC GAMMA3333(-2w;w,w,0): ',F10.5)
WRITE(4,2995)G1122
2995  FORMAT(1X,'DYNAMIC GAMMA1122(-2w;w,w,0): ',F10.5)
WRITE(4,2996)G2211

```

```

2996  FORMAT(1X, 'DYNAMIC GAMMA2211(-2w;w,w,0):      ',F10.5)
      WRITE(4,2997)G1221
2997  FORMAT(1X, 'DYNAMIC GAMMA1221(-2w;w,w,0):      ',F10.5)
      WRITE(4,2998)G2112
2998  FORMAT(1X, 'DYNAMIC GAMMA2112(-2w;w,w,0):      ',F10.5)
      WRITE(4,2999)G1133
2999  FORMAT(1X, 'DYNAMIC GAMMA1133(-2w;w,w,0):      ',F10.5)
      WRITE(4,3000)G3311
3000  FORMAT(1X, 'DYNAMIC GAMMA3311(-2w;w,w,0):      ',F10.5)
      WRITE(4,3001)G1331
3001  FORMAT(1X, 'DYNAMIC GAMMA1331(-2w;w,w,0):      ',F10.5)
      WRITE(4,3002)G3113
3002  FORMAT(1X, 'DYNAMIC GAMMA3113(-2w;w,w,0):      ',F10.5)
      WRITE(4,3003)G2233
3003  FORMAT(1X, 'DYNAMIC GAMMA2233(-2w;w,w,0):      ',F10.5)
      WRITE(4,3004)G3322
3004  FORMAT(1X, 'DYNAMIC GAMMA3322(-2w;w,w,0):      ',F10.5)
      WRITE(4,3005)G2332
3005  FORMAT(1X, 'DYNAMIC GAMMA2332(-2w;w,w,0):      ',F10.5)
      WRITE(4,3006)G3223
3006  FORMAT(1X, 'DYNAMIC GAMMA3223(-2w;w,w,0):      ',F10.5)

      WRITE(4,2190)Q1
2190  FORMAT(1X, 'THETA11:                          ',F10.5)
      WRITE(4,2241)Q2
2241  FORMAT(1X, 'THETA22:                          ',F10.5)
      WRITE(4,2210)R
2210  FORMAT(1X, 'R(0):                              ',F10.5)
      WRITE(4,2220)SHAPE1
2220  FORMAT(1X, 'SHAPE FACTOR 1:                    ',F10.5)
      WRITE(4,2221)SHAPE2
2221  FORMAT(1X, 'SHAPE FACTOR 2:                    ',F10.5)
      WRITE(4,2230)PARAM2
2230  FORMAT(1X, 'E/K:                              ',F10.5)
      WRITE(4,2235)AMIN1,AMAX1
2235  FORMAT(1X, 'MIN AND MAX POINTS OF RANGE:',2(F10.5,3X))
      WRITE(4,2240)
2240  FORMAT(1X, 'END B_eshg')
      WRITE(4,2261)
2261  FORMAT(1X, '  ')

      close(unit=4)
      END

```

Bibliography

1. M. Göppert-Mayer, “Über elementarakte mit zwei quantensprüngen,” *Ann. Phys.*, **9**, 273–294 (1931).
2. W. Kaiser and C. G. B. Garrett, “Two-photon excitation in $\text{CaF}_2:\text{Eu}^{2+}$,” *Phys. Rev. Lett.*, **7**, 229–231 (1961).
3. P. A. Franken, A. E. Hill, C. W. Peters, and G. Weinreich, “Generation of optical harmonics,” *Phys. Rev. Lett.*, **7**, 118–119 (1961).
4. P. Norman and K. Ruud, “Microscopic Theory of Nonlinear Optics,” in “Non-Linear Optical Properties of Matter,” vol. 1, M. G. Papadopoulos, A. J. Sadlej, and J. Leszczynski, eds. (Springer, Dordrecht, 2006), chap. 1, pp. 1–49.
5. P. Norman, K. Ruud, and T. Saue, *Principles and Practices of Molecular Properties: Theory, Modeling, and Simulations* (John Wiley & Sons, 2018).
6. R. W. Boyd, *Nonlinear Optics* (Elsevier, New York, 2020), 4th ed.
7. N. Bloembergen, *Nonlinear Optics* (Benjamin, New York, 1965).
8. “The Nobel Prize in Physics 1981 — nobelprize.org,” <https://www.nobelprize.org/prizes/physics/1981/ceremony-speech/>. [Accessed 06-12-2024].
9. P. A. Franken and J. F. Ward, “Optical harmonics and nonlinear phenomena,” *Rev. Mod. Phys.*, **35**, 23–39 (1963).

10. R. W. Terhune, P. D. Maker, and C. M. Savage, "Optical harmonic generation in calcite," *Phys. Rev. Lett.*, **8**, 404–406 (1962).
11. P. D. Maker and R. W. Terhune, "Study of optical effects due to an induced polarization third-order in the electric field strength," *Phys. Rev.*, **137A**, 801–818 (1965).
12. J. A. Armstrong, N. Bloembergen, J. Ducuing, and P. S. Pershan, "Interactions between light waves in a nonlinear dielectric," *Phys. Rev.*, **127**, 1918–1939 (1962).
13. P. S. Pershan, "Nonlinear optical properties of solids: Energy considerations," *Phys. Rev.*, **130**, 919–928 (1963).
14. A. Adler, "Nonlinear optical frequency polarization in a dielectric," *Phys. Rev.*, **134A**, 728–733 (1964).
15. N. Bloembergen, R. K. Chang, S. S. Jha, and C. H. Lee, "Optical second-harmonic generation in reflection from media with inversion symmetry," *Phys. Rev.*, **174**, 813–822 (1968).
16. G. Mayer, "Even-harmonic light radiation by molecules in a dc electric field," *Compt. Rend. Acad. Sci. (Paris)*, **267B**, 54–57 (1968).
17. S. Kielich, "dc electric field-induced optical second harmonic light generation by interacting multipolar molecules," *Chem. Phys. Lett.*, **2**, 569–572 (1968).
18. S. Kielich, "Second-harmonic generation of light by dipolar molecules totally aligned in a dc electric field," *Acta Phys. Polonica*, **XXXVI**, 621–631 (1969).
19. S. Kielich, "Optical second-harmonic generation by electrically polarized isotropic media," *IEEE J. Quantum Electron.*, **5**, 562–568 (1969).
20. S. Kielich, "dc electric field-induced second harmonic light generation in gases and liquids," *Acta Phys. Polonica*, **A37**, 205–219 (1970).

21. S. Kielich, "Frequency doubling of laser light in an isotropic medium with electrically destroyed centre of inversion," *J. Opto-Electron.*, **2**, 5–20 (1970).
22. R. S. Finn and J. F. Ward, "dc-induced optical second-harmonic generation in the inert gases," *Phys. Rev. Lett.*, **26**, 285–289 (1971).
23. I. J. Bigio and J. F. Ward, "Measurement of the hyperpolarizability ratio $X_{yyyy}(-2\omega; 0, \omega, \omega)/X_{yyxx}(-2\omega; 0, \omega, \omega)$ for inert gases," *Phys. Rev. A*, **9**, 35–39 (1974).
24. R. S. Finn and J. F. Ward, "Measurements of hyperpolarizabilities for some halogenated methanes," *J. Chem. Phys.*, **60**, 454–458 (1974).
25. J. F. Ward and I. J. Bigio, "Molecular second- and third-order polarizabilities from measurements of second-harmonic generation in gases," *Phys. Rev. A*, **11**, 60–66 (1975).
26. C. K. Miller and J. F. Ward, "Measurements of nonlinear optical polarizabilities for some halogenated methanes: The role of bond-bond interactions," *Phys. Rev. A*, **16**, 1179–1185 (1977).
27. J. F. Ward and D. S. Elliott, "Measurements of molecular hyperpolarizabilities for ethylene, butadiene, hexatriene, and benzene," *J. Chem. Phys.*, **69**, 5438–5440 (1978).
28. J. F. Ward and C. K. Miller, "Measurements of nonlinear optical polarizabilities for twelve small molecules," *Phys. Rev. A*, **19**, 826–833 (1979).
29. J. W. Dudley and J. F. Ward, "Measurements of second- and third-order nonlinear polarizabilities for HF and HCl," *J. Chem. Phys.*, **82**, 4673–4677 (1985).
30. D. P. Shelton and A. D. Buckingham, "Optical second-harmonic generation in gases with a low-power laser," *Phys. Rev. A*, **26**, 2787–2798 (1982).

31. V. Mizrahi and D. P. Shelton, "Nonlinear susceptibility of H₂ and D₂ accurately measured over a wide range of wavelengths," *Phys. Rev. A*, **32**, 3454–3460 (1985).
32. D. P. Shelton, "Dispersion of the nonlinear susceptibility measured for benzene," *J. Opt. Soc. Am. B*, **2**, 1880–1882 (1985).
33. V. Mizrahi and D. P. Shelton, "Dispersion of nonlinear susceptibilities of Ar, N₂ and O₂ measured and compared," *Phys. Rev. Lett.*, **55**, 696–699 (1985).
34. V. Mizrahi and D. P. Shelton, "Deviations from Kleinman symmetry measured for several simple atoms and molecules," *Phys. Rev. A*, **31**, 3145–3154 (1985).
35. D. P. Shelton and V. Mizrahi, "Frequency dependence of the hyperpolarizability measured for SF₆," *Chem. Phys. Lett.*, **120**, 318–320 (1985).
36. D. P. Shelton, "The hyperpolarizability of benzene measured in the presence of absorption," *Chem. Phys. Lett.*, **121**, 69–72 (1985).
37. D. P. Shelton, "Hyperpolarizability dispersion measured for CH₄," *Phys. Rev. A*, **34**, 304–308 (1986).
38. D. P. Shelton, "Hyperpolarizability dispersion measured for Kr and Xe," *J. Chem. Phys.*, **84**, 404–407 (1986).
39. D. P. Shelton, "Hyperpolarizability dispersion measured for CO₂," *J. Chem. Phys.*, **85**, 4234–4239 (1986).
40. Z. Lu and D. P. Shelton, "Vibrational contributions to the second hyperpolarizability of CF₄," *J. Chem. Phys.*, **87**, 1976–1976 (1987).
41. R. E. Cameron and D. P. Shelton, "Non-resonant third-order susceptibilities measured for ethane, propane and *n*-butane," *Chem. Phys. Lett.*, **133**, 520–524 (1987).

42. D. P. Shelton and Z. Lu, “Kleinman symmetry deviations for hydrogen,” *Phys. Rev. A*, **37**, 2231–2233 (1988).
43. D. P. Shelton and Z. Lu, “Hyperpolarizability dispersion measured for neon,” *Phys. Rev. A*, **37**, 3813–3817 (1988).
44. D. P. Shelton, “Anomalous hyperpolarizability dispersion measured for neon,” *Phys. Rev. Lett.*, **62**, 2660–2663 (1989).
45. D. P. Shelton, “Nonlinear-optical susceptibilities of gases measured at 1064 and 1319 nm,” *Phys. Rev. A*, **42**, 2578–2592 (1990).
46. D. P. Shelton and E. A. Donley, “The hyperpolarizability dispersion of neon is not anomalous,” *Chem. Phys. Lett.*, **195**, 591–595 (1992).
47. M. Stähelin, C. R. Moylan, D. M. Burland, A. Willetts, J. E. Rice, D. P. Shelton, and E. A. Donley, “A comparison of calculated and experimental hyperpolarizabilities for acetonitrile in gas and liquid phases,” *J. Chem. Phys.*, **98**, 5595–5603 (1993).
48. E. A. Donley and D. P. Shelton, “Hyperpolarizabilities measured for interacting molecular pairs,” *Chem. Phys. Lett.*, **215**, 156–162 (1993).
49. E. A. Donley and D. P. Shelton, “Erratum: Hyperpolarizabilities measured for interacting molecular pairs (Chem. Phys. Letters 215 (1993) 156),” *Chem. Phys. Lett.*, **228**, 701 (1994).
50. P. Kaatz, E. A. Donley, and D. P. Shelton, “A comparison of molecular hyperpolarizabilities from gas and liquid phase measurements,” *J. Chem. Phys.*, **108**, 849–856 (1998).
51. V. W. Couling and D. P. Shelton, “Hyperpolarizability dispersion measured for $(\text{CH}_3)_2\text{O}$,” *J. Chem. Phys.*, **143**, 224307 (2015).

52. R. M. Ellis and D. P. Shelton, "Vibration overtone hyperpolarizability measured for H₂," *J. Chem. Phys.*, **152**, 154301 (2020).
53. R. N. Fernandez and D. P. Shelton, "Hyperpolarizability dispersion measured for CS₂ vapor," *J. Opt. Soc. Am. B*, **37**, 1769–1774 (2020).
54. L. R. Dalton, P. A. Sullivan, and D. H. Bale, "Electric field poled organic electro-optic materials: state of the art and future prospects," *Chem. Rev.*, **110**, 25–55 (2010).
55. L. R. Dalton, "Rational design of organic electro-optic materials," *J. Phys.: Condens. Matter*, **15**, R897–R934 (2003).
56. N. I. Zheludev and Y. S. Kivshar, "From metamaterials to metadevices," *Nat. Mater.*, **11**, 917–924 (2012).
57. J. R. Hammond and K. Kowalski, "Parallel computation of coupled-cluster hyperpolarizabilities," *J. Chem. Phys.*, **130**, 194108 (2009).
58. A. V. Gubskaya and P. G. Kusalik, "The multipole polarizabilities and hyperpolarizabilities of the water molecule in liquid state: an *ab initio* study," *Mol. Phys.*, **99**, 1107–1120 (2001).
59. C. H. Kwak and G. Y. Kim, "Rigorous theory of molecular orientational nonlinear optics," *AIP Adv.*, **5**, 017124 (2015).
60. M. Kuzyk, K. Singer, and G. Stegeman, "Theory of molecular nonlinear optics," *Adv. Opt. Photon.*, **5**, 4–82 (2013).
61. E. P. Concannon, "*Hyperpolarizabilities of Interacting Atoms*," Ph.D. thesis, University of Cambridge (1996).
62. A. D. Buckingham, E. P. Concannon, and I. D. Hands, "Hyperpolarizability of Interacting Atoms," *J. Phys. Chem.*, **98**, 10455–10459 (1994).

63. K. L. C. Hunt, "Long-range dipoles, quadrupoles, and hyperpolarizability of interacting inert-gas atoms," *Chem. Phys. Lett.*, **70**, 336–342 (1980).
64. A. D. Buckingham and B. D. Utting, "Intermolecular forces," *Ann. Rev. Phys. Chem.*, **21**, 287–316 (1970).
65. D. M. Bishop and M. Dupuis, "The interaction polarizability and interaction second-hyperpolarizability for $\text{He} \cdots \text{He}$," *Mol. Phys.*, **88**, 887–898 (1996).
66. X. Li, K. L. C. Hunt, J. Pipin, and D. M. Bishop, "Long-range, collision-induced hyperpolarizabilities of atoms or centrosymmetric linear molecules: Theory and numerical results for pairs containing H or He," *J. Chem. Phys.*, **105**, 10954–10968 (1996).
67. B. Fernández, C. Hättig, H. Koch, and A. Rizzo, "*Ab initio* calculation of the frequency-dependent interaction induced hyperpolarizability of Ar_2 ," *J. Chem. Phys.*, **110**, 2872–2882 (1999).
68. C. Hättig, H. Larsen, J. Olsen, P. Jørgensen, H. Koch, B. Fernández, and A. Rizzo, "The effect of intermolecular interactions on the electric properties of helium and argon. I. *Ab initio* calculation of the interaction induced polarizability and hyperpolarizability in He_2 and Ar_2 ," *J. Chem. Phys.*, **111**, 10099–10107 (1999).
69. H. Koch, C. Hättig, H. Larsen, J. Olsen, P. Jørgensen, B. Fernández, and A. Rizzo, "The effect of intermolecular interactions on the electric properties of helium and argon. II. The dielectric, refractivity, Kerr, and hyperpolarizability second virial coefficients," *J. Chem. Phys.*, **111**, 10108–10118 (1999).
70. G. Maroulis, "Computational aspects of interaction hyperpolarizability calculations. A study on $\text{H}_2 \cdots \text{H}_2$, $\text{Ne} \cdots \text{HF}$, $\text{Ne} \cdots \text{FH}$, $\text{He} \cdots \text{He}$, $\text{Ne} \cdots \text{Ne}$, $\text{Ar} \cdots \text{Ar}$, and $\text{Kr} \cdots \text{Kr}$," *J. Phys. Chem. A*, **104**, 4772–4779 (2000).

71. J. L. Cacheiro, B. Fernández, D. Marchesan, S. Coriani, C. Hättig, and A. Rizzo, "Coupled cluster calculations of the ground state potential and interaction induced electric properties of the mixed dimers of helium, neon and argon," *Mol. Phys.*, **102**, 101–110 (2004).
72. A. Rizzo, S. Coriani, D. Marchesan, J. L. Cacheiro, B. Fernández, and C. Hättig, "Density dependence of electric properties of binary mixtures of inert gases," *Mol. Phys.*, **104**, 305–318 (2006).
73. G. Maroulis, "Interaction-induced electric properties," in "Chemical Modelling: Applications and Theory," (The Royal Society of Chemistry, 2012).
74. A. D. Buckingham and J. A. Pople, "Theoretical studies of the Kerr effect I. Deviations from a linear polarization law," *Proc. Phys. Soc. A*, **68**, 905–909 (1955).
75. A. D. Buckingham, "Theoretical studies of the Kerr effect II. The influence of pressure," *Proc. Phys. Soc. A*, **68**, 910–919 (1955).
76. A. D. Buckingham, P. A. Galwas, and L. Fan-Chen, "Polarizabilities of interacting polar molecules," *J. Mol. Struct.*, **100**, 3–12 (1983).
77. V. W. Couling and C. Graham, "Second Kerr effect virial coefficients of polar molecules with linear and lower symmetry," *Mol. Phys.*, **93**, 31–47 (1998).
78. V. W. Couling and C. Graham, "Calculation of second Kerr effect virial coefficients of H₂S," *Mol. Phys.*, **98**, 135–138 (2000).
79. V. W. Couling, B. W. Halliburton, R. I. Keir, and G. L. D. Ritchie, "Anisotropic molecular polarizabilities of HCHO, CH₃CHO, and CH₃COCH₃. Rayleigh depolarization ratios of HCHO and CH₃CHO and first and second Kerr virial coefficients of CH₃COCH₃," *J. Phys. Chem. A*, **105**, 4365–4370 (2001).

80. P. Naidoo, “*Second Kerr-effect Virial Coefficients of Non-dipolar Molecules with Axial and Lower Symmetry*,” Master’s thesis, University of KwaZulu-Natal (2017).
81. M. M. Mhlongo, “*Hyperpolarizability Contributions to the Second Kerr-effect Virial Coefficients of Non-dipolar Molecules*,” Master’s thesis, University of KwaZulu-Natal (2019).
82. S. Kielich, M. Kozierowski, Z. Ozgo, and R. Zawodny, “Second-harmonic electric quadrupolar elastic scattering by atoms and centro-symmetric molecules,” *Acta Phys. Pol.*, **A45**, 9–19 (1974).
83. A. D. Buckingham, “Permanent and induced molecular moments and long-range intermolecular forces,” *Adv. Chem. Phys.*, **12**, 107–142 (1967).
84. A. D. Buckingham, “Molecular quadrupole moments,” *Quart. Rev.*, **13**, 183–214 (1959).
85. L. D. Barron, *Molecular Light Scattering and Optical Activity* (Cambridge University Press, Cambridge, 2004).
86. R. E. Raab and O. L. de Lange, *Multipole Theory in Electromagnetism* (Clarendon Press, Oxford, 2005).
87. D. A. Imrie, “*The Measurement of Electric Quadrupole Moments of Gas Molecules by Induced Birefringence*,” Ph.D. thesis, University of Natal (1993).
88. C. A. Coulson, A. Maccoll, and L. E. Sutton, “The polarizability of molecules in strong electric fields,” *Trans. Faraday Soc.*, **48**, 106–113 (1952).
89. M. P. Bogaard and B. J. Orr, “Electric Dipole Polarisabilities of Atoms and Molecules,” in “International Review of Science, Physical Chemistry, Molecular Structure and Properties,” vol. 2 of *Ser. 2*, A. D. Buckingham, ed. (Butterworths, London, 1975), chap. 5, pp. 149–194.

90. D. M. Bishop and J. Pipin, "Improved dynamic hyperpolarizabilities and field-gradient polarizabilities for helium," *J. Chem. Phys.*, **91**, 3549–3551 (1989).
91. P. N. Butcher and D. Cotter, *The Elements of Nonlinear Optics*, Cambridge Studies in Modern Optics, reprint edition (Cambridge University Press, Cambridge, 1993).
92. H. Reis, "Problems in the comparison of theoretical and experimental hyperpolarizabilities revisited," *J. Chem. Phys.*, **125**, 014506 (2006).
93. J. F. Ward and G. H. C. New, "Optical third harmonic generation in gases by a focused laser beam," *Phys. Rev.*, **185**, 57–72 (1969).
94. B. J. Orr and J. F. Ward, "Perturbation theory of the non-linear optical polarization of an isolated system," *Mol. Phys.*, **20**, 513–526 (1971).
95. D. M. Bishop, "Molecular vibrational and rotational motion in static and dynamic electric fields," *Rev. Mod. Phys.*, **62**, 343–374 (1990).
96. D. M. Bishop, J. Pipin, and S. M. Cybulski, "Theoretical investigation of the nonlinear optical properties of H₂ and D₂: Extended basis set," *Phys. Rev. A*, **43**, 4845–4853 (1991).
97. J. Olsen and P. Jørgensen, "Linear and nonlinear response functions for an exact state and for an MCSCF state," *J. Chem. Phys.*, **82**, 3235–3264 (1985).
98. J. Olsen and P. Jørgensen, *Modern Electronic Structure Theory, Part II* (World Scientific, Singapore, 1995).
99. T. Helgaker, S. Coriani, P. Jørgensen, K. Kristensen, J. Olsen, and K. Ruud, "Recent advances in wave function-based methods of molecular-property calculations," *Chem. Rev.*, **112**, 543–631 (2012).
100. C. J. F. Böttcher, *Theory of Electric Polarization*, vol. I (Elsevier, Amsterdam, 1973).

101. F. N. H. Robinson, *Macroscopic Electromagnetism* (Pergamon Press, Oxford, 1973).
102. A. Zangwill, *Modern Electrodynamics* (Cambridge University Press, Cambridge, 2013).
103. H. A. Lorentz, *The Theory of Electrons* (Dover, New York, 1952).
104. J. G. Kirkwood, "The dielectric polarization of polar liquids," *J. Chem. Phys.*, **7**, 911–919 (1939).
105. L. Onsager, "Electric moments of molecules in liquids," *J. Am. Chem. Soc.*, **58**, 1486–1493 (1936).
106. N. Bloembergen, *Nonlinear Optics* (World Scientific, Singapore, 1996), 4th ed.
107. A. Willetts, J. E. Rice, D. M. Burland, and D. P. Shelton, "Problems in the comparison of theoretical and experimental hyperpolarizabilities," *J. Chem. Phys.*, **97**, 7590–7599 (1992).
108. A. Hourri, J. M. St-Arnaud, and T. K. Bose, "Dielectric and pressure virial coefficients of imperfect gases: CO₂–SF₆ mixtures," *J. Chem. Phys.*, **106**, 1780–1785 (1997).
109. J. W. Schmidt and M. R. Moldover, "Dielectric permittivity of eight gases measured with cross capacitors," *Int. J. Thermophys.*, **24**, 375–403 (2003).
110. A. D. Buckingham, "Frequency dependence of the Kerr constant," *Proc. Roy. Soc. London A* **267**, 271–282 (1962).
111. M. H. Protter and C. B. Morrey Jr, "Differentiation under the Integral Sign," in "Intermediate Calculus," (Springer, New York, 1985), chap. 8, pp. 421–426, 2nd ed.

112. A. L. Andrews and A. D. Buckingham, "The effect of strong electric and magnetic fields on the depolarization ratios of gases," *Mol. Phys.*, **3**, 183–189 (1960).
113. P. Langevin, "Sur la théorie du magnétisme," *J. Phys. Theor. Appl.*, **4**, 678–693 (1905).
114. P. Langevin, "Magnétisme et théorie des électrons," *Ann. Chim. Phys.*, **5**, 70–127 (1905).
115. P. Debye, "Einige resultate einer kinetischen theorie der isolatoren," *Phys. Z.*, **13**, 97–100 (1912).
116. P. Debye, *Polar Molecules* (Chemical Catalog Company, New York, 1929).
117. R. Clausius, *Die Mechanische Wärmetheorie* (Vieweg, Braunschweig, 1879), vol. II, p. 62.
118. O. F. Mossotti, *Discussione analitica sull'influenza che l'azione di un mezzo dielettrico ha sulla distribuzione dell'elettricità alla superficie di più corpi elettrici disseminati in esso*, *Memorie di Mathematica e di Fisica della Società Italiana della Scienza Residente in Modena* (1850), vol. 24, pp. 49–74.
119. A. D. Buckingham and C. Graham, "The density dependence of the refractivity of gases," *Proc. Roy. Soc. Lond. A*, **337**, 275–291 (1974).
120. U. Hohm, "Frequency-dependence of second refractivity virial coefficients of small molecules between 325 nm and 633 nm," *Mol. Phys.*, **81**, 157–168 (1994).
121. P. F. Egan, J. A. Stone, J. K. Scherschligt, and A. H. Harvey, "Measured relationship between thermodynamic pressure and refractivity for six candidate gases in laser barometry," *J. Vac. Sci. Technol. A*, **37**, 031603 (2019).

122. H. A. Lorentz, "Ueber die beziehung zwischen der fortpflanzungsgeschwindigkeit des lichtes und der körperdichte," *Ann. Phys. Chem.*, **245**, 641–665 (1880).
123. L. Lorenz, "Ueber die refractionsconstante," *Ann. Phys. Chem.*, **247**, 70–103 (1880).
124. A. D. Buckingham and J. A. Pople, "Electromagnetic properties of compressed gases," *Disc. Faraday Soc.*, **22**, 17–21 (1956).
125. V. W. Couling and C. Graham, "Calculation and measurement of the second light-scattering virial coefficients of nonlinear molecules: a study of ethene," *Mol. Phys.*, **87**, 779–799 (1996).
126. V. W. Couling and C. Graham, "Measurement and interpretation of the second light-scattering virial coefficients of linear and quasi-linear molecules," *Mol. Phys.*, **82**, 235–244 (1994).
127. V. W. Couling and C. Graham, "Depolarized interaction-induced Rayleigh light scattering in gaseous SO₂," *Mol. Phys.*, **96**, 921–925 (1999).
128. V. W. Couling and R. V. Nhlelela, "Calculation and measurement of the second light-scattering virial coefficient of (CH₃)₂O," *Phys. Chem. Chem. Phys.*, **3**, 4551–4554 (2001).
129. R. R. Birss, "Macroscopic symmetry in space-time," *Rep. Prog. Phys.*, **26**, 307–360 (1963).
130. R. R. Birss, *Symmetry and Magnetism* (North-Holland, Amsterdam, 1966).
131. J. O. Hirschfelder, C. F. Curtiss, and R. B. Bird, *Molecular Theory of Gases and Liquids* (Wiley, New York, 1954).

132. A. D. Buckingham, S. Coriani, and A. Rizzo, "Investigation of electric-field-gradient-induced birefringence in H₂ and D₂," *Theor. Chem. Acc.*, **117**, 969–977 (2007).
133. J. H. Dymond, K. N. Marsh, R. C. Wilhoit, and K. C. Wong, *The Virial Coefficients of Pure Gases and Mixtures* (Springer-Verlag, Berlin, 2002).
134. A. Kumar and W. J. Meath, "Constrained anisotropic dipole oscillator strength distribution techniques, and reliable results for anisotropic and isotropic dipole molecular properties, with applications to H₂ and N₂," *Theoret. Chim. Acta*, **82**, 131–152 (1992).
135. D. M. Bishop and J. Pipin, "Ab initio study of third-order nonlinear optical properties of the H₂ and D₂ molecules," *Phys. Rev. A*, **36**, 2171–2181 (1987).
136. D. M. Bishop and B. Lam, "Calculation of the dc Kerr and electric-field-induced second-harmonic generation susceptibilities for H₂ and D₂," *J. Chem. Phys.*, **89**, 1571–1579 (1988).
137. D. M. Bishop, J. Pipin, and M. Rérat, "Nonlinear optical properties of H₂ and D₂," *J. Chem. Phys.*, **92**, 1902–1908 (1990).
138. A. D. Buckingham, "Direct method of measuring molecular quadrupole moments," *J. Chem. Phys.*, **30**, 1580–1585 (1959).
139. A. D. Buckingham and R. L. Disch, "The quadrupole moment of the carbon dioxide molecule," *Proc. R. Soc. London A*, **273**, 275–289 (1963).
140. D. E. Woon and T. H. Dunning, "Gaussian basis sets for use in correlated molecular calculations. IV. Calculation of static electrical response properties," *J. Chem. Phys.*, **100**, 2975–2988 (1994).
141. E. Miliordos and K. L. C. Hunt, "Dependence of the multipole moments, static polarizabilities, and static hyperpolarizabilities of the hydrogen molecule on

- the H–H separation in the ground singlet state,” *J. Chem. Phys.*, **149**, 234103 (2018).
142. “NIST Chemistry WebBook,” <http://webbook.nist.gov/chemistry/>. [Accessed 06-12-2024].
143. C. Graham, “Calculations of second light-scattering virial coefficients of linear and quasi-linear molecules,” *Mol. Phys.*, **77**, 291–309 (1992).
144. G. L. D. Ritchie, J. N. Watson, and R. I. Keir, “Temperature dependence of electric field-gradient induced birefringence (Buckingham effect) and molecular quadrupole moment of N₂. Comparison of experiment and theory,” *Chem. Phys. Lett.*, **370**, 376–380 (2003).
145. C. Hättig, O. Christiansen, and P. Jørgensen, “Frequency-dependent second hyperpolarizabilities using coupled cluster cubic response theory,” *Chem. Phys. Lett.*, **282**, 139–146 (1998).
146. F. Pawłowski, P. Jørgensen, and C. Hättig, “The second hyperpolarizability of the N₂ molecule calculated using the approximate coupled cluster triples model CC3,” *Chem. Phys. Lett.*, **413**, 272–279 (2005).
147. G. Maroulis, “Accurate electric multipole moment, static polarizability and hyperpolarizability derivatives for N₂,” *J. Chem. Phys.*, **118**, 2673–2687 (2003).
148. D. P. Shelton and J. E. Rice, “Measurements and calculations of the hyperpolarizabilities of atoms and small molecules in the gas phase,” *Chem. Rev.*, **94**, 3–29 (1994).
149. N. Chetty and V. W. Couling, “Measurement of the electric quadrupole moments of CO₂ and OCS,” *Mol. Phys.*, **109**, 655–666 (2011).
150. P. C. Balachandran Pillai and V. W. Couling, “Dispersion of the Rayleigh

- light-scattering virial coefficients and polarisability anisotropy of CO₂,” *Mol. Phys.*, **117**, 289–297 (2019).
151. H. Sekino and R. J. Bartlett, “Molecular hyperpolarizabilities,” *J. Chem. Phys.*, **98**, 3022–3037 (1993).
152. D. M. Bishop and E. K. Dalskov, “Analysis of the vibrational, static and dynamic, second hyperpolarizability of five small molecules,” *J. Chem. Phys.*, **104**, 1004–1011 (1996).
153. G. Maroulis, “Polarizabilities and hyperpolarizabilities of carbon dioxide,” *J. Chem. Phys.*, **93**, 4164–4171 (1990).
154. V. W. Couling and C. Graham, “Higher-order dipole-dipole, dipole-quadrupole and field gradient contributions to the second light-scattering virial coefficient,” *Mol. Phys.*, **79**, 859–867 (1993).
155. R. Tammer and W. Hüttner, “Kerr effect and polarizability tensor of gaseous ethene,” *Mol. Phys.*, **83**, 579–590 (1994).
156. Y. Das Gupta, Y. Singh, and S. Singh, “Effect of shape of molecules on transport and equilibrium properties of nonpolar polyatomic gases,” *J. Chem. Phys.*, **59**, 1999–2006 (1973).
157. W. Majer, P. Lutzmann, and W. Hüttner, “The molecular electric quadrupole tensor of ethene from the rotational Zeeman effect of CH₂=CD₂,” *Mol. Phys.*, **83**, 567–578 (1994).
158. G. Maroulis, “A study of basis set and electron correlation effects in the *ab initio* calculation of the electric dipole hyperpolarizability of ethene (H₂C=CH₂),” *J. Chem. Phys.*, **97**, 4188–4194 (1992).

159. O. Quinet and B. Champagne, "Hybridization effect upon the vibrational second hyperpolarizability: An *ab initio* study of acetylene, ethylene, and ethane," *Int. J. Quantum Chem.*, **80**, 871–881 (2000).